The Design and Synthesis of ß-Keto Vinyl Sultams and Macrocyclic ß-Keto Vinyl Sultams: Novel Analogs of Tetramic Acids

The Design and Synthesis of *β*-Keto Vinyl Sultams and Macrocyclic *β*-Keto Vinyl Sultams: Novel Analogs of Tetramic Acids

By

Jay Shankar Jha

Submitted to the graduate degree program in the Department of Chemistry and the Graduate Faculty of the University of Kansas in partial fulfillment of the requirements of Master of Science

Paul R. Hanson, Chair

Michael Rubin

Michael Clift

July 24th, 2018
Date Defended

The Dissertation Committee of Jay Shankar Jha certifies that this is the approved version of the following dissertation

The Design and Synthesis of *β*-Keto Vinyl Sultams and Macrocyclic *β*-Keto Vinyl Sultams: Novel Analogs of Tetramic Acids

Paul R. Hanson, Chair

July 24th, 2018
Date Approved

Abstract

Jay Shankar Jha

Department of Chemistry

University of Kansas, July 24th, 2018

Sulfur (*S*)-containing heterocyclic compounds possessing $R^1R^2N–SO_2R^3$ functionality have been recognized as important due to their innate physical properties that affect biological systems marking them as attractive targets for probing biological pathways. Specifically, sulfonamides and sultams represent two significant compound classes, which exhibit broad ranges of biological activities. Similarly, natural products possessing the tetramic acid core structural motif have emerged as a rich chemotype due to their potent and broad biological activities. Several bioactive tetramic acid-containing compounds have been reported with a variety of activities, including antibacterial, anticancer and anti-inflammatory activities, as well as unique biological profiles in different cell assays. Tetramic acid analogs are also known to modulate protein-protein interactions.

In light of the biological significance of the tetramic acid subunit, and the notable physical properties of sulfur containing compounds, we have become interested in the generation of *S*-analogs of tetramic acids in order to screen for biological activity, and to serve as new probes in Chemical Biology studies with our collaborators. One such class is *β*-keto sultams, and their unsaturated analogs, both of which represent relatively unexplored chemical space. While there are several reports in the literature for the synthesis of tetramic acid-containing compounds, there are a relatively limited number of examples of the corresponding *β*-keto sultam analogs. Moreover, their unsaturated analogs are even more limited. It is the purpose of this thesis to start our investigations to explore the substitution of the *β*-keto sultam group for the

β-keto lactam subunit in drug-like tetramic acid-containing molecules, which ultimately has the potential to modulate biological activity as well as ADME profiles of the resulting analogs compounds. This thesis will describe the design and synthesis of *β*-keto sultam analogs of tetramic acids and their corresponding unsaturated and macrocyclic derivatives as novel electrophilic probes that can be modulated electronically, sterically, and stereochemically.

Acknowledgement

I would like to acknowledge Prof. Paul R. Hanson for his supervision and guidance over the years, especially during my rough phase of academic life. I am grateful to the Chemistry Department and Graduate School of KU for accepting me at KU. Most importantly, I would like to thank my lab mates, friends and family members for their prayers, support and encouragement throughout my stay here in Lawrence.

I also appreciate the help and support I received from Dr. Justin Douglas and Sarah Neuenswander for NMR spectroscopy, Lawrence Seib for mass spectroscopy and Dr. Victor Day for the X-ray crystallography.

Table of Contents

Abbreviations

$(COCl)_2$	oxalyl chloride
ABPP	activity-based protein profiling
Ac_2O	acetic anhydride
AcOH	acetic acid
$AgNO_3$	silver nitrate
Al_2O_3	aluminium oxide
$B(OAc)_3$	boron acetate
$B_2(pin)_2$	bis(pinacolato)diboron
BnOLi	Benzyloxylithium
Boc_2O	di-tert-butyldicarbonate
$CaCl_2$	calcium chloride
CbzCl	benzyl chloroformate
CF_3CH_2OH	trifluoroethanol
CH_2N_2	diazomethane
CH_3SO_2Cl (MsCl)	methanesulfonyl chloride
$CHCl_3$	chloroform
Cs_2CO_3	cesium carbonate
$Cu(OAc)_2$	copper(II) acetate
CuCl	copper(I) Chloride
DABCO	1,4-diazabicyclo[2.2.2]octane
DBU	1,8-diazabicyclo[5.4.0]undec-7-ene
DCC	*N,N'*-dicyclohexylcarbodiimide
DCM (CH_2Cl_2)	dichloromethane
DDQ	2,3-dichloro-5,6-dicyano-1,4-benzoquinone
DEAD	diethyl azodicarboxylate
DIAD	diisopropyl azocarboxylate
DIBAL	diisobutylaluminium hydride

DIPEA	*N,N*-diisopropylethylamine
DMA	dimethylacetamide
DMAP	4-dimethylaminopyridine
DMF	N,N-dimethyl formamide
DMFDMA	N,N-dimethylformamide dimethyl acetal
DMP	Dess-Martin periodinane
DMSO	dimethyl sulfoxide
EDC	1-ethyl-3-(dimethylaminopropyl)carbodiimide
equiv.	equivalent
Et_2O	diethyl ether
Et_3N (TEA)	triethylamine
EtOAc	ethyl acetate
EtOH	ethanol
FBLD	fragment-based ligand design
h	hours
H_2O	water
H_3PO_4	phosphoric acid
HCl	hydrochloric acid
HCO_2NH_4	ammonium formate
HDAC	histone deacetylase
HIV	human immunodeficiency virus
HMPA	hexamethylphosphoramide
$InCl_3$	indium chloride
IPCC	isopropenyl chlorocarbonate
K_2CO_3	potassium carbonate
KOH	potassium hydroxide
KO_tBu	potassium tert-butoxide
LDA	lithium diisopropylamide

L-DET	diethyl L-tartrate
$LiAlH_4$	lithium aluminium hydride
LiBr	lithium bromide
LiHMDS	lithium bis(trimethylsilyl)amide
$LiN(iPr)_2$	lithium diisopropylamide
LiOAc	lithium acetate
LiOH	lithium hydroxide
MeCN	acetonitrile
MeI	methyl iodide
MeOH	methanol
$MgSO_4$	magnesium sulfate
Min.	minute
MPa	megapascal
MS	molecular sieves
Na_2SO_3	sodium sulfite
$NaBO_3$	sodium perborate
NaH	sodium hydride
NaHMDS	sodium bis(trimethylsilyl)amide
NaI	sodium iodide
NaOH	sodium hydroxide
NaOMe	sodium methoxide
nBu_4NF	tetrabutylammonium fluoride
n-BuLi	butyllithium
NH_3	ammonia
NMO	*N*-methylmorpholine N-oxide
PCl_5	phosphorous pentachloride
$Pd(OAc)_2$	palladium(II) acetate
PDC	pyridinium dichromate

$PhCH_3$	Toluene
PivCl	trimethylacetyl chloride (pivaloyl chloride)
PMB	4-methoxybenzyl ether
PPh_3	triphenylphosphine
PPTS	pyridinium *p*-toluenesulfonate
p-TsOH	*p*-toluenesulfonic acid
quant.	quantitative
RCM	ring closing metathesis
Rf	retention factor
RT	room temperature
SmI_2	samarium(II) iodide
$SOCl_2$	thionyl chloride
TA	tetramic acid
TBAF	tetrabutylammonium fluoride
TBAI	tetrabutylammonium iodide
TBDPS	*tert*-butyldiphenylsilane
TBSCl	*tert*-butyldimethylsilyl chloride
t-BuO_2H	*tert*-butylhydroperoxide
TFA	trifluoroacetic acid
TfOH	trifluoromethanesulfonic acid
THF	tetrahydrofuran
$Ti(i\text{-}PrO)_4$	titanium isopropoxide
$TiCl_4$	titanium tetrachloride
TMSOTf	trimethylsilyl trifluoromethanesulfonate
Tol	toluene
TPAP	tetrapropylammonium perruthenate
TsCl	*p*-toluenesulfonyl chloride
Ugi-4CR	Ugi four component reaction

Chapter: 1

Synthesis of β-Keto Vinyl Sultams:

Novel Tetramic Acid Analogs

Overview:

1.1 Introduction

Sulfur (*S*)-containing heterocyclic compounds possessing $R^1R^2N–SO_2R^3$ functionality have been recognized as important due to their innate physical properties that affect biological systems marking them as attractive targets for probing biological pathways. Specifically, sulfonamides and sultams represent two significant compound classes, which exhibit broad ranges of biological activities. Similarly, natural products possessing the tetramic acid core structural motif have emerged as a rich chemotype due to their potent and broad biological activities.[1] Several bioactive tetramic acid-containing compounds, such as,

equisetin, integramycin, janolusimide etc. have been reported with a variety of activities, including antibacterial, anticancer and anti-inflammatory activities, as well as unique biological profiles in different cell assays.[1] Tetramic acid analogs are also known to modulate protein-protein interactions.[1d,e]

In light of the biological significance of the tetramic acid subunit, and the notable physical properties of sulfur-containing compounds such as enhanced Mulliken charge, ability of mild *N*-alkylation etc., we have become interested in the generation of *S*-analogs of tetramic acids in order to screen for biological activity, and to serve as new probes in Chemical Biology studies with our collaborators. One such class is *β*-keto sultams, and their unsaturated analogs, both of which represent relatively unexplored chemical space. While there are several reports in the literature for the synthesis of tetramic acid-containing compounds, there are a relatively limited number of examples of the corresponding *β*-keto sultam analogs. Moreover, their unsaturated analogs are even more limited. It is the purpose of this thesis to start our investigations to explore the substitution of the *β*-keto sultam group for the *β*-keto lactam subunit in drug-like tetramic acid-containing molecules, which ultimately has the potential to modulate biological activity as well as ADME profiles of the resulting analogs compounds.

This thesis will describe the design and synthesis of *β*-keto sultam analogs of tetramic acids and their corresponding unsaturated derivatives as novel electrophilic probes that can be modulated electronically, sterically, and stereochemically. A modular approach is described, whereby these compounds can be simply accessed from amino acids/esters and can be converted to the corresponding *β*-keto sultams by mesylation, *N*-sulfonylation and Dieckmann cyclization (Figure 1.1). Their unsaturated and macrocyclic counterparts can be

obtained by Knoevenagel condensation using several different aldehydes in short adaptable synthetic routes. Varying substituents and ring size, as well as adjusting electronic, steric and stereochemical parameters will modulate the properties of these compounds. These compounds represent excellent starting points in the development of specific molecular probes for identifying hotspots in reactive proteins and enzymes.[2] Understanding the reactivity of such probes is a primary goal of this project, whereby compounds will be assessed against cysteine- and serine-based biological nucleophiles and whole proteome screening using activity-based protein profiling (ABPP).[3]

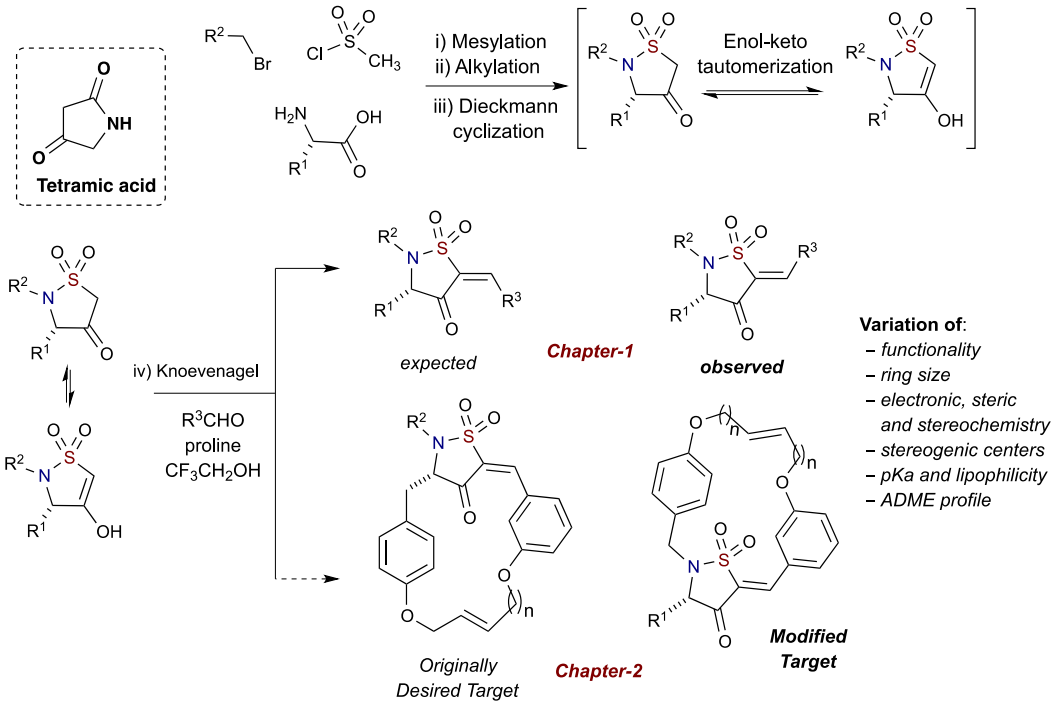

Figure 1.1: *Synthetic strategy of sultam analogs of tetramic acids.*

1.1.1 Sulfonamides and sultams: Properties and role in biological systems.

Sulfonamides are one of the well-known functional groups in the field of pharmacology. Sulfonamides drugs are bacteriostatic and are one of the first drugs used for

chemotherapeutics and preventive care.[4] This premise has inspired the proposed development of a number of modular methods within our laboratory for the construction of new electrophilic *S*-chemotypes with the aim of producing small libraries with attenuated thiol- and oxo-reactivity patterns, and improved selectivity. Efforts directed towards the synthesis and applications of these *S*-heterocycles will exploit their unique chemical properties, which are many-fold as outlined in Figure 1.2[5] and include, (i) Mulliken charge enhancement at the heteroatom, (ii) tunable pKa, which affects differential rate and conditions for *N*-alkylation enabling modular synthesis, (iii) hard P=O/soft SO_2 - engendering potential chemoselectivity with nucleophilic additions, (iv) variable oxidation states, (v) multivalency, (vi) Thorpe-Ingold enhancement of cyclization rates, (vii) tunable electrophilicity to affect modulation within reactivity profiling and ABPP studies, (viii) the ability of sulfur nuclei to exist with stable tetrahedral geometry, thus presenting them as an ideal mimic of tetrahedral transition

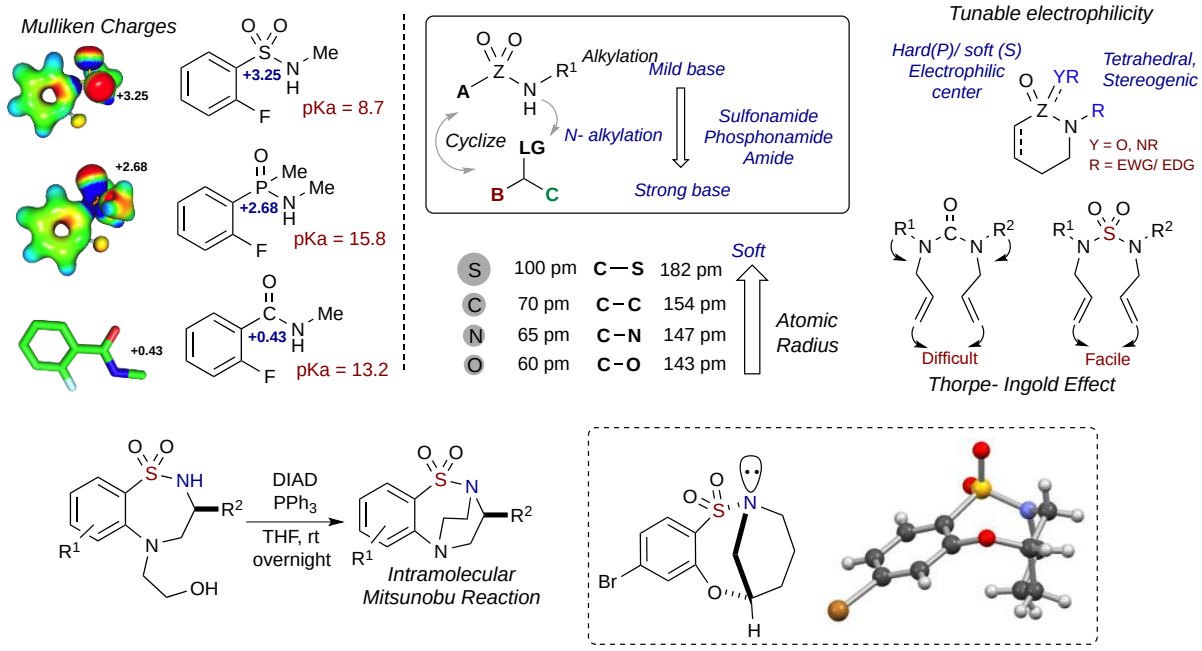

Figure 1.2: *Salient features of sulfur*

states involved in key biological processes, and (ix) the sp^3 character of sultams relegates them to 'non-flatland' status in molecular architecture unlike their planar amide counterparts.

Although sulfonamides are prevalent in drugs, their cyclic forms (sultams) are unnatural and less prevalent in the literature. Some of the synthesized sultam compounds are known to exhibit anti-proliferative and anti-HIV activities[6a] Others demonstrate inhibitory activity of trypsin-like serine protease factor XIa involved in blood coagulation,[6b] and modulator of lysosomal acidification involved in cellular function (Figure 1.3).[6c]

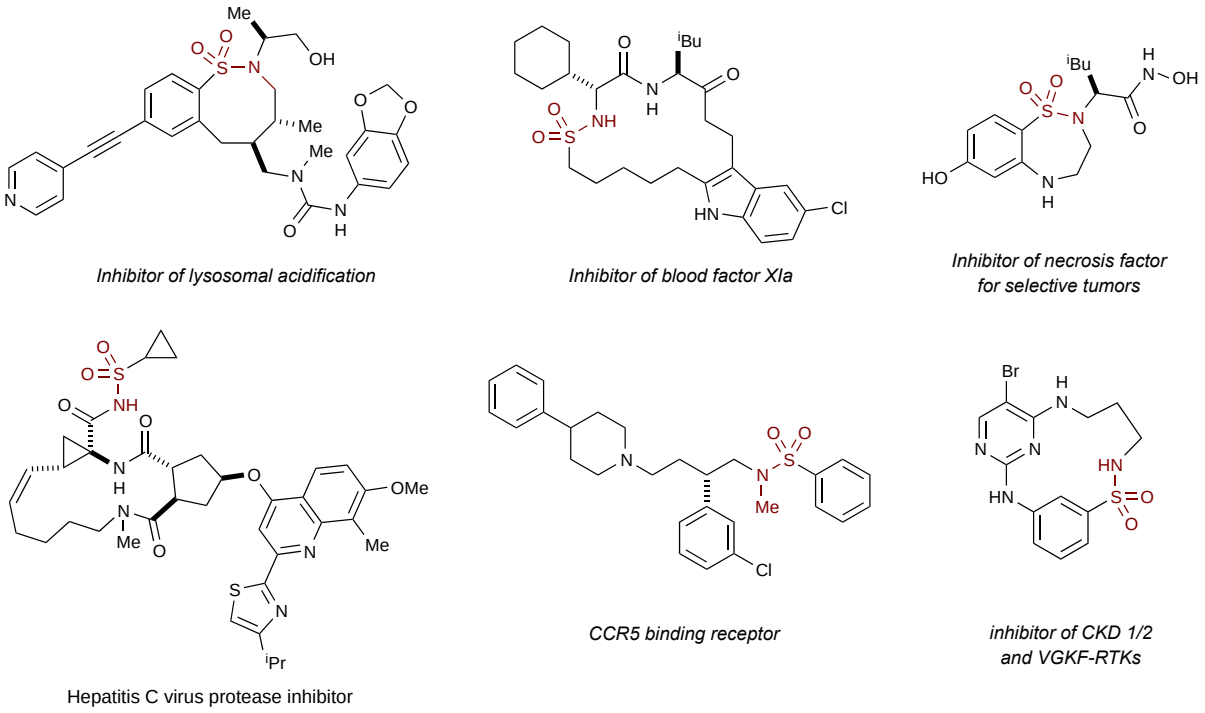

Figure 1.3: *Activity of sulfonamides and sultam compounds.*

The above discussion highlights the interesting properties of the $R^1R^2N–SO_2R^3$ moiety in both sulfonamides and sultams. The broad biological activity of sulfonamides and sultams is intriguing and has motivated our group to design and synthesize sultam compounds with unique properties using modular methods employing multi-functional

sulfonamide building blocks/linchpins for the synthesis of diverse array of sultams with variable ring size and functionality (Figure 1.4). This body of work includes use of: vinyl sulfonamide linchpins in Michael addition and double aza-Michael addition reactions[7], vinyl and allyl sulfonamides building blocks/linchpins in RCM reactions and RCM-Mitsunobu sequences.[8], and vinyl sulfonamides, α-halo aryl sulfonamides and α-halo aryl aziridinyl sulfonamides in various complementary pairing (CP) and complimentary ambiphile pairing (CAP) strategies.[9] In addition, the chemistry of mesylated amino esters was employed in Dieckmann cyclization strategies to generate novel amino acid derived *β*-keto sultams as highlighted in Chapter 3 of Moon Young Hur's thesis, and serves as the foundation for this dissertation.[10]

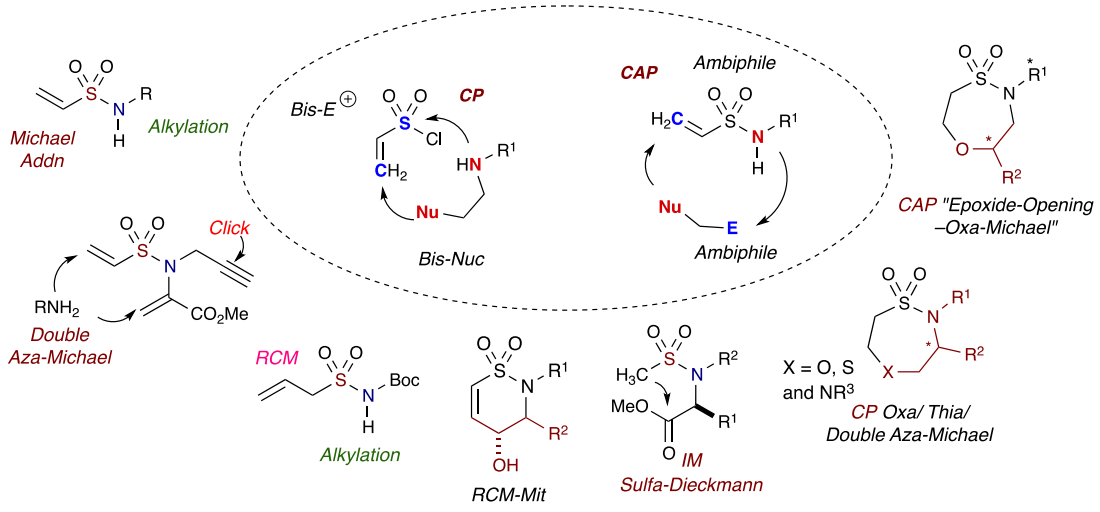

Figure 1.4: *Multi-Functional Sulfonamide Building Blocks.*

1.1.2 Tetramic acids: Natural products and their biological activities

Tetramic acids, formally 2,4-pyrrolidinediones, normally exist in equilibrium with their enol form. Tetramic acids have been known since the early 20th century, but gained prominence after the 1960s when they were found to be a key structural moiety in a variety

of natural products.[11] Tetramic acid-containing compounds are often secondary metabolites isolated from a wide range of terrestrial and marine organisms such as fungi, cyanobacteria, bacteria, and sponges.[12] They have attracted large interest in the field due to their broad range of bioactivities, including: antibiotic, antiviral, cytotoxicity, cell cycle inhibitory, and mycotoxicity.[13] Some of the examples of prominent natural products containing tetramic acid as a core structural motif have been listed in Figure 1.5. The list contains: spirotetramat, a spirocyclic tetramic acid derivative and a lipid biosynthesis inhibitor, which has been postulated to block acetyl-coenzyme A carboxylase and has been used as a pesticide and insecticide.[14] Streptosetin A is derived from marine actinomycetes and has been reported as a histone deacetylase (HDAC) inhibitor.[15] Spiroscytalin is a fungus metabolite having phenylalanine-derived tetramic acid core, and was found to exhibit anti-proliferative activity against human tumor cell lines and is also known to have antimicrobial activities.[16] Reutericyclin is isolated from bacteria *Lactobacillus reuteri*, and has a 5-membered core, structurally related to the tetramic acid core. Reutericyclin is bactericidal to gram-positive bacteria and a broad range of food-related spoilage organisms and pathogens.[17] Cryptocin, isolated from fungus, is a 3-acyl tetramic acid having a trans-decalin as a generic skeleton and is found to be antimycotic against *Pyricularia oryzae*, an agent that causes rice blast disease.[18] Equisetin is an *N*-methyl serine-derived acyl tetramic acid produced by various *Fusarium* species fungi and possesses antibiotic and cytotoxic activity as well as inhibitory activity against mitochondrial ATPases and HIV-1 integrase *in vitro*.[19] Integramycin is a hexacyclic tetramic acid-containing natural product that inhibits recombinant HIV-1 integrase.[20] Sch210972 is a decalin-containing tetramic acid derivative that inhibits cytokine receptor and is also a potential antiretroviral drug.[21] JBIR-22 is reported as a proteasome

inhibitor,[22] and inhibits protein-protein interaction by binding to the interface of the PAC3-binding domain. Janolusimide is a lipophilic tripeptide, isolated from the nudibranch mollusk and is known to be a neurotoxin.[23] Fusarisetin A, isolated form soil fungus, is a pentacyclic natural product consisting of a 5,5,5-angular tricycle motif, and is known to display inhibition of acinar morphogenesis along with cell migration and inhibition.[24] Diaporthichalasin, isolated form endophytic fungus, is a potent inhibitor of drug-metabolizing enzyme CYP3A4.[25]

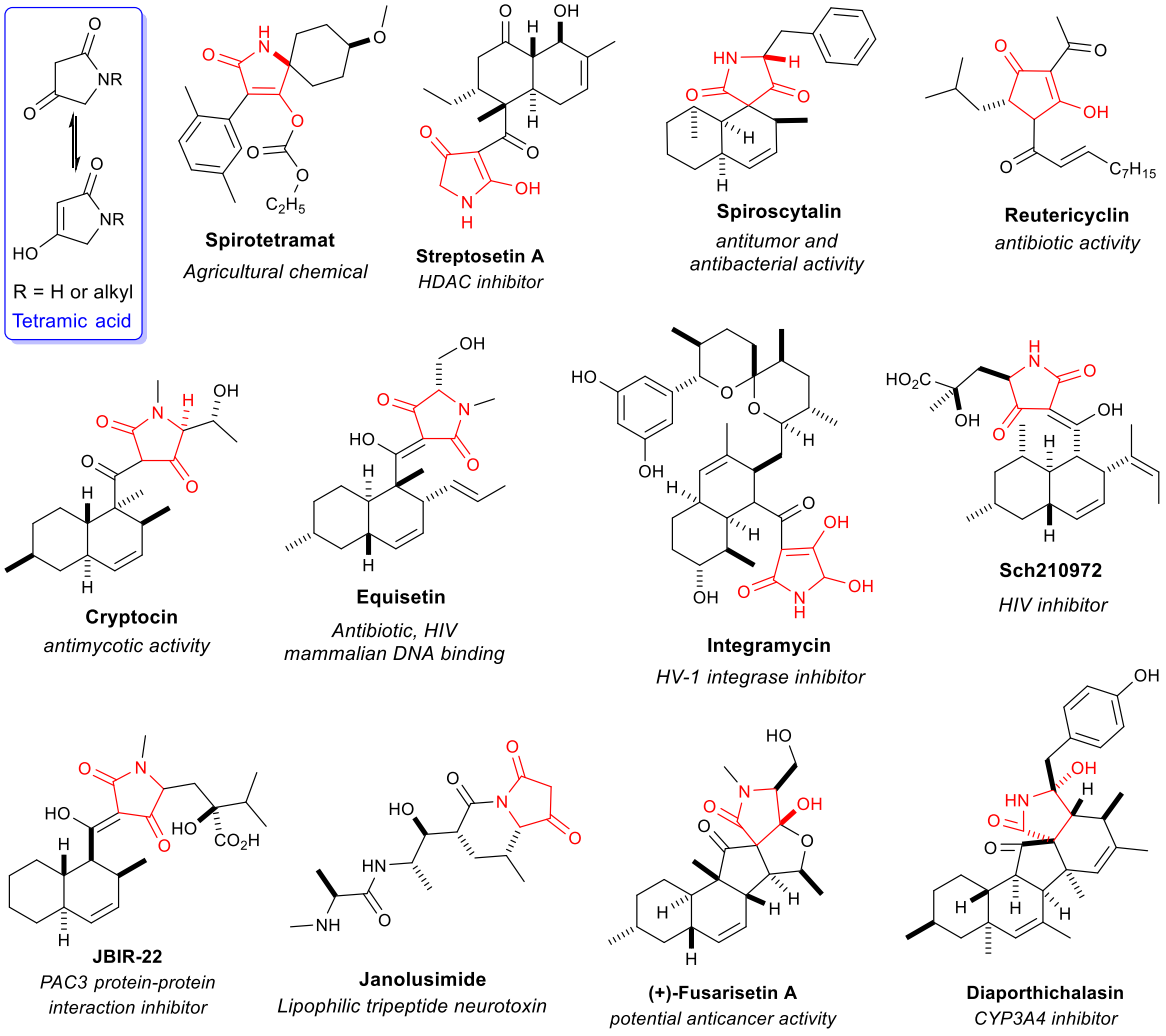

Figure. 1.5*: Natural products containing a tetramic acid as a core structural motif.*

The above discussion highlights the tetramic acid core as an important structural motif in natural products that display diverse biological activities. Similarly, from the earlier discussion, it has been revealed that sulfonamides and sultams are an important class of compounds known to possess interesting biological properties. Collectively, the synergy in these two motifs has inspired studies aimed at the production of sultam analogs of tetramic acid that will incorporate diverse biological activities associated to tetramic acids, and compelling molecular features from the sultam moiety.

In the course of designing and synthesizing several β-keto sultams, we have focused on the synthesis of small molecule electrophilic probes, namely β-keto vinyl sultams, as shown in Figure 1.6. These covalent probes possess doubly-activated Michael systems that are also present in a number of biologically active molecules and potential drug candidates such as bardoxolone methyl, cryptoquinone, and pyrrocidine A (Figure 1.6).[26]

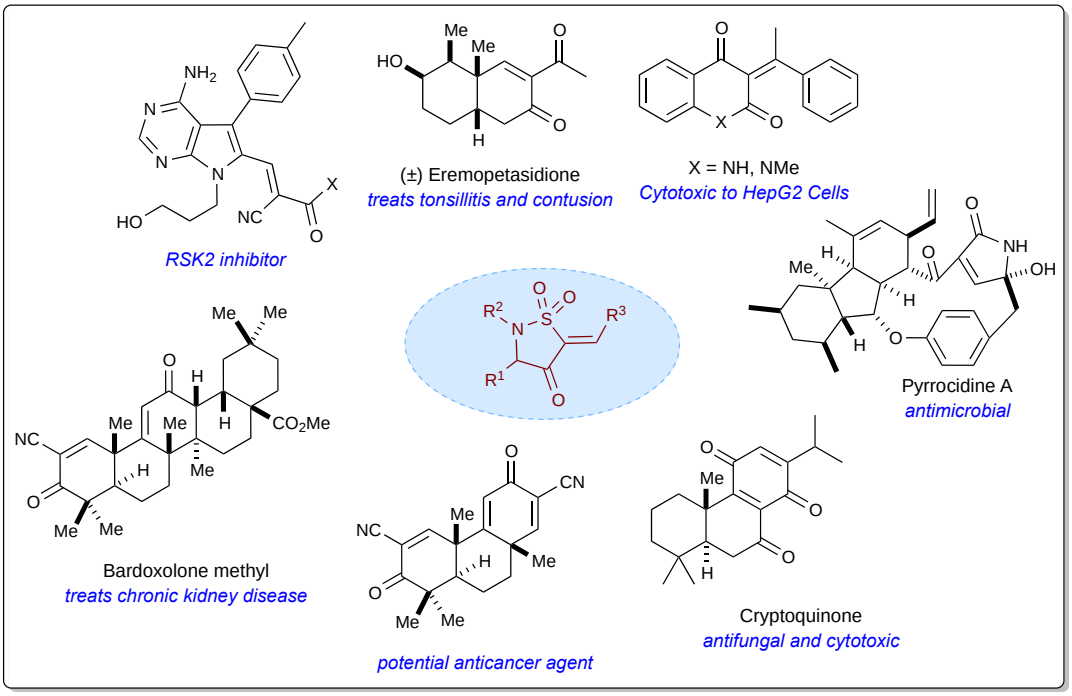

Figure 1.6: *Bioactive compounds having doubly activated Michael acceptors.*

Scifinder and PubChem database search of tetramic acids and their corresponding sultam analogs highlight that sultam analogs of tetramic acids are limited in the literature (Figure 1.7).[27] Although the number of reports of incorporation of the β-keto sultam moiety has increased over the last few years, collectively they are still limited when compared to their amide counterparts. Moreover, the reports of β-keto vinyl sultams are still relatively void, which when coupled with their aforementioned potential as novel electrophilic probes, has inspired our work in this area.

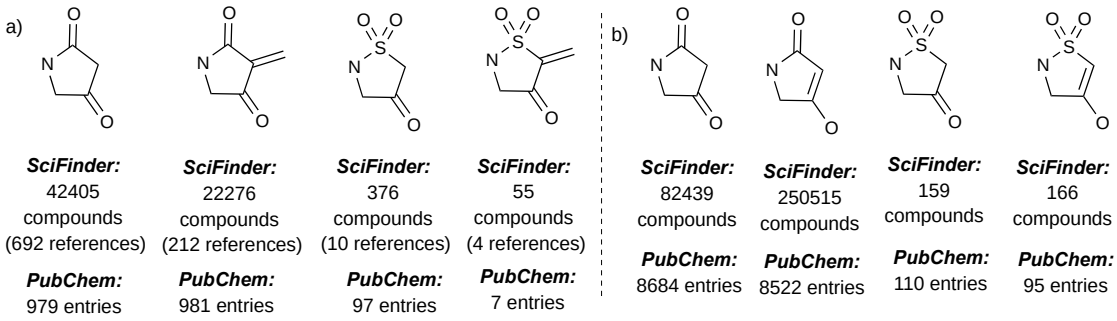

Figure 1.7: *SciFinder and PubChem substructure searches carried out on the following dates (a) 7-16-2018 and (b) 4-7-2015*

1.1.3 Tetramic acids: Representative known synthetic methods

Historically, several methods for the synthesis of the tetramic acid core have been reported, and have been extensively covered in two excellent reviews reported in 2008 and 2010.[28] Discussions of Dieckmann- and non-Dieckmann-derived tetramic acids, as well as derivatizations of the tetramic acid core, were covered in the dissertation of Moon Young Hur (PhD, 2015).[10] Additional relatively recent work in the construction of the tetramic acid core is discussed further below.

In 2010, Spatz and coworkers demonstrated the synthesis of the tetramic acid core using an Ugi–Dieckmann-reaction (Scheme 1.1).[29] The authors used isocyano methylcarbonate **1.1.4** as a cleavable isocyanate for the Ugi 4-component-coupling reaction.

The Ugi reaction was performed by the condensation of amine **1.1.1** and aldehyde/ketone **1.1.2** to generate an imine, which in due course reacted with acid **1.1.3** and isocyanate **1.1.4** to furnish amide **1.1.5**. Deprotonation of amide **1.1.5** with potassium *t*-butoxide initiates the Dieckmann-type cyclization of **1.1.6** by the enolized carboxylic acid to afford tetramic acid **1.1.7a** or **1.1.7b**, along with the oxazolidinone leaving group **1.1.8**.

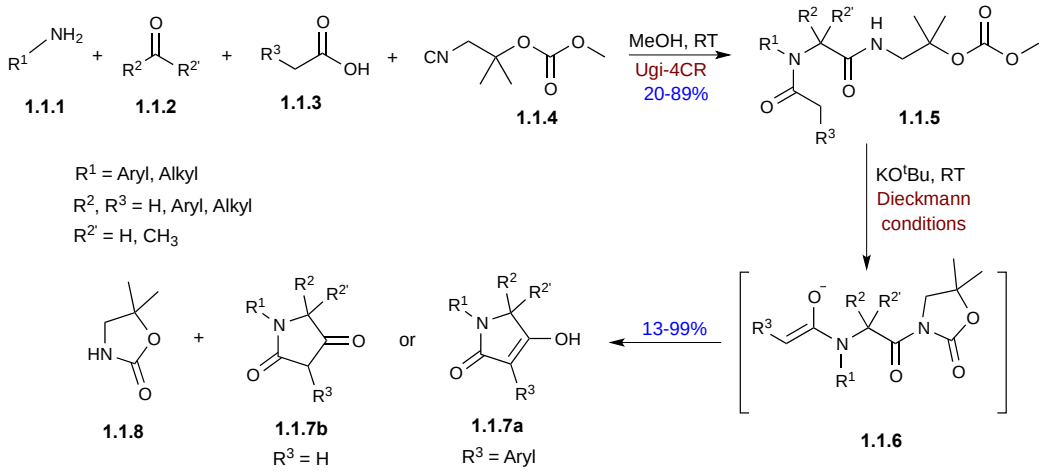

Scheme 1.1: *Synthesis of tetramic acid core by Ugi–Dieckmaan condensation method.*

In 2010, Sarpong and Marcus synthesized the tetracyclic core of tetrapetalone A using a reductive alkylation of pyrrole (Scheme 1.2).[30] En route to the synthesis, they constructed the tetramic acid core by alkylation of the ene-lactam moiety **1.2.1** using sequential treatment with LDA and MeI to yield **1.2.2**. Conjugate addition of boron pinacolato ester to **1.2.2**, followed by oxidation with sodium perborate, and Swern oxidation installed the tetramic acid moiety within **1.2.3**.

In 2010, Gu and Zakarian reported the synthesis of sintokamide A, and demonstrated the construction of the tetramic acid moiety (Scheme 1.3).[31] En route to the synthesis of sintokamide A, the authors performed methyl ester hydrolysis of dipeptide **1.3.1** to furnish a

carboxylic acid, which was coupled with Meldrum's acid using the Jouin procedure to generate **1.3.2**.[31] Intermediate **1.3.2** was next heated in the presence of MeCN, followed by addition of DEAD and PPh_3 to afford the tetramic acid derivative **1.3.3**.

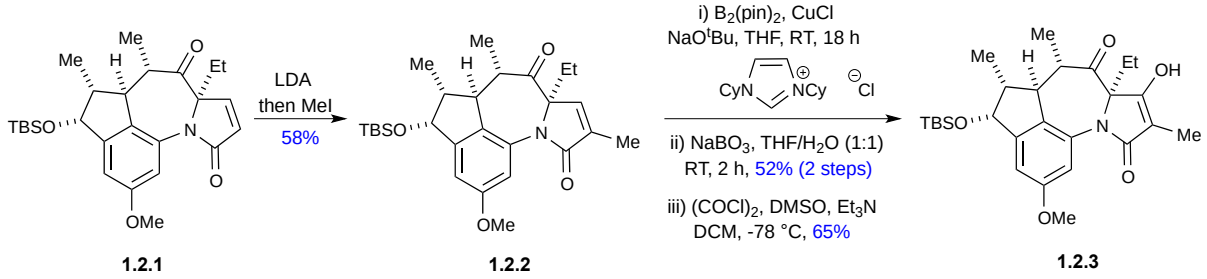

Scheme 1.2: *Construction of the tetramic acid core during the synthesis of tetrapetalone A.*

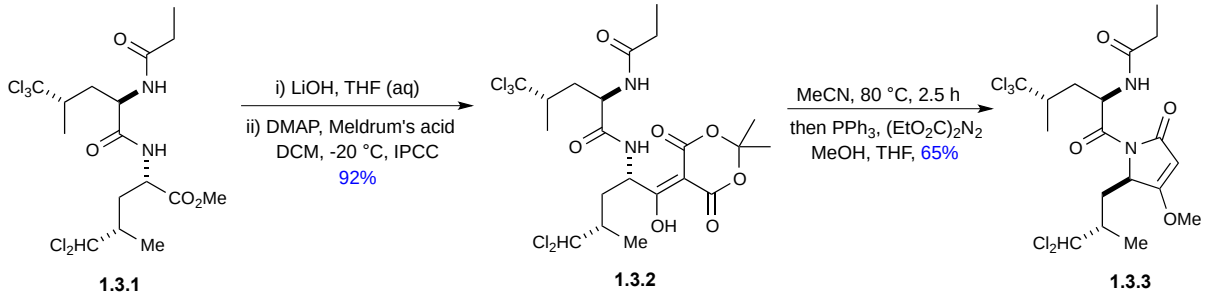

Scheme 1.3: *Construction of the tetramic acid core during the synthesis of sintokamide A.*

In 2012, Pettus and coworkers reported the synthesis of 3-methyl tetramic acid **1.4.3** using a SmI_2-promoted cyclization approach (Scheme 1.4).[32] The authors used amino acid ester **1.4.1** to generate amino acid derivative **1.4.2** by first protecting the amine with CbzCl and next reacting with 2-bromopropionyl bromide. Intermediate **1.4.2** was cyclized to tetramic acid **1.4.3** using SmI_2, in the presence of HMPA, with subsequent exposure of the reaction mixture to diazomethane. This method was applicable to a wide range of amino acids such as valine, proline, leucine, phenylalanine and alanine.

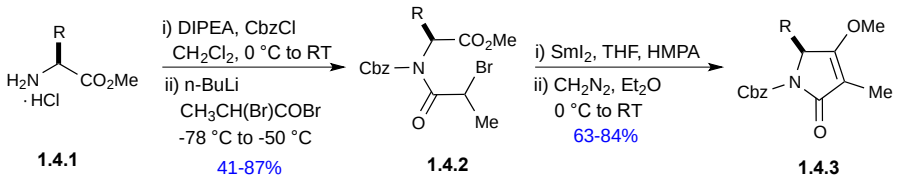

Scheme 1.4: *Construction of 3-methyl tetramic acid using SmI_2.*

In 2013, Gao and coworkers demonstrated the cyclization of TBS-protected *N*-methyl amino alcohol **1.5.3** during the synthesis of Equisetin (Scheme 1.15).[19d] The authors started the synthesis using (+)-citronellal **1.5.1,** and in several steps, converted it to alkene **1.5.2**. Subsequent protection afforded TBS-protected alcohol **1.5.3** in nine linear steps. Dieckmann cyclization of **1.5.3** in the presence of sodium methoxide and MeOH constructed the tetramic acid core of equisetin **1.5.4**.

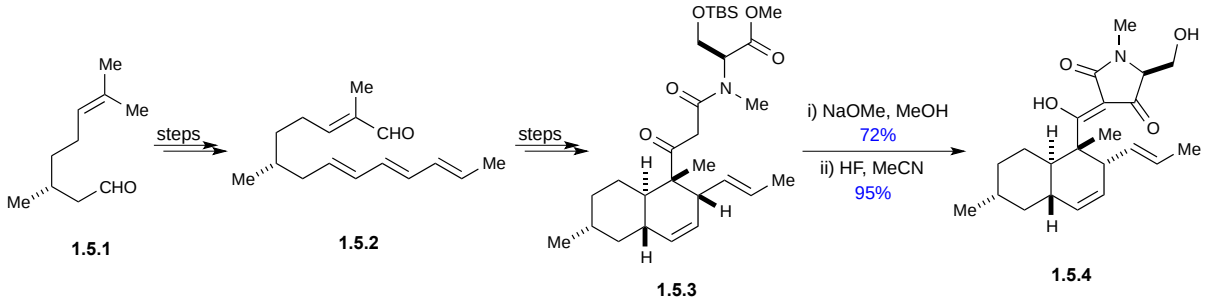

Scheme 1.5: *Tetramic acid core construction during the synthesis of Equisetin.*

In 2014, Wang and coworkers demonstrated the synthesis of pyrrolidine-diones (Scheme 1.16).[33] The authors coupled mono-ethyl malonate **1.6.1** and α-amino esters in the presence of EDC and DMAP to synthesize amide **1.6.2**. Subsequent cyclization using sodium methoxide (Na/MeOH) in the presence of toluene furnished 3-methoxycarbonyl tetramic acid **1.6.3**. Finally, pyrrolidine-2,4-dione **1.6.4** was obtained by refluxing **1.6.3** in a mixture of acetonitrile and water.

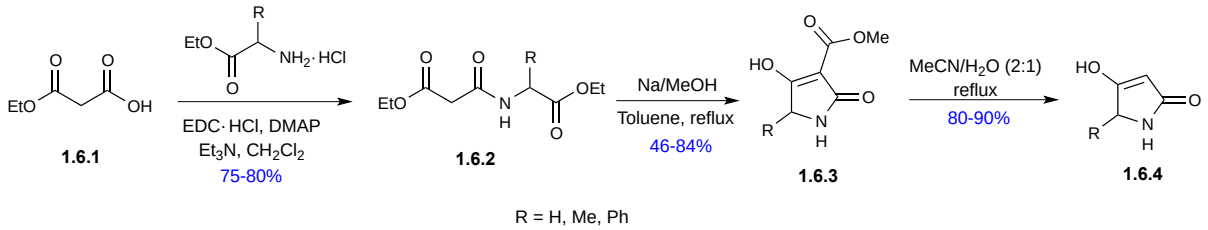

Scheme 1.6: *Synthesis of pyrrolidine-2,4-diones from mono-ethyl malonate.*

In 2014, Frontier and coworkers reported the total synthesis of tetrapetalone A-Me aglycon (Scheme 1.7).[34] During their total synthesis, the authors subjected alcohol **1.7.1** to the Ley TPAP-oxidation conditions to furnish the corresponding aldehyde, which was subsequently cyclized to produce tetracycle **1.7.2** using an intramolecular Baylis-Hillman cyclization with Stryker's reagent. Swern oxidation of **1.7.2** afforded the chlorinated tetramic acid tetracycle **1.7.3**.

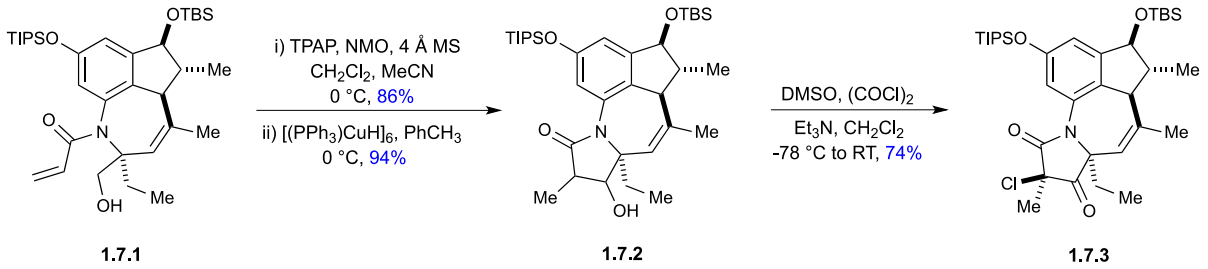

Scheme 1.7: *Construction of the tetramic acid core during the synthesis of tetrapetalone A.*

In 2015, Yamada and coworkers demonstrated the silver-catalyzed synthesis of several tetramic acid derivatives (Scheme 1.8).[35] The authors used readily available and cheap propargylic amines **1.8.1** and carbon dioxide as starting materials. The reaction lead to the formation of oxazolidinone **1.8.2**, which in the presence of DBU, underwent rearrangement to produce the corresponding tetramic acid **1.8.3**.

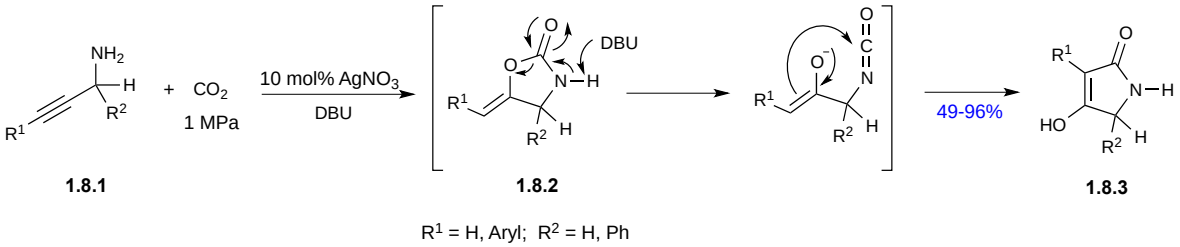

Scheme 1.8: *A one-pot synthesis of tetramic acids starting from propargyl amine.*

1.1.4 *β*-Keto sultams: Methods of synthesis

Sulfur analogs of tetramic acids, termed *β*-keto sultams, belong to an attractive chemotype class for probe and drug development due to the aforementioned bioisosteric equivalence of sulfonamides with corresponding amides.[36] Over past few decades, a number of classical synthesis of *β*-keto sultams has been reported, mostly using an intramolecular cyclization pathway, some representative synthetic strategies are discussed below.

Stachel and Drasch, in 1976, described the synthesis of sultams using an intramolecular CSIC reaction involving esters as the electrophilic component (Scheme 1.9).[37] The authors synthesized several substituted sulfonates and sulfonamides **1.9.1** and prepared respective *β*-keto sultone and sultams **1.9.2** in 30–60% yield using sodium methoxide as base in dry EtOH. Based on pKa analysis, it was revealed that most of the sultones and sultams existed in the enol form.

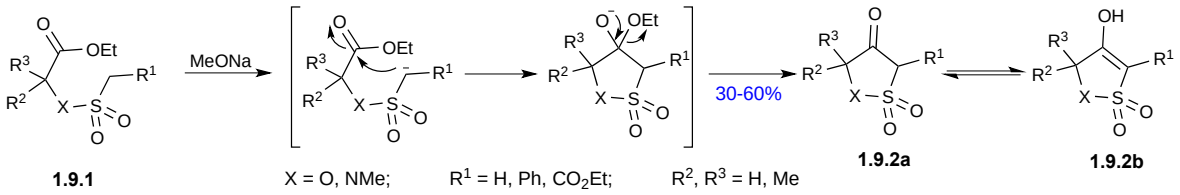

Scheme 1.9: *Synthesis of sultones and sultams involving ester electrophile.*

In 1966, Snader and coworkers demonstrated the synthesis of benzofused sultams during the synthesis of Sulfostyril (Scheme 1.10a).[38] The authors started their synthesis with sulfoacetic acid **1.10.1** and converted it to sulfoanilide **1.10.2** in three steps. Sulfoanilide was then hydrolyzed to acid and then cyclized to *β*-keto sultam **1.10.3** in the presence of polyphosphoric acid in excellent yield.

In 1996, Tornus and Schaumann synthesized a six-membered *β*-keto sultam using a novel Diels-Alder reaction (Scheme 1.10b).[39] The authors prepared the *N*-sulfonyl-alkyl-amines **1.10.5** *in situ* using the corresponding sulfamoyl chlorides **1.10.4**. A formal Diels-Alder reaction between dienophile **1.10.5** and diene **1.10.6** generated *β*-keto sultam **1.10.7**.

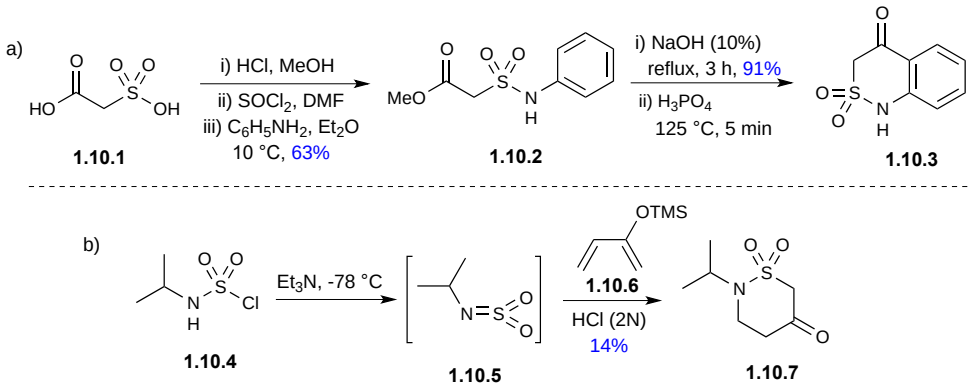

Scheme 1.10: *Synthesis of β-keto sultams*

Coppo and Fawzi in 1998, and Volovenko and coworkers in 2007, reported the synthesis of *N*-substituted benzofused *β*-keto sultams (Scheme 1.11).[40] The authors began the synthesis with 2-aminobenzoic acid methyl ester **1.11.1**, subsequent sulfonylation using methanesulfonyl chloride, followed by *N*-alkylation, generated aminobenzoates **1.11.2**. Dieckmann ring closure of **1.11.2** was achieved using NaH in DMF to afford sultam **1.11.3** in good to excellent yield.

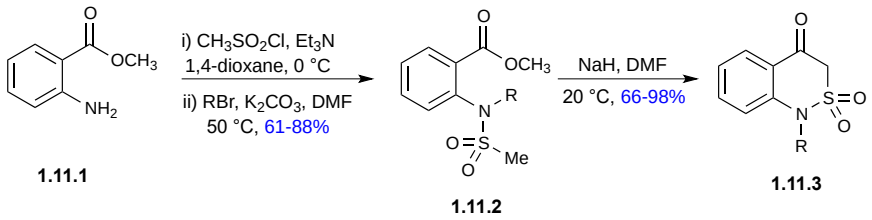

Scheme 1.11: *Synthesis of N-substituted benzofused β-keto sultams.*

In 2012, Tabarrini and coworkers demonstrated the synthesis of a unique subclass of *β*-keto sultams, namely, benzothiazine dioxide derivatives (Scheme 1.12).[41] The authors commenced the synthesis with bromoacetate **1.12.1** and reacted it with sodium sulfite, followed by treatment with PCl_5, to generate the corresponding sulfonyl chloride, which was subsequently treated with cyclopropyl amine to furnish sulfonamide **1.12.2**. The sulfonamide **1.12.2** was treated with substituted benzoyl chloride **1.12.3** to afford sultam intermediate **1.12.4**. The sultam intermediate was next converted to benzofused *β*-keto sultam **1.12.5** by *N*-methylpiperazine installation, nitro group reduction, and ester hydrolysis.

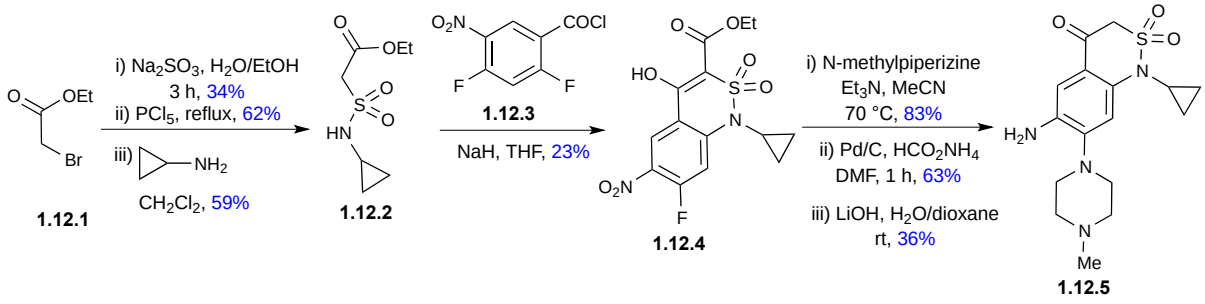

Scheme 1.12: *Synthesis of benzothiazine dioxide derivatives.*

1.1.5 Vinyl sultams and *β*-keto vinyl sultams: Methods of synthesis

There are several examples of the synthesis of vinyl sultams reported in the literature (Figure 1.8a) that will be outlined in the following pages.[42] Reports of the corresponding *β*-keto vinyl sultams are relatively rare to the best of our knowledge, as are reports of the

corresponding naturally occurring unsaturated tetramic acids of general structure **1.8.1** (Figure 1.8b).[43] Various acyclic vinyl sulfones, vinyl sulfonate, and vinyl sulfonamides (Figure 1.8c) have been reported as novel cysteine protease inhibitors[44] In 1992, Hanzlik and Liu carried out thiol reactivity screening for known targets, and discovered that vinyl sulfones are inhibitors of cysteine proteases in papain and parasitic cruzain.[44a] In 2001 and 2003, Roush[44b–d] reported that a series of vinyl sulfone, vinyl sulfonate and vinyl sulfonamide scaffolds were potent inhibitors of cruzain for the treatment of Chagas disease.

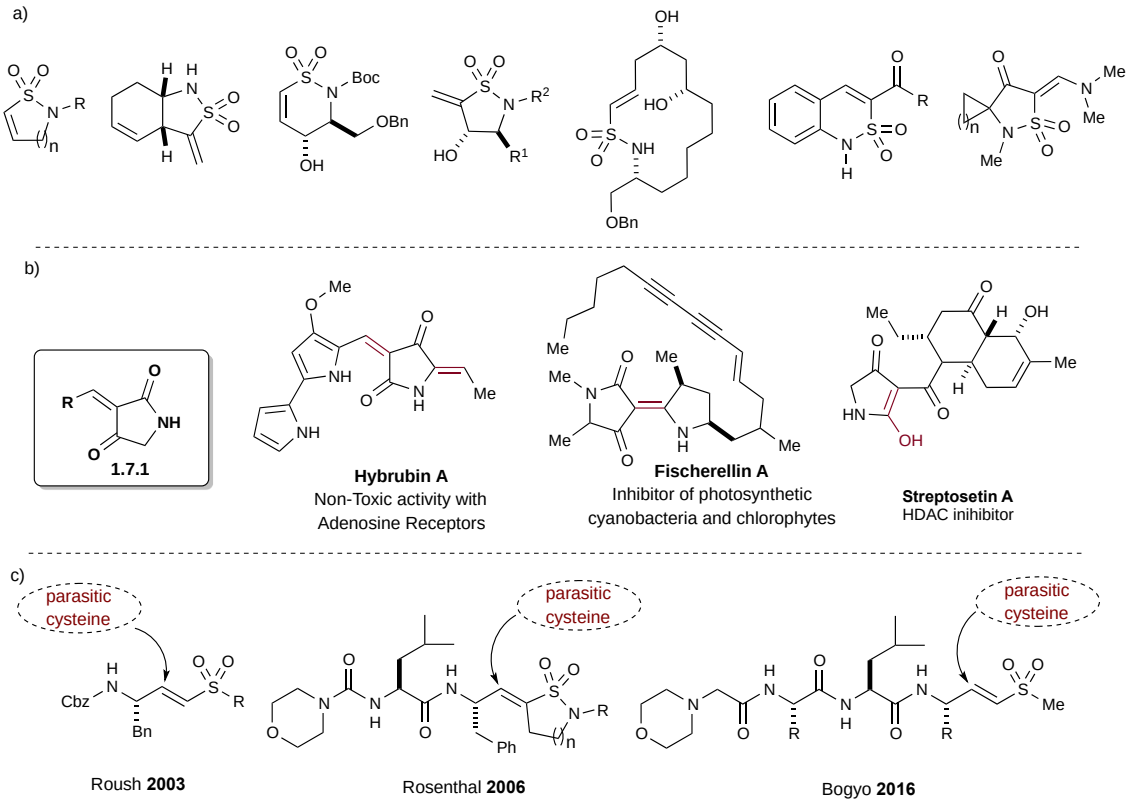

Figure 1.8: *β-Keto vinyl sultams, vinyl tetramic acids and acyclic vinyl sulfones, vinyl sulfonamides and vinyl sulfonates*.

In 2006, Rosenthal[44e] synthesized a dipeptide vinyl sultam that demonstrated mild selectivity against falcipain-2 over papain. In 2016, Bogyo[44f] reported a dipeptide vinyl sulfone as a cysteine protease inhibitor capable of killing the malarial parasite, *Plasmodium*

falciparum. These examples qualify unsaturated sultams to be an important moiety in the field of drug discovery. Some of the examples for the synthesis of unsaturated sultams are discussed below.In 1999, Hanson and coworkers reported the synthesis of vinyl sultams employing an RCM strategy (Scheme 1.13).[45] The authors synthesized vinyl sulfonamides **1.13.2** by the reaction of amines with vinyl chlorides **1.13.1**. The vinyl sulfonamides were next *N*-alkylated with 1-bromoalkene **1.13.3** to obtain diene **1.13.4**, which underwent RCM to afford vinyl sultams **1.13.5** in excellent yields. The vinyl sultams **1.13.7** underwent stereoselective Diels-Alder reaction with cyclopentadiene in the presence of Lewis acid catalyst to obtain tricyclic sulfonamides **1.13.8** (Scheme 1.13b).[46]

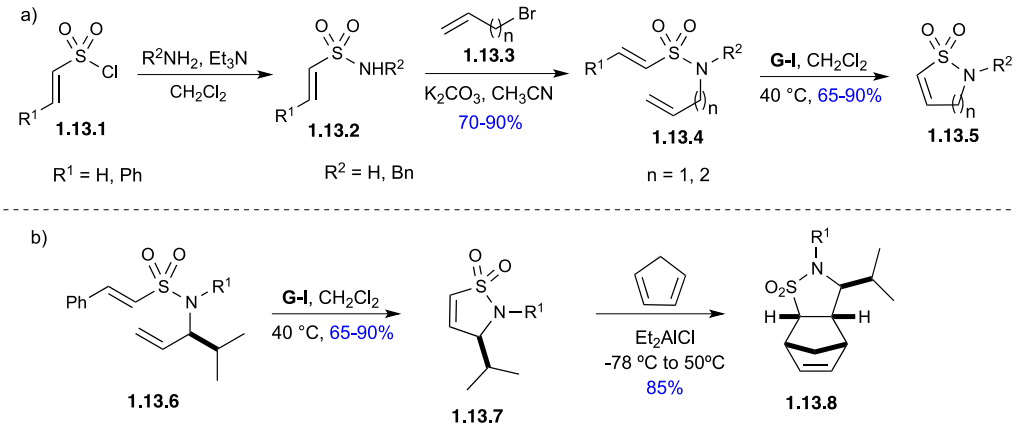

Scheme 1.13: *Synthesis of a) vinyl sultams and b) tricyclic sulfonamides.*

In 2003, Hanessian and coworkers demonstrated the synthesis of functionally diverse bicyclic sulfonamides (Scheme 1.14). [47] The authors commenced the reaction by deprotecting Boc-protected propenyl proline benzyl ester **1.14.1**, followed by the reaction with ethenesulfonyl chloride to afford the diene intermediate **1.14.2**, which under RCM conditions, yielded bicyclic vinyl sultams **1.14.3** in moderate yield.

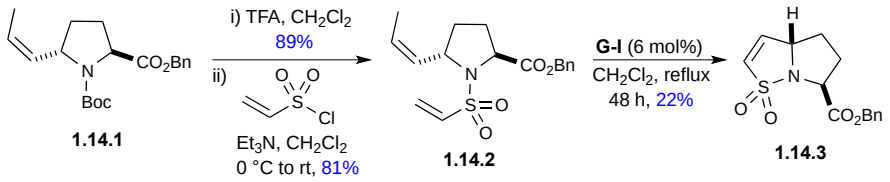

Scheme 1.14: *Synthesis of bicyclic sultams via RCM*

In 2005, Metz and coworkers demonstrated the synthesis of sultams via use of an intramolecular Heck reaction (Scheme 1.15).[48] The authors converted cyclic bromides **1.15.1** to amines **1.15.2**, which was next reacted with sulfonyl chloride **1.15.3** to afford the desired sulfonamides **1.15.4**. Intramolecular Heck reaction on sulfonamides **1.15.4** yielded bicyclic exo-vinyl sultams **1.15.5** in good yield.

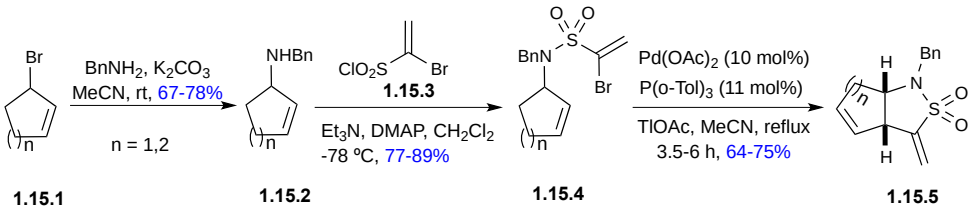

Scheme 1.15: *Synthesis of bicyclic exo-vinyl sultams via intramolecular Heck reaction*.

In 2008, Jimenez-Hopkins and Hanson reported a ring-closing metathesis (RCM) strategy for the synthesis of γ-hydroxy vinyl sultams (Scheme 1.16).[49] The authors started the synthesis with amination of allylsulfonyl chloride **1.16.1** followed by Boc-protection to afford sulfonamide **1.16.2**. Mitsunobu reaction on **1.16.2** with chiral, non-racemic alcohol **1.16.3**, obtained from corresponding glycidyl ether, furnished diene **1.16.4**. The sulfonamide **1.16.4** was cyclized using an RCM reaction and was next dihydroxylated, followed by conversion to the respective carbonate using phosgene. Final base-promoted elimination afforded the γ-hydroxy sultam **1.16.5**.

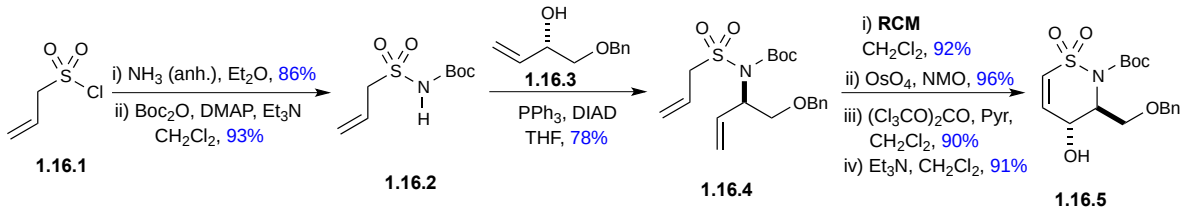

Scheme 1.16: *RCM strategy for the synthesis of γ-hydroxy vinyl sultams.*

In 2008, Zhou and Hanson developed intramolecular oxa-Michael and diastereoselective Baylis-Hillman reactions for the synthesis various sultam scaffolds (Scheme 1.17).[50] The authors commenced the synthesis with amino alcohols **1.17.1**, which were next TBS-protected, sulfonylated and *N*-alkylated to afford vinyl sulfonamides **1.17.2**. The intramolecular oxa-Michael reaction was initiated by TBS-deprotection of **1.17.2** to afford medium-sized sultams **1.17.3** in good yields. Similarly, TBS-deprotection of **1.17.2** using 10% HCl and conversion to the corresponding aldehyde *via* Dess–Martin oxidation, followed by Baylis-Hillman cyclization performed using DABCO, yielded a range of exo-vinyl sultams **1.17.4**.

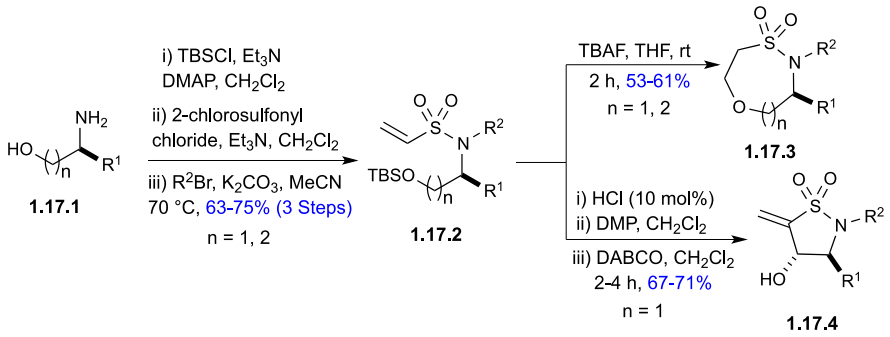

Scheme 1.17: *Synthesis of sultam via oxa-Michael and Baylis-Hillman reactions.*

In 2016, Hanson and coworkers reported one-pot sequential protocols for the synthesis of several novel macrocycles bearing α,β-chemotypes (Scheme 1.18).[42d] The authors began the synthesis by coupling phosphate triene **1.18.1** with cross-metathesis

partner **1.18.2** using RCM/CM/chemoselective hydrogenation protocol to afford phosphate triester **1.18.3**. Next, Pd-catalyzed, reductive allylic transposition and phosphate tether removal protocol provided 1,3-*anti*-diol **1.18.4**. MOM protection and TBS deprotection of alcohols in **1.18.4** yielded carbinol **1.18.5**. Mitsunobu reaction on **1.18.5** followed by reduction and sulfonylation afforded the sulfonamide **1.18.7**. The desired macrocyclic α,β-unsaturated sultam **1.18.8** was obtained by RCM of diene **1.18.7** followed by MOM-deprotection.

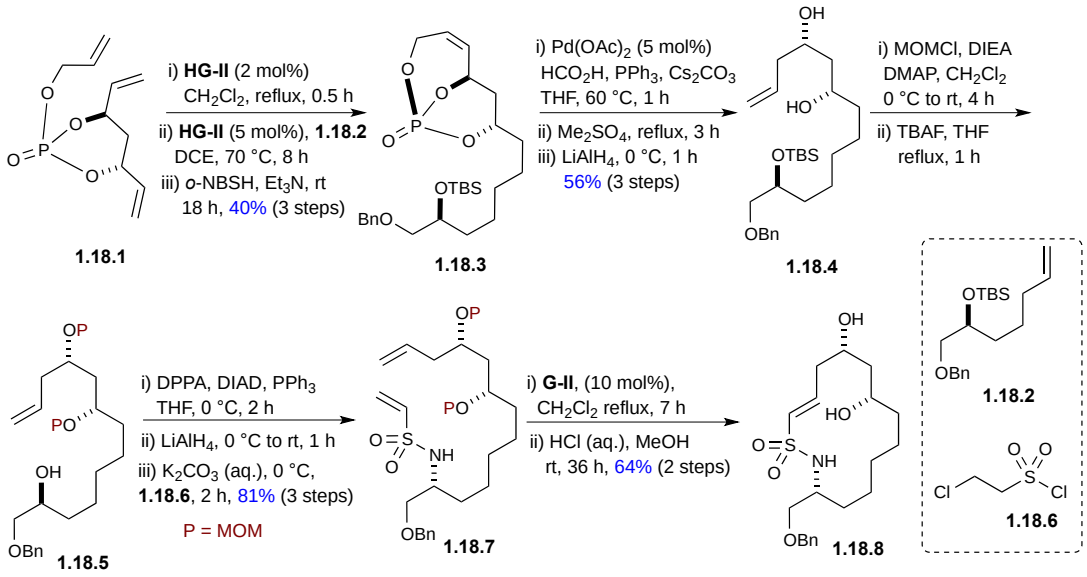

Scheme 1.18*: Synthesis of α,β-unsaturated sultam using one-pot sequential protocols.*

In 2017, Banerjee and coworkers reported the synthesis of fused vinyl sultams (Scheme 1.19).[51] The fused vinyl sultams **1.19.3** were synthesized by the reaction of pyrrole-2-carboxaldehydes **1.19.1** and arylmethanesulfonyl chloride **1.19.2** in the presence of sodium hydride in a one-pot tandem synthesis.

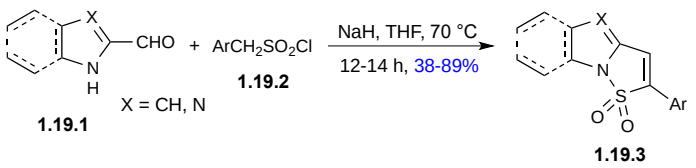

Scheme 1.19: *One-pot tandem synthesis of fused vinyl sultams.*

In 2017, Nguyen and Retailleau reported the atom-economical synthesis of a variety of benzofused sultams (Scheme 1.20).[52] The authors incorporated elemental sulfur into 2-nitrochalcones **1.20.1** in the presence of 3-picoline to synthesize benzofused sultam **1.20.2**. They were also able to derive the same product **1.20.2** using the *β*-hydroxy analogs of nitrochalcone **1.20.3** in a relatively lower yield.

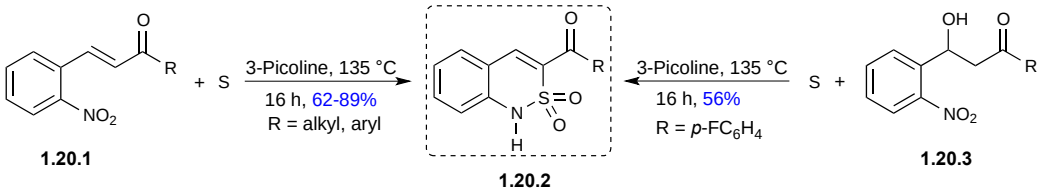

Scheme 1.20: *Atom-economical synthesis of benzofused sultams*.

In 2017, Volovenko and coworkers reported the synthesis of sultam analogs of tetramic acid using amino esters (Scheme 1.21).[53] The authors synthesized a series of tetramic acid sultam analogs using amino ester-containing cycloalkanes **1.21.1**. The amine was mesylated and *N*-alkylated to afford **1.21.2**. Sultam analog of tetramic acid **1.21.3** was obtained, when **1.21.2** was cyclized under sulfa-Dieckmann condition using KOtBu in DMF. The exo-vinyl sultam analog of tetramic acid **1.21.4** was obtained by treating **1.21.3** with DMF/DMA in MeOH under Knoevenagel conditions.

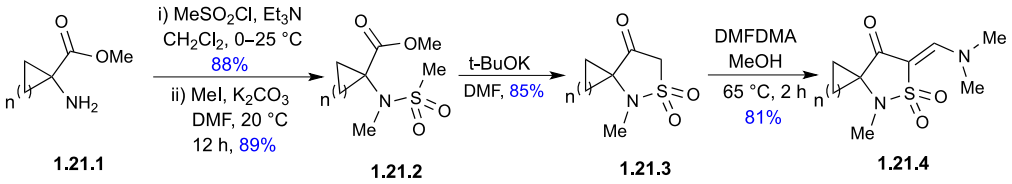

Scheme 1.21*: Synthesis of unsaturated sultam analog of tetramic acid.*

1.2 Results

Intrigued by the potent bioactivities of tetramic acid-containing natural products, sulfonamides and sultams, we began the design and synthesis of *β*-keto sultam analogs of tetramic acids. The key modification in the tetramic acid moiety is the replacement of the amide group (-NH-CO-) with a sulfonamide group (-NH-SO_2-). The synthesis of sultams has been reviewed in 2011, 2013 and recently in 2018.[54] Our lab has a long history in the development of several different methods for the facile synthesis of diverse *S*-heterocycles and sultam compounds.[55] Among these, highlights include, (i) a number of transition metal-catalyzed approaches using RCM, (ii) "click-click-cyclize", (iii) complementary pairing (CP) and complementary ambiphile pairing (CAP) strategies, and (iv) reagent-based diversity-oriented synthesis (DOS). The click-click-cyclize strategy has been explored for the synthesis of skeletally diverse sultams via functional group pairing between vinyl sulfonamides linchpins and an array of functional groups.

In 2015, Moon Young reported new syntheses of β-keto sultam analogs of tetramic acid involving acyclic and cyclic amino esters (PhD Thesis, 2015), as well derivatization chemistry.[10] This thesis aims to extend on the body of work on *β*-keto sultams and targets unsaturated sultam analogs, namely *β*-keto vinyl sultams, which can be modulated electronically, sterically and stereochemically. These unique *S*-containing electrophiles will

be assessed as molecular probes in order to assist in targeting rare protein residues and shallow binding sites to alleviate or eliminate drug resistance, mutation, and toxicity.[56] Reactivity profiling studies using ^{19}F–NMR are being conducted to monitor the rate at which the unsaturated sultams react with cysteine residue and hence give an idea of ranking them with several other known electrophilic probes, which will test our above mentioned hypothesis on the unsaturated sultams. Our ultimate goal is to use these chemotypes in activity–based protein profiling (ABPP) studies.

Previously, we have reported the synthesis of unsaturated sultam analogs of tetramic acids using a strategy we term 'click-click-cyclize'.[55e] This concept, a variant of build-couple-pair (BCP)[57] utilizes two simple click reactions as defined by Sharpless[58] namely *N*-sulfonylation and *N*-alkylation, followed by a cyclization event, to construct core sultam subunits. In this thesis, a variety of *β*-keto vinyl sultam analogs of tetramic acids have been targeted using a modular method employing (i) simple *N*-mesylation, followed by (ii) *N*-sulfonamide alkylation under mild conditions, (iii) Dieckmann-type cyclization and a (iv) simple Knoevenagel condensation reaction with a range of aldehydes (Figure 1.9). Chapter 2 aims to embed the *β*-keto vinyl sultam moiety in a macrocyclic framework.

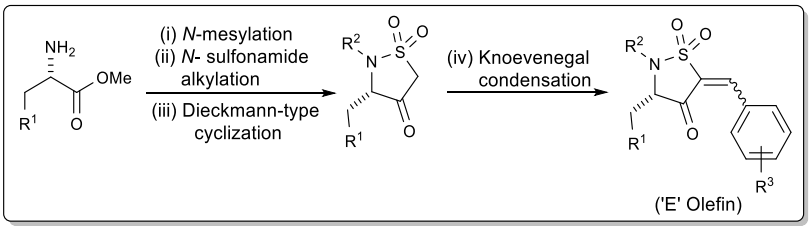

Figure 1.9: *Synthetic strategy for the synthesis of unsaturated sultams*

1.2.1 Synthetic design of β-keto vinyl sultam analogs of tetramic acids

As highlighted in Figure 1.10, we are implementing a simple 'click–click–cyclize' strategy utilizing amino acids, methane sulfonyl chloride and benzyl bromides that will be attenuated electronically, sterically, and stereochemically. Attention to the enol-keto tautomerization equilibrium will also be sought with the employment of functionality and ring size expansion. The targeted sultam analogs of tetramic acids can be readily converted to structurally diverse β-keto vinyl sultam analogs (**1.10-A**, **1.10-D**) by reacting with an array of aldehydes, carboxylic acids while enolic-type unsaturated sultams (**1.10-B**, **1.10-C**) can be obtained by reacting with alkylisocynate and alkyl halides.

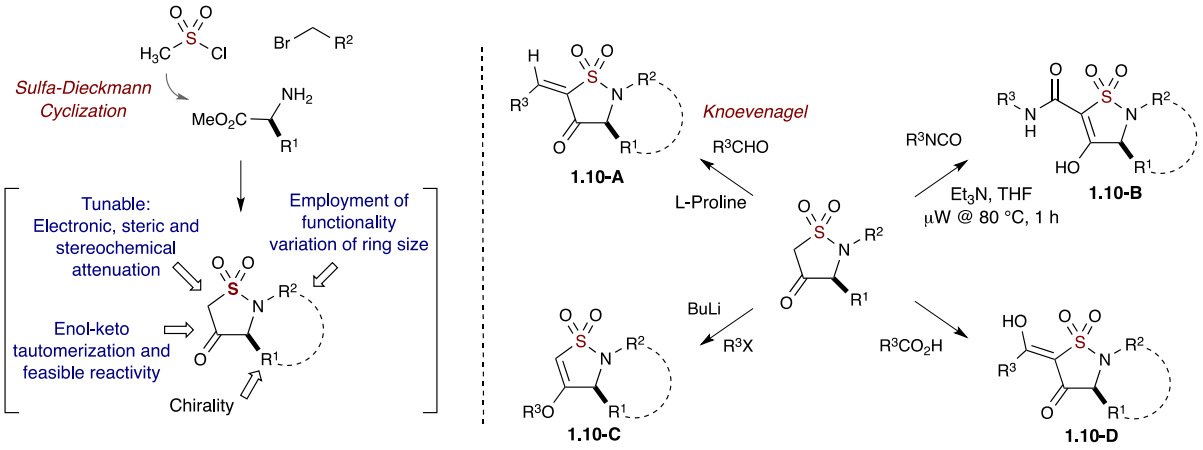

Figure 1.10: *Synthetic design for unsaturated sultams.*

1.2.2 Synthesis of β-keto vinyl sultam analogs of tetramic acids

We started this project using an array of amino acids, namely, valine, leucine, isoleucine, phenylalanine and 4-nitro phenylalanine. This thesis chapter is specific to phenylalanine and 4-nitro phenylalanine. Thus, amino acid **1.22.1** was esterified using thionyl chloride in the presence of MeOH at 60 ˚C (Scheme 1.22). After 6 h, MeOH was removed via reduced pressure evaporation and the reaction mixture was dissolved in dry

CH_2Cl_2. The crude reaction mixture was subjected to mesylation using MsCl/Et_3N, to generate the mesylated amino ester **1.22.3**. The reaction was completed in 6 to 8 hours with excellent yields of 85–90% over two steps. Subsequent benzylation furnished *N*-benzylated amino ester **1.22.4**. To carry out this reaction, the amino ester was dissolved in dry acetonitrile and was refluxed with benzyl bromide in the presence of K_2CO_3. The acyclic intermediate **1.22.4** was then cyclized under Dieckmann-like condition to afford the *β*-keto sultam **1.22.5**. This crucial cyclization was optimized using LiHMDS in dry THF at low temperature. Several runs demonstrated that dry solvent was a very important requirement for this reaction, as the presence of moisture in the reaction mixture resulted in no reaction, leaving behind unreacted starting material.

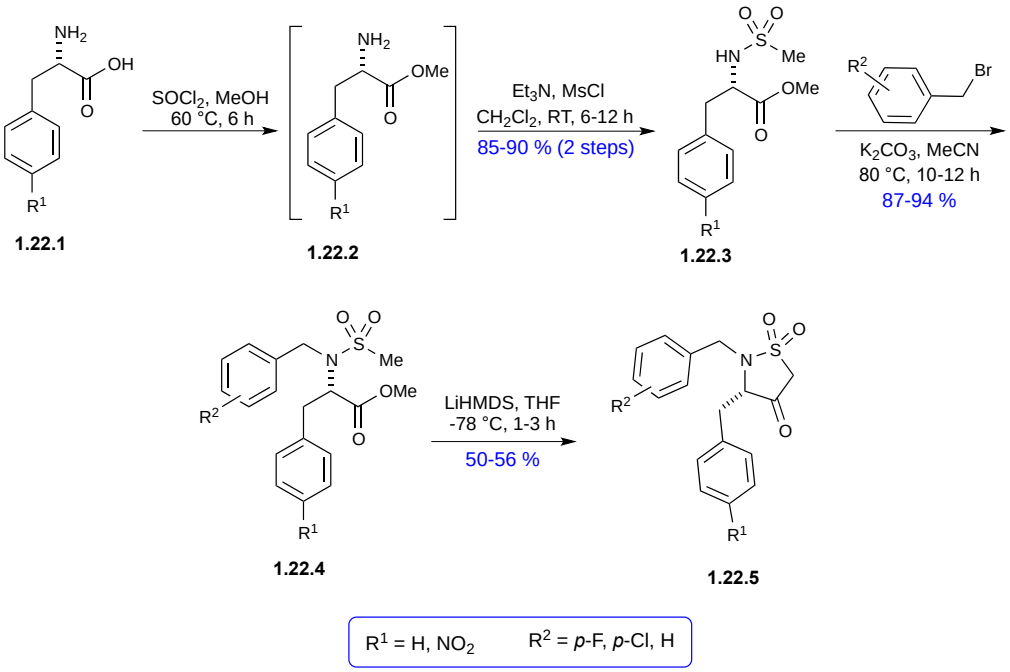

Scheme 1.22: *Synthesis of β-keto sultam analogs of tetramic acids.*

Tetramic acids can exhibit keto-enol tautomerization. There are several literature examples indicating the keto-form as the predominant tautomer in a tetramic acid.[59]

However, in 1984, Rooney and coworkers reported the predominance of the enol-form in diketo-sultam **1.11-A** (Figure 1.12a), which was verified by ^{13}C NMR in Me_2CO-d_6 and solid-state IR studies.[60] Stachel and Drasch reported predominance of the enol-form in sultams **1.11-B** (Figure 1.12b), which was verified by both pKa and IR studies.[61] In 2009, Jeong and Moloney reported the tautomeric behavior of the tetramic acid **1.11-C** in solution along with computational calculations, and mentioned the characteristic ^{13}C NMR chemical shift for both the keto and enol-forms of tetramic acid **1.11-C** (Figure 1.12C).[62]

We have observed the methylene protons at the C5 position (Figure 1.12d) in the ^1H NMR spectra in $CDCl_3$ for the *β*-keto sultam analogs **1.11-D**. In the NMR of **1.11-D**, the ^{13}C carbon resonance at C5 appears between 195.1–206.1 ppm and also lacks the expected sp^2-CH resonance at 170–175 ppm for the enol tautomer. The keto-form is further verified by

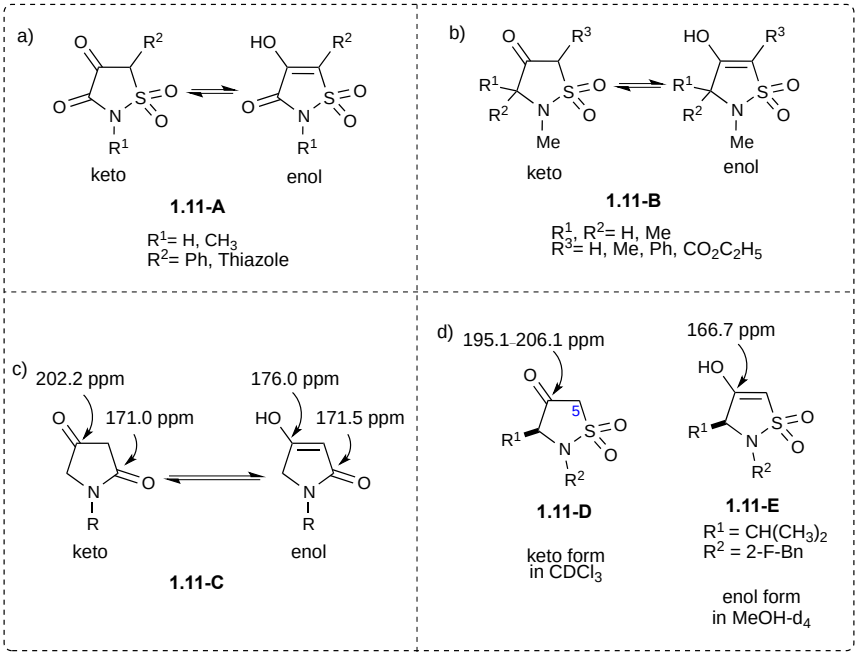

Figure 1.11. *Keto-enol tautomerism of in tetramic acid and β-keto-sultam analogs of tetramic acids a) and b) literature precedence c) characteristics ^{13}C-NMR chemical shift for tetramic acid d) our observation of ^{13}C-NMR chemical shift on β-keto sultam analogs of tetramic acids.*

the carbonyl absorption (1748-1767 cm^{-1}) in the IR spectrum without any detection of the hydroxyl absorption. However, when MeOH-*d4* was used as the NMR solvent we also observed an additional ^{13}C carbon resonance for C5 at 166.7 ppm for the *β*-keto sultam **1.12-E**, suggesting the enol tautomer. From ^{1}H NMR analysis, the enol-tautomer in MeOH-d_4 was found to be ~ 21–25%. Additionally, two peaks at -64.00 and -64.05 ppm in the ^{19}F NMR spectrum in MeOH-d_4 provides additional evidence for the enol-keto tautomerization in MeOH.

1.2.3 Knoevenagel condensation to unsaturated tetramic acids

With the *β*-keto sultam analogs in hand, efforts focused on the generation of β-keto vinyl sultam analogs, utilizing literature precedent employing Knoevenagel condensations with a set of aromatic aldehydes. The Knoevenagel condensation,[63] described by Emil Knoevenagel, is a classic organic synthesis reaction in which an active hydrogen compound (nucleophile) undergoes nucleophilic addition with an aldehyde or ketone in the presence of a basic catalyst, to form a C–C bond (Figure 1.12). The reaction normally undergoes spontaneous dehydration to generate an unsaturated product.

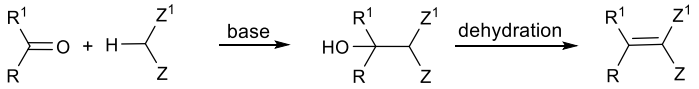

Figure 1.12: *General scheme of Knoevenagel condensation.*

Some notable examples of the Knoevenagel condensation carried on tetramic acids related to our work are mentioned below. In 2002, Saudi and coworkers demonstrated a Knoevenagel condensation on tetramic acid **1.23.1** (Scheme 1.23).[64] The authors used the reaction of 1,5-diphenylpyrrolidine-2,4-dione **1.23.1** with several carbonyl compounds,

whereby they reported the Knoevenagel condensation with a range of carbonyl compounds in acidic medium to afford unsaturated tetramic acid **1.23.5**. **1.23.1** when reacted with isatin **1.23.2** in acidic medium, a Knoevenagel condensation product **1.23.3** was formed. The same reaction in alkaline medium produced the 4-quinoline carboxylic acid derivative **1.23.4**. In contrast, amines react with **1.23.1** to yield 4-substituted amino pyrroline-2-ones **1.23.6**.

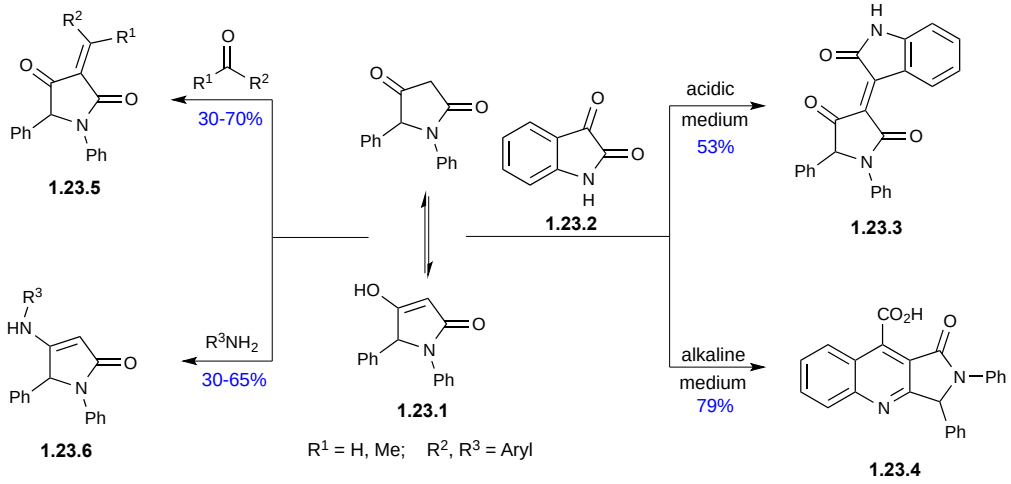

Scheme 1.23*: Reactions of tetramic acid with carbonyl compounds and amines.*

In 2011, Beyer and coworkers reported the asymmetric total synthesis of the indole alkaloid cyclopiazonic acid (Scheme 1.24).[65] En route towards their synthesis, the authors prepared chiral indole-ester derivative **1.24.1**, which underwent cationic cyclization in the presence of triflic acid to form the 5-membered ring of pyrrolidine **1.24.2** simultaneously in a 1:1 diastereomeric ratio. The next synthetic step was a mercaptomethanol-mediated denosylation and construction of the tetramic acid core using acetyl-Meldrum's acid (AMA), to afford the *N*-protected cyclopiazonic acid **1.24.3** in an overall one-pot process.

In 2014, Sengoku and coworkers demonstrated that phenylalanine-derived tetramic acid **1.25.1**, when treated with acetone or sterically hindered 9-anthraldehyde, leads to the

formation of corresponding ene-dione **1.25.2** in excellent yield (Scheme 1.25).[66] The authors demonstrated that such a reaction was only possible with ketones and hindered aldehydes in the presence of L-proline as catalyst. Unhindered aldehydes produced the dimerized product **1.25.3.** Use of base catalysts such as piperidine, pyrrolidine, L-serine, L-lysine and L-aspartic acid also failed to produce the desired Knoevenagel condensation product.

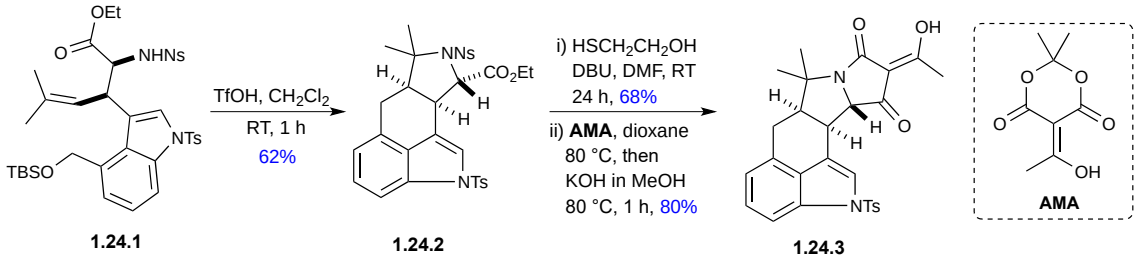

Scheme 1.24*: Asymmetric synthesis of cyclopiazonic acid*

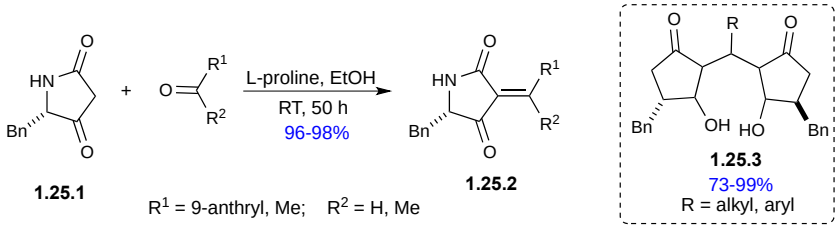

Scheme 1.25: *Knoevenagel condensation between tetramic acid and carbonyl compounds.*

In 2012, Sengoku and coworkers demonstrated the synthesis of tetramic acids **1.26.2** using condensation-decarboxylation reactions starting from *N*-protected amino acids **1.26.1** (Scheme 1.26).[67] The tetramic acids **1.26.2** were then condensed with a carboxylic acid in the presence of EDCI and DMAP to provide 4-*O*-acetyltetramic acid **1.26.3**, which underwent 1,3-acyl transfer to afford the 3-acyl tetramic acid **1.26.4**. In this work, the authors used a rearrangement reaction rather than a Knoevenagel condensation reaction to synthesize 3-acyl tetramic acids. Similarly, in 2005, Piric and coworkers reported the synthesis of tetramic

acid **1.26.2**. The authors further reacted **1.26.2** with DMF/DMA in the presence of CH_2Cl_2 to synthesize unsaturated tetramic acid **1.26.5** employing the Knoevenagel condensation (Scheme 1.26).[68]

In 2017, Volovenko and coworkers reported use of a Knoevenagel condensation of the β-keto sultam analog of the tetramic acid previously described in Scheme 1.21.[53] The authors synthesized β-keto vinyl sultams **1.13-A** from β-keto sultams **1.13-B** using DMF/DMA in MeOH under Knoevenagel condition (Figure 1.13a).

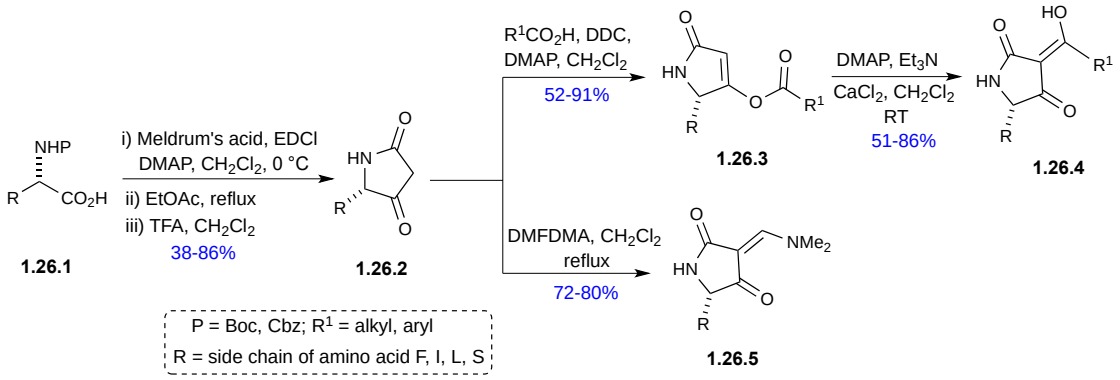

Scheme 1.26*: Synthesis of 3-substituted tetramic acid.*

The above discussion reveals that the common method for Knoevenagel condensation is the use of bases such as proline, piperidine, Et_3N, in polar protic solvents such as EtOH. Unfortunately, most of the sultam analogs of tetramic acid failed to deliver the desired condensation product under these conditions. The only reaction that was successful using these conditions was between the valine-derived β-keto sultam with piperonal, yielding 56% of the desired product (Figure 1.13b). Regrettably, we were not able to reproduce similar types of result with other amino acid-derived β-keto sultams and various aldehydes.

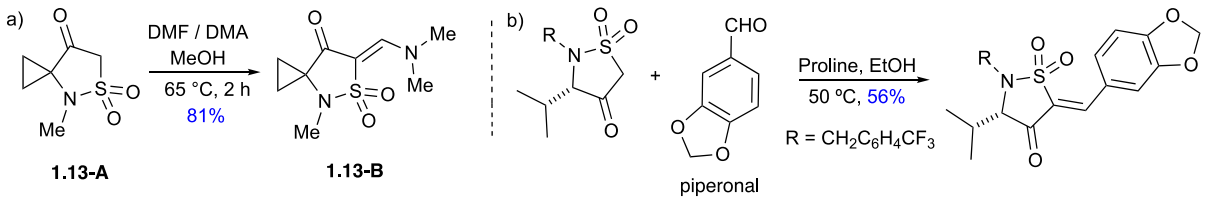

Figure 1.13: *Knoevenagel condensation with β-keto sultam*

In studies attempting to find suitable conditions for the Knoevenagel condensation that will be applicable for a wide range of tetramic acid analogs and aldehydes, we screened several bases, catalysts, solvents and temperature conditions. The list of several conditions is mentioned in Table 1. Several bases were tested, including proline, piperidine, Et_3N, diisopropylethyl amine (Hunig's base), and DBU. In addition, the Lewis acids $InCl_3$ and $TiCl_4$ were also screened for the reaction. Two different temperature conditions i.e. room temperature and 50 ˚C were maintained for the reaction. Polar solvents like THF, EtOH, and CH_3CN were considered for the reaction. None of the above-mentioned reagents, solvents and catalyst was helpful for the desired product formation. After initial failure of the condensation step, a more thorough literature search revealed the use of trifluoroethanol (TFE) by several laboratories as the solvent of choice in a range of condensation and multicomponent reactions.[69] We felt that TFE being a polar solvent with high ionizing capability and low nucleophilicity, should be an effective solvent for our condensation reaction condition. Gratifyingly, use of TFE in the presence of L-proline as catalyst at 50 ˚C, we were able to condense the sultam analog of tetramic acid **1.22.5** with several aromatic aldehydes (R^3CHO) such as benzaldehyde, 4-fluoro benzaldehyde, p-anisaldehyde, piperonal, and 4-fluorocinnamaldehyde to afford the desired β-keto vinyl sultams of general structure **1.27.1** (Scheme 1.27). Following this protocol, a small library of **1.27.1** analogs has been synthesized, and summarized in Table 2.

Table 1*: Conditions for Knoevenagel condensation*

SN	*Base*	*Catalyst*	*Temp. (˚C)*	*Solvent*	*Observation*
1	-	Proline	50	EtOH	Decomposition of starting material
2	-	Piperidine	50	EtOH	Decomposition of starting material
3	-	Piperidine	50	THF	Decomposition of starting material
4	-	Piperidine	RT	THF	Decomposition of starting material
5	-	Piperidine	RT	MeCN	Decomposition of starting material
6	TEA	-	Microwave	MeCN	Decomposition of starting material
7	TEA	NaI/TMSOTf[a]	RT	MeCN	Decomposition of starting material
8	-	$InCl_3/Ac_2O$[a]	RT	THF	Decomposition of starting material
9	TEA	$TiCl_4$	-78	THF	Decomposition of starting material
10	DIPEA	$TiCl_4$	-78	THF	Decomposition of starting material
11	DBU	$TiCl_4$	-78	THF	Decomposition of starting material
12	-	Proline	50	CF_3CH_2OH	Reaction occurred

a = used in stoichiometric amount as a reagent.

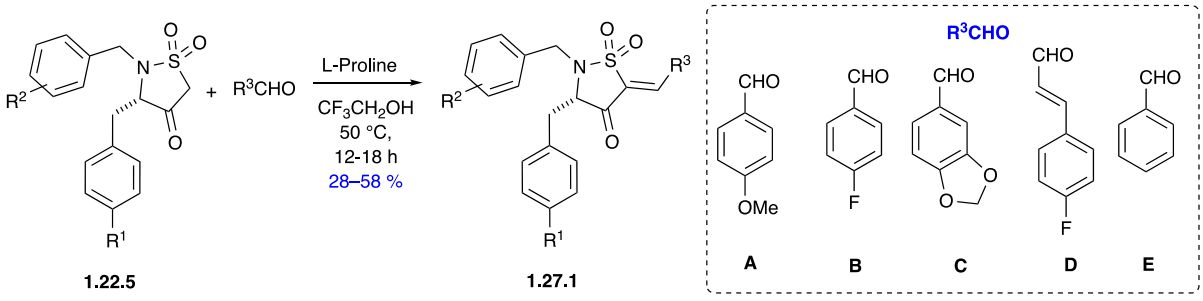

Scheme 1.27: *Synthesis of β-keto-vinyl sultam analog of tetramic acid.*

An analysis of the Knoevenagel condensation products reveals that electron donating groups on the aldehyde component enhances the yield of the product (reaction involving aldehyde

A), whereas electron withdrawing effect (reaction involving aldehyde **B**), decreases the yield. Introduction of substituents to the aldehyde had little effect in the overall yield of the product (reaction involving aldehyde **C**).

In the course of this work, efforts to generate macrocyclic isomers through an RCM approach revealed that our originally desired target possessing an *E*-configured olefin geometry, which we sought in the Knoevenagel strategy, actually produced the *Z*-configured olefin, as revealed by X-ray crystal structure (Figure 1.14).

Table 2: *β-Keto vinyl sultam of tetramic acids.*

Entry	***R^1***	***R^2***	***R^3CHO***	***Yield (%)***	***Entry***	***R^1***	***R^2***	***R^3CHO***	***Yield (%)***
1	H	H	A	***54***	10	NO_2	H	B	***45***
2	H	F	A	***50***	11	NO_2	F	C	***58***
3	H	Cl	A	***49***	12	NO_2	Cl	C	***52***
4	NO_2	H	A	***57***	13	H	Cl	C	***44***
5	NO_2	F	A	***57***	14	H	F	C	***41***
6	NO_2	Cl	B	***40***	15	NO_2	Cl	C	***51***
7	H	H	B	***47***	16	NO_2	H	D	***51***
8	H	F	B	***28***	17	NO_2	F	D	***55***
9	H	Cl	B	***43***	18	H	Cl	E	***42***

In order to further assess this result, we compared the ^{1}H NMR chemical shift of the vinyl proton within *β*-keto vinyl sultams analogs **1.15-A**, **B** and **C**, and the literature reported spirocyclic vinyl sultam **1.15-D** (Figure 1.15). The chemical shift for the vinylic proton of all three *β*-keto vinyl sultams analogs **1.15-A**, and **B** fall in the range of 7.72–7.85 ppm and all

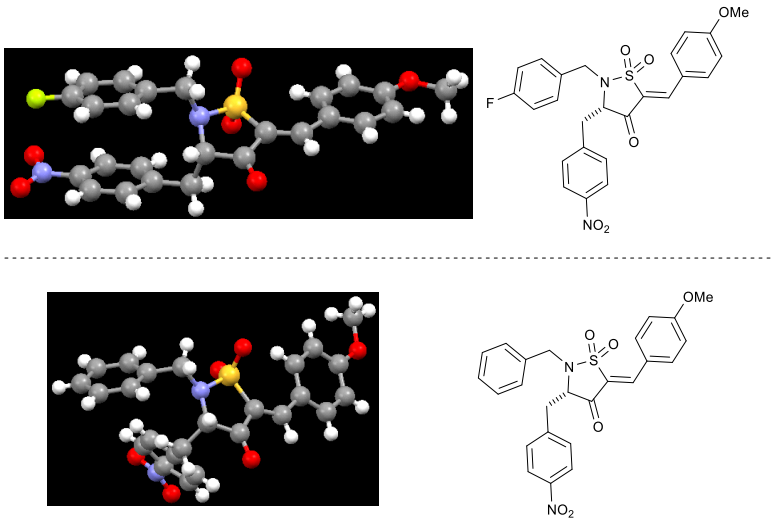

Figure 1.14: X-ray *structure of the exo-vinyl sultam analog of tetramic acid.*

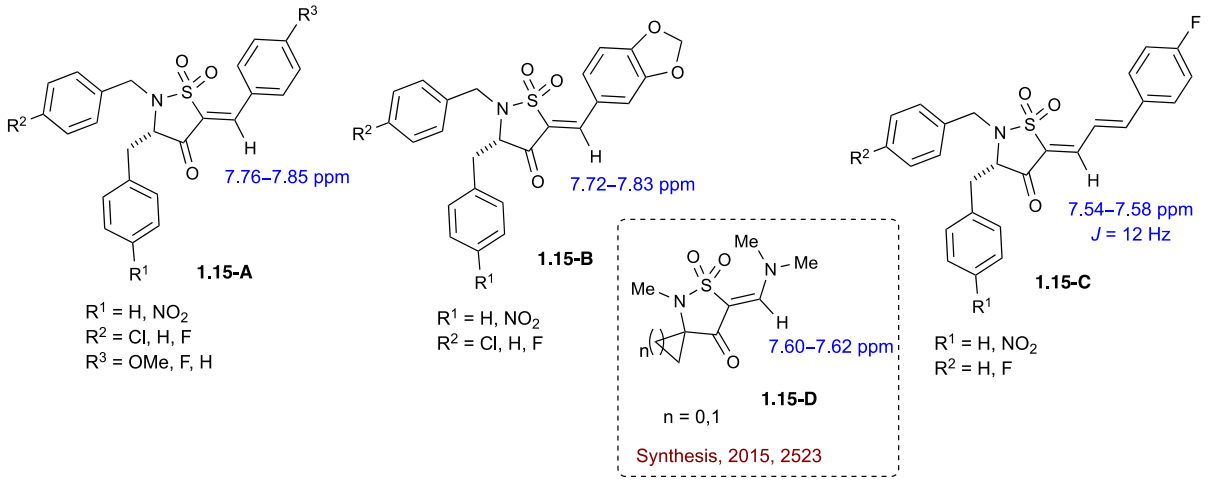

Figure 1.15: *Chemical shift of vinylic protons of β-keto vinyl sultams.*

appear as a singlet. The *β*-keto vinyl sultams **1.15-C** (possessing styrene substitution) has doublet splitting for the vinylic proton with a coupling constant of 12.0 Hz. Volovenkoa and coworkers synthesized the spirocyclic *β*-keto vinyl sultam **1.15–D** and reported the chemical shift of the vinylic proton to be in the7.60–7.62 ppm.[53] Collectively, the chemical shifts of the vinylic protons provide additional evidence for the *Z*-configured isomers of the *β*-keto vinyl sultam analogs **1.15- A**, **B** and **C**.

Although, we succeeded in the Knoevenagel condensation of aromatic aldehydes with the amino acid-derived *β*-keto sultams, the yields are moderate, ranging from 28–56%. We still seek more optimized conditions using TFE as a solvent. Also, suitable conditions for the condensation of aliphatic aldehydes should be analyzed as we were unable to link aliphatic aldehydes to tetramic acid analogs.

1.2.4 Reactivity profiling of *β*-keto vinyl sultams using fluorine NMR.

With the *β*-keto vinyl sultam analogs in hand, we have begun initial investigations involving reactivity profiling with thiols and cysteine residues to establish reactivity patterns in order to provide emperical data for their concurrent use as electrophilic probes in activity-based protein profiling (ABPP) investigations in the laboratories of our collaborators. ABPP is a technology to broadly assess reactive protein functionality and aid in the identification and mapping of ligandable hotspots in whole proteomes and allow pharmacological interrogation of difficult targets.[70]

Recently, chemical biology ABPP studies have been augmented by a number of thiol reactivity studies in order to identify and rank reactivity trends among chemotypes, and are a "natural fit" for prescreening electrophilic covalent modifiers (CMs) for ABPP studies (Figure 1.16). In 2003, Roush and coworkers[44a-d] carried out thiol reactivity studies related to the inhibition of cysteine proteases papain and parasitic cruzain using vinyl sulfones, sulfonates, sulfonamides and their derivatives of general structure **1.16a**. This study was further substantiated by Rosenthal in 2006-using exo-vinyl sultams **1.16-b**,[44e] Love in 2016-using arylvinyl sulfones **1.16-c** and alkynamides **1.16-d**,[71] and Bogyo in 2016-using peptidic vinylsulfones **1.16-e**.[44f] Studies involving hetero-Michael additions into α,β-unsaturated carbonyl systems were recently detailed in a 2017 perspective co-authored by Brummond

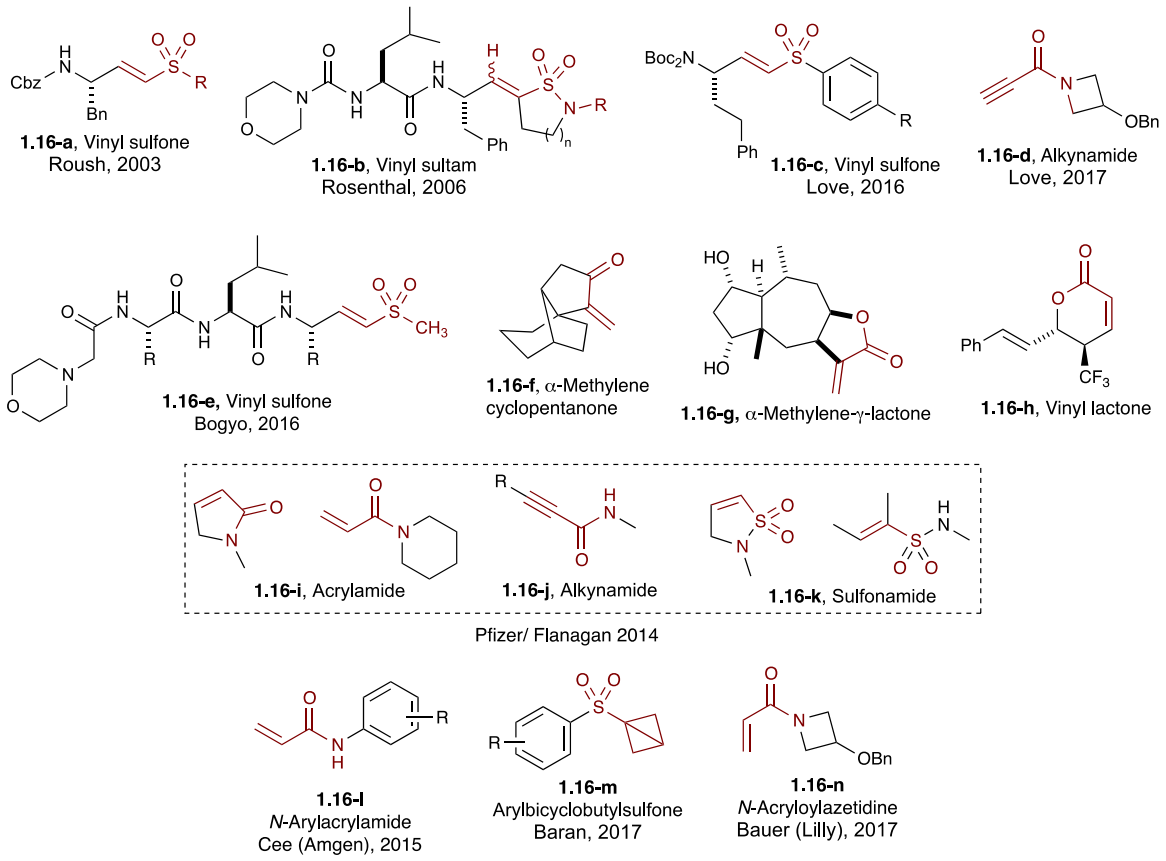

Figure 1.16: *Electrophilic covalent modifiers for ABPP studies.*

and Harki,[72] including α-methylene cyclopentanones **1.16-f**,[73] α-methylene-γ-lactone **1.16-g**[74] and vinyl lactones **1.16-h**.[75] This detailed perspective sheds light on extensive biological activities of a number of natural products and drugs bearing α,β-unsaturated carbonyls, and details studies quantifying thiol reactivity patterns using various kinetic techniques. Overarching systematic investigations comparing thiol-electrophile reactivity patterns across compound classes, however, have only recently begun to emerge.A seminal paper in 2014 by Flanagan and co-scientists at Pfizer[76] characterized and reported glutathione (GSH) reactivity with simple electrophilic warheads, and elevated the concept of reactivity-based thiol screening assays for chemotypes. In this study, thiol/nucleophilic/GSH reactivity data was reported on a number of simple acrylamides **1.16-i**, alkynamides **1.16-j**, and their

sulfonamide/sultam derivatives **1.16-k**, which were elegantly detailed. Augmenting this work were (i) a 2015 systematic study by Cee and co-scientists at Amgen detailing GSH reactivity patterns within a set of aryl substituted *N*-arylacrylamides **1.16-l**,[77] (ii) the novel strain release studies using substituted arylbicyclo[1.1.0]butylsulfones **1.16-m** as chemoselective Cys-reactive probes reported by Baran/Pfizer in 2017 in a joint academic-industrial collaboration,[78] and (iii) a 2017 study by Palkowitz and co-scientists at Eli Lilly reporting the enhanced thiol reactivity patterns of a diverse set of *N*-acryloyl azetidines **1.16-n**.[79] Collectively, these studies have yielded notable data, whereby small acyclic fragment-based modifiers are in the majority.

For these initial reactivity studies, we have employed ^{19}F–NMR as an analytical tool. ^{19}F–NMR studies is a well established method for the elucidation of protein folding, protein dynamics, enzyme kinetics, and ligand interaction both *in vivo* and *in vitro*.[80] Although ^{19}F NMR has been extensively reported to monitor protein dynamics, *vide infra*, and has been termed by Pomerantz as a bioorthogonal method,[81] its use to monitor reactions is much less prevalent.[82,83] Use of ^{19}F to monitor reactions, while less prevalent, has been reported by Berkowitz.[84]

Following our goal of synthesizing electrophilic probes and their potenital use as inhibitors in ABPP studies, we carried out initial reactivity profiling experiments by reacting the *β*-keto vinyl sultam **1.17-A** with *N*-acetylcysteine methyl ester **1.17-B** (Figure 1.17). The reactions were carried out in an NMR tube and the rate of decrease in the intensity of fluorine peak of starting material was monitored and plotted against time in order to measure the rate of the reaction.

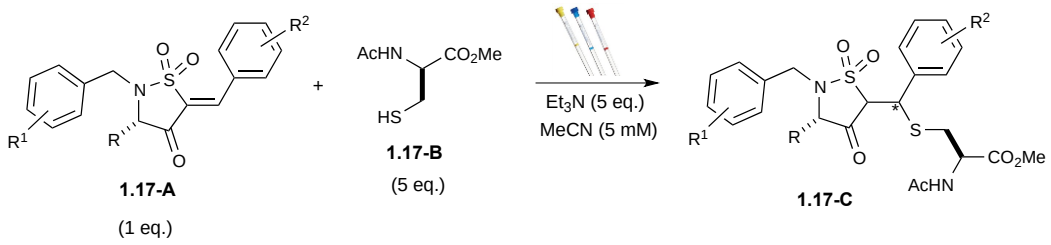

Figure 1.17: *^{19}F-NMR studies of β-keto vinyl sultam*

To perform the aforementioned reaction, 25 mM stock solution of **1.17-A** was prepared in CH_3CN. Similarly, 125 mM stock solutions each of Et_3N, *N*-acetylcysteine methyl ester and internal standard (Trifluorotoluene or trichlorofluoromethane was used as internal standard) were also prepared in CH_3CN. 100 µL each of **1.17-A**, internal standard, and nucleophile were added, followed by the addition of the required amount of CH_3CN to maintain the concentration of reaction at 5 mM. Finally, Et_3N was added to the NMR tube and was immediately subjected to obtain ^{19}F-NMR spectrum. ^{19}F-NMR intensities at different time intervals were noted to obtain a concentration *vs* time plot along with % conversion graph.

The log of concentration *vs* time plot revealed a linear dependence between time and log of concentration of starting material when subjected to pseudo-first order conditions. The pseudo-first order condition was maintained by adding excess of nucleophile and base (5 equiv. each) compared with **1.17-A**. A representative plot of pseudo-first order conditions for the reaction of **1.27.3** with *N*-acetylcysteine methyl ester is shown in Figure 1.18.

The % conversion graph for the Michael addition reaction performed in NMR tube is shown in Figure 1.19 as reported by Baran and coworkers.[78] The difference in reactivity of some of the *β*-keto vinyl sultams (**1.27.2–1.27.5**) can be rationalized from their distinct electrophilic nature. Nucleophilic attack by *N*-acetylcysteine methyl ester is less pronounced

at the electrophilic site of **1.27.5** due to the electron-donating nature of the methoxy substituent that decreases the Michael accepting electrophilicity *via* resonance. In the case of **1.27.2**, which lacks an electron- donating group, a faster nucleophilic reaction is seen. The % conversion graph shown in Figure 1.19 also implies that the substituent at the olefin of the *β*-keto vinyl sultam governs the relative reactivity of the nucleophile to Michael addition. While the amino acid side chain, as well as the *N*-substituent, has no effect in these simple addition reactions, their affect using more elaborate cysteine-containing small peptides in in vitro reactivity profiling studies, as well as in ABPP experiments, awaits to be seen.

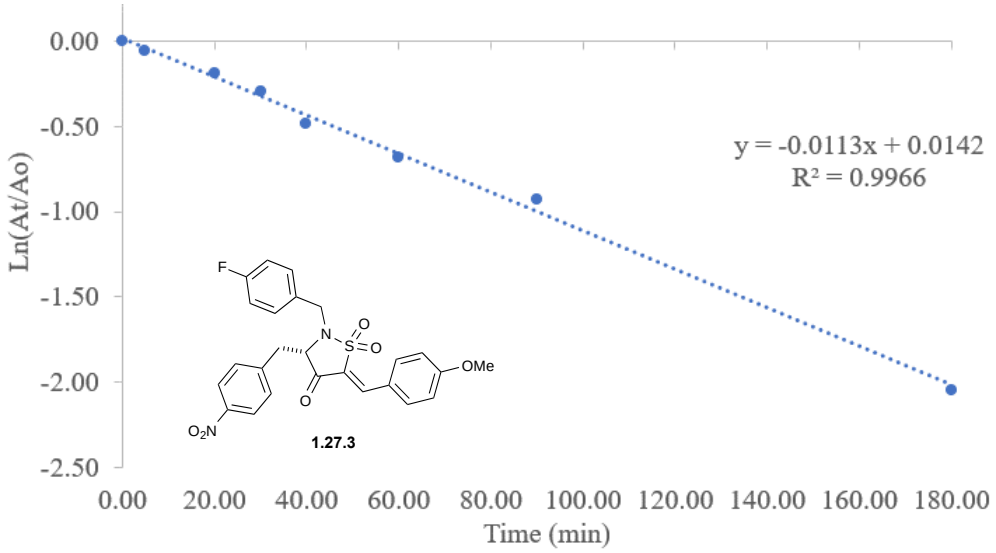

Figure 1.18: *Pseudo-first order reaction of β-keto vinyl sultam analog **1.27.3** with N-acetyl cysteine methyl ester.*

Notably, the reaction between *β*-keto vinyl sultam analogs and *N*-acetylcysteine methyl ester resulted in the appearance of two fluorine peaks in the ^{19}F–NMR spectrum, that appear in equal intensity, which are tentatively assigned as two of four possible diastereomeric addition products. In the case of the reaction with **1.27.3**, four fluorine peaks were seen suggesting all four possible diastereomeric products were seen.

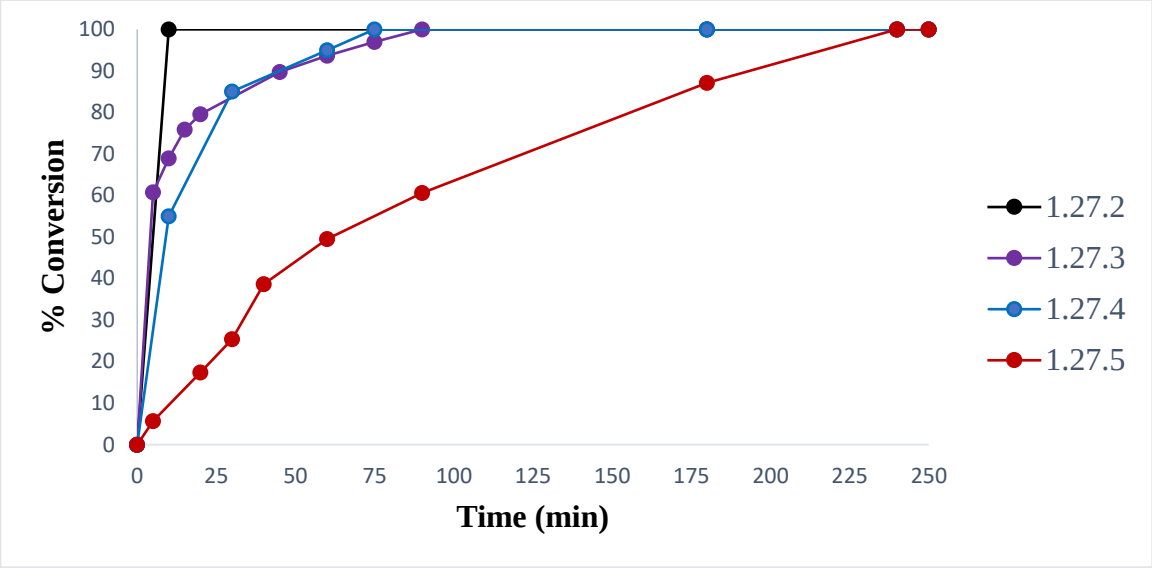

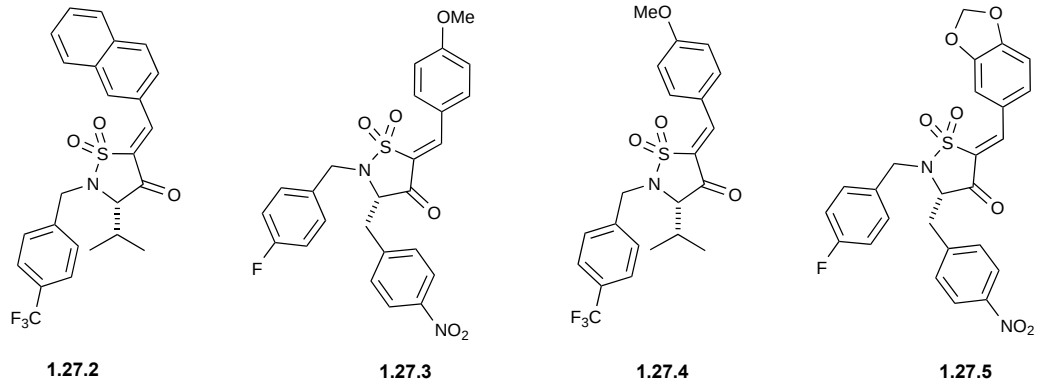

Figure 1.19: *Percentage conversion vs time graph for reaction between β-keto vinyl sultams with N-acetyl cysteine methyl ester.*

1.3 Future work

We have reported synthetic studies and initial reactivity profiling of β-keto vinyl sultam analogs of tetramic acids. With these results in hand, we are providing a list of work to be carried out by subsequent researchers in the group on this project, which includes:

(i) Detailed studies on reactivity profiling with several different thiols and cysteine containing peptides are forthcoming and will be conducted to rank the reactivity of each *β*-keto vinyl sultam.

(ii) Complete characterization of the thiol addition products obtained by the reaction between *β*-keto vinyl sultams and several different thiols will be conducted to confirm the identity of the products.

(iii) The yield of *β*-keto vinyl sultams during the Knoevenagel condensation was moderate, further optimization of the reaction will be done to enhance the yield of the reaction.

(iv) We were not able to obtain *β*-keto vinyl sultams when aliphatic aldehydes were used in the Knoevenagel condensation. Effort will be made to synthesize *β*-keto vinyl sultams using aliphatic aldehydes.

1.4 Conclusion

An efficient method for the synthesis of a small library of *β*-keto vinyl sultams, analogs of tetramic acids, has been reported. This method is applicable to a variety of aromatic aldehydes and sultam analogs of tetramic acids derived from several amino acids. Initial reactivity profiling results of a small set of these *β*-keto vinyl sultams, varying in olefinic substituents, using *N*–acetylcysteine methyl ester as the nucleophile, and monitoring with ^{19}F–NMR has been reported. Using a simple percent conversion versus time metric, appreciable differences in reactivity between these *β*-keto vinyl sultam analogs is seen, and indicates that the substituent at the olefin of the *β*-keto vinyl sultam governs the relative reactivity of the *N*-acetylcysteine methyl ester nucleophile. Data reported herein, warrants further reactivity profiling studies, including use of small peptides in aqueous solvent, as well as in collaborative ABPP studies in whole proteomes.

1.4 References

[1] (a) Royles, B. J. Naturally occurring tetramic acids: structure, Isolation and synthesis. *Chem. Rev*. **1995**, *95*, 1981−2001. (b) Schobert, R.; Schlenk, A. Tetramic and tetronic acids: An update on new derivatives and biological aspects. *Bioorg. Med. Chem*. **2008**, *16*, 4203–4221. (c) Zhao, H. P.; Cui, Z. P.; Gu, Y. C.; Liu, Y. X.; Wang, Q. M. The phytotoxicity of natural tetramic acid derivatives. *Pest Manag. Sci.* **2011,** *67*, 1059–1061. (d) Mo, X. H.; Li, Q. L.; Ju, J. H. Naturally occurring tetramic acid products: isolation, structure elucidation and biological activity. *RSC Adv*. **2014,** *4*, 50566–50593. (e) Boettger, D.; Hertweck, C. Molecular Diversity Sculpted by Fungal PKS–NRPS Hybrids. *ChemBioChem*. **2013**, *14*, 28–42.

[2] (a) Gordon, S. E.; Weber, D. K.; Downton, M. T.; Wagner, J.; Perugini, M. A. Dynamic Modelling Reveals 'Hotspots' on the Pathway to Enzyme-Substrate Complex Formation. *Plos Comp. Biol.* **2016,** *12*. (b) Medina-Cleghorn, D.; Bateman, L. A.; Ford, B.; Heslin, A.; Fisher, K. J.; Dalvie, E. D.; Nomura, D. K. Mapping Proteome-Wide Targets of Environmental Chemicals Using Reactivity-Based Chemoproteomic Platforms. *Chem. Biol.* **2015,** *22*, 1394–1405.

[3] (a) Serwa, R.; Tate, E. W. Activity-Based Profiling for Drug Discovery. *Chem. Biol.* **2011,** *18*, 407–409. (b) Cravatt, B. F.; Wright, A. T.; Kozarich, J. W. Activity-based protein profiling: From enzyme chemistry. *Ann. Rev. Biochem.* **2008,** *77*, 383–414. (c) Niphakis, M. J.; Cravatt, B. F. Enzyme Inhibitor Discovery by Activity-Based Protein Profiling. *Ann. Rev. Biochem.* **2014**, *83*, 341–377.

[4] (a) Haim, A. Sulfonamide group of drugs: General properties, use and dosage. *Cal. West. Med.* **1941**, *55*, 123–125. (b) Ajeet, A.; Mishra, A. K.; Kumar, A. Recent advances in development of sulfonamide derivatives and their pharmacological effects–A review. *Am. J. Pharmacol. Sci.* **2015**, *3*, 18–24.

[5] (a) Udugamasooriya, D. G.; Spaller, M. R. Conformational constraint in protein ligand design and the inconsistency of binding entropy. *Biopolymers* **2008**, *89*, 653–667. (b) Bauer, R. A.; Wurst, J. M.; Tan, D. S. Expanding the range of 'druggable'

targets with natural product-based libraries: an academic perspective. *Curr. Opin. Chem. Biol.* **2010**, *14*, 308–314. (c) Doak, B. C.; Zheng, J.; Dobritzsch, D.; Kihlberg, J. How Beyond Rule of 5 Drugs and Clinical Candidates Bind to Their Targets. *J. Med. Chem.* **2015**, 59, 2312–2327. (d) Knudtson, C. A. Intramolecular oxa-Michael and Baylis hillman strategies towards sultam library production, MS Dissertation, University of Kansas, Lawrence, KS, April **2011**. (e) The calculations of electronegativity and pKa were completed by Gerald H. Lushington using the link provided. MOPAC 2012 http://OpenMOPAC.net

[6] (a) Lucking, U.; Siemeister, G.; Schafer, M.; Briem, H.; Kruger, M.; Lienau, P.; Jautelat, R. Macrocyclic aminopyrimidines as multitarget CDK and VEGF−R inhibitors with potent antiproliferative activities. *ChemMedChem.* **2007**, *2*, 63−77. (b) Hanessian, S.; Larsson, A.; Fex, T.; Knecht, W.; Blomberg, N. Design and synthesis of macrocyclic indoles targeting blood coagulation cascade Factor XIa. *Bioorg. Med. Chem. Lett.* **2010**, *20*, 6925−6928. (c) Aldrich, L. N.; Kuo, S.-Y.; Castoreno, A. B.; Goel, G.; Petric Kuballa, P.; Rees, M. G.; Seashore-Ludlow, B. A.; Cheah, J. H.; Latorre, I. J.; Stuart, L.; Schreiber, S. L.; Shamji, A. F.; Xavier, R. J. Discovery of a small-molecule probe for V-ATPase function. *J. Am. Chem. Soc.* **2015**, *137*, 5563−5568.

[7] (a) Zang, Q.; Javed, S.; Hill, D.; Ullah, F.; Bi, D.; Porubsky, P.; Neuenswander, B.; Lushington, G. H.; Santini, C.; Organ, M. G.; Hanson, P. R. Automated Synthesis of a Library of Triazolated 1,2,5-Thiadiazepane 1,1-Dioxide via a Double aza-Michael Strategy. *ACS Combi. Sci*. **2012**, *14*, 456–459. (b) Zang, Q.; Javed, S.; Porubsky, P.; Ullah, F.; Neunswander, B.; Lushington, G.; Basha, F.; Organ, M. G.; Hanson, P. R. Synthesis of a Unique Isoindoline/Tetrahydroisoquinoline-based Tricyclic Sultam Library Utilizing a Heck-aza-Michael Strategy. *ACS Comb. Sci.* **2012**, *14*, 211–217. (c) Zang, Q.; Javed, S.; Ullah, F.; Zhou, A.; Knudtson, C. A.; Bi, D.; Bashac, F. Z.; Organ, M. G.; Hanson, P. R. Application of a Double aza-Michael Reaction in a "Click, Click, Cy-Click" Strategy: From Bench to Flow. *Synthesis* **2011**, 2743–2750.

[8] (a) Jeon, K. O.; Rayabarapu, D.; Rolfe, A.; Volp, K.; Omar, I.; Hanson, P. R. Metathesis Cascade Strategies (ROM-RCM-CM): A DOS Approach to Skeletally

Diverse Sultams. *Tetrahedron*, **2009**, *65*, 4992–5000. (b) Rolfe, A.; Lushington, G. H.; Hanson, P. R. Reagent based DOS: A "Click, Click, Cyclize" strategy to probe chemical space. *Org. Biomol. Chem.* **2010,** *8*, 2198–2203.

[9] (a) Rayabarapu, D. K.; Zhou, A.; Jeon, K. O.; Samarakoon, T.; Rolfe, A.; Siddiqui, H.; Hanson, P. R. α-Haloarylsulfonamides: multiple cyclization pathways to skeletally diverse benzofused sultams. *Tetrahedron* **2009,** *65*, 3180–3188. (b) Rolfe, A.; Samarakoon, T. B.; Hanson, P. R. Formal [4+3] Epoxide Cascade Reaction via a Complementary Ambiphilic Pairing Strategy. *Org. Lett.* **2010,** *12*, 1216–1219. (c) Loh, J. K.; Yoon, S. Y.; Samarakoon, T. B.; Rolfe, A.; Porubsky, P.; Neuenswander, B.; Lushington, G. H.; Hanson, P. R. Exploring chemical diversity via a modular reaction pairing strategy. *Beilstein J. Org. Chem.* **2012,** *8*, 1293–1302.

[10] Hur, M. Y. Synthesis of novel sultam scaffolds: Method and library development. PhD Dissertation, University of Kansas, Lawrence, August **2015**.

[11] Royles, B. J. Naturally occurring tetramic acids: structure, Isolation and synthesis. *Chem. Rev*. **1995**, *95*, 1981−2001.

[12] (a) Putri, S. P.; Kinoshita, H.; Ihara, F.; Igarashi, Y.; Nihira, T. Ophiosetin, a new tetramic acid derivative from the mycopathogenic fungus *Elaphocordyceps ophioglossoides*. *J. Antibiot*. **2010**, *63*, 195−198. (b) Marfori, E. C.; Kajiyama, S.; Fukusaki, E.; Kobayashi, A. Trichosetin, a novel tetramic acid antibiotic produced in dual culture of *trichoderma harzianum* and *catharanthus roseus. Z Naturforsch C* **2002**, *57*, 465−470. (c) Zhou, M.; Miao, M.-M.; Du, G.; Li, X.-N.; Shang, S.-Z.; Zhao, W.; Liu, Z.-H.; Yang, G.-Y.; Che, C.-T.; Hu, Q.-F.; Gao, X.-M. Aspergillines A–E, Highly Oxygenated Hexacyclic Indole–Tetrahydrofuran–Tetramic Acid Derivatives from *Aspergillus versicolor*. *Org. Lett.* **2014**, *16*, 5016−5019. (d) Carlsen, P. N.; Mann, T. J.; Hoveyda, A. M.; Frontier, A. J. Synthesis of (±)-Tetrapetalone A−Me Aglycon *Angew. Chem., Int. Ed.* **2014**, *53*, 9334–9338.

[13] (a) Henning, H.-G.; Gelbin, A. Advances in tetramic acid chemistry. *Adv. Heterocycl. Chem.* **1993**, *57*, 139–185. (b) Royles, B. J. L. Naturally occurring tetramic acids: structure, isolation and synthesis. *Chem. Rev.* **1995**, *95*, 1981–2001. (c) Tejedor, D.;

Garcia-Tellado, F. Synthesis and chemistry of tetronic acids. *Org. Prep. Proced. Int.* **2004**, *36*, 35–59. (d) Sims, J. W.; Fillmore, J. P.; Warner, D. D.; Schmidt, E. W. Equisetin biosynthesis in *Fusarium heterosporum. Chem. Comm.* **2005**, 186−188.

[14] (a) Dekeyser, M. A. Acaricide mode of action. *Pest. Manag. Sci*. **2005**, *61*, 103−110; (b) Brück, E.; Elbert, A.; Fischer, R.; Krueger, S.; Kühnhold, J.; Klueken, A. M.; Nauen, R.; Niebes, J.-F.; Reckmann, U.; Schnorbach, H.-J.; Steffens, R.; Waetermeulen, X. Movento®, an innovative ambimobile insecticide for sucking insect pest control in agriculture: biological profile and field performance. *Crop Prot.* **2009**, *28*, 838−844. (c) Nauen, R.; Reckmann, U.; Thomzik, J.; Thielert, W. Biological profile of spirotetramat (Movento®) – a new two-way systemic (ambimobile) insecticide against sucking pest species. *Bayer Crop Science Journal* **2008**, *61*, 245−278.

[15] Amagata, T.; Xiao, J.; Chen, Y.-P.; Holsopple, N.; Oliver, A. G.; Gokey, T.; Guliaev, A. B.; Minoura, K. Creation of an HDAC-based yeast screening method for evaluation of marine−derived actinomycetes: Discovery of streptosetin A. *J. Nat. Prod.* **2012**, *75*, 2193−2199.

[16] (a) Sycorderoa, A. A.; Figueroab, M.; Rajaa, H. A. Avinaa, M. E. M.; Croatta, M. P.; Adcockc, A. F.; Krollc, D. J.; Wanid, M. C.; Pearcee, C. J.; Oberliesa, N. H. Spiroscytalin, a new tetramic acid and other metabolites of mixed biogenesis from *Scytalidium cuboideum. Tetrahedron* **2015**, *71*, 8899–8904. (b) Kempf, K.; Kempf, O.; Orozco, M.; Bilitewski, U.; Schobert, R. Synthesis and structural revision of the fungal tetramic acid metabolite spiroscytalin. *J. Org. Chem.* **2017**, *82*, 7791−7795.

[17] (a) Ganzle, M. G. Reutericyclin: biological activity, mode of action, and potential applications. *Appl. Microbiol. Biotechnol.* **2004**, *64*, 326−332. (b) Cherian, P. T.; Wu, X.; Maddox, M. M.; Singh, A. P.; Lee, R. E.; Hurdle, J. G. Chemical modulation of the biological activity of reutericyclin: a membrane-active antibiotic from *Lactobacillus reuteri*. *Scientific Reports*, **2014**, *4*, 4721.

[18] (a) Strobel, G. A.; Miller, R. V.; Miller, C.-M.; Condron, M. M.; Teplow, D. B. Cryptocandin, a potent antimycotic from the endophytic fungus Cryptosporiopsis cf.

quercina. *Microbiol.* **1999**, *145*, 1919–1926. (b) Li, J. Y.; Strobel, G.; Harper, J.; Lobkovsky, E.; Clardy, J. Cryptocin, a Potent Tetramic Acid Antimycotic from the Endophytic Fungus *Cryptosporiopsis cf. quercina. Org. Lett.* **2000**, *2*, 767–770.

[19] (a) Burmeister, H. Antibiotic equisetin and method of production. *Patent USPTO 3,959,468*; May 25, **1976**; (b) Vesonder, R. F.; Tjarks, L. W.; Rohwedder, W. K.; Burmeister, H. R.; Laugal, J. A. Equisetin, an antibiotic from Fusarium equiseti NRRL 5537, identified as a derivative of N-methyl-2,4-pyrollidone. *J. Antibiot.* **1979**, *32*, 759−761; (c) Yin, J.; Wang, C.; Kong, L. L.; Cai, S. J.; Gao, S. H. Asymmetric synthesis and biosynthetic implications of (+)-Fusarisetin A. *Angew. Chem. Int. Ed.* **2012**, *51*, 7786–7789; (d) Yin, J.; Kong, L.; Wang, C.; Shi, Y.; Cai, S.; Gao, S. Biomimetic synthesis of equisetin and (+)-fusarisetin A. *Chem. Eur. J.* **2013**, *19*, 13040–13046; (e) Li, g.; Kusari, S.; Spiteller, M. Natural products containing 'decalin' motif in microorganisms. *Nat. Prod. Rep.* **2014**, *31*, 1175–1201.

[20] (a) Singh, S. B.; Zink, D. L.; Heimbach, B.; Genilloud, O.; Teran, A.; Silverman, K. C.; Lingham, R. B.; Felock, P.; Hazuda, D. J. Structure, Stereochemistry, and Biological Activity of Integramycin, a Novel Hexacyclic Natural Product Produced by *Actinoplanes* sp. that Inhibits HIV-1 Integrase. *Org. Lett.* **2002**, *4*, 1123−1126; (b) Kim, D.-H.; Creek, D. J. What role can metabolomics play in the discovery and development of new medicines for infectious diseases? *Bioanalysis* **2015**, *7*, 629−631.

[21] (a) Tian, Z.; Sun, P.; Yan, Y.; Wu, Z.; Zheng, Q.; Zhou, S.; Zhang, H.; Yu, F.; Jia, X.; Chen, D.; Mándi, A.; Kurtán, T.; Liu, W. An enzymatic [4+2] cyclization cascade creates the pentacyclic core of pyrroindomycins. *Nat. Chem. Biol.* **2015**, *11*, 259–265. (b) Watanabe, K. Effective use of heterologous hosts for characterization of biosynthetic enzymes allows production of natural products and promotes new natural product discovery. *Chem. Pharm. Bull.* **2014**, *62*, 1153–1165. (c) Kakule, T. B.; Zhang, S.; Zhan J.; Schmidt, E. W. Biosynthesis of the tetramic acids Sch210971 and Sch210972. *Org. Lett*. **2015**, *17*, 2295–2297. (d) Yang, S. W.; Mierzwa, R.; Terracciano, J.; Patel, M.; Gullo, V.; Wagner, N.; Baroudy, B.; Puar, M.; Chan, T.

M.; Chu, M. Sch 213766, A novel chemokine receptor CCR-5 inhibitor from *Chaetomium globosum*. *J. Antibiot.* **2007**, *60*, 524–528.

[22] (a) Izumikawa, M.; Hashimoto, J.; Hirokawa, T.; Sugimoto, S.; Koto, T.; Takai, M.; Shin-ya, K. JBIR-22, An inhibitor for protein-protein interaction of the homodimer of proteasome assembly factor 3. *J. Nat. Prod.* **2010**, *73*, 628–631. (b) Healy A. R.; Westwood, N. Synthetic studies on the bioactive tetramic acid JBIR-22 using a late stage Diels–Alder reaction. *J. Org. Biomol. Chem.* **2015**, 10527−10531.

[23] (a) Sodano, G.; Spinella, A. Janolusimide, a lipophilic tripeptide toxin from the nudibranch mollusc *janolus cristatus*. *Tetrahedron Lett.* **1986**, *27*, 2505−2508; (b) Giordano, A.; Spinella, A.; Sodano, G. Stereoselective synthesis of 4-amino-3-hydroxy-2-methylpentanoic acids: stereochemistry of the amino acid occurring in the marine toxin janolusimide. *Tetrahedron: Asymmetry* **1999**, *10*, 1851–1854; (c) Wang, J.; Prinsep, M. R.; Gordon, D. P.; Page, M. J.; Copp, B. R. Isolation and stereospecific synthesis of Janolusimide B from a New Zealand collection of the bryozoan *Bugula flabellate. J. Nat. Prod.* **2015**, *78*, 530–533.

[24] (a) Jang, J.-H.; Asami, Y.; Jang, J.-P.; Kim, S.-O.; Moon, D. O.; Shin, K.-S.; Hashizume, D.; Muroi, M.; Saito, T.; Oh, H.; Kim, B. Y.; Osada, H.; Ahn, J. S. Fusarisetin A, an acinar morphogenesis inhibitor from a soil fungus, *Fusarium* sp. FN080326. *J. Am. Chem. Soc.* **2011**, *133*, 6865–6867. (b) Deng, J.; Zhu, B.; Lu, Z. Y.; Yu H. X.; Li, A. Total synthesis of (−)-Fusarisetin A and reassignment of the absolute configuration of its natural counterpart. *J. Am. Chem. Soc.* **2012**, *134*, 920–923.

[25] (a) Pornpakakul, S.; Roengsumran, S.; Deechangvipart, S.; Petsom, A.; Muangsin, N.; Ngamrojnavanich, N.; Sriubolmas, N.; Chaichit, N.; Ohta, T. Diaporthichalasin, a novel CYP3A4 inhibitor from an endophytic *Diaporthe* sp. *Tetrahedron Lett.* **2007**, *48*, 651–655; (b) Shionozaki, N.; Iwamura, N.; Tanaka, R.; Makino, K.; Uchiro H. Total synthesis of Diaporthichalasin by using the intramolecular Diels–Alder reaction of an α,*β*−unsaturated γ−hydroxylactam in aqueous media. *Chem Asian J.* **2013**, *8*, 1243–1252.

[26] (a) Honda, T.; Yoshizawa, H.; Sundararanjan, C.; David, E.; Lajoie, M. J.; Favaloro Jr., F. G.; Janosik, T.; Su, X.; Honda, Y.; Roebuck, B. D.; Gribble, G. W. Tricyclic compounds containing nonenolizable cyano enones. A novel class of highly potent anti-inflammatory and cytoprotective agents. *J. Med. Chem.* **2011**, *54*, 1762−1778. (b) Hsu, D.-S.; Hsu, P.-Y.; Liao, C.-C. The first total synthesis of (±)-Eremopetasidione. *Org. Lett.* **2001**, *3*, 263−265. (c) Yajima, A.; Yamaguchi, A.; Saitou, F.; Nukada, T.; Yabuta, G. Asymmetric synthesis of abietane diterpenoids via *B*-alkyl Suzuki–Miyaura coupling. Formal total asymmetric synthesis of 12-deoxyroyleanone and cryptoquinone. *Tetrahedron* **2007**, *63*, 1080−1084. (d) Refouvelvet, B.; Guyon, C.; Jacquot, Y.; Girard, C.; Fein, H.; Bevalot, F.; Robert, J.-F.; Heyd, B.; Mantion, G.; Richert, L.; Xicluna, A. Synthesis of 4-hydroxycoumarin and 2,4-quinolinediol derivatives and evaluation of their effects on the viability of HepG2 cells and human hepatocytes culture. *Eur. J. Med. Chem.* **2004**, *39*, 931−937. (e) Krishnan, S.; Miller, R. M.; Tian, B.; Mullins, R. D.; Jacobson, M. P.; Taunton, J. Design of reversible, cysteine-targeted Michael acceptors guided by kinetic and computational analysis. *J. Am. Chem. Soc.* **2014**, *136*, 12624−12630.

[27] The databases were searched by Jay Jha on 07/16/2018 and by Moon Young Hur on 04/07/2015. The method of search was drawing the desired moiety in database followed by pressing search button.

[28] (a) Schobert, R.; Schlenk, A. Tetramic and tetronic acids: An update on new derivatives and biological aspects. *Bioorg. Med. Chem.* **2008**, *16*, 4203–4221. (b) Athanasellis, G.; Igglessi-Markopoulou, O.; Markopoulos, J. Tetramic and Tetronic Acids as Scaffolds in Bioinorganic and Bioorganic Chemistry. *Bioinorg. Chem. Appl.* **2010**, *2010*, 1–11.

[29] Spatz, J. H.; Welsch, S. J.; Duhaut, D-E.; Jager, N.; Boursier, T.; Fredrich, M.; Allmendinger, L.; Ross, G.; Kolb, J.; Burdack, C.; Umkehrer, M. Tetramic acid derivatives via Ugi–Dieckmann-reaction. *Tetrahedron Lett.* **2009**, *50*, 1705–1707.

[30] Marcus, A. P.; Sarpong, R. Synthesis of the tetracyclic core of tetrapetalone A enabled by a pyrrole reductive alkyation. *Org. Lett.* **2010**, *12*, 4560−4563.

[31] Gu, Z.; Zakarian, A. Concise total synthesis of Sintokamides A, B, and E by a unified, protecting-group-free strategy. *Angew. Chem. Int. Ed.* **2010**, *49*, 9702 –9705.

[32] Bai, W.-J.; Jackson, S. K.; Pettus, T. R. R. Mild construction of 3-methyl tetramic acids enabling a formal synthesis of Palauimide. *Org. Lett.* **2012**, *14*, 3862–3865.

[33] Liu, Y. X.; Zhao, H. P.; Song, H. B.; Gu, Y. C.; Wang, Q. M. Studies on the synthesis and bioactivities of 4-amino derivatives of tetramic acid. *J. heterocyclic chemistry* **2014**, *51*, E25–E33.

[34] Carlsen, P. N.; Mann, T. J.; Hoveyda, A. H.; and Frontier, A. J. Synthesis of (±)−Tetrapetalone A-Me aglycon. *Angew. Chem. Int. Ed.* **2014**, *53*, 9334 –9338.

[35] Ishida, T.; Kobayashi, R.; Yamada, T. Novel method of tetramic acid synthesis: Silver-catalyzed carbon dioxide incorporation into propargylic amine and intramolecular rearrangement. *Org. Lett.* **2014**, *16*, 2430−2433.

[36] Dobrydnev, A. V.; Popova, M. V.; Saffon-Merceron, N.; Listunov, D.; Volovenko, Y. M. Synthesis of the first representatives of spiro-1-(6)-isothiazolidine-1,1,4-triones. *Synthesis-Stuttgart* **2015,** *47*, 2523−2528.

[37] Stachel, H.-D.; Drasch, G. Synthesis and properties of *β*-oxopropanesultones and-sultams. *Arch. Pharm.***1985**, *318*, 304−311.

[38] Loev, B.; Kormendy, M. F.; Snader, K. M. Sulfostyril (2,1-Benzothiazine 2,2-Dioxide). II synthesis. *J. Org. Chem.* **1966**, *31*, 3531–3534.

[39] Tornus, I.; Schaumann, E. Novel applications of N-sulfonyl-alkylamines in [2+4] cycloadditions. *Tetrahedron* **1996**, *52*, 725−732.

[40] (a) Coppo, F. T.; Fawzi, M. M. Synthesis of 1-methyl-7-(trifluoromethyl)-1*H*-pyrido[2,3-*c*][1,2]thiazin-4(3*H*)-one 2,2-dioxide. *J. Heterocyclic Chem.* **1998**, *35*, 499–501. (b) Volovenko, Y.; Volovnenko, T.; Popov, K. N-alkyl-4-chloro-1*H*-benzo[*c*][1,2]thiazine-3-carbaldehyde-2,2-dioxides–New functional benzothiazine derivatives. *J. Heterocyclic Chem.* **2007**, *44*, 1413–1419.

[41] Pieroni, M.; Sabatini, S.; Massari, S.; Kaatz, G. W.; Cecchetti, V.; Tabarrini, O. Searching for innovative quinolone-like scaffolds: synthesis and biological evaluation of 2,1-benzothiazine 2,2-dioxide derivatives. *Med. Chem. Commun.* **2012**, *3*, 1092–1097.

[42] (a) Karsch, S.; Freitag, D.; Schwab, P.; Metz, P. Ring closing metathesis in the synthesis of sultones and sultams. *Synthesis*. **2004**, *10*, 1696–1712. (b) Ho, K. F.; Fung, D. C. W.; Wong, W. Y.; Chan, W. H.; Lee, A. W. M. Synthesis and Diels–Alder reactions of *α,β*–unsaturated–*γ*–sultams. *Tetrahedron Lett*. **2001**, *42*, 3121–3124. (c) Majumdar, K. C.; Mondal, S. Recent developments in the synthesis of fused sultams. *Chem. Rev*. **2011**, *111*, 7749–7773. (d) Javed, S.; Bodugam, M.; Torres, J.; Ganguly, A.; Hanson, P. Modular synthesis of novel macrocycles bearing *α,β*–unsaturated chemotypes through a series of one–pot, sequential protocols. *Chem. Eur. J*. **2016**, *22*, 6755–6758.

[43] (a) Jeffries, D. E.; Lindsley, C. W. Total synthesis and biological evaluation of Hydrubin A. *J. Org. Chem*. **2017**, *82*, 431–437. (b) Hagmann, L.; Juttner, F. Fischerellin A, a novel photosystem-II-inhibiting allelochemical of the cyanobacterium Fischerella muschicola with antifungal and herbicidal activity. Tetrahedron Lett. **1996**, *37*, 6539–6542. (c) Amagata, T.; Xiao, J.; Chen, Y. P.; Holsopple, N.; Oliver, A. G.; Gokey, T.; Guliaev, A. B.; Minoura, K. Creation of an HDAC-based yeast screening method for evaluation of marine-derived actinomycetes: discovery of streptosetin A. *J Nat Prod*. **2012**, *75*, 2193–2199.

[44] (a) Liu, S.; Hanzlik, R. P. Structure–Activity Relationships for Inhibition of Papain by Peptide Michael Acceptors. *J. Med. Chem.* **1992**, *35*, 1067–1075. (b) Roush, W. R.; Cheng, J.; Knapp-Reed, B.; Alvarez-Hernandez, A.; McKerrow, J. H.; Hansell, E.; Engel, J. C. Potent second generation vinyl sulfonamide inhibitors of the trypanosomal cysteine protease cruzain**.** *Bioorg. Med. Chem. Lett*. **2001**, *11*, 2759–2762. (c) Alvarez-Hernandez, A.; Roush, W. R. Recent advances in the synthesis, design and selection of cysteine protease inhibitors. *Curr. Opin. Chem. Biol*. **2002**, *6*, 459–465. (d) Reddick, J. J.; Cheng, J.; Roush, W. R. Relative rates of Michael reactions of 2'-(phenethyl)thiol with vinyl sulfones, vinyl sulfonate Esters, and vinyl sulfonamides relevant to vinyl sulfonyl cysteine protease inhibitors. *Org. Lett*. **2003**,

5, 1967–1970. (e) Valente, C.; Guedes, R. C.; Moreir, R.; Iley, J.; Gut, J.; Rosenthal P. J. Dipeptide vinyl sultams: Synthesis via the Wittig–Horner reaction and activity against papain, falcipain-2 and *Plasmodium falciparum*. *Bioorg. Med. Chem. Lett*. **2006**, *16*, 4115–4119. (f) Li, H.; O'Donoghue, A. J.; van der Linden, W. A.; Xie, S. C.; Yoo, E.; Foe, I. T.; Tilley, L.; Craik, C. S.; da Fonseca, P. C. A.; Bogyo, M. Structure- and function-based design of Plasmodium-selective proteasome inhibitors. *Nature*. **2016**, *530*, 233–236.

[45] Hanson, P. R.; Probst, D. A.; Robinson, R. E.; Yau, M. Cyclic sulfonamides via the ring-closing methathesis reaction. *Tetrahedron Lett*. **1999**, *40*, 4761–4764.

[46] Wanner, J.; Harned, A. M.; Probst, D. A.; Poon, K. W. C.; Klein, T. A.; Snelgrove, K. A.; Hanson, P. R. A dual metathesis route to oligomeric sulfonamides. *Tetrahedron Lett*. **2002**, *43*, 917–921.

[47] Hanessian, S.; Sailes, H.; Therrien, E. Synthesis of functionally diverse bicyclic sulfonamides as constrained proline analogs and application to the design of potential thrombin inhibitors. *Tetrahedron* **2003**, *59*, 7047–7056.

[48] Merten, S.; Frohlich, R.; Kataeva, O.; Metz, P. Synthesis of sultams by intramolecular Heck reaction. *Adv. Synth. Catal*. **2005**, *347*, 754–758.

[49] Jimenez-Hopkins, M.; Hanson, P. R. An RCM strategy to stereodiverse δ-sultam scaffolds. *Org. Lett.* **2008**, *10*, 2223–2226.

[50] Zhou, A.; Hanson, P. R. Synthesis of sultam scaffolds via intramolecular oxa-Michael and diastereoselective Baylis−Hillman reactions. *Org. Lett.* **2008**, *10*, 2951–2954.

[51] Laha, J. K.; Sharma, S.; Kirar, S.; Banerjee, U. C. Design, sustainable synthesis, and programmed reactions of templated *N*-heteroaryl-fused vinyl sultams. *J. Org. Chem.* **2017**, *82*, 9350−9359.

[52] Nguyen, T. B.; Retailleau, P. Redox-neutral access to sultams from 2-nitrochalcones and sulfur with complete atom economy. *Org. Lett.* **2017**, *19*, 3879−3882.

[53] Popova, M. V.; Dobrydnev, A. V.; Dyachenko, M. S.; Duhayon, C.; Listunov, D. Volovenko, Y. M. Synthesis of a series of tetraminic acid sulfone analogs. *Monatsh Chem.* **2017**, *148*, 939–946.

[54] (a) Majumdar, K. C.; Mondal, S. Recent developments in the synthesis of fused sultams. *Chem. Rev.* **2011**, *111*, 7749–7773. (b) Rassadin V. A.; Grosheva, D. S.; Tomashevskii, A. A.; Sovolov, V. V. Methods of sultam synthesis. *Chem. Heterocycl. Comp*. **2013**, *49*, 39–65. (c) Debnath, S.; Mondal, S. Sultams: Syntheses and application. *Eur. J. Org. Chem*. **2018**, 933–956.

[55] (a) Rolf, A.; Hanson, P. R. Microwave-assisted sequential one-pot protocol to benzothiadiazin-3-one-1,1-dioxides via a copper-catalyzed *N*-arylation strategy. *Tetrahedron Lett*. **2009**, *50*, 6935–6937. (b) Rolfe, A.; Young, K.; Volp, K.; Schoenen, F.; Neuenswander, B.; Lushington, G. H.; Hanson, P. R. A one-pot, 3-component, domino Heck-aza-Michael approach to libraries of functionalized 1,1-dioxido-1,2-benzisothiazoline-3-acetic acids. *J. Comb. Chem*. **2009**, *11*, 732–738. (c) Jeon, K. O.; Rayabarapu, D.; Rolfe, A.; Volp, K.; Omar, I.; Hanson, P. R. Metathesis cascade strategies (ROM-RCM-CM): A DOS approach to skeletally diverse sultams. *Tetrahedron* **2009**, *65*, 4992–5000. (d) Rayabarapu, D.; Zhou, A.; Jeon, K. O.; Samarakoon, T.; Rolfe, A.; Siddiqui, H.; Hanson, P. R. α-haloarylsulfonamides: Multiple cyclization pathways to skeletally diverse benzofused sultams. *Tetrahedron* **2009**, *65*, 3180–3188. (e) Zhou, A.; Rayabarapu, D.; Hanson, P. R. 'Click-click-cyclize': A DOS approach to sultams utilizing vinyl sulfonamides linchpins. *Org. Lett*. **2009**, *11*, 531–534. (f) Zhou, A.; Hanson, P. R. Synthesis of sultams scaffolds via intramolecular oxa-Michael and diastereoselective Baylis-Hillman reactions. *Org. Lett*. **2008**, *10*, 2951–2954. (g) Rolfe, A.; Samarakoon, T. B.; Hanson, P. R. Formal [4+3] epoxide cascade reaction via a complementary ambiphilic pairing. *Org. Lett*. **2010**, *12*, 1216–1219. (h) Rolfe, A.; Lushington, G. H.; Hanson, P. R. Reagent based DOS: A 'Click-click-cyclize' strategy to probe chemical space. *Org. Biomol. Chem*. **2010**, *8*, 2198–2203.

[56] Gupta, V.; Yang, J.; Liebler, D. C.; Carroll, K. S. Diverse redoxome reactivity profiles of carbon nucleophiles. *J. Am. Chem. Soc.* **2017**, *139*, 5588−5595.

[57] (a) Nielsen, T. E.; Schreiber, S. L. Diversity–oriented synthesis using the build/couple/pair strategy. *Angew. Chem. Int. ed.* **2007**, *47*, 48–56. (b) Takuya Uchida, T.; Manuela Rodriquez, M.; Stuart L. Schreiber, S. L. Skeletally diverse small molecules using a build/couple/pair strategy. *Org. Lett.* **2009**, *11*, 1559–1562. (c) Fitzgerald, M. E.; Mulrooney, C. A.; Duvall, J. R.; Wei, J.; Suh, B–C.; Akella, L. B.; Vrcic, A.; Marcaurelle, L. A. Build/couple/pair strategy for the synthesis of stereochemically diverse macrolactams via head–to–tail cyclization. *ACS Comb. Sci.* **2012**, *14*, 89–96.

[58] Kolb, H. C.; Finn, M. G.; Sharpless, K. B. Click chemistry: Diverse chemical function from a few good reactions. *Angew. Chem. Int. ed.* **2001**, *40*, 2004–2021.

[59] (a) Boeckman, R. K.; Starrett, J. E.; Nickell, D. G.; Sum, P. E. Synthetic studies directed toward the naturally occurring acyl tetramic acids. 1. Convergent total synthesis of (+)-tirandamycin A. *J. Am. Chem. Soc.* **1986**, *108*, 5549–5559; (b) Boeckman, R. K.; Potenza, J. C.; Enholm, E. J. Synthetic studies directed toward naturally occurring tetramic acids. 3. Synthesis of (-)-methyl ydiginate and the tetramic acid subunit for streptolydigin *J. Org. Chem.* **1987**, *52*, 469–472; (c) Skylaris, C. K.; Igglessi-Markopoulou, O.; Detsi, A.; Markopoulos, J. Density functional and ab initio study of the tautomeric forms of 3-acetyl tetronic and 3-acetyl tetramic acids. *Chem. Phys.* **2003**, *293*, 355–363; (d) Detsi, A.; Afantitis, A.; Athanasellis, G.; Markopoulos, J.; Igglessi-Markopoulou, O.; Skylaris, C. K. Cyclisation of novel amino oxo esters to tetramic acids − density functional theory study of the reaction mechanism. *Eur. J. Org. Chem.* **2003**, 4593–4600; (e) Schobert, R.; Schlenk, A. Tetramic and tetronic acids: an update on new derivatives and biological aspects. *Bioorg. Med. Chem.* **2008**, *16*, 4203–4221.

[60] Rooney, C. S.; Cochran, D. W.; Ziegler, C.; Cragoe, Jr., E. J.; Williams, H. W. R. 5-Aryl-4-hydroxy-3(2H)-isothiazolone 1,1-dioxide derivatives. Synthesis and carbon-13 NMR characterization. *J. Org. Chem.* **1984**, *49*, 2212–2217.

[61] (a) Stachel, H.-D.; Drasch, G. Herstellung und Eigenschaften von β-ketopropansultonen und –sultamen. *Arch. Pharm.* **1985**, *318*, 304–311.

[62] Jeong, Y-C.; Moloney, M. G. Tetramic acids as scaffolds: Synthesis, tautomeric and antibacterial behaviour. *Synlett*, **2009**, *15*, 2487–2491.

[63] Knoevenagel, E. Condensation of malonic acid with aromatic aldehydes via ammonia and amines. *Berichte der deutschen chemischen Gesellschaft* **1898**, *31*, 2596–2619.

[64] Saudi, M. N. S.; EL Semary, M. M. A.; EL Sawaf, G. Synthesis of some 3- and 4-substituted 1,5-diphenylpyrrolidine-2,4-diones as potential antimicrobial and antineoplastic agents. Reactions with tetramic acid, Part 5. *Pharmazie* **2002**, *57*, 519–522.

[65] Beyer, W. R. C.; Woithe, K.; Luke, B.; Schindler, M.; Antonicek, H.; Scherkenbeck, J. Asymmetric total synthesis of the indole alkaloid cyclopiazonic acid and first structure–activity data. *Tetrahedron* **2011**, *67*, 3062–3070.

[66] Sengoku, T.; Suzuki, K.; Nakayama, K.; Yagishita, F.; Sakamoto, M.; Takahashi, M.; Yoda, H. Novel chiral tetramic acid–derived diols: organocatalytic facile synthesis and unique structural properties. *RSC. Adv.* **2014**, *4*, 30775–30779.

[67] Sengoku, T.; Nagae, Y.; Ujihara, Y.; Takahashi, M.; Yoda, H. A synthetic approach to diverse 3-acyltetramic acids via *O*– to *C*–acyl rearrangement and application to the total synthesis of penicillenol series. *J. Org. Chem.* **2012**, *77*, 4391−4401.

[68] Pirc, S.; Bevk, D.; Jakse, R.; Recnik, S.; Golic, L.; Golobic, A.; Meden, A.; Stanovnik, B.; Svete, J. Synthesis of N-substituted 3–aminomethylidenetetramic acids. *Synthesis* **2005**, *17*, 2969–2988.

[69] (a) Khaksar, S.; Heydari, A.; Tajbakhsh, M.; Bikanzadeh, H. R. A facile and efficient synthesis of β-amino alcohols using 2,2,2-trifluoroethanol as a metal-free and reusable medium. *J. Fluorine Chem.* **2010**, *131*, 106–110. (b) Balalaie, S.; Azizian, J.; Shameli, A.; Bijanzadeh, H. R. Trifluoroethanol as an efficient reaction media for the synthesis of pyran skeleton through domino Knoevenagel-hetero-Diels-Alder reaction with non-activated alkynes. *J. Iran. Chem. Soc*. **2015**, *12*, 631−637. (c) Dandia, A.; Khan, S.; Soni, P.; Indora, A.; Mahawar, D. K.; Pandya, P.; Chauhan, C. S. Diversity-oriented sustainable synthesis of antimicrobial spiropyrrolidine/thiapyrrolizidine

oxindole derivatives: New ligands for a metallo-b-lactamase from Klebsiella pneumonia. *Bioorg. Med. chem. Lett*. **2017**, *27*, 2873−2880.

70. (a) Serwa, R.; Tate, E. W., Activity-Based Profiling for Drug Discovery. *Chem. Biol.* **2011,** *18*, 407-409. (b) Cravatt, B. F.; Wright, A. T.; Kozarich, J. W., Activity-based protein profiling: From enzyme chemistry. *Ann. Rev. Biochem.* **2008,** *77*, 383–414. (c) Niphakis, M. J.; Cravatt, B. F., Enzyme Inhibitor Discovery by Activity-Based Protein Profiling. *Ann. Rev. Biochem.* **2014,** *83*, 341–377. (d) Roberts, A. M.; Ward, C. C.; Nomura, D. K. Activity-based protein profiling for mapping and pharmacologically interrogating proteome-wide ligandable hotspots. *Curr. Opin. Biotechnol.* **2017**, *43*, 25–33.

[71] Kiemele, E. R.; Wathier, M.; Bichler, P.; Love, J. A. Total Synthesis of K777: Successful Application of Transition-Metal-Catalyzed Alkyne Hydrothiolation toward the Modular Synthesis of a Potent Cysteine Protease Inhibitor. *Org. Lett.* **2016**, *18*, 492–495.

[72] Jackson, P. A.; Widen, J. C.; Harki, D. A.; Brummond, K. M. Covalent Modifiers: A Chemical Perspective on the Reactivity of α,β-Unsaturated Carbonyls with Thiols via Hetero-Michael Addition Reactions. *J. Med. Chem.* **2017**, *60*, 839–885.

[73] Kakiuchi, K.; Ue, M.; Takeda, M.; Tadaki, T.; Kato, Y.; Nagashima, T.; Tobe, Y.; Koike, H.; Ida, N.; Odaira, Y. Antiproliferating polyquinanes .5. Diquinanes and triquinanes involving α-methylene or α -alkylidene cyclopentanone, cyclopentenone, and γ-lactone systems *Chem. Pharm. Bull.* **1987**, *35*, 617.

[74] Schmidt, T. J.; Lyss, G.; Pahl, H. L.; Merfort, I. Helenanolide type sesquiterpene lactones. Part 5: The role of glutathione addition under physiological conditions *Bioorg. Med. Chem.* **1999**, *7*, 2849.

[75] Chen, J. L.; You, Z. W.; Qing, F. L. Total synthesis of γ-trifluoromethylated analogs of goniothalamin and their derivatives *J. Fluorine Chem.* **2013**, *155*, 143.

[76] (a) Flanagan, M. E.; Abramite, J. A.; Anderson, D. P.; Aulabaugh, A.; Dahal, U. P.; Gilbert, A. M.; Li, C.; Montgomery, J.; Oppenheimer, S. R.; Ryder, T.; Schuff, B. P.;

Uccello, D. P.; Walker, G. S.; Wu, Y.; Brown, M. F.; Chen, J. S. M.; Hayward, M. M.; Noe, M. C.; Obach, R. S.; Philippe, L.; Shanmugasundaram, V.; Shapiro, M. J.; Starr, J.; Stroh, J.; Che, Y., Chemical and Computational Methods for the Characterization of Covalent Reactive Groups for the Prospective Design of Irreversible Inhibitors. *J. Med. Chem.* **2014**, *57*, 10072–10079. See also: Pfizer **2016** study on *N*-α-acetyl-L-lysine as a model amine-based nucleophile for a series of electrophiles (acrylamides, nitriles, cyanamides, sulfones, and sulfonamides) and compared with results using GSH. (b) Dahal U. P.; Gilbert, A. M.; Obach, R. S.; Flanagan, M. E.; Chen, J. M.; Garcis-Irizarry, C.; Starr, J. T.; Schuff, B. Uccello, D. P.; Young, J. R. Intrinsic reactivity profile of electrophilic moieties to guide covalent drug design: *N*-α-acetyl-L-lysine as an amine nucleophile. *Med. Chem. Comm* **2016**, *7*, 864–872.

[77] Cee, V. J.; Volak, L. P.; Chen, Y.; Bartberger, M. D.; Tegley, C.; Arvedson, T.; McCarter, J.; Tasker, A. S.; Fotsch, C. Systematic Study of the Glutathione (GSH) Reactivity of *N*-Arylacrylamides: 1. Effects of Aryl Substitution. *J. Med. Chem.* **2015**, *58*, 9171−9178.

[78] Lopchuk, J. M.; Fjelbye, K.; Kawamata, Y.; Malins, L. R.; Pan, C. M.; Gianatassio, R.; Wang, J.; Prieto, L.; Bradow, J.; Brandt, T. A.; Collins, M. R.; Elleraas, J.; Ewanicki, J.; Farrell, W.; Fadeyi, O. O.; Gallego, G. M.; Mousseau, J. J.; Oliver, R.; Sach, N. W.; Smith, J. K.; Spangler, J. E.; Zhu, H. C.; Zhu, J. J.; Baran, P. S., Strain-Release Heteroatom Functionalization: Development, Scope, and Stereospecificity. *J. Am. Chem. Soc.* **2017**, *139*, 3209–3226.

[79] Palkowitz, M. D.; Tan, B.; Hu, H.; Roth, K.; Bauer, R. A. Synthesis of Diverse *N*-Acryloyl Azetidines and Evaluation of Their Enhanced Thiol Reactivities**.** *Org. Lett.* **2017**, *19*, 2270–2273.

[80] (a) Li, C.; Wang, G-F.; Wang, Y.; Creager-Allen, R.; Lutz, E. A.; Scronce, H.; Slade, K. M.; Ruf, R. A. S.; Mehl, R. A.; Pielak, G. J. Protein ^{19}F NMR in *Escherichia coli*. *J. Am. Chem. Soc.* **2010**, *132*, 321–327. (b) Chen, H.; Viel, S.; Ziarelli, F.; Peng, L. ^{19}F NMR: a valuable tool for studying biological events. *Chem. Soc. Rev*. **2013**, *42*,

7971–7982. (c) Marsh, E. N. G.; Suzuki, Y. Using ^{19}F NMR to probe biological interactions of proteins and peptides. *ACS Chem. Biol.* **2014**, *9*, 1242–1250. (d) Arntson, K. E.; Pomerantz, W. C. K. Protein-observed fluorine NMR: A bioorthogonal approach for small molecule discovery. *J. Med. Chem.* **2016**, *59*, 5158–5171.

[81] (a) Arntson, K. E.; Pomerantz, W. C. K. Protein-Observed Fluorine NMR: A Bioorthogonal Approach for Small Molecule Discovery. *J. Med. Chem.* **2016**, *59*, 5158–5171. (b) Mishra, N. K.; Urick, A. K.; Ember, S. W. J.; Schönbrunn, E.; Pomerantz, W. C. Fluorinated Aromatic Amino Acids Are Sensitive 19F NMR Probes for Bromodomain-Ligand Interactions. *ACS Chem. Biol*. **2014**, *9*, 2755–2760. (c) Pomerantz, W. C.; Hadley, E. B.; Fry, C. G.; Gellman, S. H. *In Situ* Monitoring of Backbone Thioester Exchange by 19F NMR. *ChemBioChem.* **2009**, *10*, 2177–2181.

[82] Krolikowski, P. "The Use of 19F NMR to Monitor Organic Reactions on Solid Supports" (**2004**) *Theses and Dissertations.* Paper 841.

[83] Woods, J. R.; Mo, H.; Bieberich, A. A.; Alavanja, T.; Colby, D. A. Fluorinated Amino-Derivatives of the Sesquiterpene Lactone Parthenolide, as 19F NMR Probes in Deuterium-Free Environments. *J. Med. Chem.* **2011**, *54*, 7934–7941.

[84] (a) Panigrahi, K.; Applegate, G. A.; Malik, G.; Berkowitz, D. W. Combining a *Clostridial* enzyme exhibiting unusual active site plasticity with a remarkably facile sigmatropic rearrangement: Rapid, stereocontrolled entry into densely functionalized fluorinated phosphonates for chemical biology. *J. Am. Chem. Soc*. **2015**, *137*, 3600–3609. (b) McCune, C. D.; Beio, M. L.; Sturdivant, J. M.; Salud-Bea, R.; Darnel, B. M.; Berkowitz, D. W. Synthesis and development of an elusive fluorovinyl cation equivalent: Access to quaternary a-(1'-fluoro)vinyl amino acids as potential PLP enzyme Inactivators. *J. Am. Chem. Soc*. **2017**, *139*, 14077–14089. (c) Malik, G.; Swyka, R. A.; Tiwari, V. K.; Fei, X.; Applegate, G. A.; Berkowitz, D. W. A thiocyanopalladation/carbocyclization transformation identified through enzymatic screening: Stereocontrolled tandem C–SCN and C–C bond formation. *Chem. Sci*. **2017**, *8*, 8050–8060. (d) Karukurichi, K. R.; Fei, X.; Swyka, R. A.; Broussy, S.; Shen,

W.; Dey, S.; Roy, S. K.; Berkowitz, D. W. Mini-ISES identifies promising carbafructopyranose-based salens for asymmetric catalysis: Tuning ligand shape via the anomeric effect. *Sci. Adv*. **2015**, *1*, 1–20.

Chapter: 2

Synthetic Approach towards Macrocyclic *β*-Keto Vinyl Sultams: Novel Macrocidin-like Tetramic Acid Analogs

Overview:

2.1 Introduction

2.1.1 Macrocycle-containing tetramic acids: Natural products and biological activities

2.1.2 Synthesis: Macrocidin and macrocidin-like molecules

2.2 Results

2.2.1 Synthetic design of β-keto vinyl sultam analogs of macrocidin A-like molecule

2.2.2 Synthesis of β-keto vinyl sultam analogs of macrocidin A-like molecule

2.3 Future work

2.4 Conclusion

2.1 Introduction

The design and development of efficient and economical protocols for the synthesis of medium- and large-sized bioactive heterocycles is an important component of the screening campaign for facilitating drug discovery. In particular, macrocyclic tetramic acid-containing natural products demonstrate a wide range of bioactivities and hence construction of macrocycles with the tetramic acid core is synthetically noteworthy. Macrocycles containing sulfur analogs of tetramic acids are also of great interest as they may lead to a new sub-class of heterocyclic molecules.

Macrocyclic tetramic acid-containing compounds are also prevalent in the literature; however, their macrocyclic *β*-keto sultam counterparts are void. As noted in Chapter 1, sulfur (*S*)-based heterocycles possessing the $R^1R^2N–SO_2R^3$ functional group have been

recognized as important due to their intrinsic physical properties capable of influencing biological systems.

Macrocyclic sultams are beginning to emerge in the literature[1] as seen in Figure 2.1 [**2.1-A–D**], however, to the best of our knowledge, reports of macrocyclic *β*-keto and *β*-keto vinyl sultam analogs are void in the literature. This portion of the thesis will describe the design and attempted routes toward the synthesis of macrocyclic *β*-keto vinyl sultam analogs of tetramic acids (Figure 2.1), that can be modulated electronically, sterically, and stereochemically.

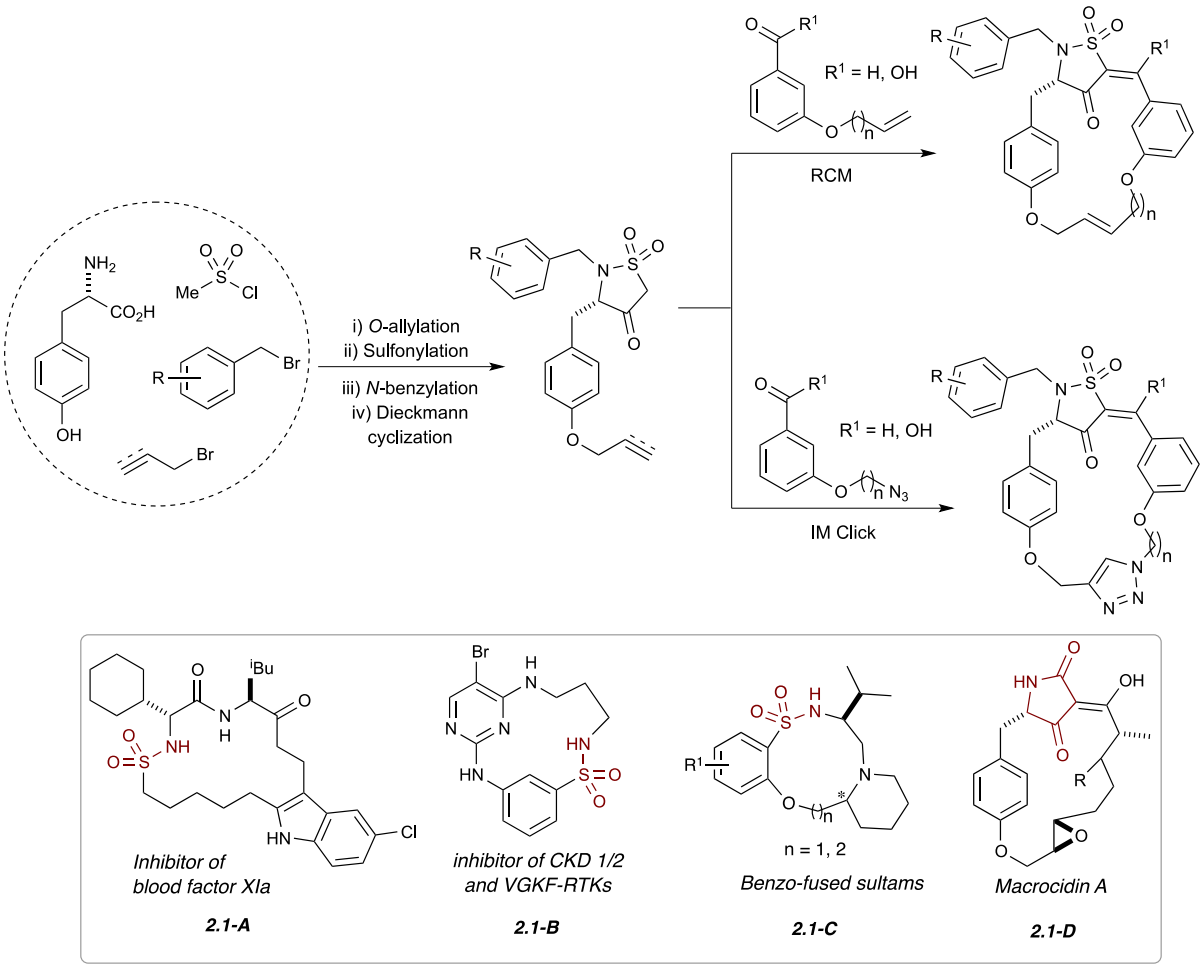

Figure 2.1: *Synthetic strategy of macrocyclic β-keto sultam analogs of tetramic acids.*

2.1.1 Macrocyclic tetramic acids: Natural products and biological activities

Macrocyclic compounds have an immense importance in applied chemistry. They have attracted a huge interest in research and development in the field of organic synthesis. Macrocycles can display remarkable features, such as selectivity, flexibility, conformational pre-organization, and high affinity with protein targets and hence are promising molecules for the modulation of protein-protein interactions.[2] Both natural and synthetic macrocyclic analogs display a wide range of biological activities ranging from anti-fungal, anti-helminthic, antibiotics, anti-viral and insecticidal agents in agriculture.[3] Macrocyclic organic compounds also demonstrate inhibitory effects, such as CDK2/cyclin A, Hsp90 and protein kinase C inhibitions in drug discovery.[4] Additionally, the significance of macrocycles has been demonstrated in drug development with more than a hundred naturally occurring and synthetic macrocycle-containing compounds currently being explored in therapy.[5]

Compared to small-molecules, macrocyclic compounds can address challenging and biologically compelling targets, such as protein-protein interface in a more efficient way.[6] Macrocycles have both pharmacological and physiochemical advantages over acyclic molecules in modulation of problematic molecular targets[7] and decreasing binding affinity by the preorganization of bioactive conformations.[8] The physiochemical advantages of macrocycles result from their structure, lower rotatable bond-count and ability to mask polar functionality by forming stable intramolecular H-bonds in low-dielectric environment.[9] Macrocyclic compounds containing highly reactive functional groups are particularly interesting as they provide an opportunity to modulate the physical and chemical properties of the compound. Such macrocycles possess structure-specific interactions and are therefore highly selective for their target molecules.[10]

As discussed in Chapter 1, tetramic acids represent an important structural motif that is present in many bioactive natural products. There are abundant examples of macrocyclic natural products containing a tetramic acid moiety in the literature that have excellent biological activities (Figure 2.2). Some of them are described here: Macrocidins A and B, both are acyltetramic acid isolated from *Phoma macrostoma* and are inhibitors of weeds growth and chlorosis.[11] Cylandrimide A, which is extracted from the Halichondria sponge, is potent against various cancer cell lines.[12] HSAF (heat-stable antifungal factor) is a known herbicide that controls plant fungal disease in agriculture and are also known to inhibit several fungal pathogens.[13] Frontalamides A and B were discovered from *Streptomyces* species while Frontalamide FI-2 was obtained by genetic engineering on *Streptomyces* species[14]. All variants of this macrocyclic tetramic acid family show antifungal activity. Clifednamides are also macrocyclic tetramic acid analogs obtained by genetic engineering from the strain of *Streptomyces* species and display antifungal activity.[15] Discodermide has been isolated from *Discodermia* species and is known to possess cytotoxic and antifungal properties.[16] Ikarugamycin is a macrocyclic antibiotic isolated from *Streptomyces* species of symbiotic bacteria and demonstrates potent antiprotozoal activity as well as cytotoxic effects in cancer cell lines via genotoxicity and caspase activation ultimately leading to apoptosis.[17] Aburatubolactam A is a tetramic acid containing a macrolactam and is isolated form the bacteria of *Streptomyces* species found in marine mollusk.[18] Aburatubolactam A is known to possess cytotoxicity, antimicrobial activity and the inhibition of superoxide generation.

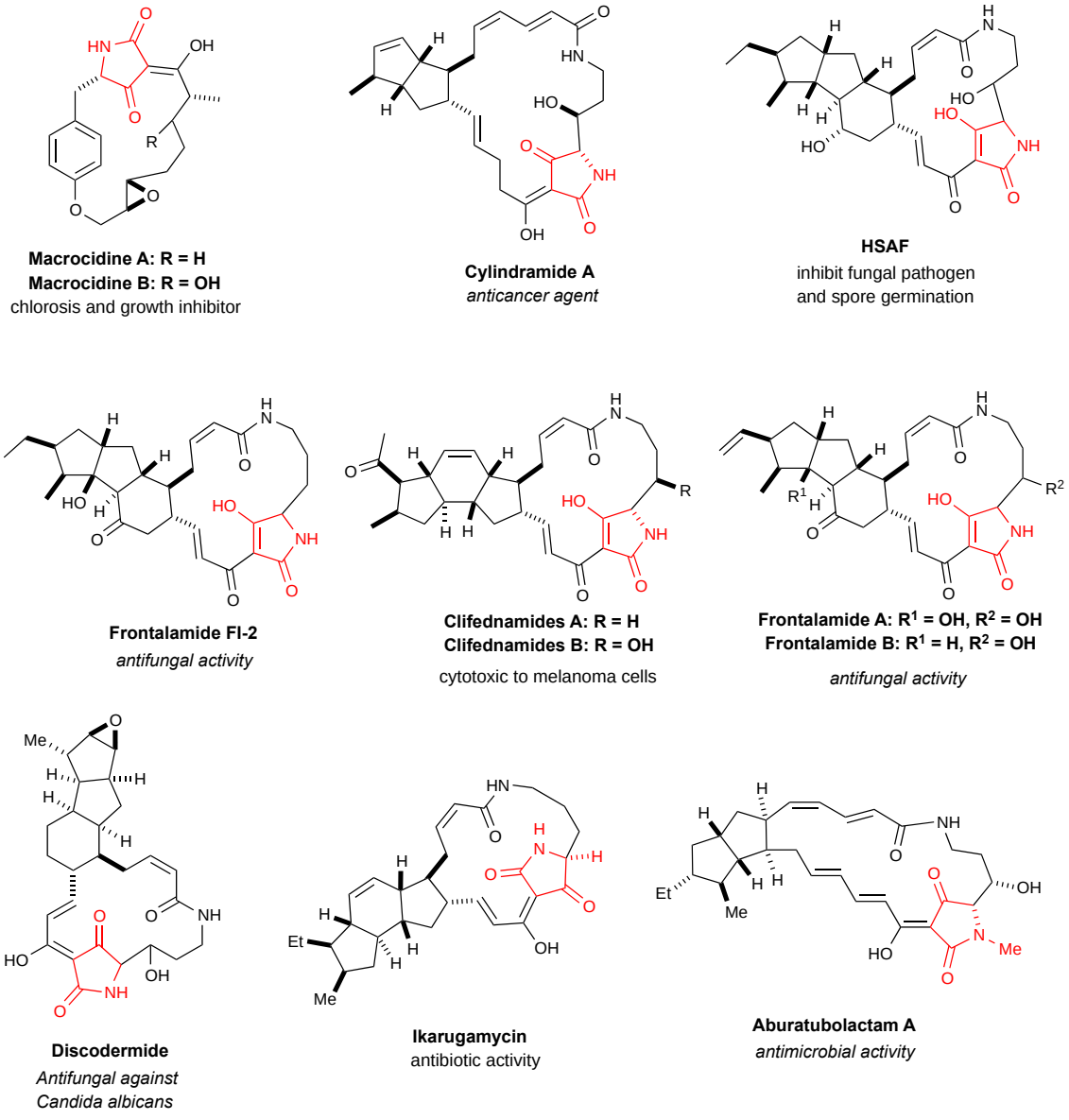

Figure 2.2: *Macrocyclic natural products having tetramic acid core.*

2.1.2 Synthesis: Macrocidin and macrocidin-like molecules

Macrocidin has garnered lots of interest in the synthetic world since it was first isolated from the liquid culture of *Phoma macrostoma* that was obtained from a diseased Canada thistle.[11] The interest was mainly because of its selective activity on broadleaf weeds while remaining inactive on grass weeds. Several attempts have been put forward for the

synthesis of Macrocidin and in these attempts; some of macrocidin-like molecules have also been made and tested for biological activity.[19]

In 2006, Ramana and coworkers attempted to synthesize *des*-methylmacorcidin A using PMB-protected *O*-allyl-L-tyrosine methyl ester **2.1.1** and protected *β*-keto ester **2.1.2** to afford the *β*-ketoamide **2.1.3** (Scheme 2.1)[20]. The diene **2.1.3** was subjected to Lacey–Dieckmann cyclization condition to obtain the RCM precursor containing tetramic acid core **2.1.4** in 91% yield. **G-II**-catalyzed RCM on diene **2.1.4** afforded the macrocidin analog **2.1.6** in poor yield. In an alternative strategy, **2.1.3** was first subjected to a **G-I** catalyzed RCM to form the macrocycle **2.1.5** with a good yield of 63%, followed by *t*-butoxide-mediated cyclization, to obtain *des*-methylmacrocidin A **2.1.6** in good yield. The authors also mentioned that they were unsuccessful in both Lacey–Dieckmann cyclization and RCM,

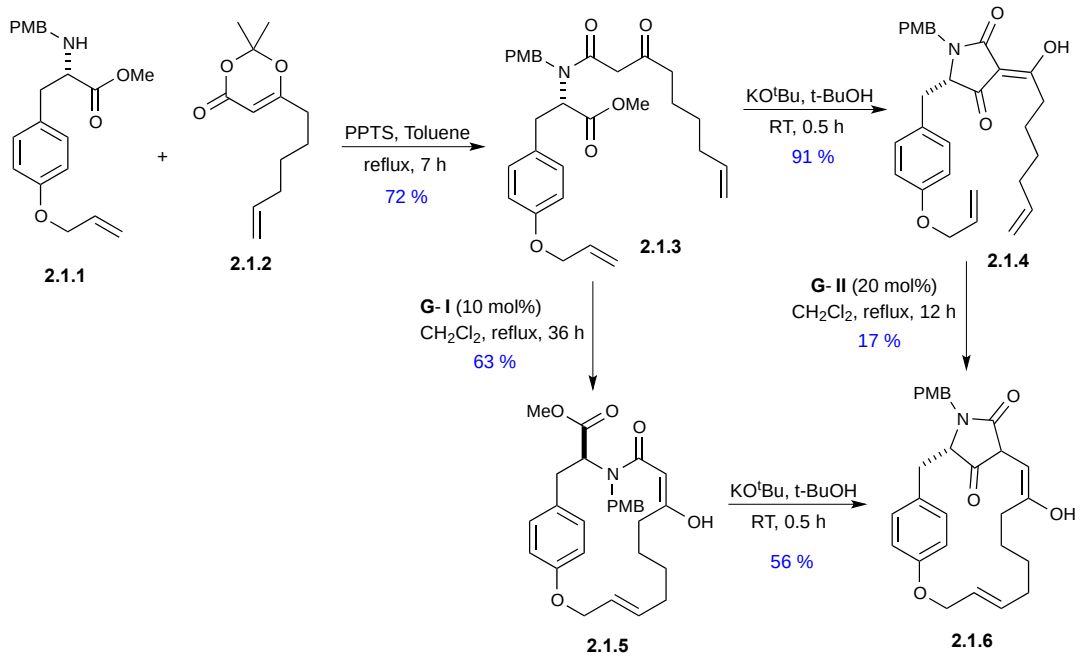

Scheme 2.1: *Synthesis of des-methylmacrocidin A.*

without PMB-protection of the amine functional group. Although several attempts were made to install the epoxide in **2.1.6**, none of them were successful as the starting material was decomposing in all the cases.

In 2010, Schobert and coworkers demonstrated the synthesis of nor-macrocidin A based on C3-acylation of tyrosine-derived tetramic acid **2.2.1**, followed by Williamson etherification (Scheme 2.2).[21] For proof-of-concept, the authors started with the bis-protected tyrosine **2.2.1** to generate the corresponding tetramic acid **2.2.2** using Meldrum's acid. Subsequent acylation with ω-bromo acid at the C3 position of **2.2.2** afforded the C3-acylated tetramic acids **2.2.3**. $Pd(PPh_3)_4$ was used for deallylation of **2.2.3**, which promoted *in situ* etherification via the phenolate anion, to afford macrocycle **2.2.4**.

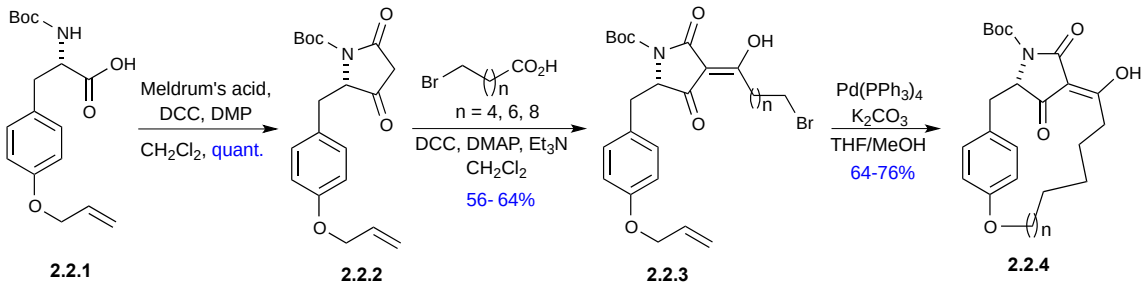

Scheme 2.2*: Synthesis of Macrocidin like molecule **2.2.4**.*

After successful synthesis of tetramic acid macrocycle **2.2.4**, the authors applied a similar strategy to synthesize nor-macrocidin A **2.3.2** using the acetonide-bearing ω-bromo acid **2.3.6** and tyrosine-derived tetramic acid **2.2.2** (Scheme 2.3). For the synthesis of **2.3.6**, the authors used caprolactone **2.3.3** and reduced it to the corresponding lactol, followed by Wittig alkenylation, and PMB-protection to afford **2.3.4**. The resulting olefin was subjected to asymmetric dihydroxylation using AD-mix, followed by acetonide protection of diol and $LiAlH_4$ reduction of ester to yield the corresponding primary alcohol **2.3.5**. The resulting

alcohol was converted to the corresponding bromide in a couple of steps. DDQ-mediated PMB-deprotection and oxidation of the resulting alcohol using PDC furnished the corresponding carboxylic acid within the coupling partner **2.3.6**.

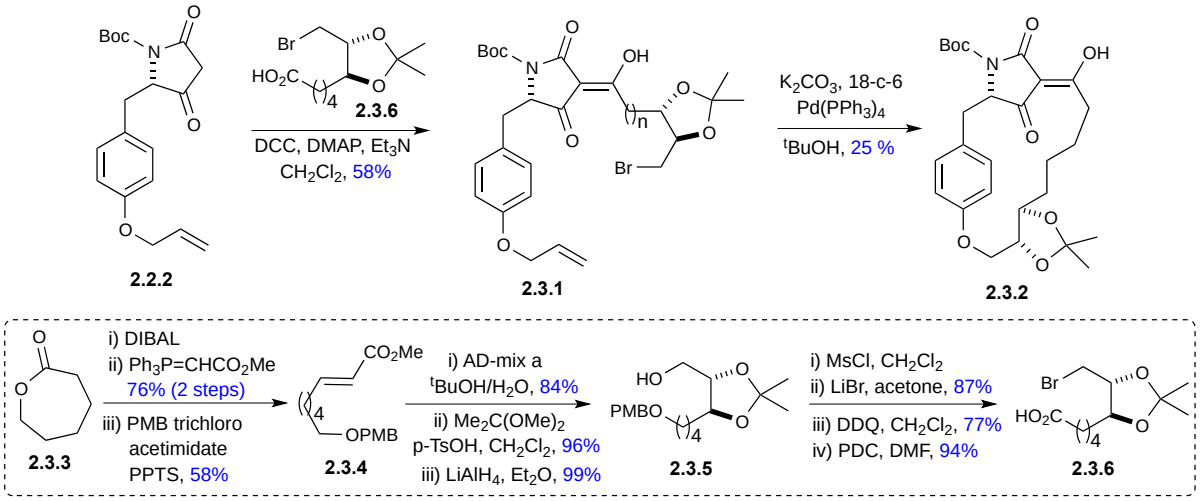

Scheme 2.3*: Synthesis of nor–Macrocidin A.*

In 2010, Suzuki and coworkers reported the first total synthesis of Macrocidin A (Scheme 2.4).[22] The authors started their synthesis with propargyl alcohol to generate the desired acid for reaction with tyrosine. In two steps, propargyl alcohol was converted to allylic alcohol and next to epoxide **2.4.2** using the Katsuki-Sharpless asymmetric epoxidation. The primary alcohol was protected as silyl ether before subjecting the compound to an Rh-catalyzed hydroboration-oxidation sequence, which was followed by Swern oxidation to furnish aldehyde **2.4.3**. Horner-Emmons olefination with phosphonate **2.4.4**, followed by desilylation and epoxide ring opening, yielded the 1,3-diol **2.4.5**. The desired epoxy alcohol **2.4.6** was synthesized from **2.4.5** using an Ir-catalyzed asymmetric hydrogenation. Final regeneration of the epoxide was accomplished using potassium carbonate in MeOH.

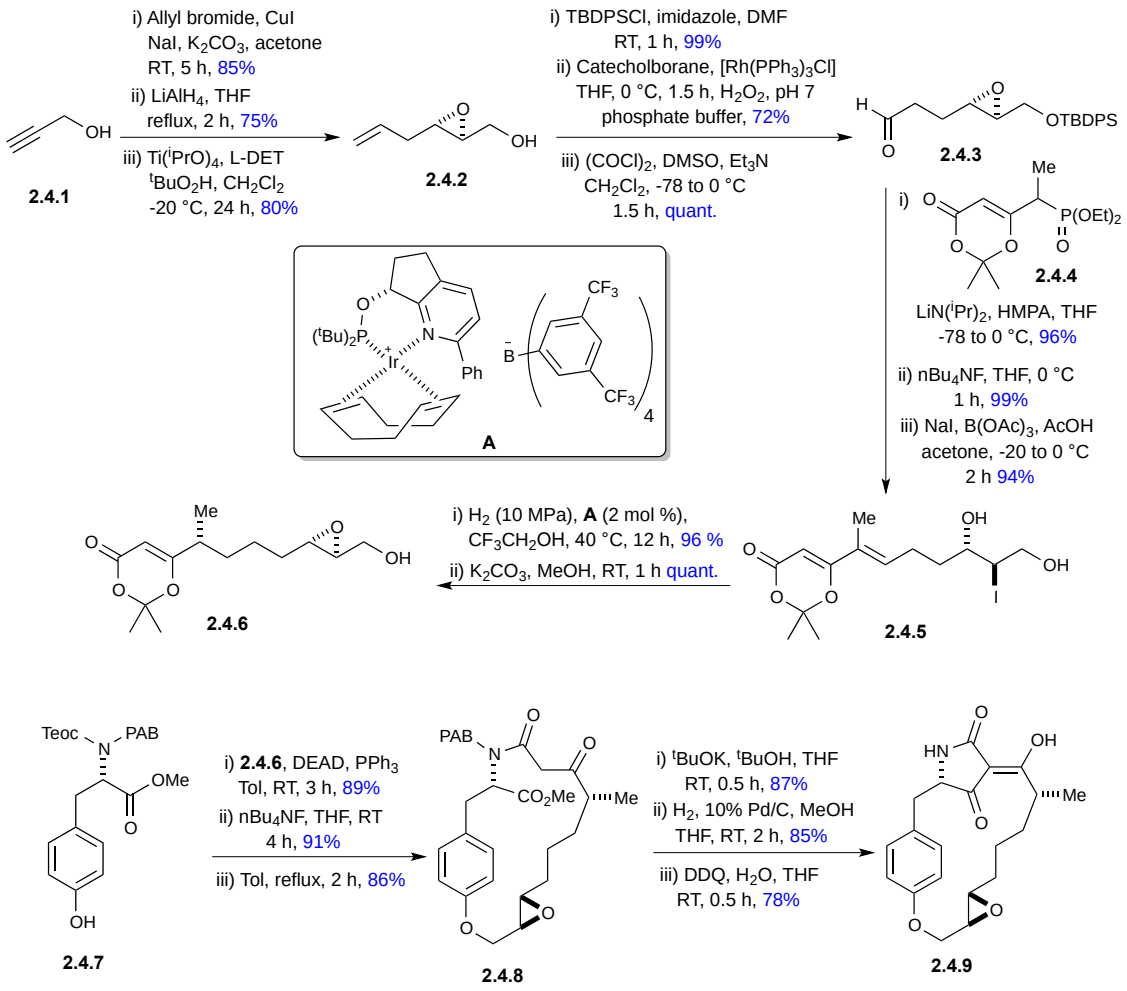

Scheme 2.4: *Total synthesis of macrocidin A*

With **2.4.6** in hand, the authors coupled with bis-*N*-protected tyrosine precursor **2.4.7** using Mitsunobu conditions. Next, TBAF-mediated deprotection of the 2-(trimethylsilyl) ethoxycarbonyl (Teoc) group was performed to furnish the macrolactam precursor, which was next subjected to acyl-ketene cyclization in refluxing toluene to afford macrocycle **2.4.8**. Lacey–Dieckmann cyclization on macrolactam **2.4.8** using KOtBu in *t*-butanol provided the tetramic acid core. The final product, macrocidin A (**2.4.9**) was obtained by the deprotection of the PAB-group using hydrogenation conditions, followed by treatment with DDQ.

In 2016, Schobert and coworkers reported the total synthesis of macrocidin A (Scheme 2.5).[23] The authors started the synthesis of side chain fragment **2.5.5** from 5-bromovaleric acid **2.5.1**, which was converted to a mixed anhydride and allowing coupling with the Evans auxiliary, followed by enolate formation, and subsequent methylation to furnish **2.5.2** in 84% yield. This intermediate **2.5.2** was subjected to Finkelstein halogen exchange, followed by *in situ* generation of the organozincate, which on Pd(0) catalyzed coupling with vinyl iodide, afforded **2.5.3**. Removal of the auxiliary from intermediate **2.5.3** followed by silyl deprotection and diastereoselective Sharpless epoxidation furnished epoxy alcohol **2.5.4**. Epoxy alcohol was mesylated and converted to the corresponding bromide using LiBr. The desired carboxylic acid **2.5.5** was obtained by hydrogenolytic cleavage of the benzyl ester. After the synthesis of the side-chain fragment, the next step was coupling with tyrosine. To commence the coupling step, the authors used *O*-allylated tyrosine **2.6.1** and treated with Meldrum's acid in the presence of EtOAc to construct the tetramic acid core within **2.6.2** (Scheme 2.6). The tetramate **2.6.2** was next coupled with the carboxylic acid

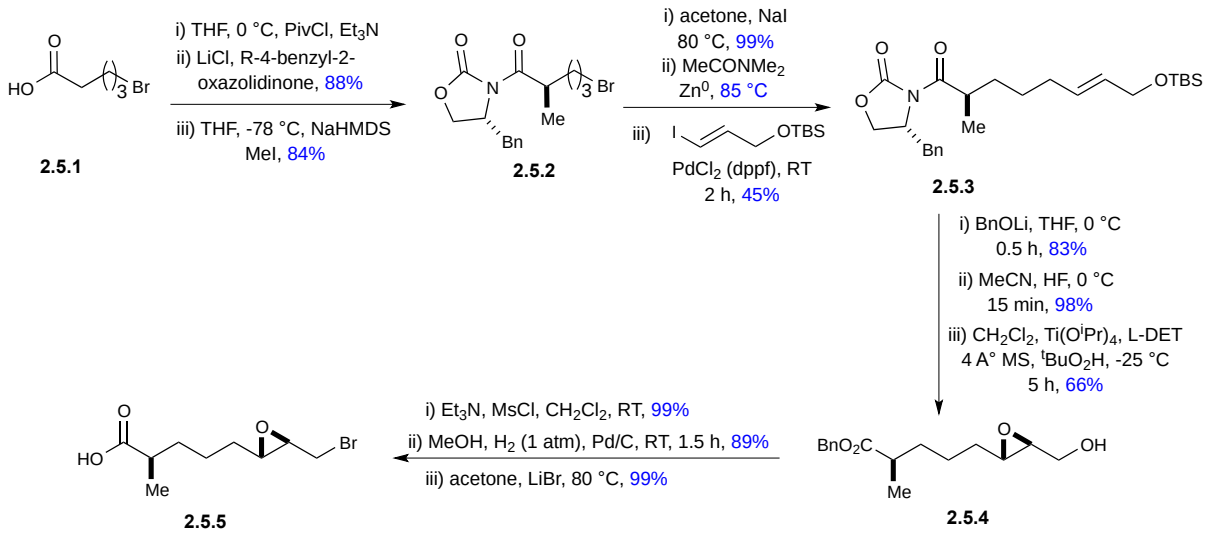

Scheme 2.5: *Synthesis of epoxy bromide.*

2.5.5 to furnish the 4-*O*-acyltetramate **2.6.3**, which subsequently underwent a Fries-type acyl rearrangement, to furnish 3-acyltetramic acid **2.6.4**. The final step in the total synthesis of macrocidin A was Pd(0)-catalyzed deallylation of **2.6.4** followed by Williamson etherification to achieve the desired product **2.6.5**.

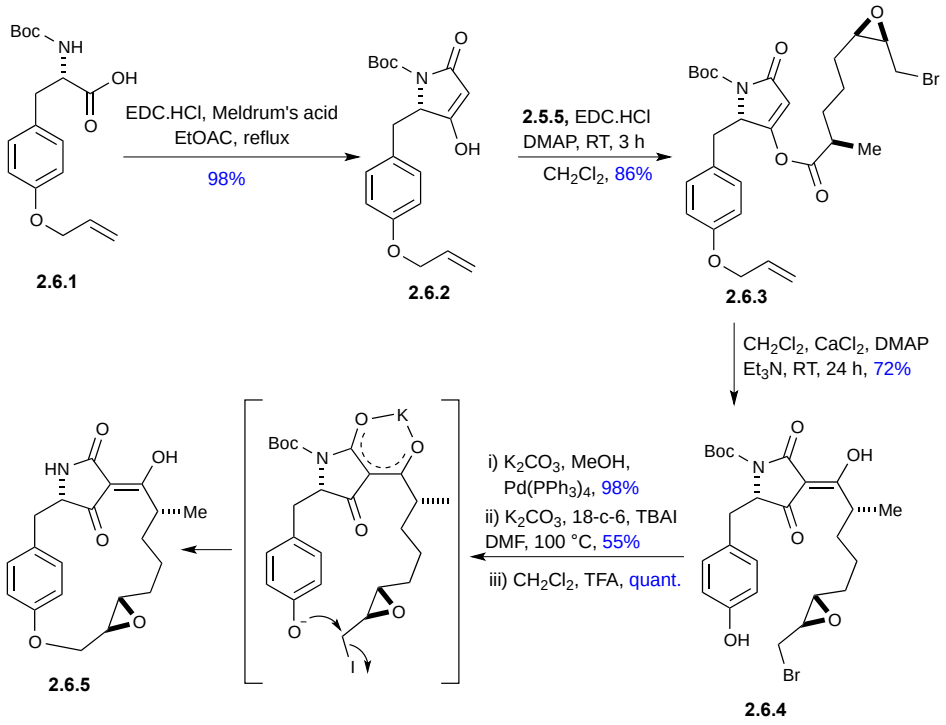

Scheme 2.6: *Synthesis of macrocidin A via Williamson's etherification.*

2.2 Results

Inspired by the potent bioactivities of macrocyclic tetramic acid, more specifically macrocidin A, sulfonamides and sultams, we are interested in the design and synthesis of macrocyclic *β*-keto vinyl sultam analogs of tetramic acids that can be modulated electronically, sterically and stereochemically. We also aim for future reactivity profiling studies of these novel *S*-containing unsaturated macrocyclic electrophiles with thiols and cysteine residues to test our hypothesis of them being used as macrocyclic covalent

inhibitors. Our ultimate aim is to use these compounds as probes that can target the shallow binding sites of rare protein residues and enzymes.

2.2.1 Synthetic design of sultam analogs of macrocidin A-like molecule

Our lab has been interested in the synthesis of diverse sultam scaffolds as discussed earlier in chapter 1. Along this line, we have designed the synthesis of sulfur containing macrocyclic compounds. Such compounds will help in comparative and comprehensive ranking of elaborate electrophilic compounds, such as macrocycles bearing complex stereochemical arrays, structural conformations, ring size, and attenuated *S*-warheads.

Our design is based on the synthesis of a tyrosine-derived tetramic acid, which can be achieved by esterification, *O*-allylation/propargylation, mesylation, *N*-benzylation and cyclization of tyrosine (Figure 2.3). Once the tyrosine-derived tetramic acid is formed, macrocyclization is envisioned via a ring-closing metathesis (RCM) reaction (**2.3-A** and **2.3-C**) or intra molecular click (IM click) reaction (**2.3-B** and **2.3-D**). The reactivity of the resulting macrocycles will be assessed using different thiol- and oxo-nucleophiles and the progression of the reactions will be monitored by ^{1}H, ^{19}F NMR and LC-MS.

2.2.2 Synthesis of sultam analogs of macrocidin A-like molecule

Our synthesis commenced with the generation of tyrosine methyl ester **2.7.2** by the reaction of L-tyrosine **2.7.1** and thionyl chloride in MeOH and heating the reaction mixture at 60 ˚C for 6 hours (Scheme 2.7). The solvent, MeOH, was evaporated under reduced pressure and the reaction mixture was directly subjected to TBS-protection of the phenol moiety. This method gave us 37% yield of the TBS-protected L-tyrosine methyl ester **2.7.3**.

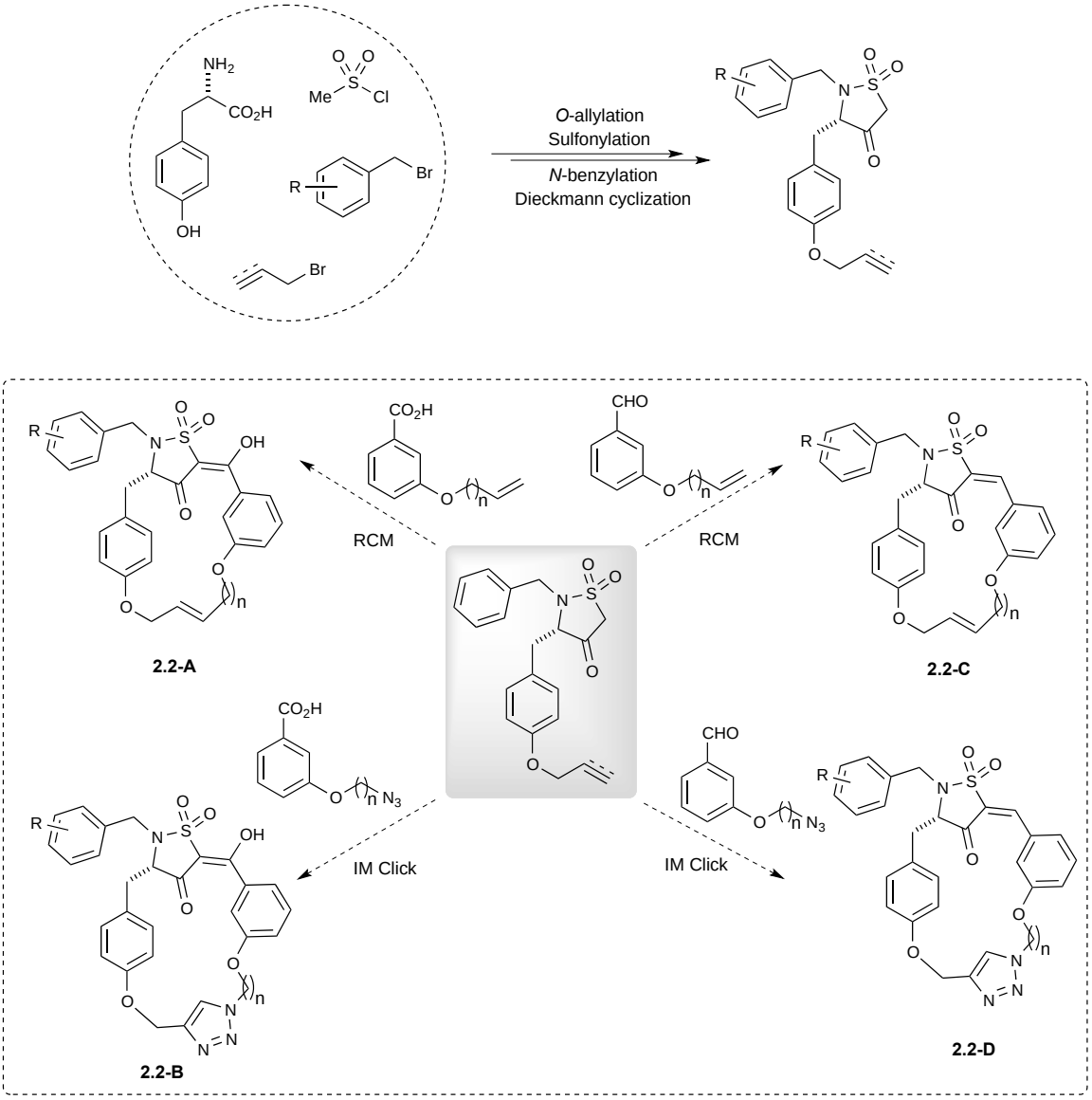

Figure 2.3: *Design and synthetic strategy for the synthesis of macrocidin-like compound.*

We realized that the low yield of **2.7.3** might be due to the protonation of **2.7.2** by the HCl formed during esterification. So, the reaction mixture of esterification reaction was washed with water and extracted with EtOAc several times until the aqueous portion did not show the presence of the compound by TLC. This improvised procedure yielded 77% over two steps. The next step involved simple mesylation of **2.7.3**, which was accomplished by use of MsCl and Et_3N to generate the mesylated tyrosine derivative **2.7.4**.

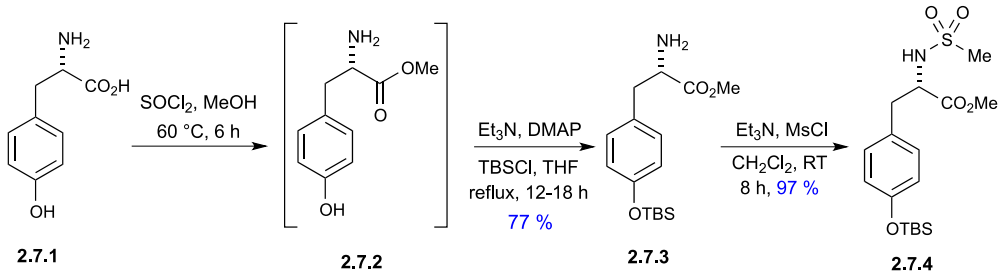

Scheme 2.7: *Synthesis of mesylated L-tyrosine methyl ester.*

Compound **2.7.4** was *N*-benzylated using several substituted benzyl bromides in the presence of potassium carbonate as base to furnish **2.8.1** (Scheme 2.8). The acyclic intermediate **2.8.1** was then subjected to Dieckmann-type cyclization conditions. In this method, the compound was dissolved in dry THF and the temperature was lowered to -78 ˚C, then LiHMDS was added dropwise to the cold reaction mixture to generate the tetramic acid analog **2.8.2**. The reaction was very sensitive to moisture as any hint of moisture in the reaction medium completely prevented the reaction, resulting in full recovery of starting material. The TBS-protected phenol of tetramic acid analog **2.8.2** was deprotected using TBAF in THF to afford the *β*-keto sulfonamide **2.8.3**.

Our next step towards macrocyclization was to introduce an allyl group to the phenol of **2.8.3**. Several attempts of allylation gave unsatisfactory low yields (<27%) with multiple spots in TLC. After obtaining multiple spots in the TLC across several runs, combined with a low yield of the desired product, we reasoned that we were generating more than one nucleophilic site within the starting material (ie, the pKa of phenol is roughly equal to or lower than the proton at the C3 position of the sultam tetramate **2.8.3**). Therefore, to avoid competitive reactions, we took an alternative approach.

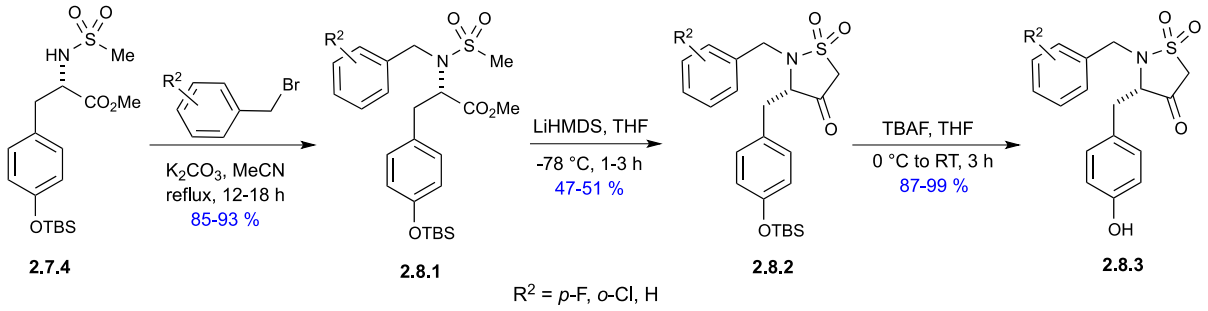

Scheme 2.8: *Tyrosine derived β-keto sultam.*

We decided to install the allyl group prior to Dieckmann cyclization. Hence compound **2.8.1** was treated with TBAF in THF to deprotect the TBS group to generate **2.9.1**, which was subsequently allylated using allyl bromide in the presence of K_2CO_3 with refluxing in CH_3CN to generate compound **2.9.2**. Subsequent Dieckmann cyclization of **2.9.2** afforded *β*-keto sulfonamide **2.9.3**.

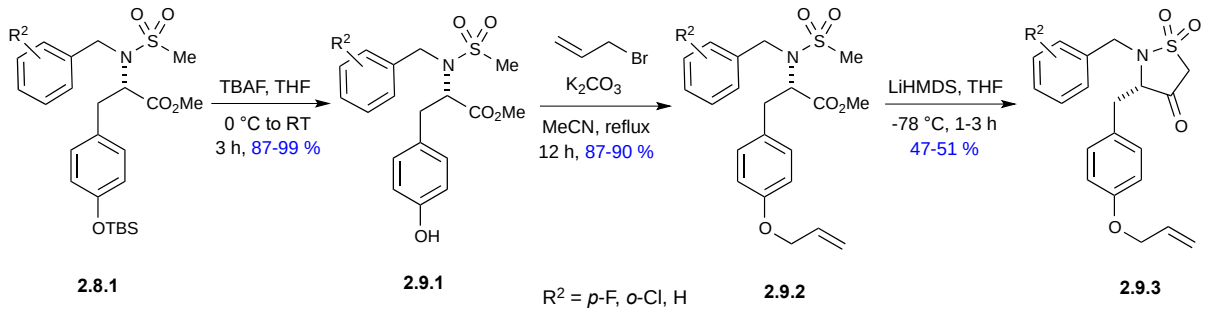

Scheme 2.9: *Synthesis of β-keto sultam.*

Besides tyrosine, serine was also used for the purpose of macrocyclization (Scheme 2.10). Similar sets of reactions, as performed with tyrosine, were conducted in an attempt to obtain a serine-based macrocycle. It will be interesting to see the differences in the properties of these macrocycles and their roles as electrophilic probes.

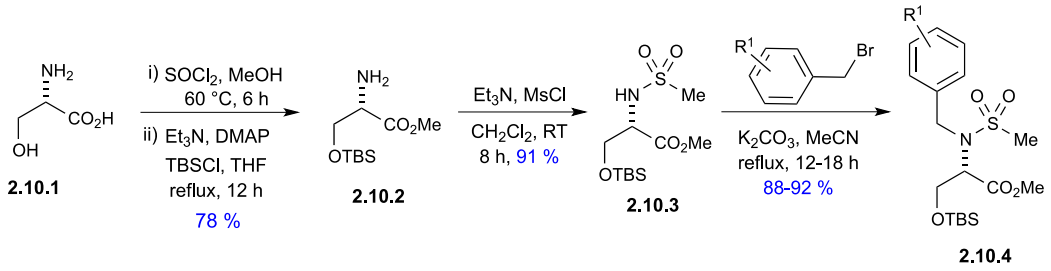

Scheme 2.10: *Synthesis of mesylated L-serine methyl ester.*

With construction of the *β*-keto sulfonamide core, we next needed an aldehyde to couple with the allylated tetramic acid **2.9.3**. Several aldehydes with varying chain lengths were made using 3-hydroxybenzaldehyde **2.11.1** (Scheme 2.11). The aldehyde **2.11.1** was reacted with allyl bromide and two other terminal alkene bromides to generate the *O*-substituted 3-hydroxy aldehydes **2.11.2**–**2.11.5**. The substituted aldehyde **2.11.8** was formed by reacting **2.11.1** with tosylated allyloxyethanol **2.11.7** in the presence of cesium carbonate (Cs_2CO_3).

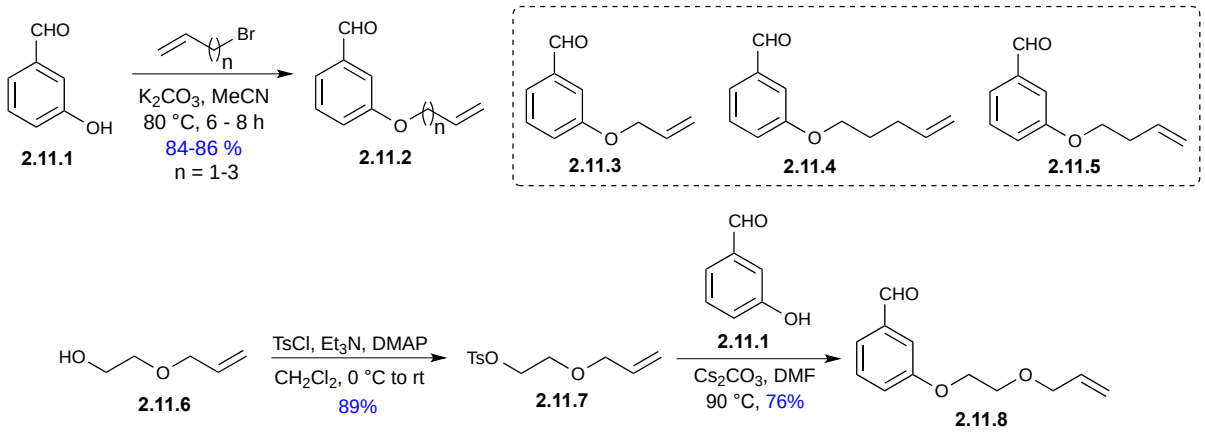

Scheme 2.11: *Synthesis of O-substituted 3-hydroxy aldehydes.*

With the desired aldehydes in hand, we coupled aldehyde **2.11.3** with the allylated *β*-keto sulfonamide **2.12.1** using the aforementioned Knoevenagel conditions (Chp-1) employing L-proline as a catalyst in the polar protic solvent trifluoroethanol. After 12 h of

stirring at 50 ˚C, the coupled product **2.12.2** was obtained in 34% yield (Scheme 2.12). The lower yield was mainly due to a challenge in purification of this product. It was observed that the product was highly unstable on silica gel and converted back to starting material during column separation. Several modification and alternatives were tried to enhance the yield of the reaction, such as use of neutral alumina, using small amount of 0.1% acetic acid or 0.1% of triethyl amine to column. So far, we were not able to increase the yield of the Knoevenagel condensation reaction.

Our attempt of RCM of **2.12.2** remained unsuccessful. Several cyclization conditions were investigated, the first of which consisted of 5 mol% of Grubbs II catalyst in CH_2Cl_2 and refluxing for an hour. Further optimizations were done by increasing the amount of catalyst to 15 mol% as well as changing the solvent to toluene. In all these cases decomposition of starting material was observed. These failures prompted us to question the stereochemistry at the olefin of the Knoevenagel products, and drove the aforementioned X-ray and NMR studies outlined at the end of Chapter 1, where we were able to obtain crystals of some of the unsaturated *β*-keto sultams. As noted before, the X-ray crystal structure of those compounds

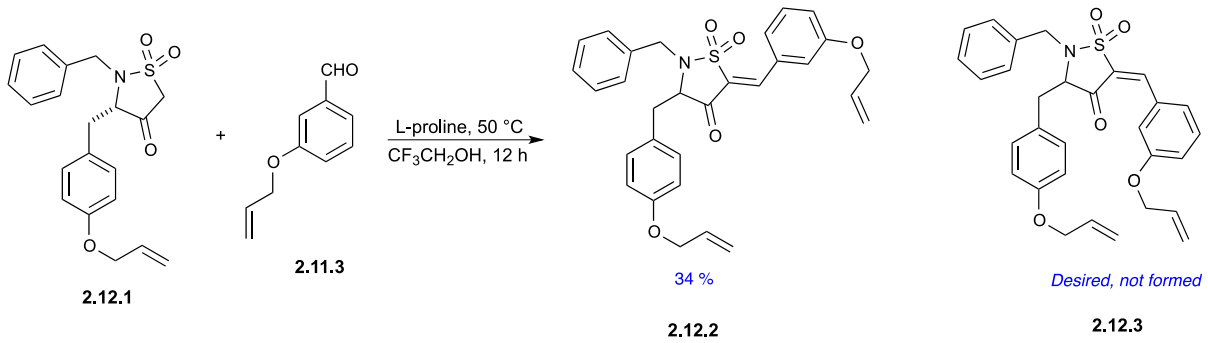

2.12.1 + 2.11.3 → 2.12.2 (34 %) + 2.12.3 (Desired, not formed)

Scheme 2.12: *Knoevenagel condensation of β-keto sulfonamide and aldehyde*.

revealed the '*Z*' configuration (Fig 1.13, Chapter-1). On the basis of the X-ray structure of **2.4-A** and **2.4-B** we rationalized that the Knoevenagel condensation of *β*-keto sultams **2.12.1** did not result in the formation of desired *E*-olefin **2.12.3**, but rather the *Z*-olefin was obtained. This finding was contrary to our targeted compound and was one of the possible reasons for RCM failure.

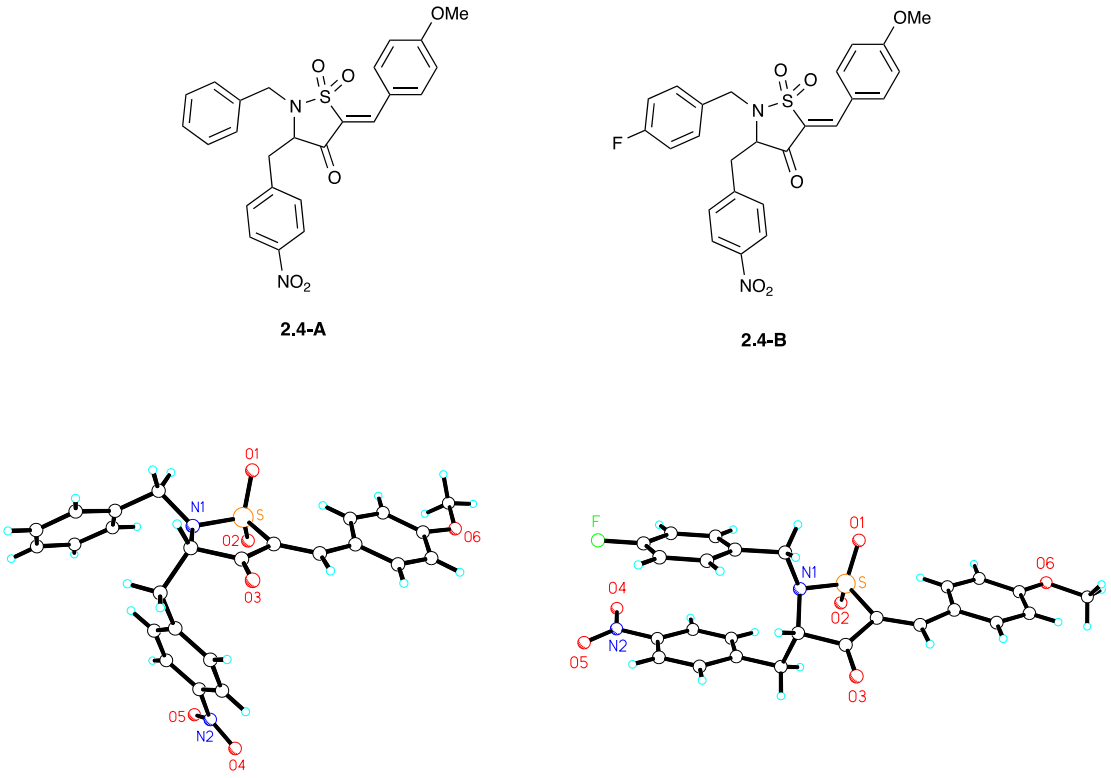

Figure 2.4: *X-ray crystal structures of β-keto vinyl sultams*

2.3 Future work

(i) After revealing the stereochemistry at the olefin position, we are now aiming to perform RCM by installing a terminal olefinic *N*-substituent rather than at the side-chain as shown in Figure 2.5. After the synthesis of the macrocyclic β-keto vinyl sultams, preliminary

reactivity profiling studies will be performed in our lab with thiols and cysteine residue as well as ABPP studies in the laboratories of our collaborators.

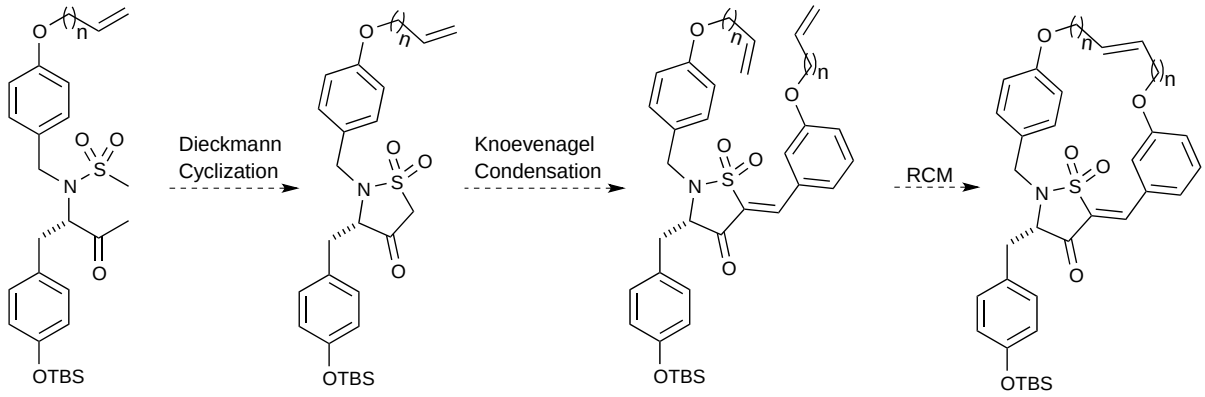

Figure 2.5: *Proposed alternative approach towards macrocyclic β-keto vinyl sultam analogs.*

2.4 Conclusion

In summary, an attempt towards the synthesis of macrocidin-like *β*-keto vinyl sultams has been reported along with the potential modification for successful synthesis. The synthetic route commences with *L*-tyrosine followed by *N*-mesylation, *O*-allylation, *N*-benzylation, Dieckmann type cyclization, and Knovenagel condensation. After identifying the probable cause for unsuccessful RCM, an alternative synthetic method has been proposed for macrocyclization, and will be reported in due course.

2.5 References

[1] (a) Hanessian, S.; Larsson, A.; Fex, T.; Knecht, W.; Blomberg, N. Design and synthesis of macrocyclic indoles targeting blood coagulation cascade Factor XIa. *Bioorg. Med. Chem. Lett.* **2010**, *20*, 6925−6928. (b) Aldrich, L. N.; Kuo, S.-Y.; Castoreno, A. B.; Goel, G.; Petric Kuballa, P.; Rees, M. G.; Seashore-Ludlow, B. A.; Cheah, J. H.; Latorre, I. J.; Stuart, L.; Schreiber, S. L.; Shamji, A. F.; Xavier, R. J. Discovery of a small-molecule probe for V-ATPase function. *J. Am. Chem. Soc.* **2015**, *137*, 5563−5568. (c) Loh, J. K.; Asad, N.; Samarakoon, T. B.; Hanson, P. R. Modular, one-pot, sequential aziridine ring opening-S_NAr strategy to 7-, 10-, and 11-membered benzo-fused sultams. *J. Org. Chem*. **2015**, *80*, 9926-9941.

[2] (a) Udugamasooriya, D. G.; Spaller, M. R. Conformational constraint in protein ligand design and the inconsistency of binding entropy. *Biopolymers* **2008**, *89*, 653–667. (b) Giordanetto, F.; Kihlberg, J. Macrocyclic drugs and clinical candidates: what can medicinal chemists learn from their properties? *J. Med. Chem.* **2014**, *57***,** 278–295. (c) Yudin, A. K. Macrocycles: lessons from the distant past, recent developments, and future directions. *Chem. Sci.* **2015**, *6*, 30–49. (d) Villar, E. A.; Beglov, D.; Chennamadhavuni, S.; Porco, J. A.; Kozakov, D.; Vajda, S.; Whitty, A. How proteins bind macrocycles. *Nat. Chem. Biol.* **2014**, *10*, 723–731. (e) Gavenonis, J.; Sheneman, B. A.; Siegert, T. R.; Eshelman, M. R.; Kritzer, J. A. Comprehensive analysis of loops at protein-protein interfaces for macrocycle design. *Nat. Chem.Biol.* **2014**, *10*, 716–722. (f) Mai, A. Targeting epigenetics in drug discovery. *Chem. Med. Chem.* **2014**, *9*, 415–417.

[3] (a) Hegde, V. R.; Patel, M. G.; Gullo, V. P.; Ganguly, A. K.; Sarre, O.; Puar, M. S. Macrolactams: a new class of antifungal agents. *J. Am. Chem. Soc.* **1990**, *112*, 6403–6405. (b) Ayers, S.; Zink, D. L.; Powell, J. S.; Brown, C. M.; Grund, A.; Genilloud, O.; Salazar, O.; Thompson, D.; Singh, S. B. Anthelmintic macrolactams from Nonomuraea turkmeniaca MA7381. *J. Antibiot.* **2008**, *61*, 59–62. (c) Velten, R.; Erdelen, C.; Gehling, M.; Gohrt, A.; Gondol, D.; Lenz, J.; Lockhoff, O.;

Wachendorff, U.; Wendisch, D. Cripowellin A and B, a novel type of amaryllidaceae alkaloid from *Crinum powellii. Tetrahedron Lett.* **1998**, *39*, 1737–1740.

[4]. (a) Patocka, J.; Soukup, O.; Kuca, K. Resorcylic acid lactones as the protein kinase inhibitors, naturally occuring toxins. *Mini-Rev. Med. Chem.* **2013**, *13*, 1873–1878. (b) Taldone, T.; Gozman, A.; Maharaj, R.; Chiosis, G. Targeting Hsp90: small-molecule inhibitors and their clinical development. *Curr. Opin. Pharmacol.* **2008**, *8*, 370–374. (c) Kollar, P.; Rajchard, J.; Balounova, Z.; Pazourek, J. Marine natural products: Bryostatins in preclinical and clinical studies. *Pharm. Biol.* **2014**, *52*, 237–242. (d) Yu, X.; Sun, D. *Molecules* **2013**, *18*, 6230–6268.

[5] Peterson, M. L. Macrocycles in Drug Discovery, RSC Drug Discovery Series, No. 40 (Ed.: J. Levin), RSC, Cambridge, **2015**, 398–486.

[6] (a) Driggers, E. M.; Hale, S. P.; Jinbo Lee, J.; Terrett, N. K. The exploration of macrocycles for drug discovery--an underexploited structural class. *Nat. Rev. Drug Discovery*. **2008**, *7*, 608−624. (b) Marsault, E.; Peterson, M. L. Macrocycles are great cycles: applications, opportunities, and challenges of synthetic macrocycles in drug discovery. *J. Med. Chem.* **2011**, *54*, 1961−2004. (c) Wells, J. A.; McClendon, L. Reaching for high-hanging fruit in drug discovery at protein-protein interfaces. *Nature*. **2007**, *450*, 1001−1009.

[7] Bogdan, A. R.; Jerome, S. V.; Houk, K. N.; James, K. Strained cyclophane macrocycles: impact of progressive ring size reduction on synthesis and structure. *J. Am. Chem. Soc.* **2012**, *134*, 2127−2138.

[8] (a) Udugamasooriya, G.; Saro, D.; Spaller, M. R. Bridged peptide macrocycles as ligands for PDZ domain proteins. *Org. Lett.* **2005**, *7*, 1203−1206. (b) Tao, Z.-F.; Le Wang, L.; Stewart, K. D.; Chen, Z.; Gu, W.; Bui, M.-H.; Merta, P.; Zhang, H.; Kovar, P.; Johnson, E.; Park, C.; Judge, R.; Rosenberg, S.; Sowin, T.; Lin., N.-H. Structure-based design, synthesis, and biological evaluation of potent and selective macrocyclic checkpoint kinase 1 inhibitors. *J. Med. Chem.* **2007**, *50*, 1514−1527.

[9] (a) Veber, D. F.; Johnson, S. R.; Cheng, H.-Y.; Smith, B. R.; Ward, K. W.; Kopple, K. D. Molecular properties that influence the oral bioavailability of drug candidates.

J. Med. Chem. **2002**, *45*, 2615−2623. (b) Rezai, T.; Yu, B.; Millhauser, G. L.; Jacobsen, M. P.; Lokey, R. S. Testing the Conformational Hypothesis of Passive Membrane Permeability Using Synthetic Cyclic Peptide Diastereomers. *J. Am. Chem. Soc.* **2006**, *128*, 2510−2511.

[10] Ogoshi, T.; Yamagishi, T.-A. Historical backgrounds of macrocyclic compounds. In *Monograph in supramolecular chemistry*, Royal Society of Chemistry, **2016**; pp 2.

[11] Graupner, P. R.; Carr, A.; Clancy, E.; Gilbert, J.; Bailey, K. L.; Derby, J.-A.; Gerwick, B. C. The Macrocidins: novel cyclic tetramic acids with herbicidal activity produced by *Phoma macrostoma*. *J. Nat. Prod.* **2003**, *66*, 1558–1561.

[12] (a) Cramer, N.; Laschat, S.; Baro, A.; Schwalbe, H.; Richter, C. Enantioselective total synthesis of cylindramide. *Angew. Chem., Int. Ed.* **2005**, *44*, 820–822. (b) Cramer, N.; Buchweitz, M.; Laschat, S.; Frey, W.; Baro, A.; Mathieu, D.; Richter, C.; Schwalbe, H. Total synthesis and NMR investigations of Cylindramide. *Chem.–Eur. J.* **2006**, *12*, 2488–2503. (c) Hart, A. C.; Phillips, A. J. Total synthesis of (+)-Cylindramide A. *J. Am. Chem. Soc.* **2006**, *128*, 1094–1095.

[13] (a) Giesler, L. J.; Yuen, G. Y. Evaluation of *Stenotrophomonas maltophilia* strain C3 for biocontrol of brown patch disease. *Crop Prot.* **1998,** *17*, 509–513. (b) Yu, F.; Zaleta-Rivera, K.; Zhu, X.; Huffman, J.; Millet, J. C.; Harris, S. D.; Yuen, G.; Li, X.-C.; Du, L. Structure and biosynthesis of heat-stable antifungal factor (HSAF), a broad-spectrum antimycotic with a novel mode of action. *Antimicrob. Agents Chemother*. **2007**, *51*, 64–72.

[14] Blodgett, J. A.; Oh, D.-C.; Cao, S.; Currie, C. R.; Kolter, R.; Clardy, J. Common biosynthetic origins for polycyclic tetramate macrolactams from phylogenetically diverse bacteria. *Proc. Natl. Acad. Sci. USA*, **2010**, *107*, 11692–11697.

[15] Cao, S.; Blodgett, J. A.; Clardy, J. Targeted Discovery of Polycyclic Tetramate Macrolactams from an Environmental *Streptomyces* Strain. *Org. Lett.* **2010**, *12*, 4652–4654.

[16] Gunasekera, S. P.; Gunasekera, M.; McCarthy, P. Discodermide: a new bioactive macrocyclic lactam from the marine sponge *Discodermia dissolute. J. Org. Chem.* **1991**, *56*, 4830–4833.

[17] (a) Jomon, K.; Kuroda, Y.; Ajisaka, M.; Sakai, H. A new antibiotic, Ikarugamycin. *J. Antibiot. (Tokyo)* **1972**, *25*, 271–280. (b) Hasumi, K.; Shinohara, C.; Naganuma, S.; Endo, A. Inhibition of the uptake of oxidized low-density lipoprotein in macrophage J774 by the antibiotic ikarugamycin. *Eur. J. Biochem.* **1992**, *205*, 841–846. (c) Luo, T.; Fredericksen, B.L.; Hasumi, K.; Endo, A.; Garcia, J. V. Human immunodeficiency virus type 1 Nef-induced CD4 cell surface downregulation is inhibited by Ikarugamycin. *J. Virol.* **2001**, *75*, 2488–2492.

[18] Henderson, J. A.; Phillips, A, J. Total synthesis of Aburatubolactam A. *Angew. Chem. Int. Ed.* **2008**, *47*, 8499–8501.

[19] Barnickela, B.; Bayliffeb, F.; Diestelc, R.; Kempfa, K.; Laschatb, S.; Pachalib, S.; Sassec, F.; Schlenka, A.; Schobert, R. Structure–activity relationships of precursors and analogs of natural 3–enoyl–tetramic acids. *Chem. Biodivers.* **2010**, *7*, 2830–2845.

[20] Ramana, C. V.; Mondal, M. A.; Puranik, V. G.; Gurjar, M. K. Synthetic studies toward macrocidins: an RCM approach for the construction of the central cyclic core. *Tetrahedron Lett.* **2006**, *47*, 4061–4064.

[21] Barnickel, B.; Schobert, R. Toward the Macrocidins: macrocyclization via Williamson etherification of a phenolate. *J. Org. Chem*. **2010**, *75*, 6716–6719.

[22] Yoshinari, T.; Ohmori, K.; Schrems, M. G.; Pfaltz, A.; Suzuki, K. Total synthesis and absolute configuration of Macrocidin A, a cyclophane tetramic acid natural product. *Angew. Chem. Int. Ed.* **2010**, *49*, 881 –885.

[23] Haase, R. G.; Schobert, R. Synthesis of the Bioherbicidal Fungus Metabolite Macrocidin A. *Org. Lett*. **2016**, *18*, 6352−6355.

Chapter: 3

Supporting Information for Chapters 1 and 2

Methods, Experimental Data and NMR Spectra

General Experimental Section

All air and moisture sensitive reactions were carried out in flame- or oven-dried glassware under argon atmosphere using standard gas tight syringes and septa. Stirring was achieved with oven-dried, magnetic stir bars. THF and CH_2Cl_2 were purified by passage through a purification system (Solv-Tek) employing activated Al_2O_3 (Pangborn, A. B.; Giardello, M. A.; Grubbs, R. H.; Rosen, R. K.; Timmers, F. J. Safe and Convenient Procedure for Solvent Purification. *Organometallics* **1996**, *15*, 1518–1520). Et_3N was purified by passage over basic alumina and stored over KOH. All olefin metathesis catalysts were acquired from Materia and used without further purification. Flash column chromatography was performed with SiO_2 obtained from Sorbent Technologies (30930M–25, Silica Gel 60 Å, 40–63 μm). Thin layer chromatography was performed on silica gel 60F254 plates (EM–5717, Merck). Deuterated solvents were purchased from Cambridge Isotope laboratories. ^1H, ^{19}F, and ^{13}C NMR spectra were recorded on a Bruker DRX–400 spectrometer operating at 400 MHz and 100 MHz respectively; or a Bruker DRX 500 operating at 500 MHz and 125 MHz respectively using $CDCl_3$ or Methanol–d_4 as solvents. Chemical shift values (δ) are reported in ppm (residual chloroform δ = 7.26 ppm and 77.0 ppm for ^1H and ^{13}C respectively). The ^1H spectra are reported as follows δ (multiplicity, coupling constant *J*, number of protons). High-resolution mass spectrometry (HRMS) was recorded on an LCT Premier Spectrometer (Micromass UK Limited) operating on ESI (MeOH). Melting points were obtained on a Thomas Hoover capillary melting point apparatus. FTIR spectroscopy was performed using a Shimadzu FTIR-8400S instrument. Observed rotations at 589 nm, were measured using AUTOPOL IV Model automatic polarimeter.

General Procedure A: To the solution of amino ester (1.0 equiv.) in CH_2Cl_2 (0.2 M), was added Et_3N (3.0 equiv.) at 0 ˚C. After 15 min of stirring, methanesulfonyl chloride (2.0 equiv.) was added to the reaction mixture, and the reaction was stirred for 15 min at 0 ˚C and warmed to room temperature. After 6 h, the reaction was quenched with water and extracted with CH_2Cl_2 (3x). The organic layer was washed with brine, dried ($MgSO_4$), filtered, and concentrated under reduced pressure.

General Procedure B: To the solution sulfonamide (1.0 equiv.) in MeCN (0.2 M), was added K_2CO_3 (3.0 equiv.) at room temperature. After 15 min of stirring, benzyl or allyl bromide (1.5 equiv.) was added to the reaction mixture, and the reaction was heated to 80 ˚C. After 14 h, MeCN was removed under reduced pressure and the compound was extracted with CH_2Cl_2 (3x). The organic layer was washed with brine, dried ($MgSO_4$), filtered, and concentrated under reduced pressure.

General Procedure C: To the solution of N–benzylated sulfonamide (1.0 equiv.) in dry THF (0.05 M), was added LiHMDS (3.0 equiv.) at -78 ˚C under argon atmosphere. After 2 h, the reaction mixture was quenched with saturated ammonium chloride solution and the compound was extracted with EtOAc (3x). The organic layer was washed with brine, dried ($MgSO_4$), filtered, and concentrated under reduced pressure.

General Procedure D: To the solution of tetramic acid analog (0.20 mmol, 1.0 equiv.) in 2,2,2-trifluoroethanol (1.5 ml), was added L-proline (20 mol%) at 50 ˚C. After 15 min of stirring, aldehyde (0.22 mmol, 1.1 equiv.) was added and stirred overnight at 50 ˚C. The reaction mixture was removed from heating and after it reached the room temperature, the reaction vessel was kept in ice-cold water. The precipitate formed was then washed with ethanol and hexane (3x each) to afford the product. If the product did not precipitate, the

reaction mixture was evaporated, and the compound was extracted with EtOAc (3x). The organic layer was washed with brine, dried ($MgSO_4$), filtered, and concentrated under reduced pressure.

General Procedure E: To the solution of amino ester (1.0 equiv.) in THF (0.2 M) at 0 ˚C, was added Et_3N (3.0 equiv.) followed by DMAP (20 mol%). After 15 min of stirring, TBSCl (2.5 equiv.) was added to the reaction mixture and refluxed overnight. The reaction mixture was quenched with water and extracted with EtOAc (3x). The organic layer was washed with brine, dried ($MgSO_4$), filtered, and the solvent removed under reduced pressure.

General Procedure F: To the solution of protected amino ester (1.0 equiv.) in THF (0.2 M) at 0 ˚C, was added TBAF (2.5 equiv.) dropwise. After 15 min of stirring, the reaction was brought to room temperature. After 2 h, the reaction was quenched with saturated ammonium chloride and the compound was extracted with EtOAc (3x). The organic layer was washed with brine, dried ($MgSO_4$), filtered, and concentrated under reduced pressure.

Methyl (methylsulfonyl)-L-phenylalaninate (1.22.3a)

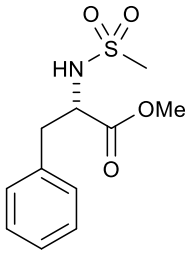

According to general procedure A; flash chromatography (100% Hexane to 15% EtOAc in Hexane) provided **1.22.3a** (2.1 g, 89%) as a pale-yellow oil.

TLC Rf = 0.4 (2:1 Hexanes/EtOAc) $[\alpha]^{25}_D$ = -29.7 (c = 2.1, $CHCl_3$)

HRMS calculated for $C_{11}H_{15}NO_4SNa$ $(M+Na)^+$ 280.0620; found 280.0627 (TOF MS ES+)

FTIR (neat): 3251, 1738, 1607, 1348, 1170 cm^{-1}

^{1}H NMR ($CDCl_3$, 400 MHz) δ 7.39 – 7.23 (m, 3H), 7.23 – 7.17 (m, 2H), 5.14 (d, *J* = 9.3 Hz, 1H), 4.38 (ddd, *J* = 9.3, 7.7, 5.1 Hz, 1H), 3.77 (s, 3H), 3.16 (dd, *J* = 13.7, 5.1 Hz, 1H), 2.99 (dd, *J* = 13.8, 7.7 Hz, 1H), 2.63 (s, 3H).

^{13}C NMR ($CDCl_3$, 126 MHz) δ 172.1, 135.7, 129.6, 128.9, 127.5, 57.3, 52.8, 41.3, 39.4.

Methyl (S)-2-(methylsulfonamido)-3-(4-nitrophenyl)propanoate (1.22.3b)

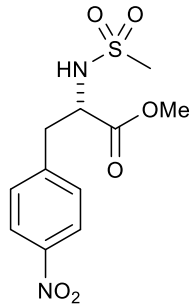

According to general procedure A; flash chromatography (5% EtOAc in Hexane to 25% EtOAc in Hexane) provided **1.22.3b** (3.25 g, 85%) as a pale orange solid.

MP = 174 – 176 ˚C; TLC Rf = 0.3 (2:1 Hexanes/EtOAc) $[\alpha]^{25}_{D}$ = 27.7 (c =1.1, $CHCl_3$)

HRMS calculated for $C_{11}H_{14}N_2O_6SNa$ $(M + Na)^+$ 325.0470; found 325.0478 (TOF MS ES+)

FTIR (KBr film): 3251, 1738, 1607, 1524, 1348, 1170 cm^{-1}

^{1}H NMR ($(CD_3)_2CO$, 400 MHz) δ 8.23 – 8.17 (m, 2H), 7.65 – 7.59 (m, 2H), 4.43 (ddd, *J* = 9.1, 5.6, 3.5 Hz, 1H), 3.74 (s, 3H), 3.34 (dd, *J* = 13.8, 5.5 Hz, 1H), 3.17 (dd, *J* = 13.8, 8.7 Hz, 1H), 2.77 (d, *J* = 1.2 Hz, 3H).

^{13}C NMR ($(CD_3)_2CO$, 126 MHz) δ 172.4, 148.1, 145.9, 131.8, 124.3, 57.8, 52.9, 41.5, 39.2.

Methyl N-(4-chlorobenzyl)-N-(methylsulfonyl)-L-phenylalaninate (1.22.4a)

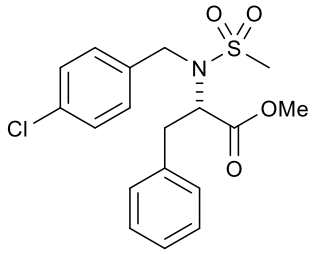

According to general procedure B; flash chromatography (5% EtOAc in Hexane to 20% EtOAc in Hexane) provided **1.22.4a** (3.32 g, 94%) as a pale-yellow oil.

TLC Rf = 0.4 (4:1 Hexanes/EtOAc) $[\alpha]^{25}_{D}$ = -33.74 (c = 2.8, $CHCl_3$)

HRMS calculated for $C_{18}H_{20}ClNO_4SNa$ $(M + Na)^+$ 404.0699; found 404.0704 (TOF MS ES+)

FTIR (neat): 3231, 1732, 1604, 1348, 1170 cm^{-1}

^1H NMR ($CDCl_3$, 400 MHz) δ 7.36 – 7.21 (m, 7H), 7.17 – 7.06 (m, 2H), 4.78 (dd, *J* = 8.6, 6.8 Hz, 1H), 4.49 (d, *J* = 15.9 Hz, 1H), 4.28 (d, *J* = 15.9 Hz, 1H), 3.66 (s, 3H), 3.26 (dd, *J* = 14.4, 6.9 Hz, 1H), 2.99 (dd, *J* = 14.4, 8.6 Hz, 1H), 2.75 (s, 3H).

^{13}C NMR ($CDCl_3$, 126 MHz) δ 171.1, 136.8, 134.9, 133.9, 130.1, 129.2, 128.7, 128.7, 127.0, 61.8, 52.5, 49.3, 40.2, 36.9.

Methyl (S)-2-(N-(4-chlorobenzyl)methylsulfonamido)-3-(4-nitrophenyl)propanoate (1.22.4b)

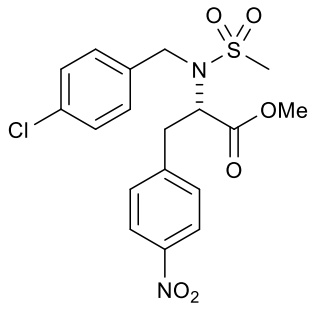

According to general procedure B; flash chromatography (10%EtOAc in Hexane to 30% EtOAc in Hexane) provided **1.22.4b** (3.2 g, 94%) as a pale-orange solid.

Mp = 103 – 105 ˚C; TLC Rf = 0.3 (1:1 Hexanes/EtOAc) $[\alpha]^{25}_{D}$ = -27.7 (c = 0.7, $CHCl_3$)

HRMS calculated for $C_{18}H_{19}ClN_2O_6SNa$ $(M + Na)^+$ 449.0550; found 449.0559 (TOF MS ES+)

FTIR (KBr Film): 1749, 1606, 1520, 1352, 1144 cm^{-1}

^{1}H NMR ($CDCl_3$, 400 MHz) δ 8.13 – 7.97 (m, 2H), 7.24 – 7.13 (m, 6H), 4.74 (dd, *J* = 8.3, 7.0 Hz, 1H), 4.50 (d, *J* = 15.7 Hz, 1H), 4.19 (d, *J* = 15.7 Hz, 1H), 3.76 (s, 3H), 3.27 (dd, *J* = 14.6, 7.0 Hz, 1H), 3.01 (dd, *J* = 14.6, 8.4 Hz, 1H), 2.96 (s, 3H).

^{13}C NMR ($CDCl_3$, 126 MHz) δ 170.5, 147.0, 144.4, 134.7, 134.4, 130.2, 130.0, 128.9, 123.7, 61.54, 52.9, 49.9, 40.2, 37.3.

Methyl N-benzyl-N-methylsulfonyl-L-phenylalaninate (1.22.4c)

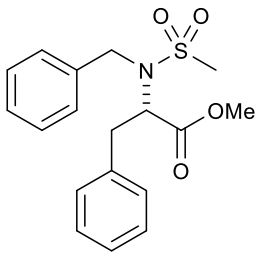

According to general procedure B; flash chromatography (5% EtOAc in Hexane to 20% EtOAc in Hexane) provided **1.22.4c** (1.12 g, 89%) as a pale-yellow oil.

TLC Rf = 0.6 (2:1 Hexanes/EtOAc) $[\alpha]^{25}_{D}$ = -55.4 (c = 2.8, $CHCl_3$)

HRMS calculated for $C_{18}H_{21}NO_4SNa$ $(M + Na)^+$ 370.1089; found 370.1103 (TOF MS ES+)

FTIR (neat): 1748, 1609, 1353, 1175 cm^{-1}

^1H NMR ($CDCl_3$, 400 MHz) δ 7.32 – 7.14 (m, 8H), 7.11 – 6.98 (m, 2H), 4.68 (dd, *J* = 8.2, 7.1 Hz, 1H), 4.44 (d, *J* = 15.6 Hz, 1H), 4.23 (d, *J* = 15.6 Hz, 1H), 3.55 (s, 3H), 3.20 (dd, *J* = 14.3, 7.0 Hz, 1H), 2.95 (dd, *J* = 14.3, 8.2 Hz, 1H), 2.65 (s, 3H).

^{13}C NMR ($CDCl_3$, 126 MHz) δ 1701.0, 137.1, 136.1, 129.3, 128.8, 128.6, 128.6, 128.0, 126.9, 61.8, 52.3, 49.9, 40.4, 36.9.

Methyl (S)-2-(N-benzylmethylsulfonamido)-3-(4-nitrophenyl)propanoate (1.22.4d)

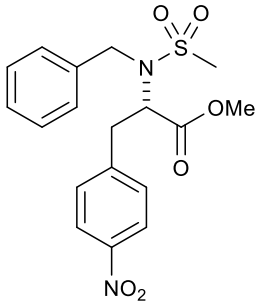

According to general procedure B; flash chromatography (5% EtOAc in Hexane to 25% EtOAc in Hexane) provided **1.22.4d** (1.84 g, 87%) as an orange solid.

Mp = 77 – 78 ˚C; TLC Rf = 0.4 (2:1 Hexanes/EtOAc) $[\alpha]^{25}_{D}$ = -37.5 (c = 1.2, $CHCl_3$)

HRMS calculated for $C_{18}H_{20}N_2O_6SNa$ $(M + Na)^+$ 415.0940; found 415.0945 (TOF MS ES+)

FTIR (KBr Film): 1743, 1606, 1515, 1345, 1147 cm^{-1}

^{1}H NMR ($CDCl_3$, 400 MHz) δ 8.07 – 7.69 (m, 2H), 7.21 – 7.06 (m, 5H), 7.04 – 6.88 (m, 2H), 4.56 (dd, *J* = 8.3, 6.8 Hz, 1H), 4.35 (d, *J* = 15.4 Hz, 1H), 4.09 (d, *J* = 15.5 Hz, 1H), 3.60 (s, 3H), 3.14 (dd, *J* = 14.5, 6.8 Hz, 1H), 2.90 (dd, *J* = 14.5, 8.4 Hz, 1H), 2.81 (s, 3H).

^{13}C NMR ($CDCl_3$, 126 MHz) δ 170.5, 146.9, 144.7, 135.9, 130.1, 128.9, 128.8, 128.3, 123.6, 61.6, 52.8, 50.7, 40.2, 37.2.

Methyl N-(4-fluorobenzyl)-N-(methylsulfonyl)-L-phenylalaninate (1.22.4e)

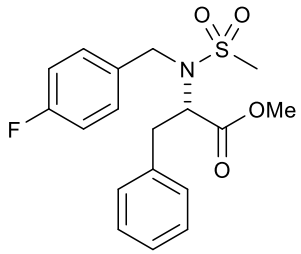

According to general procedure B; flash chromatography (5% EtOAc in Hexane to 15% EtOAc in Hexane) provided **1.22.4e** (1.16 g, 88%) as a pale-yellow solid.

Mp = 93 – 95 ˚C; TLC Rf = 0.6 (2:1 Hexanes/EtOAc) $[\alpha]^{25}_{D}$ = -44.7 (c = 1.7, $CHCl_3$)

HRMS calculated for $C_{18}H_{20}FNO_4SNa$ $(M + Na)^+$ 388.0995; found 388.1010 (TOF MS ES+)

FTIR (KBr Film): 1737, 1606, 1352, 1148 cm^{-1}

^{1}H NMR ($CDCl_3$, 400 MHz) δ 7.26 – 7.17 (m, 5H), 7.12 – 7.03 (m, 2H), 6.98 – 6.87 (m, 2H), 4.72 (dd, *J* = 8.6, 6.8 Hz, 1H), 4.42 (d, *J* = 15.7 Hz, 1H), 4.23 (d, *J* = 15.7 Hz, 1H), 3.58 (s, 3H), 3.20 (dd, *J* = 14.4, 6.8 Hz, 1H), 2.94 (dd, *J* = 14.4, 8.6 Hz, 1H), 2.66 (s, 3H).

^{13}C NMR ($CDCl_3$, 126 MHz) δ 171.0, 162.4 (d, *J* = 246.2 Hz), 136.8, 132.0 (d, *J* = 2.9 Hz), 130.5 (d, *J* = 8.1 Hz), 129.1, 128.6, 126.9, 115.3 (d, *J* = 21.7 Hz), 61.6, 52.4, 49.1, 40.1, 36.8.

Methyl (S)-2-(N-(4-fluorobenzyl)methylsulfonamido)-3-(4-nitrophenyl)propanoate (1.22.4f)

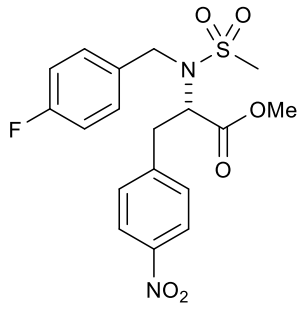

According to general procedure B; flash chromatography (5% EtOAc in Hexane to 25% EtOAc in Hexane) provided **1.22.4f** (2.00 g, 91%) as a pale-yellow solid.

Mp = 113 – 114 ˚C; TLC Rf = 0.4 (2:1 Hexanes/EtOAc) $[\alpha]^{25}_{D}$ = -51.7 (c = 1.2, $CHCl_3$)

HRMS calculated for $C_{18}H_{19}FN_2O_6SNa$ $(M + Na)^+$ 433.0846; found 433.0862 (TOF MS ES+)

FTIR (KBr Film): 1747, 1605, 1519, 1350, 1145 cm^{-1}

^{1}H NMR ($CDCl_3$, 400 MHz) δ 8.10 – 8.01 (m, 2H), 7.27 – 7.22 (m, 2H), 7.18 – 7.13 (m, 2H), 6.98 – 6.91 (m, 2H), 4.74 (dd, *J* = 8.3, 6.9 Hz, 1H), 4.49 (d, *J* = 15.6 Hz, 1H), 4.20 (d, *J* = 15.6 Hz, 1H), 3.75 (s, 3H), 3.27 (dd, *J* = 14.5, 7.0 Hz, 1H), 3.01 (dd, *J* = 14.5, 8.3 Hz, 1H), 2.95 (s, 3H).

^{13}C NMR ($CDCl_3$, 126 MHz) δ 170.5, 162.7 (d, *J* = 247.5 Hz), 147.0, 144.5, 131.9 (d, *J* = 3.5 Hz), 130.6 (d, *J* = 8.2 Hz), 130.1, 123.7, 115.7 (d, *J* = 21.1 Hz), 61.5, 52.9, 49.8, 40.2, 37.2.

(S)-3-benzyl-2-(4-chlorobenzyl)isothiazolidin-4-one 1,1-dioxide (1.22.5a)

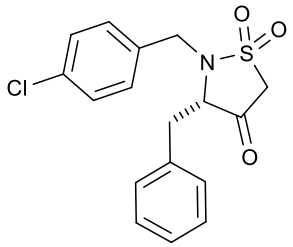

According to general procedure C; flash chromatography (100% Hexane to 10% EtOAc in Hexane) provided **1.22.5a** (0.65 g, 51%) as a pale-orange solid.

Mp = 126 – 128 ˚C; TLC Rf = 0.6 (4:1 Hexanes/EtOAc) $[\alpha]^{25}_{D}$ = -21.3 (c = 1.1, $CHCl_3$)

HRMS calculated for $C_{17}H_{17}ClNO_3S$ $(M + H)^+$ 350.0618, found 350.0624 (TOF MS ES+)

FTIR (KBr Film): 1755, 1596, 1372, 1186 cm^{-1}

^1H NMR ($CDCl_3$, 400 MHz) δ 7.36 – 7.21 (m, 5H), 7.17 – 7.10 (m, 2H), 7.06 – 6.99 (m, 2H), 4.58 (d, *J* = 15.2 Hz, 1H), 3.92 (ddd, *J* = 8.2, 4.4, 1.3 Hz, 1H), 3.84 (d, *J* = 15.1 Hz, 1H), 3.69 (d, *J* = 16.6 Hz, 1H), 3.60 (dd, *J* = 16.6, 1.4 Hz, 1H), 3.14 (dd, *J* = 14.1, 4.4 Hz, 1H), 3.06 (dd, *J* = 14.2, 8.2 Hz, 1H).

^{13}C NMR ($CDCl_3$, 126 MHz) δ 198.1, 135.7, 134.7, 132.5, 130.5, 129.6, 129.3, 129.1, 127.6, 69.3, 55.9, 47.5, 37.3.

(S)-2-(4-chlorobenzyl)-3-(4-nitrobenzyl)isothiazolidin-4-one 1,1-dioxide (1.22.5b)

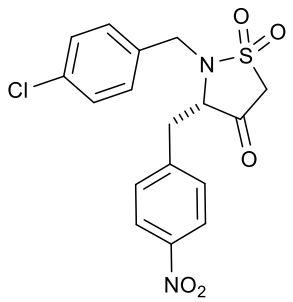

According to general procedure C; flash chromatography (100% Hexane to 15% EtOAc in Hexane) provided **1.22.5b** (0.35 g, 54%) as an orange solid.

Mp = 136 – 138 ˚C; TLC Rf = 0.7 (2:1 Hexanes/EtOAc) $[\alpha]^{25}_{D}$ = -12.6 (c = 0.1, $CHCl_3$)

HRMS calculated for $C_{17}H_{16}ClN_2O_5S$ $(M + H)^+$ 395.0468, found 395.0475 (TOF MS ES+)

FTIR (KBr Film): 1767, 1606, 1516, 1345, 1183 cm^{-1}

^1H NMR ($CDCl_3$, 400 MHz) δ 8.14 – 8.09 (m, 2H), 7.25 – 7.20 (m, 4H), 7.07 – 7.02 (m, 2H), 4.39 (d, *J* = 14.9 Hz, 1H), 4.11 (d, *J* = 14.9 Hz, 1H), 3.97 (dd, *J* = 7.9, 5.5 Hz, 1H), 3.73 (s, 2H), 3.18 (dd, *J* = 6.7, 3.4 Hz, 2H).

^{13}C NMR ($CDCl_3$, 126 MHz) δ 198.1, 147.4, 143.2, 135.1, 132.3, 130.5, 130.5, 129.4, 124.0, 69.8, 55.3, 49.8, 37.1.

(S)-2,3-dibenzylisothiazolidin-4-one 1,1-dioxide (1.22.5c)

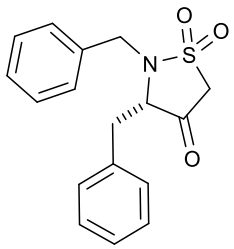

According to general procedure C; flash chromatography (100% Hexane to 10% EtOAc in Hexane) provided **1.22.5c** (0.56 g, 50%) as a pale-orange solid.

Mp = 87 – 89 ˚C; TLC Rf = 0.6 (4:1 Hexanes/EtOAc) $[\alpha]^{25}_{D}$ = -11.2 (c =1.0, $CHCl_3$)

HRMS calculated for $C_{17}H_{17}NO_3SNa$ $(M + Na)^+$ 338.0827, found 338.0844 (TOF MS ES+)

FTIR (KBr film): 3031, 2934, 1754, 1373, 1137 cm^{-1}

^{1}H NMR ($CDCl_3$, 400 MHz) δ 7.37 – 7.23 (m, 6H), 7.15 – 6.98 (m, 4H), 4.66 (d, *J* = 15.0 Hz, 1H), 3.90 (ddd, *J* = 7.9, 4.7, 1.4 Hz, 1H), 3.76 (d, *J* = 15.0 Hz, 1H), 3.62 (d, *J* = 16.5 Hz, 1H), 3.51 (dd, *J* = 16.6, 1.3 Hz, 1H), 3.08 (dd, *J* = 14.1, 4.7 Hz, 1H), 3.01 (dd, *J* = 14.1, 7.8 Hz, 1H).

^{13}C NMR ($CDCl_3$, 126 MHz) δ 198.4, 135.7, 133.94, 129.7, 129.3, 129.1, 129.0, 128.7, 127.5, 68.9, 56.1, 48.0, 37.1.

(S)-2-benzyl-3-(4-nitrobenzyl)isothiazolidin-4-one 1,1-dioxide (1.22.5d)

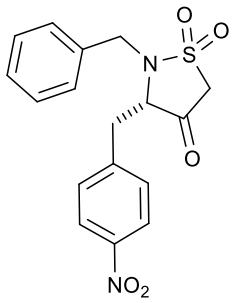

According to general procedure C; flash chromatography (100% Hexane to 15% EtOAc in Hexane) provided **1.22.5d** (0.90 g, 55%) as an orange solid.

Mp = 132 – 135 ˚C; TLC Rf = 0.6 (2:1 Hexanes/EtOAc) $[\alpha]^{25}_{D}$ = -23.6 (c = 0.1, $CHCl_3$)

HRMS calculated for $C_{17}H_{16}N_2O_5SNa$ $(M + Na)^+$ 383.0698, found 383.0706 (TOF MS ES+)

FTIR (KBr film): 1747, 1602, 1524, 1332, 1164 cm^{-1}

^{1}H NMR ($CDCl_3$, 400 MHz) δ 8.07 (d, *J* = 8.4 Hz, 2H), 7.33 – 7.23 (m, 3H), 7.20 (d, *J* = 8.3 Hz, 2H), 7.11 (d, *J* = 7.1 Hz, 2H), 4.45 (d, *J* = 14.7 Hz, 1H), 4.10 (d, *J* = 14.7 Hz, 1H), 4.00 (t, *J* = 6.6 Hz, 1H), 3.79 – 3.66 (m, 2H), 3.23 – 3.12 (m, 2H).

^{13}C NMR ($CDCl_3$, 126 MHz) δ 198.5, 147.3, 143.4, 133.7, 131.1, 130.5, 129.2, 128.9, 123.9, 69.7, 55.4, 50.5, 37.1.

(S)-3-benzyl-2-(4-fluorobenzyl)isothiazolidin-4-one 1,1-dioxide (1.22.5e)

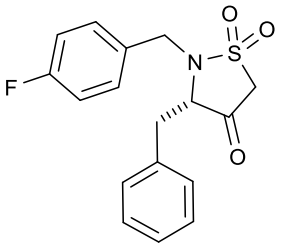

According to general procedure C; flash chromatography (100% Hexane to 10% EtOAc in Hexane) provided **1.22.5e** (0.57 g, 53%) as a pale-orange solid.

Mp = 116 – 117 ˚C; TLC Rf = 0.5 (4:1 Hexanes/EtOAc) $[\alpha]^{25}_{D}$ = -13.6 (c =0.1, $CHCl_3$)

HRMS calculated for $C_{17}H_{16}FNO_3SNa$ $(M + Na)^+$ 356.0733; found 356.0739 (TOF MS ES+)

FTIR (KBr film): 1752, 1604, 1332, 1135 cm^{-1}

^1H NMR ($CDCl_3$, 400 MHz) δ 7.35 – 7.28 (m, 3H), 7.16 – 7.04 (m, 4H), 7.00 – 6.93 (m, 2H), 4.61 (d, *J* = 15.1 Hz, 1H), 3.93 (ddd, *J* = 8.1, 4.4, 1.3 Hz, 1H), 3.83 (d, *J* = 15.1 Hz, 1H), 3.68 (d, *J* = 16.6 Hz, 1H), 3.58 (dd, *J* = 16.6, 1.3 Hz, 1H), 3.14 (dd, *J* = 14.1, 4.4 Hz, 1H), 3.06 (dd, *J* = 14.1, 8.1 Hz, 1H).

^{13}C NMR ($CDCl_3$, 126 MHz) δ 198.2, 162.8 (d, *J* = 247.9 Hz), 135.7, 131.0 (d, *J* = 8.2 Hz), 129.8 (d, *J* = 3.5 Hz), 129.6, 129.0, 127.6, 116.0 (d, *J* = 21.1 Hz), 69.1, 55.9, 47.4, 37.2.

(S)-2-(4-fluorobenzyl)-3-(4-nitrobenzyl)isothiazolidin-4-one 1,1-dioxide (1.22.5f)

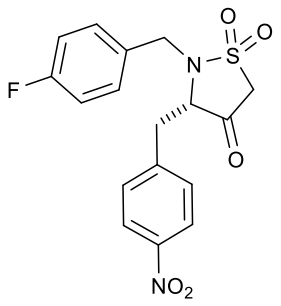

According to general procedure C; flash chromatography (100% Hexane to 15% EtOAc in Hexane) provided **1.22.5f** (0.54 g, 56%) as a pale-orange solid.

Mp = 134 – 135 ˚C; TLC Rf = 0.5 (2:1 Hexanes/EtOAc) $[\alpha]^{25}_{D}$ = -2.7 (c = 0.1, $CHCl_3$)

HRMS calculated for $C_{17}H_{16}FN_2O_5S$ $(M + H)^+$ 379.0764; found 379.0782 (TOF MS ES+)

FTIR (KBr film): 1769, 1606, 1509, 1344, 1134 cm^{-1}

^1H NMR ($CDCl_3$, 400 MHz) δ 8.17 – 8.04 (m, 2H), 7.28 – 7.20 (m, 2H), 7.15 – 7.06 (m, 2H), 7.01 – 6.92 (m, 2H), 4.44 (d, *J* = 14.9 Hz, 1H), 4.07 (d, *J* = 14.9 Hz, 1H), 3.98 (dd, *J* = 7.5, 5.7 Hz, 1H), 3.72 (d, *J* = 1.2 Hz, 2H), 3.18 (dd, *J* = 6.7, 2.5 Hz, 2H).

^{13}C NMR ($CDCl_3$, 126 MHz) δ 198.1, 162.9 (d, *J* = 249.0 Hz), 147.4, 143.2, 131.0 (d, *J* = 8.2 Hz), 130.6, 129.6 (d, *J* = 2.8 Hz), 124.0, 116.2 (d, *J* = 21.1 Hz), 69.6, 55.4, 49.5, 37.0.

(S,E)-3-benzyl-2-(4-chlorobenzyl)-5-(4-methoxybenzylidene)isothiazolidin-4-one 1,1-dioxide (1.27.1a)

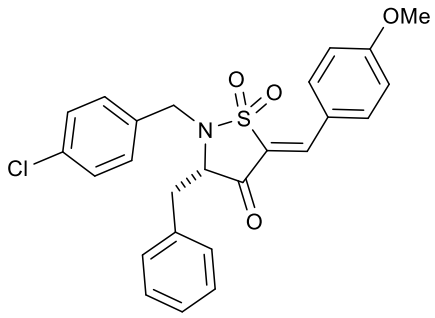

According to general procedure D; **1.27.1a** (46.2 mg, 49%) precipitated as a yellow solid.

Mp = 154 – 155 ˚C; TLC Rf = 0.3 (7:1 Hexanes/EtOAc) $[\alpha]^{25}_{D}$ = -34.0 (c = 0.2, $CHCl_3$)

HRMS calculated for $C_{25}H_{22}ClNO_4SNa$ $(M + Na)^+$ 490.0856; found 490.0866 (TOF MS ES+)

FTIR (KBr film): 1710, 1604, 1356, 1273, 1169, 1029 cm^{-1}

^{1}H NMR ($CDCl_3$, 400 MHz) δ 8.14 – 7.98 (m, 2H), 7.79 (s, 1H), 7.29 (m, 3H), 7.21 – 7.15 (m, 4H), 7.08 – 7.01 (m, 2H), 6.99 – 6.91 (m, 2H), 4.50 (d, *J* = 15.1 Hz, 1H), 3.96 (dd, *J* = 8.7, 4.9 Hz, 1H), 3.92 (s, 3H), 3.88 (d, *J* = 15.1 Hz, 1H), 3.29 – 3.04 (m, 2H).

^{13}C NMR ($CDCl_3$, 126 MHz) δ 190.2, 165.1, 145.5, 137.1, 136.4, 134.2, 133.0, 130.4, 129.7, 128.99, 128.9, 127.3, 124.8, 123.2, 115.3, 67.8, 55.9, 47.8, 38.3.

(S,E)-3-benzyl-2-(4-chlorobenzyl)-5-(4-fluorobenzylidene)isothiazolidin-4-one 1,1-dioxide (1.27.1b)

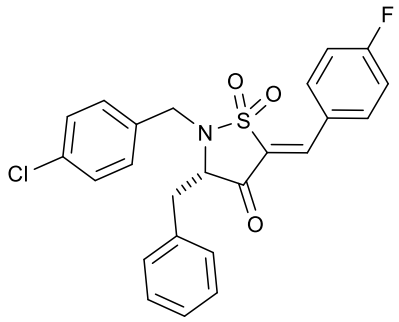

According to general procedure D; **1.27.1b** (39 mg, 43%) precipitated as a yellow solid.

Mp = 141 – 143 ˚C; TLC Rf = 0.32 (7:1 Hexanes/EtOAc) $[\alpha]^{25}_{D}$ = -11.6 (c = 0.2, $CHCl_3$)

HRMS calculated for $C_{24}H_{19}ClFNO_3SNa$ $(M + Na)^+$ 478.0656; found 478.0638 (TOF MS ES+)

FTIR (KBr film): 1716, 1611, 1338, 1164 cm^{-1}

^{1}H NMR ($CDCl_3$, 400 MHz) δ 8.16 – 7.99 (m, 2H), 7.79 (s, 1H), 7.33 – 7.28 (m, 4H), 7.25 – 7.15 (m, 5H), 6.98 – 6.88 (m, 2H), 4.52 (d, *J* = 15.0 Hz, 1H), 3.98 (dd, *J* = 8.4, 5.4 Hz, 1H), 3.86 (d, *J* = 15.0 Hz, 1H), 3.22 – 3.07 (m, 2H).

^{13}C NMR ($CDCl_3$, 126 MHz) δ 190.2, 166.3 (d, *J* = 259.7 Hz), 143.9, 136.7 (d, *J* = 9.9 Hz), 136.1, 134.4, 132.7, 130.4, 129.7, 129.1, 129.0, 127.6 (d, *J* = 2.7 Hz), 127.5, 126.7 (d, *J* = 2.8 Hz), 117.1 (d, *J* = 22.7 Hz), 67.8, 47.9, 38.2.

(S,E)-3-benzyl-5-benzylidene-2-(4-chlorobenzyl)isothiazolidin-4-one 1,1-dioxide (1.27.1c)

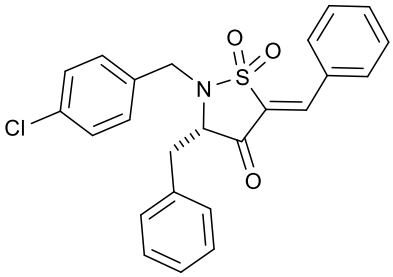

According to general procedure D; **1.27.1c** (0.37 g, 42%) precipitated as a yellow solid.

Mp = 143 – 145 ˚C; TLC Rf = 0.4 (7:1 Hexanes/EtOAc) $[\alpha]^{25}_D$ = -14.7 (c = 0.1, $CHCl_3$)

HRMS calculated for $C_{24}H_{20}ClNO_3SNa$ $(M + Na)^+$ 460.0750; found 460.0762 (TOF MS ES+)

FTIR (KBr film): 1721, 1594, 1339, 1163 cm^{-1}

^{1}H NMR ($CDCl_3$, 400 MHz) δ 8.11 – 8.02 (m, 2H), 7.85 (s, 1H), 7.69 – 7.59 (m, 1H), 7.59 – 7.50 (m, 2H), 7.31 (qd, *J* = 3.2, 2.2 Hz, 3H), 7.22 – 7.14 (m, 4H), 7.00 – 6.86 (m, 2H), 4.51 (d, *J* = 15.0 Hz, 1H), 3.98 (dd, *J* = 8.1, 5.7 Hz, 1H), 3.87 (d, *J* = 15.0 Hz, 1H), 3.20 – 3.07 (m, 2H).

^{13}C NMR ($CDCl_3$, 126 MHz) δ 190.4, 145.5, 136.2, 134.3, 134.3, 134.0, 132.8, 130.4, 130.3, 129.7, 129.6, 129.1, 129.0, 128.1, 127.4, 67.8, 48.0, 38.2.

(S,E)-2-(4-chlorobenzyl)-5-(4-fluorobenzylidene)-3-(4-nitrobenzyl)isothiazolidin-4-one 1,1-dioxide (1.27.1d)

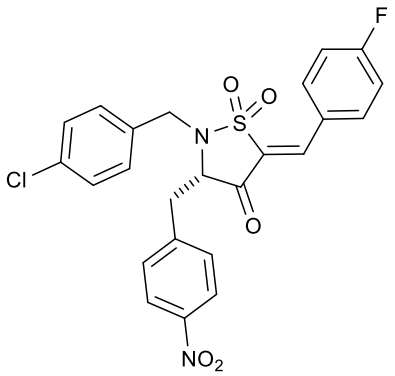

According to general procedure D; **1.27.1d** (0.36 g, 40%) precipitated as a yellow solid.

Mp = 168 – 170 ˚C; TLC Rf = 0.3 (7:1 Hexanes/EtOAc) $[\alpha]^{25}_{D}$ = -0.54 (c = 1.1, $CHCl_3$)

HRMS calculated for $C_{24}H_{18}ClFN_2O_5SNa$ $(M + Na)^+$ 523.0607, found 523.0631 (TOF MS ES+)

FTIR (KBr film): 1713, 1581, 1514, 1347, 1166, 1048 cm^{-1}

^1H NMR ($CDCl_3$, 400 MHz) δ 8.13 – 8.05 (m, 4H), 7.81 (s, 1H), 7.25 – 7.18 (m, 6H), 7.06 – 7.01 (m, 2H), 4.35 (d, *J* = 14.9 Hz, 1H), 4.21 (d, *J* = 14.9 Hz, 1H), 4.02 (dd, *J* = 8.5, 5.0 Hz, 1H), 3.24 (dd, *J* = 14.0, 8.5 Hz, 1H), 3.15 (dd, *J* = 14.1, 5.1 Hz, 1H).

^{13}C NMR ($CDCl_3$, 126 MHz δ 190.0, 166.5 (d, *J* = 260.6 Hz), 147.3, 144.9, 143.3, 136.8 (d, *J* = 9.8 Hz), 134.8, 132.4, 130.6, 130.4, 129.2, 127.1 126.6 (d, *J* = 2.8 Hz), 123.9, 117.2 (d, *J* = 22.0 Hz), 68.1, 49.6, 37.3.

(S,E)-5-(benzo[d][1,3]dioxol-4-ylmethylene)-2-(4-chlorobenzyl)-3-(4-nitrobenzyl) isothiazolidin-4-one 1,1-dioxide (1.27.1e)

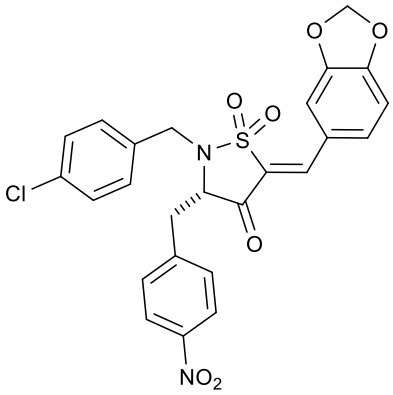

According to general procedure D; **1.27.1e** (48 mg, 51%) precipitated as a yellow solid.

Mp = 156 – 159 ˚C; TLC Rf = 0.3 (7:1 Hexanes/EtOAc) $[\alpha]^{25}_{D}$ = -24.5 (c = 0.05, $CHCl_3$)

HRMS calculated for $C_{25}H_{20}ClN_2O_7S$ $(M + H)^+$ 527.0680; found 527.0696 (TOF MS ES+)

FTIR (KBr film): 1708, 1604, 1519, 1367, 1230, 1171, 1040 cm^{-1}

^{1}H NMR ($CDCl_3$, 400 MHz) δ 8.13 – 7.97 (m, 2H), 7.81 – 7.64 (m, 2H), 7.52 (dd, *J* = 8.2, 1.9 Hz, 1H), 7.31 – 7.15 (m, 4H), 7.11 – 7.02 (m, 2H), 6.96 (d, *J* = 8.2 Hz, 1H), 6.13 (s, 2H), 4.34 (d, *J* = 15.0 Hz, 1H), 4.23 (d, *J* = 15.0 Hz, 1H), 4.00 (dd, *J* = 8.3, 4.9 Hz, 1H), 3.22 (dd, *J* = 14.0, 8.3 Hz, 1H), 3.13 (dd, *J* = 14.0, 5.0 Hz, 1H).

^{13}C NMR ($CDCl_3$, 126 MHz) δ 189.9, 154.1, 149.2, 147.3, 146.4, 143.5, 134.7, 133.7, 132.6, 130.6, 130.4, 129.2, 124.7, 124.6, 123.9, 112.0, 109.4, 102.8, 68.1, 49.5, 37.3.

(S,E)-2,3-dibenzyl-5-(4-methoxybenzylidene)isothiazolidin-4-one 1,1-dioxide (1.27.1f)

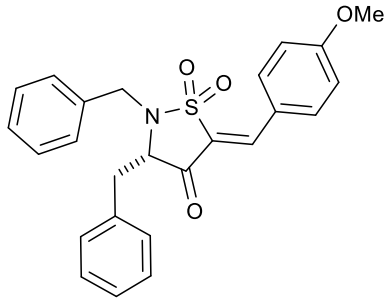

According to general procedure D; **1.27.1f** (52 mg, 54%) precipitated as a yellow solid.

Mp = 132 – 134 ˚C; TLC Rf = 0.4 (7:1 Hexanes/EtOAc) $[\alpha]^{25}_{D}$ = -27.4 (c = 0.1, $CHCl_3$)

HRMS calculated for $C_{25}H_{23}NO_4SNa$ $(M + Na)^+$ 456.1245, found 456.1249 (TOF MS ES+)

FTIR (KBr film): 1710, 1513, 1356, 1271, 1166, 1041 cm^{-1}

^1H NMR ($CDCl_3$, 400 MHz) δ 8.14 – 7.97 (m, 2H), 7.77 (s, 1H), 7.36 – 7.15 (m, 8H), 7.13 – 6.99 (m, 4H), 4.66 (d, *J* = 14.9 Hz, 1H), 3.99 (t, *J* = 6.7 Hz, 1H), 3.92 (s, 3H), 3.86 (d, *J* = 15.0 Hz, 1H), 3.12 (d, *J* = 6.8 Hz, 2H).

^{13}C NMR ($CDCl_3$, 126 MHz) δ 190.3, 165.0, 145.1, 137.1, 136.4, 134.3, 129.7, 129.1, 128.9, 128.8, 128.3, 127.3, 125.1, 123.3, 115.2, 67.3, 55.9, 47.9, 38.0.

(S,E)-2,3-dibenzyl-5-(4-fluorobenzylidene)isothiazolidin-4-one 1,1-dioxide (1.27.1g)

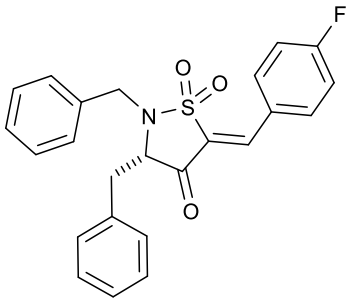

According to the general procedure D: flash chromatography (100% Hexane to 10% EtOAc in Hexane) provided **1.27.1g** (0.44 g, 47%) as a yellow solid.

Mp = 128 – 131 ˚C; TLC Rf = 0.4 (7:1 Hexanes/EtOAc) $[\alpha]^{25}_{D}$ = -24.8 (c = 0.1, $CHCl_3$)

HRMS calculated for $C_{24}H_{20}FNO_3SNa$ $(M + Na)^+$ 444.1045, found 444.1053 (TOF MS ES+)

FTIR (KBr Film): 1718, 1543, 1271, 1166 cm^{-1}

^1H NMR ($CDCl_3$, 400 MHz) δ 8.19 – 8.01 (m, 2H), 7.76 (s, 1H), 7.31 (td, *J* = 5.8, 2.8 Hz, 3H), 7.27 – 7.22 (m, 5H), 7.21 – 7.17 (m, 2H), 7.12 – 7.00 (m, 2H), 4.68 (d, *J* = 14.9 Hz, 1H), 4.02 (dd, *J* = 7.7, 5.9 Hz, 1H), 3.84 (d, *J* = 15.0 Hz, 1H), 3.20 – 3.07 (m, 2H).

^{13}C NMR ($CDCl_3$, 126 MHz) δ 190.2, 166.2 (d, *J* = 259.7 Hz), 143.6, 136.7 (d, *J* = 9.3 Hz), 136.1, 134.0, 129.7, 129.1, 128.9, 128.9, 128.4, 127.8, 127.4, 126.8 (d, *J* = 2.9 Hz), 117.0 (d, *J* = 22.5 Hz), 67.2, 47.9, 37.9.

(S,E)-2-benzyl-5-(4-methoxybenzylidene)-3-(4-nitrobenzyl)isothiazolidin-4-one 1,1-dioxide (1.27.1h)

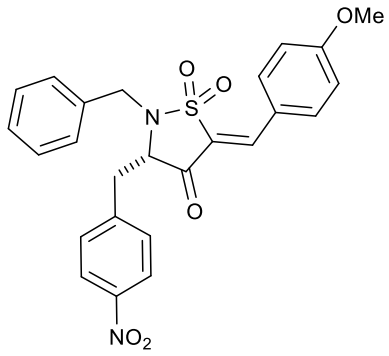

According to general procedure D; **1.27.1h** (53 mg, 57%) precipitated as a yellow solid.

Mp = 178 – 181 ˚C; TLC Rf = 0.4 (7:1 Hexanes/EtOAc) $[\alpha]^{25}_{D}$ = -14.5 (c = 0.06, $CHCl_3$)

HRMS calculated for $C_{25}H_{22}N_2O_6SNa$ $(M + Na)^+$ 501.1096, found 501.1096 (TOF MS ES+)

FTIR (KBr film): 1706, 1604, 1552, 1338, 1276, 1167, 1040 cm^{-1}

^{1}H NMR ($CDCl_3$, 400 MHz) δ 8.13 – 8.00 (m, 4H), 7.79 (s, 1H), 7.31 – 7.18 (m, 5H), 7.16 – 7.09 (m, 2H), 7.08 – 7.00 (m, 2H), 4.38 (d, *J* = 14.7 Hz, 1H), 4.29 (d, *J* = 14.8 Hz, 1H), 4.03 (dd, *J* = 8.1, 5.1 Hz, 1H), 3.92 (s, 3H), 3.22 (dd, *J* = 14.0, 8.1 Hz, 1H), 3.11 (dd, *J* = 14.0, 5.1 Hz, 1H).

^{13}C NMR ($CDCl_3$, 126 MHz) δ 190.2, 165.3, 147.2, 146.2, 143.7, 137.2, 134.1, 130.6, 129.2, 129.0, 128.5, 124.4, 123.8, 123.1, 115.4, 68.0, 56.0, 50.0, 37.3.

(S,E)-2-benzyl-5-(4-fluorobenzylidene)-3-(4-nitrobenzyl)isothiazolidin-4-one 1,1-dioxide (1.27.1i)

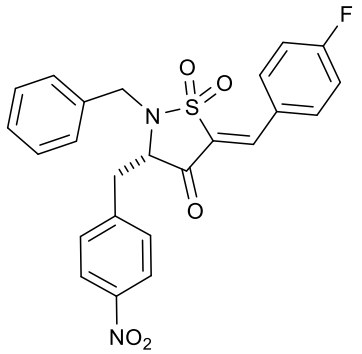

According to general procedure D; **1.27.1i** (41 mg, 45%) precipitated as a yellow solid.

Mp = 173 – 175 ˚C; TLC Rf = 0.4 (7:1 Hexanes/EtOAc) $[\alpha]^{25}_{D}$ = -13.5 (c = 1, $CHCl_3$)

HRMS calculated for $C_{24}H_{19}FN_2O_5SNa$ $(M + Na)^+$ 489.0996, found 489.0972 (TOF MS ES+)

FTIR (KBr film): 1717, 1606, 1519, 1348, 1157 cm^{-1}

^{1}H NMR ($CDCl_3$, 400 MHz) δ 8.15 – 8.00 (m, 4H), 7.80 (s, 1H), 7.35 – 7.17 (m, 7H), 7.14 – 7.05 (m, 2H), 4.39 (d, *J* = 14.8 Hz, 1H), 4.26 (d, *J* = 14.7 Hz, 1H), 4.05 (dd, *J* = 8.4, 5.2 Hz, 1H), 3.24 (dd, *J* = 14.0, 8.3 Hz, 1H), 3.12 (dd, *J* = 14.0, 5.1 Hz, 1H).

^{13}C NMR ($CDCl_3$, 126 MHz) δ 190.3, 166.4 (d, *J* = 260.1 Hz), 147.3, 144.6, 143.4, 136.8 (d, *J* = 9.9 Hz), 133.8, 130.6, 129.1, 129.1, 128.7, 127.3 (d, *J* = 2.6 Hz), 126.6 (d, *J* = 3.4 Hz), 123.9, 117.2 (d, *J* = 22.4 Hz), 68.0, 50.2, 37.2.

(S,E)-5-(benzo[d][1,3]dioxol-4-ylmethylene)-2-benzyl-3-(4-nitrobenzyl)isothiazolidin-4-one 1,1-dioxide (1.27.1j)

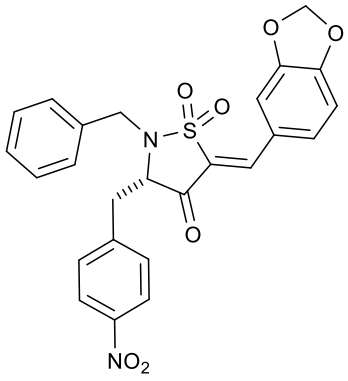

According to general procedure D; **1.27.1*j*** (46 mg, 48%) precipitated as a yellow solid.

Mp = 162 – 164 ˚C; TLC Rf = 0.3 (7:1 Hexanes/EtOAc) $[\alpha]^{25}_D$ = -14.2 (c = 0.9, $CHCl_3$)

HRMS calculated for $C_{25}H_{20}N_2O_7SNa$ $(M + Na)^+$ 515.0889, found 515.0878 (TOF MS ES+)

FTIR (KBr film): 1711, 1605, 1571, 1518, 1346, 1276, 1167, 1037 cm^{-1}

^{1}H NMR ($CDCl_3$, 400 MHz) δ 8.10 – 8.01 (m, 2H), 7.75 – 7.68 (m, 2H), 7.53 (dd, *J* = 8.2, 1.9 Hz, 1H), 7.27 – 7.18 (m, 5H), 7.15 – 7.08 (m, 2H), 6.95 (d, *J* = 8.1 Hz, 1H), 6.12 (s, 2H), 4.38 (d, *J* = 14.7 Hz, 1H), 4.28 (d, *J* = 14.7 Hz, 1H), 4.03 (dd, *J* = 8.1, 5.1 Hz, 1H), 3.22 (dd, *J* = 14.0, 8.1 Hz, 1H), 3.10 (dd, *J* = 14.0, 5.1 Hz, 1H).

^{13}C NMR ($CDCl_3$, 126 MHz) δ 190.2, 153.9, 149.1, 147.2, 146.1, 143.6, 134.0, 133.6, 130.6, 129.1, 129.0, 128.6, 124.9, 124.8, 123.8, 112.1, 109.3, 102.8, 68.0, 50.0, 37.3.

(S,E)-2-benzyl-5-((E)-3-(4-fluorophenyl)allylidene)-3-(4-nitrobenzyl)isothiazolidin-4-one 1,1-dioxide (1.27.1k)

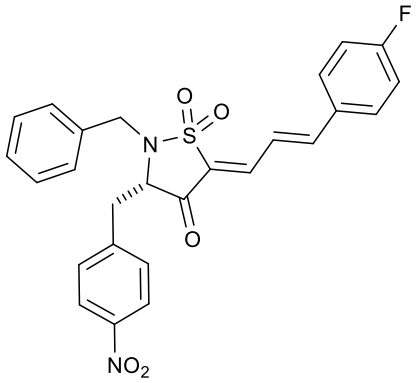

According to general procedure D; **1.27.1k** (49 mg, 51%) precipitated as a yellow solid.

Mp = 168 – 169 ˚C; TLC Rf = 0.4 (7:1 Hexanes/EtOAc) $[\alpha]^{25}_{D}$ = -27.14 (c = 0.07, $CHCl_3$)

HRMS calculated for $C_{26}H_{21}FN_2O_5SNa$ $(M + Na)^+$ 515.1053, found 515.1039 (TOF MS ES+)

FTIR (KBr film): 1703, 1607, 1550, 1347, 1315, 1158 cm^{-1}

^{1}H NMR ($CDCl_3$, 400 MHz) δ 8.08 – 7.98 (m, 2H), 7.69 – 7.61 (m, 2H), 7.58 (d, *J* = 12.0 Hz, 1H), 7.55 – 7.45 (m, 1H), 7.37 (d, *J* = 14.5 Hz, 1H), 7.30 – 7.08 (m, 9H), 4.36 (d, *J* = 14.7 Hz, 1H), 4.27 (d, *J* = 14.8 Hz, 1H), 3.96 (dd, *J* = 8.0, 5.1 Hz, 1H), 3.20 (dd, *J* = 14.1, 8.0 Hz, 1H), 3.08 (dd, *J* = 14.0, 5.1 Hz, 1H).

^{13}C NMR ($CDCl_3$, 126 MHz) δ 190.1, 165.1 (d, *J* = 255.7 Hz), 152.5, 147.2, 146.4, 144.2, 143.5, 133.9, 131.5 (d, *J* = 8.9 Hz), 130.6, 129.1, 129.0, 128.6, 123.8, 121.6 (d, *J* = 2.6 Hz), 120.6 (d, *J* = 2.5 Hz), 116.7 (d, *J* = 22.2 Hz), 67.8, 49.8, 37.0.

(S,E)-3-benzyl-2-(4-fluorobenzyl)-5-(4-methoxybenzylidene)isothiazolidin-4-one 1,1-dioxide (1.27.1l)

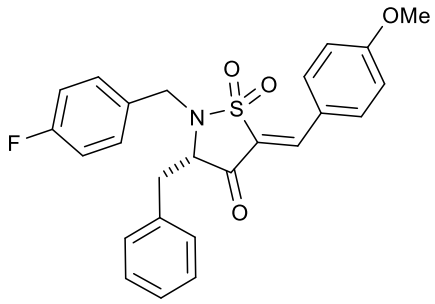

According to general procedure D; **1.27.1l** (44 mg, 50%) precipitated as a yellow solid.

Mp = 142 – 146 ˚C; TLC Rf = 0.6 (4:1 Hexanes/EtOAc) $[\alpha]^{25}_{D}$ = -26.4 (c = 0.1, $CHCl_3$)

HRMS calculated for $C_{25}H_{22}FNO_4SNa$ $(M + Na)^+$ 474.1146, found 474.1161 (TOF MS ES+)

FTIR: (KBr Film): 1714, 1612, 1276, 1167, 1040 cm^{-1}

^1H NMR ($CDCl_3$, 400 MHz) δ 8.09 – 8.04 (m, 2H), 7.78 (s, 1H), 7.33 – 7.25 (m, 3H), 7.19 (dd, *J* = 7.5, 1.9 Hz, 2H), 7.07 – 7.01 (m, 2H), 6.99 (dd, *J* = 8.6, 5.5 Hz, 2H), 6.94 – 6.85 (m, 2H), 4.54 (d, *J* = 15.0 Hz, 1H), 3.96 (dd, *J* = 8.4, 5.2 Hz, 1H), 3.92 (s, 3H), 3.86 (d, *J* = 14.9 Hz, 1H), 3.16 – 3.09 (m, 2H).

^{13}C NMR ($CDCl_3$, 126 MHz) δ 190.2, 162.7 (d, *J* = 247.1 Hz), 145.4, 137.1, 136.4, 130.8 (d, *J* = 8.2 Hz), 130.1 (d, *J* = 2.8 Hz), 129.7, 129.3, 128.9, 127.3, 124.9, 123.2, 115.7 (d, *J* = 21.8 Hz), 115.3, 67.6, 55.9, 47.6, 38.2.

(S,E)-3-benzyl-2-(4-fluorobenzyl)-5-(4-fluorobenzylidene)isothiazolidin-4-one 1,1-dioxide (1.27.1m)

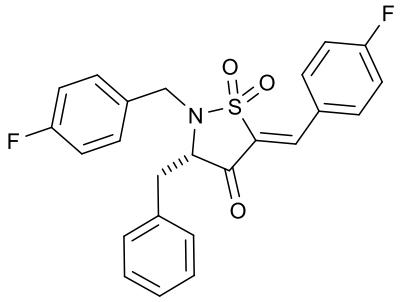

According to general procedure D; **1.27.1m** (24 mg, 28%) precipitated as a yellow solid.

Mp = 138 – 140 ˚C; TLC Rf = 0.6 (4:1 Hexanes/EtOAc) $[\alpha]^{25}_{D}$ = -24.3 (c = 0.05, $CHCl_3$)

HRMS calculated for $C_{24}H_{19}F_2NO_3SNa$ $(M + Na)^+$ 462.0946, found 462.0925 (TOF MS ES+)

FTIR (KBr film): 1714, 1612, 1276, 1167 cm^{-1}

^1H NMR ($CDCl_3$, 400 MHz) δ 8.15 – 8.04 (m, 2H), 7.78 (s, 1H), 7.31 (td, *J* = 5.2, 2.5 Hz, 3H), 7.26 – 7.15 (m, 4H), 6.98 (ddd, *J* = 8.2, 5.3, 2.5 Hz, 2H), 6.95 – 6.86 (m, 2H), 4.55 (d, *J* = 14.9 Hz, 1H), 3.99 (dd, *J* = 7.9, 5.9 Hz, 1H), 3.85 (d, *J* = 15.0 Hz, 1H), 3.21 – 3.09 (m, 2H).

^{13}C NMR ($CDCl_3$, 126 MHz) δ 190.2, 166.3 (d, *J* = 259.8 Hz), 162.7 (d, *J* = 247.1 Hz), 143.8, 136.7 (d, *J* = 9.2 Hz), 136.2, 130.8 (d, *J* = 8.2 Hz), 129.9 (d, *J* = 3.5 Hz), 129.7, 129.0, 127.7, 127.5, 126.8 (d, *J* = 2.9 Hz), 117.09 (d, *J* = 21.8 Hz), 115.8 (d, *J* = 21.7 Hz), 67.6, 47.7, 38.1.

(S,E)-5-(benzo[d][1,3]dioxol-4-ylmethylene)-3-benzyl-2-(4-fluorobenzyl)isothiazolidin-4-one 1,1-dioxide (1.27.1n)

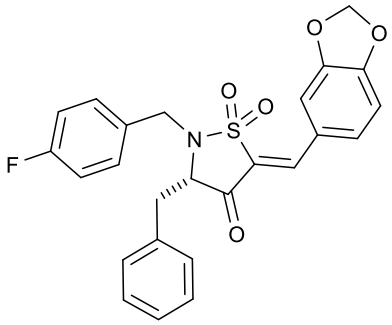

According to general procedure D; **1.27.1n** (37 mg, 41%) precipitated as a yellow solid.

Mp = 144 – 146 ˚C; TLC Rf = 0.6 (4:1 Hexanes/EtOAc) $[\alpha]^{25}_{D}$ = -31.4 (c = 0.1, $CHCl_3$)

HRMS calculated for $C_{25}H_{20}FNO_5SNa$ $(M + Na)^+$ 488.0944, found 488.0928 (TOF MS ES+)

FTIR (KBr film): 1701, 1605, 1276, 1167, 1037 cm^{-1}

^{1}H NMR ($CDCl_3$, 400 MHz) δ 7.73 (d, *J* = 1.9 Hz, 1H), 7.71 (s, 1H), 7.53 (dd, *J* = 8.3, 1.9 Hz, 1H), 7.35 – 7.27 (m, 3H), 7.22 – 7.16 (m, 2H), 7.04 – 6.89 (m, 5H), 6.11 (q, *J* = 1.1 Hz, 2H), 4.54 (d, *J* = 15.3 Hz, 1H), 3.97 (dd, *J* = 8.2, 5.3 Hz, 1H), 3.87 (d, *J* = 15.0 Hz, 1H), 3.13 (td, *J* = 8.4, 3.2 Hz, 2H).

^{13}C NMR ($CDCl_3$, 126 MHz) δ 190.2, 162.7 (d, *J* = 247.1 Hz), 153.6, 149.1, 145.4, 136.3, 133.2, 130.8 (d, *J* = 8.2 Hz), 130.1 (d, *J* = 2.8 Hz), 129.7, 129.2, 128.9, 127.3, 124.9, 115.7 (d, *J* = 21.7 Hz), 112.1, 109.3, 102.7, 67.6, 47.6, 38.2.

(S,E)-3-benzyl-2-(4-fluorobenzyl)-5-((E)-3-(4-fluorophenyl)allylidene)isothiazolidin-4-one 1,1-dioxide (1.27.1o)

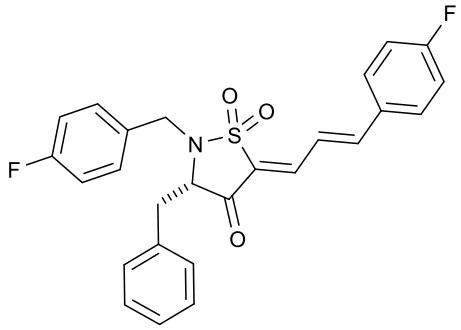

According to general procedure D; **1.27.1o** (44 mg, 49%) precipitated as a yellow solid.

Mp = 150 – 152 ˚C; TLC Rf = 0.6 (4:1 Hexanes/EtOAc) $[\alpha]^{25}_{D}$ = -22.6 (c = 0.05, $CHCl_3$)

HRMS calculated for $C_{26}H_{21}F_2NO_3SNa$ $(M + Na)^+$ 488.1102, found 488.1097 (TOF MS ES+)

FTIR (KBr film): 1716, 1607, 1315, 1158, 982 cm^{-1}

^{1}H NMR ($CDCl_3$, 400 MHz) δ 7.65 (ddd, *J* = 8.7, 5.4, 3.2 Hz, 2H), 7.57 – 7.54 (m, 1H), 7.53 – 7.46 (m, 1H), 7.34 – 7.27 (m, 4H), 7.21 – 7.10 (m, 4H), 7.01 (ddd, *J* = 8.7, 5.4, 3.2 Hz, 2H), 6.95 – 6.88 (m, 2H), 4.49 (dd, *J* = 18.6, 15.0 Hz, 1H), 4.04 – 3.76 (m, 2H), 3.25 – 3.03 (m, 2H).

^{13}C NMR ($CDCl_3$, 126 MHz) δ 190.1, 165.0 (d, *J* = 255.2 Hz), 162.7 (d, *J* = 247.1 Hz), 151.8, 145.6, 143.5, 136.3, 131.4 (d, *J* = 8.3 Hz), 130.8 (d, *J* = 8.2 Hz), 130.0 (d, *J* = 3.6 Hz), 129.7, 128.9, 127.4, 121.8 (d, *J* = 2.6 Hz), 120.7, 116.7 (d, *J* = 21.9 Hz), 115.8 (d, *J* = 21.7 Hz), 67.5, 47.4, 37.9.

(S,E)-2-(4-fluorobenzyl)-5-(4-methoxybenzylidene)-3-(4-nitrobenzyl)isothiazolidin-4-one 1,1-dioxide (1.27.1p)

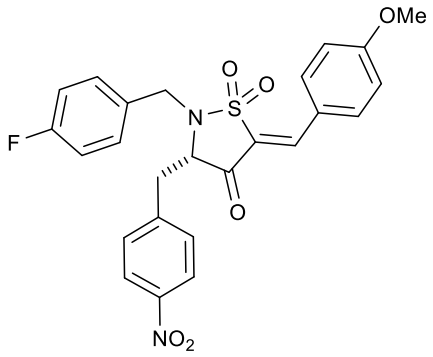

According to general procedure D; **1.27.1p** (52 mg, 57%) precipitated as a yellow solid.

Mp = 168 – 171 ˚C; TLC Rf = 0.3 (7:1 Hexanes/EtOAc) $[\alpha]^{25}_{D}$ = -29.4 (c = 0.05, $CHCl_3$)

HRMS calculated for $C_{25}H_{21}FN_2O_6SNa$ $(M + Na)^+$ 519.1002, found 519.1017 (TOF MS ES+)

FTIR (KBr film): 1709, 1606, 1512, 1347, 1290, 1166, 1054 cm^{-1}

^{1}H NMR ($CDCl_3$, 400 MHz) δ 8.13 – 8.08 (m, 2H), 8.07 – 8.02 (m, 2H), 7.79 (s, 1H), 7.26 (m, 2H), 7.15 – 7.08 (m, 2H), 7.07 – 7.02 (m, 2H), 6.97 – 6.89 (m, 2H), 4.40 (d, *J* = 14.9 Hz, 1H), 4.21 (d, *J* = 14.9 Hz, 1H), 4.01 (dd, *J* = 8.1, 5.0 Hz, 1H), 3.93 (s, 3H), 3.24 (dd, *J* = 14.1, 8.1 Hz, 1H), 3.13 (dd, *J* = 14.1, 5.0 Hz, 1H).

^{13}C NMR ($CDCl_3$, 126 MHz) δ 189.9, 165.4, 162.8 (d, *J* = 248.4 Hz), 147.3, 146.3, 143.6, 137.3, 130.9 (d, *J* = 8.5 Hz), 130.7, 129.9 (d, *J* = 3.5 Hz), 124.3, 123.8, 123.1, 116.0 (d, *J* = 21.7 Hz), 115.4, 67.8, 56.0, 49.1, 37.3.

(S,E)-5-(benzo[d][1,3]dioxol-4-ylmethylene)-2-(4-fluorobenzyl)-3-(4-nitrobenzyl) isothiazolidin-4-one 1,1-dioxide (1.27.1q)

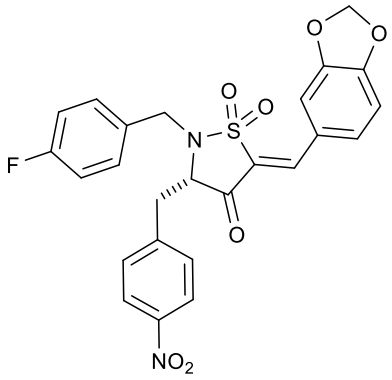

According to general procedure D; **1.27.1q** (55 mg, 58%) precipitated as a yellow solid.

Mp = 168 – 172 ˚C; TLC Rf = 0.3 (7:1 Hexanes/EtOAc) $[\alpha]^{25}_{D}$ = -22.4 (c = 0.1, $CHCl_3$)

HRMS calculated for $C_{25}H_{19}FN_2O_7SNa$ $(M + Na)^+$ 533.0795, found 533.0810 (TOF MS ES+)

FTIR (KBr film): 1710, 1604, 1510, 1346, 1277, 1157, 1038 cm^{-1}

^{1}H NMR ($CDCl_3$, 400 MHz) δ 8.17 – 8.05 (m, 2H), 7.72 (s, 1H), 7.70 (d, *J* = 1.9 Hz, 1H), 7.52 (dd, *J* = 8.4, 1.9 Hz, 1H), 7.27 (d, *J* = 2.0 Hz, 1H), 7.25 (d, *J* = 1.9 Hz, 1H), 7.10 (ddd, *J* = 8.4, 5.3, 2.6 Hz, 2H), 7.01 – 6.83 (m, 3H), 6.13 (s, 2H), 4.40 (d, *J* = 15.0 Hz, 1H), 4.20 (d, *J* = 14.9 Hz, 1H), 4.01 (dd, *J* = 8.1, 5.0 Hz, 1H), 3.23 (dd, *J* = 14.0, 8.1 Hz, 1H), 3.13 (dd, *J* = 14.0, 5.0 Hz, 1H).

^{13}C NMR ($CDCl_3$, 126 MHz) δ 189.9, 162.8 (d, *J* = 248.2 Hz), 154.0, 149.2, 147.3, 146.3, 143.5, 133.7, 130.9 (d, *J* = 8.2 Hz), 130.7, 129.9 (d, *J* = 2.9 Hz), 124.7, 124.7, 123.9, 116.0 (d, *J* = 21.8 Hz), 112.1, 109.4, 102.8, 67.8, 49.1, 37.3.

(S,E)-2-(4-fluorobenzyl)-5-((E)-3-(4-fluorophenyl)allylidene)-3-(4-nitrobenzyl) isothiazolidin-4-one 1,1-dioxide (1.27.1r)

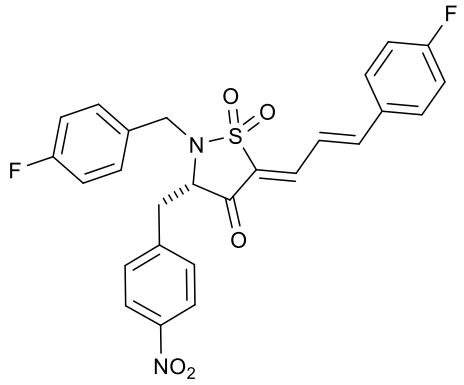

According to general procedure D; **1.27.1r** (52 mg, 55%) precipitated as a yellow solid.

Mp = 162 – 165 ˚C; TLC Rf = 0.3 (7:1 Hexanes/EtOAc) $[\alpha]^{25}_{D}$ = -26 .2 (c = 0.01, $CHCl_3$)

HRMS calculated for $C_{26}H_{20}F_2N_2O_5SNa$ $(M + Na)^+$ 533.0959, found 533.0951 (TOF MS ES+)

FTIR (KBr film): 1706, 1606, 1509, 1347, 1313, 1158 cm^{-1}

^1H NMR ($CDCl_3$, 400 MHz) δ 8.14 – 8.06 (m, 2H), 7.70 – 7.62 (m, 2H), 7.58 (d, *J* = 11.9 Hz, 1H), 7.54 – 7.44 (m, 1H), 7.38 (d, *J* = 14.6 Hz, 1H), 7.26 – 7.22 (m, 2H), 7.19 – 7.07 (m, 4H), 6.98 – 6.90 (m, 2H), 4.38 (d, *J* = 14.9 Hz, 1H), 4.19 (d, *J* = 14.9 Hz, 1H), 3.94 (dd, *J* = 8.0, 5.0 Hz, 1H), 3.21 (dd, *J* = 14.1, 8.0 Hz, 1H), 3.11 (dd, *J* = 14.1, 5.1 Hz, 1H).

^{13}C NMR ($CDCl_3$, 126 MHz) δ 189.7, 165.2 (d, *J* = 255.8 Hz), 162.8 (d, *J* = 248.0 Hz), 152.8, 147.3, 146.6, 144.4, 143.5, 131.6 (d, *J* = 9.0 Hz), 130.9 (d, *J* = 8.2 Hz), 130.7, 129.8 (d, *J* = 3.6 Hz), 127.3, 123.8, 120.6 (d, *J* = 2.6 Hz), 116.8 (d, *J* = 22.5 Hz), 116.0 (d, *J* = 21.7 Hz), 67.6, 48.9, 37.0.

Methyl (S)-2-amino-3-(4-((tert-butyldimethylsilyl)oxy)phenyl)propanoate (2.7.3)

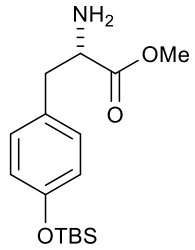

According to general procedure E; flash chromatography (5% EtOAc in Hexane to 25% EtOAc in Hexane) provided **2.7.3** (2.86 g, 67%) as a pale-yellow oil.

TLC Rf = 0.5 (2% Methanol in EtOAc) $[\alpha]^{25}_{D}$ = -39.4 (c = 0.1, $CHCl_3$)

HRMS calculated for $C_{16}H_{28}NO_3Si$ $(M + H)^+$ 310.1838, found 310.1851 (TOF MS ES+)

FTIR (neat): 3210, 1742, 1675, 920 cm^{-1}

^1H NMR ($CDCl_3$, 400 MHz) δ 7.02 (d, *J* = 8.5 Hz, 2H), 6.76 (d, *J* = 8.4 Hz, 2H), 3.76 – 3.61 (m, 4H), 2.99 (dd, *J* = 13.6, 5.3 Hz, 1H), 2.80 (dd, *J* = 13.6, 7.7 Hz, 1H), 1.46 (s, 2H), 0.96 (s, 9H), 0.17 (s, 6H).

^{13}C NMR ($CDCl_3$, 126 MHz) δ 175.7, 154.7, 130.3, 129.9, 120.2, 56.1, 52.0, 40.5, 25.8, 18.3, -4.3.

Methyl O-(tert-butyldimethylsilyl)-L-serinate (2.10.2)

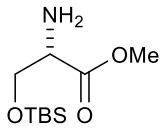

According to general procedure E; flash chromatography (5% EtOAc in Hexane to 25% EtOAc in Hexane) provided **2.10.2** (3.6 g 80%) as an off-white oil.

TLC Rf = 0.5 (2% Methanol in EtOAc) $[\alpha]^{25}_D$ = -34.4 (c = 0.5, $CHCl_3$)

HRMS calculated for $C_{10}H_{24}NO_3Si$ $(M + H)^+$ 234.1525, found 234.1535 (TOF MS ES+)

FTIR (neat): 3213, 1751, 1679, 882 cm^{-1}

^1H NMR ($CDCl_3$, 400 MHz) δ 3.86 (ddd, *J* = 9.7, 4.5, 1.3 Hz, 1H), 3.76 (ddd, *J* = 9.7, 3.8, 1.3 Hz, 1H), 3.67 (d, *J* = 1.3 Hz, 3H), 3.47 (td, *J* = 4.1, 1.4 Hz, 1H), 1.64 (s, 2H), 0.82 (d, *J* = 1.3 Hz, 9H), -0.01 (dd, *J* = 4.6, 1.3 Hz, 6H).

^{13}C NMR ($CDCl_3$, 126 MHz) δ 174.6, 65.5, 56.6, 52.0, 25.8, 18.2, -5.5 (d, *J* = 15.0 Hz).

Methyl (S)-3-(4-((tert-butyldimethylsilyl)oxy)phenyl)-2-(methylsulfonamido)propanoate (2.7.4)

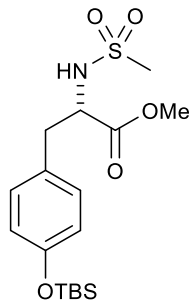

According to general procedure A; flash chromatography (5% EtOAc in Hexane to 20% EtOAc in Hexane) provided **2.7.4** (3.48 g, 97%) as an off-white solid.

Mp = 121 – 124 ˚C; TLC Rf = 0.4 (1:1 Hexanes/EtOAc) $[\alpha]^{25}_D$ = -14.15 (c =0.03, $CHCl_3$)

HRMS calculated for $C_{17}H_{29}NO_5SSiNa$ $(M + Na)^+$ 410.1433, found 410.1443 (TOF MS ES+)

FTIR (KBr film): 1753, 1657, 1367, 1152, 927 cm^{-1}

^{1}H NMR ($CDCl_3$, 400 MHz) δ 7.10 – 6.97 (m, 2H), 6.86 – 6.73 (m, 2H), 4.84 (d, *J* = 9.2 Hz, 1H), 4.34 (ddd, *J* = 9.2, 7.4, 5.1 Hz, 1H), 3.77 (s, 3H), 3.08 (dd, *J* = 13.9, 5.1 Hz, 1H), 2.94 (dd, *J* = 13.9, 7.4 Hz, 1H), 2.68 (s, 3H), 0.97 (s, 9H), 0.17 (s, 6H).

^{13}C NMR ($CDCl_3$, 126 MHz) δ 172.1, 155.3, 130.7, 128.1, 120.6, 57.4, 52.8, 41.5, 38.9, 25.8, 18.3, -4.3.

Methyl O-(tert-butyldimethylsilyl)-N-(methylsulfonyl)-L-serinate (2.10.3)

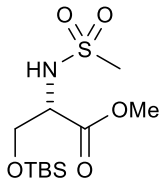

According to general procedure A; flash chromatography (5% EtOAc in Hexane to 20% EtOAc in Hexane) provided **2.10.3** (1.28 g, 91%) as a pale-yellow solid.

Mp = 107 – 109 ˚C; TLC Rf = 0.5 (1:1 Hexanes/EtOAc) $[\alpha]^{25}_{D}$ = -21.3 (c = 0.5, $CHCl_3$)

HRMS calculated for $C_{11}H_{25}NO_5SSiNa$ $(M + Na)^+$ 334.1120, found 334.1128 (TOF MS ES+)

FTIR (Kbr film): 1750, 1322, 1126, 838 cm^{-1}

^{1}H NMR ($CDCl_3$, 400 MHz) δ 5.35 (d, *J* = 9.2 Hz, 1H), 4.17 (dt, *J* = 9.2, 3.2 Hz, 1H), 4.01 (dd, *J* = 10.0, 3.3 Hz, 1H), 3.82 (dd, *J* = 10.0, 3.2 Hz, 1H), 3.72 (s, 3H), 2.95 (s, 3H), 0.80 (s, 9H), -0.01 (d, *J* = 6.4 Hz, 5H).

^{13}C NMR ($CDCl_3$, 126 MHz) δ 170.8, 64.8, 57.9, 52.6, 41.8, 25.6, 18.1, -5.6 (d, *J* = 26.2 Hz).

Methyl (S)-3-(4-((tert-butyldimethylsilyl)oxy)phenyl)-2-(N-(2-chlorobenzyl)methyl sulfonamido)propanoate (2.8.1a)

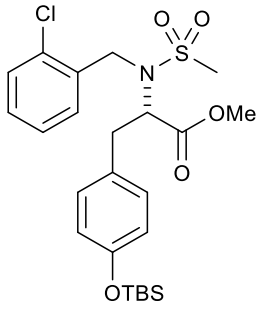

According to general procedure B; flash chromatography (5% EtOAc in Hexane to 20% EtOAc in Hexane) provided **2.8.1a** (3.36 g, 85%) as an off-white solid.

Mp = 126 – 128 ˚C; TLC Rf = 0.4 (4:1 Hexanes/EtOAc) $[\alpha]^{25}_{D}$ = -26.6 (c = 0.1, $CHCl_3$)

HRMS calculated for $C_{24}H_{34}ClNO_5SSiNa$ $(M + Na)^+$ 534.1508, found 534.1532 (TOF MS ES+)

FTIR (KBr film): 1756, 1643, 1360, 1142, 934 cm^{-1}

^{1}H NMR ($CDCl_3$, 400 MHz) δ 7.57 – 7.48 (m, 1H), 7.36 – 7.29 (m, 1H), 7.23 – 7.14 (m, 2H), 7.02 – 6.93 (m, 2H), 6.77 – 6.68 (m, 2H), 4.74 (dd, *J* = 8.3, 7.2 Hz, 1H), 4.68 – 4.53 (m, 2H), 3.61 (s, 3H), 3.12 (dd, *J* = 14.5, 7.2 Hz, 1H), 2.96 (dd, *J* = 14.4, 8.3 Hz, 1H), 2.79 (s, 3H), 0.97 (s, 9H), 0.17 (s, 6H).

^{13}C NMR ($CDCl_3$, 126 MHz) δ 171.1, 154.8, 134.3, 132.9, 130.5, 130.2, 129.4, 129.4, 129.0, 127.1, 120.3, 62.1, 52.4, 46.9, 39.7, 36.0, 25.8, 18.3, -4.3.

Methyl (S)-2-(N-benzylmethylsulfonamido)-3-(4-((tert-butyldimethylsilyl)oxy)phenyl) propanoate (2.8.1b)

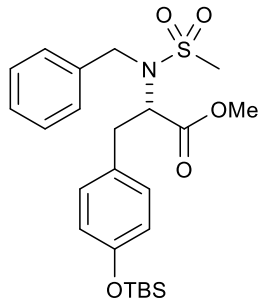

According to general procedure B; flash chromatography (5% EtOAc in Hexane to 15% EtOAc in Hexane) provided **2.8.1b** (2.48 g, 93%) as an off-white solid.

Mp = 102 – 104 ˚C; TLC Rf = 0.4 (2:1 Hexanes/EtOAc) $[\alpha]^{25}_{D}$ = -24.5 (c = 0.1, $CHCl_3$)

HRMS calculated for $C_{24}H_{35}NO_5SSiNa$ $(M + Na)^+$ 500.1903, found 500.1893 (TOF MS ES+)

FTIR (KBr film): 1734, 1607, 1326, 1143, 914 cm^{-1}

^{1}H NMR ($CDCl_3$, 400 MHz) δ 7.45 – 7.18 (m, 5H), 6.99 (d, *J* = 8.5 Hz, 2H), 6.74 (d, *J* = 8.5 Hz, 2H), 4.68 (dd, *J* = 8.4, 7.0 Hz, 1H), 4.50 (d, *J* = 15.6 Hz, 1H), 4.29 (d, *J* = 15.6 Hz, 1H), 3.58 (s, 3H), 3.17 (dd, *J* = 14.4, 7.0 Hz, 1H), 2.95 (dd, *J* = 14.4, 8.4 Hz, 1H), 2.68 (s, 3H), 0.98 (s, 9H), 0.18 (s, 6H).

^{13}C NMR ($CDCl_3$, 126 MHz) δ 171.1, 154.6, 136.3, 130.3, 129.7, 128.8, 128.6, 128.0, 120.3, 61.9, 52.3, 49.8, 40.4, 36.2, 25.8, 18.3, -4.4.

Methyl (S)-3-(4-((tert-butyldimethylsilyl)oxy)phenyl)-2-(N-(4-fluorobenzyl)methyl sulfonamido)propanoate (2.8.1c)

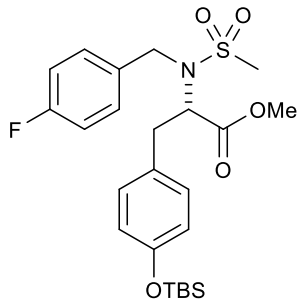

According to general procedure B; flash chromatography (5% EtOAc in Hexane to 15% EtOAc in Hexane) provided **2.8.1c** (3.48 g, 91%) as an off-white solid.

Mp = 112 – 114 ˚C; TLC Rf = 0.4 (2:1 Hexanes/EtOAc) $[\alpha]^{25}_{D}$ = -34 (c = 0.5, $CHCl_3$)

HRMS calculated for $C_{24}H_{34}FNO_5SSiNa$ $(M + Na)^+$ 518.1809, found 518.1820 (TOF MS ES+)

FTIR (KBr film): 1734, 1606, 1327, 1142, 911 cm^{-1}

^1H NMR ($CDCl_3$, 400 MHz) δ 7.34 – 7.27 (m, 2H), 6.98 (ddd, *J* = 8.7, 5.6, 2.7 Hz, 4H), 6.79 – 6.69 (m, 2H), 4.70 (dd, *J* = 8.6, 6.9 Hz, 1H), 4.46 (d, *J* = 15.7 Hz, 1H), 4.27 (d, *J* = 15.7 Hz, 1H), 3.60 (s, 3H), 3.16 (dd, *J* = 14.5, 6.9 Hz, 1H), 2.91 (dd, *J* = 14.4, 8.6 Hz, 1H), 2.68 (s, 3H), 0.97 (s, 9H), 0.17 (s, 6H).

^{13}C NMR ($CDCl_3$, 126 MHz) δ 171.2, 162.6 (d, *J* = 246.2 Hz), 154.8, 132.2 (d, *J* = 2.9 Hz), 130.6 (d, *J* = 8.2 Hz), 130.2, 129.5, 120.4, 115.5 (d, *J* = 21.0 Hz), 61.8, 52.4, 49.1, 40.34, 36.1, 25.8, 18.4, -4.3.

Methyl O-(tert-butyldimethylsilyl)-N-(2-chlorobenzyl)-N-(methylsulfonyl)-L-serinate (2.10.4a)

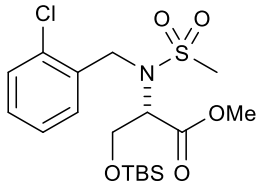

According to general procedure B; flash chromatography (5% EtOAc in Hexane to 15% EtOAc in Hexane) provided **2.10.4a** (2.46 g, 88%) as an off-white solid.

Mp = 104 – 107 ˚C; TLC Rf = 0.4 (4:1 Hexanes/EtOAc) $[\alpha]^{25}_{D}$ = -21.34 (c = 0.5, $CHCl_3$)

HRMS calculated for $C_{18}H_{30}ClNO_5SSiNa$ $(M + Na)^+$ 458.1200, found 458.1194 (TOF MS ES+)

FTIR (KBr film): 1753, 1340, 1143, 913 cm^{-1}

^{1}H NMR ($CDCl_3$, 400 MHz) δ 7.73 – 7.68 (m, 1H), 7.32 – 7.23 (m, 2H), 7.17 (td, *J* = 7.6, 1.7 Hz, 1H), 4.78 – 4.64 (m, 3H), 4.13 (dd, *J* = 10.9, 6.0 Hz, 1H), 3.98 (dd, *J* = 10.9, 3.0 Hz, 1H), 3.74 (s, 3H), 3.00 (s, 3H), 0.73 (s, 9H), -0.11 (s, 3H), -0.23 (s, 3H).

^{13}C NMR ($CDCl_3$, 126 MHz) δ 170.1, 135.9, 132.4, 129.2, 128.8, 128.3, 126.8, 63.1, 62.4, 52.5, 48.8, 39.0, 25.7, 18.2, -5.9 (d, *J* = 5.1 Hz).

Methyl N-benzyl-O-(tert-butyldimethylsilyl)-N-(methylsulfonyl)-L-serinate (2.10.4b)

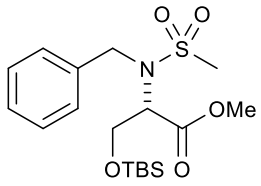

According to general procedure B; flash chromatography (5% EtOAc in Hexane to 15% EtOAc in Hexane) provided **2.10.4b** (1.21 g, 91%) as an off-white solid.

Mp = 107 – 109 ˚C; TLC Rf = 0.4 (4:1 Hexanes/EtOAc) $[\alpha]^{25}_{D}$ = -34.4 (c = 0.1, $CHCl_3$)

HRMS calculated for $C_{18}H_{31}NO_5SSiNa$ $(M + Na)^+$ 424.1590, found 424.1585 (TOF MS ES+)

FTIR (KBr film): 1749, 1311, 1147, 964 cm^{-1}

^1H NMR ($CDCl_3$, 400 MHz) δ 7.44 – 7.39 (m, 2H), 7.31 (tt, *J* = 6.5, 1.0 Hz, 2H), 7.28 – 7.22 (m, 1H), 4.66 – 4.60 (m, 2H), 4.55 (d, *J* = 16.1 Hz, 1H), 4.04 (dd, *J* = 11.0, 7.1 Hz, 1H), 3.97 (dd, *J* = 10.9, 4.2 Hz, 1H), 3.67 (s, 3H), 2.88 (s, 3H), 0.83 (s, 9H), -0.02 (s, 3H), -0.08 (s, 3H).

^{13}C NMR ($CDCl_3$, 126 MHz) δ 170.2, 137.3, 128.5, 128.2, 127.6, 62.4, 62.0, 52.3, 50.4, 40.3, 25.9, 18.3, -5.7 (d, *J* = 13.7 Hz).

Methyl O-(tert-butyldimethylsilyl)-N-(4-fluorobenzyl)-N-(methylsulfonyl)-L-serinate (2.10.4c)

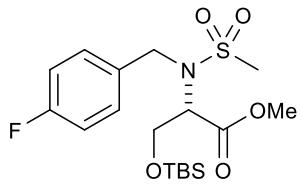

According to general procedure B; flash chromatography (5% EtOAc in Hexane to 15% EtOAc in Hexane) provided **2.10.4c** (2.49 g, 92%) as an off-white solid.

Mp = 106 – 107 ˚C; TLC Rf = 0.4 (4:1 Hexanes/EtOAc) $[\alpha]^{25}_{D}$ = -28.4 (c = 0.5, $CHCl_3$)

HRMS calculated for $C_{18}H_{30}FNO_5SSiNa$ $(M + Na)^+$ 442.1496, found 442.1498 (TOF MS ES+)

FTIR (KBr film): 1754, 1325, 1141, 916 cm^{-1}

^{1}H NMR ($CDCl_3$, 400 MHz) δ 7.43 – 7.37 (m, 2H), 7.03 – 6.96 (m, 2H), 4.66 – 4.57 (m, 2H), 4.51 (d, *J* = 15.7 Hz, 1H), 4.03 (dd, *J* = 11.0, 7.0 Hz, 1H), 3.95 (dd, *J* = 11.0, 4.0 Hz, 1H), 3.68 (s, 3H), 2.87 (s, 3H), 0.82 (s, 9H), -0.02 (s, 3H), -0.07 (s, 3H).

^{13}C NMR ($CDCl_3$, 126 MHz) δ 170.1, 162.4 (d, *J* = 246.0 Hz), 133.3 (d, *J* = 2.8 Hz), 129.8 (d, *J* = 7.7 Hz), 115.3 (d, *J* = 21.1 Hz), 62.5, 62.0, 52.4, 49.7, 40.1, 25.8, 18.2, -5.7 (d, *J* = 15.4 Hz).

Methyl N-(2-chlorobenzyl)-N-(methylsulfonyl)-L-tyrosinate (2.9.1a)

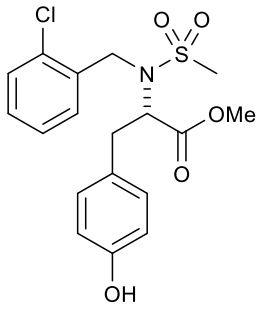

According to general procedure F; flash chromatography (5% EtOAc in Hexane to 25% EtOAc in Hexane) provided **2.9.1a** (2.37 g, 87%) as an off-white solid.

Mp = 136 – 138 ˚C; TLC Rf = 0.5 (2:1 Hexanes/EtOAc) $[\alpha]^{25}_{D}$ = -36.2 (c = 0.05, $CHCl_3$)

HRMS calculated for $C_{18}H_{20}ClNO_5SNa$ $(M + Na)^+$ 420.0648, found 420.0660 (TOF MS ES+)

FTIR (KBr film): 3356, 1718, 1605, 1346, 1154 cm^{-1}

^{1}H NMR ($CDCl_3$, 400 MHz) δ 7.48 (dd, *J* = 7.4, 2.1 Hz, 1H), 7.36 – 7.29 (m, 1H), 7.23 – 7.12 (m, 2H), 7.01 – 6.89 (m, 2H), 6.74 – 6.65 (m, 2H), 5.19 (s, 1H), 4.73 (dd, *J* = 8.4, 7.0 Hz, 1H), 4.61 (d, *J* = 16.9 Hz, 1H), 4.56 (d, *J* = 16.9 Hz, 1H), 3.63 (s, 3H), 3.13 (dd, *J* = 14.5, 7.0 Hz, 1H), 2.95 (dd, *J* = 14.5, 8.4 Hz, 1H), 2.83 (s, 3H).

^{13}C NMR ($CDCl_3$, 126 MHz) δ 171.1, 154.9, 134.0, 132.9, 130.5, 130.3, 129.4, 129.1, 128.4, 127.1, 115.6, 62.3, 52.5, 47.0, 39.8, 35.9.

Methyl N-benzyl-N-(methylsulfonyl)-L-tyrosinate (2.9.1b)

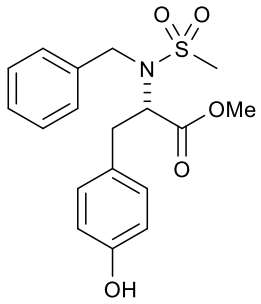

According to general procedure F; flash chromatography (5% EtOAc in Hexane to 25% EtOAc in Hexane) provided **2.9.1b** (1.66 g, 91%) as an off-white solid.

Mp = 142 – 144 ˚C; TLC Rf = 0.6 (1:1 Hexanes/EtOAc) $[\alpha]^{25}_D$ = - 34.6 (c = 0.05, $CHCl_3$)

HRMS calculated for $C_{18}H_{21}NO_5SNa$ $(M + Na)^+$ 386.1033, found 386.1049 (TOF MS ES+)

FTIR (KBr film): 3364, 1712, 1615, 1336, 1150 cm^{-1}

^{1}H NMR (($CDCl_3$, 400 MHz) δ 7.38 – 7.22 (m, 5H), 7.03 – 6.92 (m, 2H), 6.79 – 6.65 (m, 2H), 5.42 (s, 1H), 4.66 (dd, *J* = 8.3, 7.0 Hz, 1H), 4.48 (d, *J* = 15.6 Hz, 1H), 4.28 (d, *J* = 15.6 Hz, 1H), 3.61 (s, 3H), 3.17 (dd, *J* = 14.4, 7.0 Hz, 1H), 2.93 (dd, *J* = 14.4, 8.3 Hz, 1H), 2.74 (s, 3H).

^{13}C NMR (($CDCl_3$, 126 MHz) δ 171.2, 154.8, 136.2, 130.5, 128.9, 128.9, 128.7, 128.1, 115.6, 62.1, 52.5, 50.0, 40.5, 36.1.

Methyl N-(4-fluorobenzyl)-N-(methylsulfonyl)-L-tyrosinate (2.9.1c)

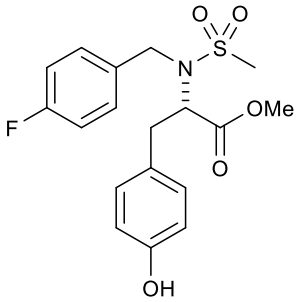

According to general procedure F; flash chromatography (5% EtOAc in Hexane to 25% EtOAc in Hexane) provided **2.9.1c** (2.64 g, 99%) as an off-white solid.

Mp = 138 – 140 ˚C; TLC Rf = 0.5 (1:1 Hexanes/EtOAc) $[\alpha]^{25}_{D}$ = -22.8 (c = 0.05, $CHCl_3$)

HRMS calculated for $C_{18}H_{20}FNO_5SNa$ $(M + Na)^+$ 404.0938, found 404.0948 (TOF MS ES+)

FTIR (KBr film): 3404, 1713, 1614, 1331, 1149 cm^{-1}

^{1}H NMR (($CDCl_3$, 400 MHz) δ 7.32 – 7.24 (m, 2H), 7.01 – 6.91 (m, 4H), 6.75 – 6.68 (m, 2H), 5.45 (s, 1H), 4.67 (dd, *J* = 8.6, 6.8 Hz, 1H), 4.45 (d, *J* = 15.7 Hz, 1H), 4.25 (d, *J* = 15.7 Hz, 1H), 3.63 (s, 3H), 3.15 (dd, *J* = 14.4, 6.8 Hz, 1H), 2.90 (dd, *J* = 14.5, 8.6 Hz, 1H), 2.74 (s, 3H).

^{13}C NMR (($CDCl_3$, 126 MHz) δ 171.2, 162.6 (d, *J* = 246.3 Hz), 154.9, 132.0 (d, *J* = 2.8 Hz), 130.6 (d, *J* = 8.2 Hz), 130.4, 128.6, 115.6, 115.5 (d, *J* = 19.9 Hz), 62.0, 52.6, 49.2, 40.4, 36.1.

Methyl (S)-3-(4-(allyloxy)phenyl)-2-(N-(2-chlorobenzyl)methylsulfonamido)propanoate (2.9.2a)

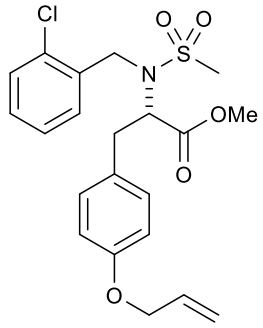

According to general procedure B; flash chromatography (5% EtOAc in Hexane to 15% EtOAc in Hexane) provided **2.9.2a** (2.13 g, 89%) as an off-white solid.

Mp = 144 – 146 ˚C; TLC Rf = 0.3 (4:1 Hexanes/EtOAc) $[\alpha]^{25}_{D}$ = -21.3 (c = 0.05, $CHCl_3$)

HRMS calculated for $C_{21}H_{24}ClNO_5SNa$ $(M + Na)^+$ 460.0956, found 460.0970 (TOF MS ES+)

FTIR (KBr film): 1719, 1616, 1336, 1141, 891 cm^{-1}

^{1}H NMR (($CDCl_3$, 400 MHz) δ 7.52 – 7.47 (m, 1H), 7.35 – 7.30 (m, 1H), 7.23 – 7.13 (m, 2H), 7.04 – 6.97 (m, 2H), 6.82 – 6.75 (m, 2H), 6.03 (ddt, *J* = 17.3, 10.5, 5.3 Hz, 1H), 5.39 (dq, *J* = 17.3, 1.7 Hz, 1H), 5.27 (dq, *J* = 10.5, 1.4 Hz, 1H), 4.73 (dd, *J* = 8.2, 7.2 Hz, 1H), 4.59 (d, *J* = 4.0 Hz, 2H), 4.49 (dt, *J* = 5.3, 1.6 Hz, 2H), 3.62 (s, 3H), 3.14 (dd, *J* = 14.4, 7.2 Hz, 1H), 2.96 (dd, *J* = 14.5, 8.2 Hz, 1H), 2.82 (s, 3H).

^{13}C NMR (($CDCl_3$, 126 MHz) δ 171.0, 157.6, 134.2, 133.3, 132.8, 130.4, 130.1, 129.3, 128.9, 128.8, 127.0, 117.6, 114.8, 68.8, 62.1, 52.4, 46.9, 39.6, 35.9.

Methyl (S)-3-(4-(allyloxy)phenyl)-2-(N-benzylmethylsulfonamido)propanoate (2.9.2b)

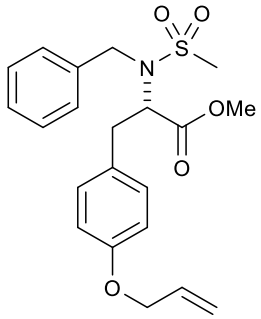

According to general procedure B; flash chromatography (5% EtOAc in Hexane to 15% EtOAc in Hexane) provided **2.9.2b** (1.85 g, 90%) as an off-white solid.

Mp = 138 – 141 ˚C; TLC Rf = 0.3 (4:1 Hexanes/EtOAc) $[\alpha]^{25}_{D}$ = -32.4 (c = 0.05, $CHCl_3$)

HRMS calculated for $C_{21}H_{25}NO_5SNa$ $(M + Na)^+$ 426.1351, found 426.1353 (TOF MS ES+)

FTIR (KBr film): 1744, 1626, 1513, 1321, 1141, 804 cm^{-1}

^1H NMR ($CDCl_3$, 400 MHz) δ 7.36 – 7.23 (m, 5H), 7.06 – 6.98 (m, 2H), 6.86 – 6.76 (m, 2H), 6.04 (ddt, *J* = 17.2, 10.5, 5.3 Hz, 1H), 5.40 (dq, *J* = 17.3, 1.6 Hz, 1H), 5.27 (dq, *J* = 10.5, 1.4 Hz, 1H), 4.67 (dd, *J* = 8.2, 7.1 Hz, 1H), 4.53 – 4.44 (m, 3H), 4.29 (d, *J* = 15.6 Hz, 1H), 3.60 (s, 3H), 3.18 (dd, *J* = 14.3, 7.1 Hz, 1H), 2.94 (dd, *J* = 14.4, 8.2 Hz, 1H), 2.72 (s, 3H).

^{13}C NMR ($CDCl_3$, 126 MHz) δ 171.0, 157.5, 136.3, 133.3, 130.3, 129.1, 128.8, 128.5, 128.0, 117.6, 114.8, 68.8, 61.9, 52.3, 49.9, 40.3, 36.1.

Methyl (S)-3-(4-(allyloxy)phenyl)-2-(N-(4-fluorobenzyl)methylsulfonamido)propanoate (2.9.2c)

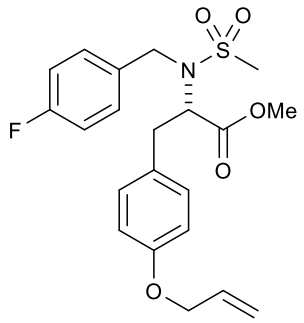

According to general procedure b; flash chromatography (5% EtOAc in Hexane to 15% EtOAc in Hexane) provided **2.9.2c** (2.60 g, 87%) as an off-white solid.

Mp = 144 – 146 ˚C; TLC Rf = 0.3 (4:1 Hexanes/EtOAc) $[\alpha]^{25}_{D}$ = -24.4 (c = 0.05, $CHCl_3$)

HRMS calculated for $C_{21}H_{24}NO_5SNa$ $(M + Na)^+$ 444.1257, found 444.1277 (TOF MS ES+)

FTIR (KBr film): 1742, 1611, 1514, 1321, 1116, 824 cm^{-1}

1H NMR (400 MHz, Chloroform-d) δ 7.32 – 7.24 (m, 2H), 7.05 – 6.91 (m, 4H), 6.83 – 6.76 (m, 2H), 6.03 (ddt, *J* = 17.3, 10.5, 5.3 Hz, 1H), 5.39 (dq, *J* = 17.3, 1.6 Hz, 1H), 5.27 (dq, *J* = 10.5, 1.4 Hz, 1H), 4.68 (dd, *J* = 8.5, 6.9 Hz, 1H), 4.49 (dt, *J* = 5.3, 1.6 Hz, 2H), 4.44 (d, *J* = 15.7 Hz, 1H), 4.26 (d, *J* = 15.7 Hz, 1H), 3.61 (s, 3H), 3.16 (dd, *J* = 14.4, 6.9 Hz, 1H), 2.90 (dd, *J* = 14.4, 8.5 Hz, 1H), 2.71 (s, 3H).

^{13}C NMR ($CDCl_3$, 126 MHz) δ 171.0, 162.4 (d, *J* = 246.3 Hz), 157.6, 133.3, 132.1 (d, *J* = 3.4 Hz), 130.5 (d, *J* = 8.0 Hz), 130.2, 128.9, 117.7, 115.3 (d, *J* = 21.1 Hz), 114.8, 68.8, 61.8, 52.4, 49.1, 40.2, 36.0.

(S)-3-(4-(allyloxy)benzyl)-2-(2-chlorobenzyl)isothiazolidin-4-one 1,1-dioxide (2.9.3a)

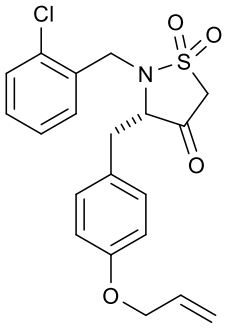

According to general procedure C; flash chromatography (100% Hexane to 10% EtOAc in Hexane) provided **2.9.3a** (0.90 g, 51%) as a pale-orange solid.

Mp = 152 – 154 ˚C; TLC Rf = 0.3 (3:1 Hexanes/EtOAc) $[\alpha]^{25}_{D}$ = -18.2 (c = 0.01, $CHCl_3$)

HRMS calculated for $C_{20}H_{20}ClNO_4SNa$ $(M + Na)^+$ 428.0700, found 428.0718 (TOF MS ES+)

FTIR (KBr film): 1763, 1611, 1512, 1323, 1138, 826 cm^{-1}

^{1}H NMR (($CDCl_3$, 400 MHz) δ 7.35 – 7.31 (m, 1H), 7.30 – 7.19 (m, 3H), 7.02 – 6.93 (m, 2H), 6.82 – 6.75 (m, 2H), 6.05 (ddt, *J* = 17.3, 10.5, 5.3 Hz, 1H), 5.41 (dq, *J* = 17.3, 1.6 Hz, 1H), 5.29 (dq, *J* = 10.5, 1.4 Hz, 1H), 4.60 (d, *J* = 15.3 Hz, 1H), 4.53 – 4.44 (m, 3H), 3.98 (td, *J* = 6.1, 1.4 Hz, 1H), 3.75 (d, *J* = 16.6 Hz, 1H), 3.53 (dd, *J* = 16.6, 1.4 Hz, 1H), 3.04 (d, *J* = 6.1 Hz, 2H).

^{13}C NMR (($CDCl_3$, 126 MHz) δ 198.5, 158.0, 134.1, 133.3, 132.1, 131.6, 130.8, 130.0, 129.9, 127.5, 127.2, 117.9, 115.0, 70.5, 68.9, 55.6, 45.7, 36.4.

(S)-3-(4-(allyloxy)benzyl)-2-benzylisothiazolidin-4-one 1,1-dioxide (2.9.3b)

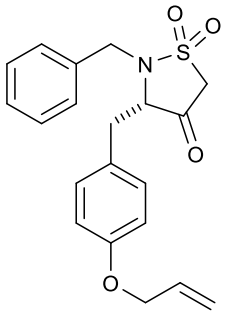

According to general procedure C; flash chromatography (100% Hexane to 10% EtOAc in Hexane) provided **2.9.3b** (0.68 g, 47%) as a pale-orange solid.

Mp = 148 – 150 ˚C; TLC Rf = 0.3 (3:1 Hexanes/EtOAc) $[\alpha]^{25}_{D}$ = -28.2 (c = 0.01, $CHCl_3$)

HRMS calculated for $C_{20}H_{21}NO_4SNa$ $(M + Na)^+$ 394.1089, found 394.1095 (TOF MS ES+)

FTIR (KBr film): 1753, 1609, 1512, 1331, 1136, 821 cm^{-1}

^{1}H NMR ($CDCl_3$, 400 MHz) δ 7.34 – 7.29 (m, 3H), 7.17 (dd, *J* = 6.6, 2.9 Hz, 2H), 7.06 – 7.01 (m, 2H), 6.89 – 6.82 (m, 2H), 6.06 (ddt, *J* = 17.3, 10.6, 5.3 Hz, 1H), 5.42 (dq, *J* = 17.2, 1.6 Hz, 1H), 5.30 (dq, *J* = 10.5, 1.4 Hz, 1H), 4.71 (d, *J* = 15.0 Hz, 1H), 4.54 (dt, *J* = 5.3, 1.6 Hz, 2H), 3.90 (ddd, *J* = 7.6, 4.7, 1.4 Hz, 1H), 3.85 (d, *J* = 15.1 Hz, 1H), 3.65 (d, *J* = 16.5 Hz, 1H), 3.52 (dd, *J* = 16.5, 1.4 Hz, 1H), 3.09 – 2.94 (m, 2H).

^{13}C NMR ($CDCl_3$, 126 MHz) δ 198.3, 157.9, 133.9, 133.2, 130.6, 129.2, 129.0, 128.6, 127.5, 117.9, 115.1, 69.0, 68.9, 56.0, 47.9, 36.1.

(S)-3-(4-(allyloxy)benzyl)-2-(4-fluorobenzyl)isothiazolidin-4-one 1,1-dioxide (2.9.3c)

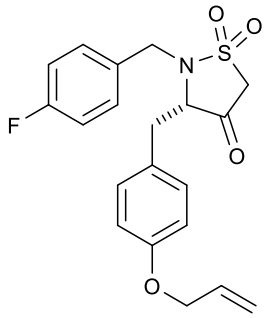

According to general procedure C; flash chromatography (100% Hexane to 10% EtOAc in Hexane) provided **2.9.3c** (0.70 g, 51%) as a pale-orange solid.

Mp = 154 – 156 ˚C; TLC Rf = 0.4 (3:1 Hexanes/EtOAc) $[\alpha]^{25}_{D}$ = -22.8 (c = 0.05, $CHCl_3$)

HRMS calculated for $C_{20}H_{20}FNO_4SNa$ $(M + Na)^+$ 412.0995, found 412.1014 (TOF MS ES+)

FTIR (KBr film): 1753, 1609, 1512, 1331, 1136, 821 cm^{-1}

^1H NMR ($CHCl_3$, 400 MHz) δ 7.15 – 7.09 (m, 2H), 7.06 – 6.95 (m, 4H), 6.89 – 6.81 (m, 2H), 6.06 (ddt, *J* = 17.3, 10.6, 5.3 Hz, 1H), 5.43 (dq, *J* = 17.2, 1.6 Hz, 1H), 5.31 (dq, *J* = 10.5, 1.4 Hz, 1H), 4.61 (d, *J* = 15.1 Hz, 1H), 4.53 (dt, *J* = 5.4, 1.5 Hz, 2H), 3.91 – 3.86 (m, 2H), 3.66 (d, *J* = 16.6 Hz, 1H), 3.54 (dd, *J* = 16.6, 1.3 Hz, 1H), 3.10 – 2.96 (m, 2H).

^{13}C NMR ($CHCl_3$, 126 MHz) δ 198.3, 162.8 (d, *J* = 247.9 Hz), 158.1, 133.2, 131.1 (d, *J* = 8.2 Hz), 130.7, 129.9 (d, *J* = 3.6 Hz), 127.6, 118.0, 116.0 (d, *J* = 21.7 Hz), 115.2, 69.3, 69.0, 56.0, 47.4, 36.3.

3-(but-3-en-1-yloxy)benzaldehyde (2.11.5)

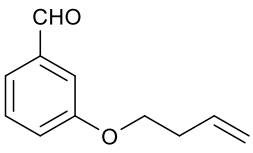

According to general procedure B; flash chromatography (100% Hexane to 2% EtOAc in Hexane) provided **2.11.5** (1.90 g, 88%) as a pale-yellow liquid.

TLC Rf = 0.7 (7:1 Hexanes/EtOAc); FTIR (neat): 1699, 1599, 1386, 1263, 1040 cm^{-1}

HRMS calculated for $C_{11}H_{12}O_2Na$ $(M + Na)^+$ 199.0735, found 199.0749 (TOF MS ES+)

^1H NMR ($CDCl_3$, 400 MHz) δ 9.97 (s, 1H), 7.50 – 7.35 (m, 3H), 7.18 (dt, *J* = 6.4, 2.7 Hz, 1H), 5.91 (ddt, *J* = 17.1, 10.3, 6.7 Hz, 1H), 5.18 (dq, *J* = 17.2, 1.6 Hz, 1H), 5.12 (dq, *J* = 10.2, 1.3 Hz, 1H), 4.08 (t, *J* = 6.7 Hz, 2H), 2.57 (qt, *J* = 6.7, 1.4 Hz, 2H).

^{13}C NMR ((CDCl3, 126 MHz) δ 192.3, 159.6, 137.9, 134.3, 130.2, 123.6, 122.1, 117.4, 113.0, 67.6, 33.6.

3-(pent-4-en-1-yloxy)benzaldehyde (2.11.4)

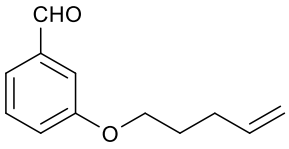

According to general procedure B; flash chromatography (100% Hexane to 2% EtOAc in Hexane) provided **2.11.4** (2.18 g, 93%) as a pale-yellow liquid.

TLC Rf = 0.6 (7:1 Hexanes/EtOAc) FTIR (neat): 1694, 1603, 1382, 1268, 1047 cm^{-1}

HRMS calculated for $C_{12}H_{14}O_2Na$ $(M + Na)^+$ 213.0891 found 213.0907 (TOF MS ES+)

^1H NMR ($CDCl_3$, 400 MHz) δ 9.96 (s, 1H), 7.47 – 7.33 (m, 3H), 7.16 (dt, *J* = 5.8, 2.7 Hz, 1H), 5.84 (ddt, *J* = 16.9, 10.2, 6.6 Hz, 1H), 5.06 (dq, *J* = 17.1, 1.7 Hz, 1H), 5.00 (ddt, *J* = 10.2, 2.2, 1.3 Hz, 1H), 4.01 (t, *J* = 6.4 Hz, 2H), 2.34 – 2.15 (m, 2H), 2.01 – 1.82 (m, 2H).

^{13}C NMR ($CDCl_3$, 126 MHz) δ 192.3, 159.8, 137.9, 137.7, 130.1, 123.5, 122.0, 115.5, 112.9, 67.5, 30.1, 28.4.

3-(hex-5-en-1-yloxy)benzaldehyde (2.11.6)

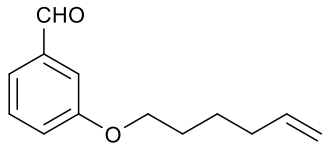

According to general procedure B; flash chromatography (100% Hexane to 2% EtOAc in Hexane) provided **2.11.6** (2.28 g, 91%) as a pale-yellow liquid.

TLC Rf = 0.6 (7:1 Hexanes/EtOAc) FTIR (neat): 1707, 1605, 1378, 1266, 1042 cm^{-1}

HRMS calculated for $C_{13}H_{16}O_2Na$ $(M + Na)^+$ 227.1048, found 227.1036 (TOF MS ES+)

^{1}H NMR ($CDCl_3$, 400 MHz) δ 9.97 (s, 1H), 7.52 – 7.32 (m, 3H), 7.22 – 7.11 (m, 1H), 5.83 (ddt, *J* = 16.9, 10.1, 6.6 Hz, 1H), 5.04 (dq, *J* = 17.1, 1.7 Hz, 1H), 4.98 (ddt, *J* = 10.2, 2.2, 1.2 Hz, 1H), 4.02 (t, *J* = 6.5 Hz, 2H), 2.18 – 2.09 (m, 2H), 1.87 – 1.78 (m, 2H), 1.58 (tt, *J* = 9.6, 6.4 Hz, 2H).

^{13}C NMR ($CDCl_3$, 126 MHz) δ 192.4, 159.8, 138.5, 137.9, 130.1, 123.5, 122.1, 115.0, 112.9, 68.2, 33.5, 28.7, 25.4.

Calculated vs found mass difference table for the synthesized compounds with error in ppm

SN	*Compound ID*	*Molecular Formula*	*Calculated Mass*	*Found Mass*	*Error (ppm)*
1	1.23.3a	$C_{11}H_{15}NO_4SNa$ (M+Na)	280.0620	280.0627	2.5
2	1.23.3b	$C_{11}H_{14}N_2O_6SNa$ (M+Na)	325.0470	325.0478	2.5
3	1.23.4a	$C_{18}H_{20}ClNO_4SNa$ (M+Na)	404.0699	404.0704	1.2
4	1.23.4b	$C_{18}H_{19}ClN_2O_6SNa$ (M+Na)	449.0550	449.0559	2.0
5	1.23.4c	$C_{18}H_{21}NO_4SNa$ (M+Na)	370.1089	370.1103	3.8
6	1.23.4d	$C_{18}H_{20}N_2O_6SNa$ (M+Na)	415.0940	415.0945	1.2
7	1.23.4e	$C_{18}H_{20}FNO_4SNa$ (M+Na)	388.0995	388.1010	3.9
8	1.23.4f	$C_{18}H_{19}FN_2O_6SNa$ (M+Na)	433.0846	433.0862	3.7
9	1.23.5a	$C_{17}H_{17}ClNO_3S$ (M+H)	350.0618	350.0624	1.7
10	1.23.5b	$C_{17}H_{16}ClN_2O_5S$ (M+H)	395.0468	395.0475	1.8
11	1.23.5c	$C_{17}H_{17}NO_3SNa$ (M+Na)	338.0827	338.0844	5.0
12	1.23.5d	$C_{17}H_{16}N_2O_5SNa$ (M+Na)	383.0698	383.0706	2.1
13	1.23.5e	$C_{17}H_{16}FNO_3SNa$ (M+Na)	356.0733	356.0739	1.7
14	1.23.5f	$C_{17}H_{16}FN_2O_5S$ (M+H)	379.0764	379.0782	4.7
15	1.24.1a	$C_{25}H_{22}ClNO_4SNa$ (M+Na)	490.0856	490.0866	2.0
16	1.24.1b	$C_{24}H_{19}ClFNO_3SNa$ (M+Na)	478.0656	478.0638	3.8
17	1.24.1c	$C_{24}H_{20}ClNO_3SNa$ (M+Na)	460.0750	460.0762	2.6
18	1.24.1d	$C_{24}H_{18}ClFN_2O_5SNa$ (M+Na)	523.0607	523.0631	4.6
19	1.24.1e	$C_{25}H_{20}ClN_2O_7S$ (M+H)	527.0680	527.0696	3.0
20	1.24.1f	$C_{25}H_{23}NO_4SNa$ (M+Na)	456.1245	456.1249	0.9
21	1.24.1g	$C_{24}H_{20}FNO_3SNa$ (M+Na)	444.1045	444.1053	1.8
22	1.24.1h	$C_{25}H_{22}N_2O_6SNa$ (M+Na)	501.1096	501.1096	0.0
23	1.24.1i	$C_{24}H_{19}FN_2O_5SNa$ (M+Na)	489.0996	489.0972	4.9
24	1.24.1j	$C_{25}H_{20}N_2O_7SNa$ (M+Na)	515.0889	515.0878	2.1
25	1.24.1k	$C_{26}H_{21}FN_2O_5SNa$ (M+Na)	515.1053	515.1039	2.7
26	1.24.1l	$C_{25}H_{22}FNO_4SNa$ (M+Na)	474.1146	474.1161	3.2

SN	*Compound ID*	*Molecular Formula*	*Calculated Mass*	*Found Mass*	*Error (ppm)*
27	1.24.1m	$C_{24}H_{19}F_2NO_3SNa$ (M+Na)	462.0946	462.0925	4.5
28	1.24.1n	$C_{25}H_{20}FNO_5SNa$ (M+Na)	488.0944	488.0928	3.3
29	1.24.1o	$C_{26}H_{21}F_2NO_3SNa$ (M+Na)	488.1102	488.1097	1.0
30	1.24.1p	$C_{25}H_{21}FN_2O_6SNa$ (M+Na)	519.1002	519.1017	2.9
31	1.24.1q	$C_{25}H_{19}FN_2O_7SNa$ (M+Na)	533.0795	533.0810	2.8
32	1.24.1r	$C_{26}H_{20}F_2N_2O_5SNa$ (M+Na)	533.0959	533.0951	1.5
33	2.7.3	$C_{16}H_{28}NO_3Si$ (M+H)	310.1838	310.1851	4.2
34	2.10.2	$C_{10}H_{24}NO_3Si$ (M+H)	234.1525	234.1535	4.3
35	2.7.4	$C_{17}H_{29}NO_5SSiNa$ (M+Na)	410.1433	410.1443	2.4
36	2.10.3	$C_{11}H_{25}NO_5SSiNa$ (M+Na)	334.1120	334.1128	2.4
37	2.8.1a	$C_{24}H_{34}ClNO_5SSiNa$ (M+Na)	534.1508	534.1532	4.5
38	2.8.1b	$C_{24}H_{35}NO_5SSiNa$ (M+Na)	500.1903	500.1893	2.0
39	2.8.1c	$C_{24}H_{34}FNO_5SSiNa$ (M+Na)	518.1809	518.1820	2.1
40	2.10.4a	$C_{18}H_{30}ClNO_5SSiNa$ (M+Na)	458.1200	458.1194	1.3
41	2.10.4b	$C_{18}H_{31}NO_5SSiNa$ (M+Na)	424.1590	424.1585	1.2
42	2.10.4c	$C_{18}H_{30}FNO_5SSiNa$ (M+Na)	442.1496	442.1498	0.5
43	2.9.1a	$C_{18}H_{20}ClNO_5SNa$ (M+Na)	420.0648	420.0660	2.9
44	2.9.1b	$C_{18}H_{21}NO_5SNa$ (M+Na)	386.1033	386.1049	4.1
45	2.9.1c	$C_{18}H_{20}FNO_5SNa$ (M+Na)	404.0938	404.0948	2.5
46	2.9.2a	$C_{21}H_{24}ClNO_5SNa$ (M+Na)	460.0956	460.0970	3.0
47	2.9.2b	$C_{21}H_{25}NO_5SNa$ (M+Na)	426.1351	426.1353	0.5
48	2.9.2c	$C_{21}H_{24}NO_5SNa$ (M+Na)	444.1257	444.1277	4.5
49	2.9.3a	$C_{20}H_{20}ClNO_4SNa$ (M+Na)	428.0700	428.0718	4.2
50	2.9.3b	$C_{20}H_{21}NO_4SNa$ (M+Na)	394.1089	394.1095	1.5
51	2.9.3c	$C_{20}H_{20}FNO_4SNa$ (M+Na)	412.0995	412.1014	4.6

Methyl (methylsulfonyl)-L-phenylalaninate (1.22.3a)

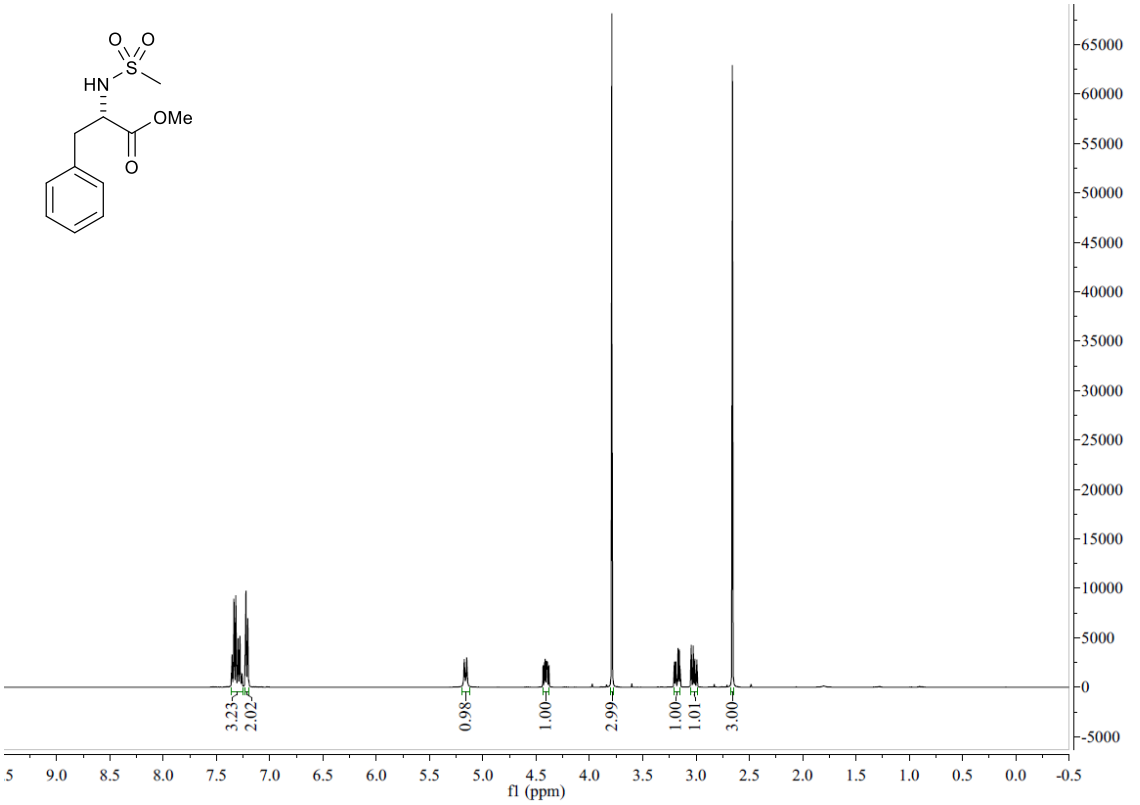

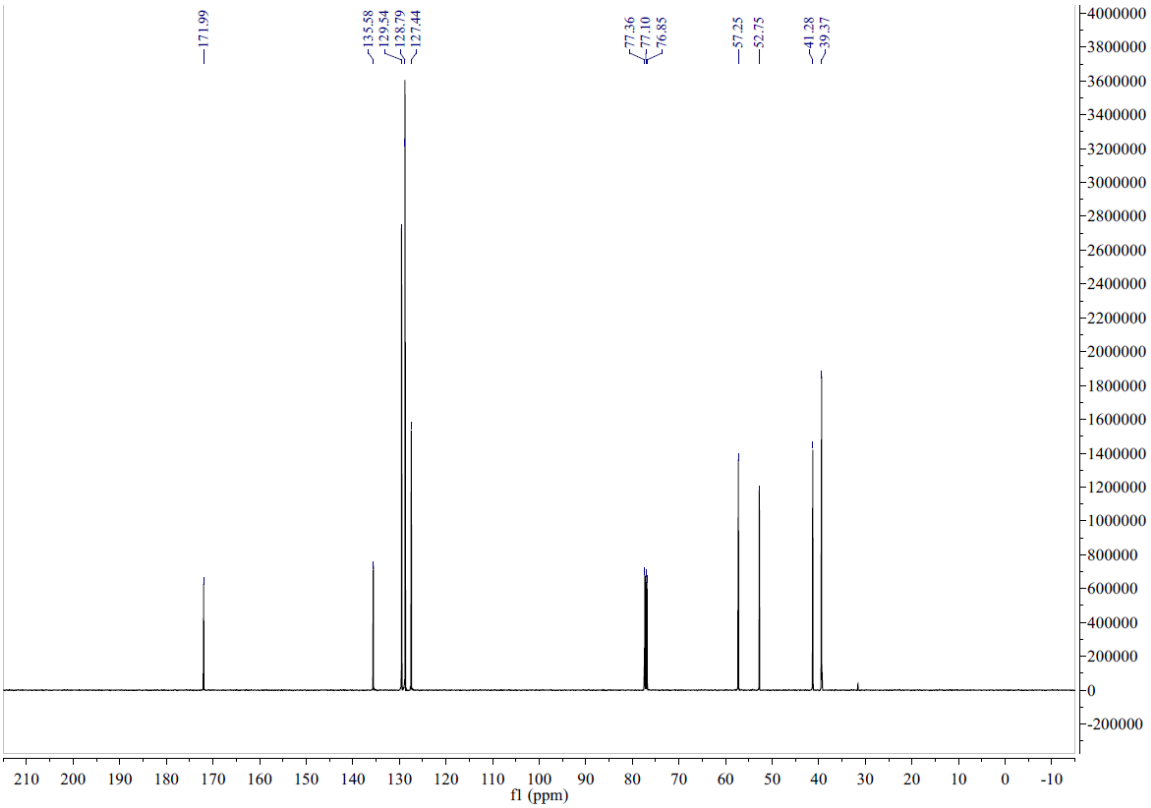

Methyl (S)-2-(methylsulfonamido)-3-(4-nitrophenyl)propanoate (1.22.3b)

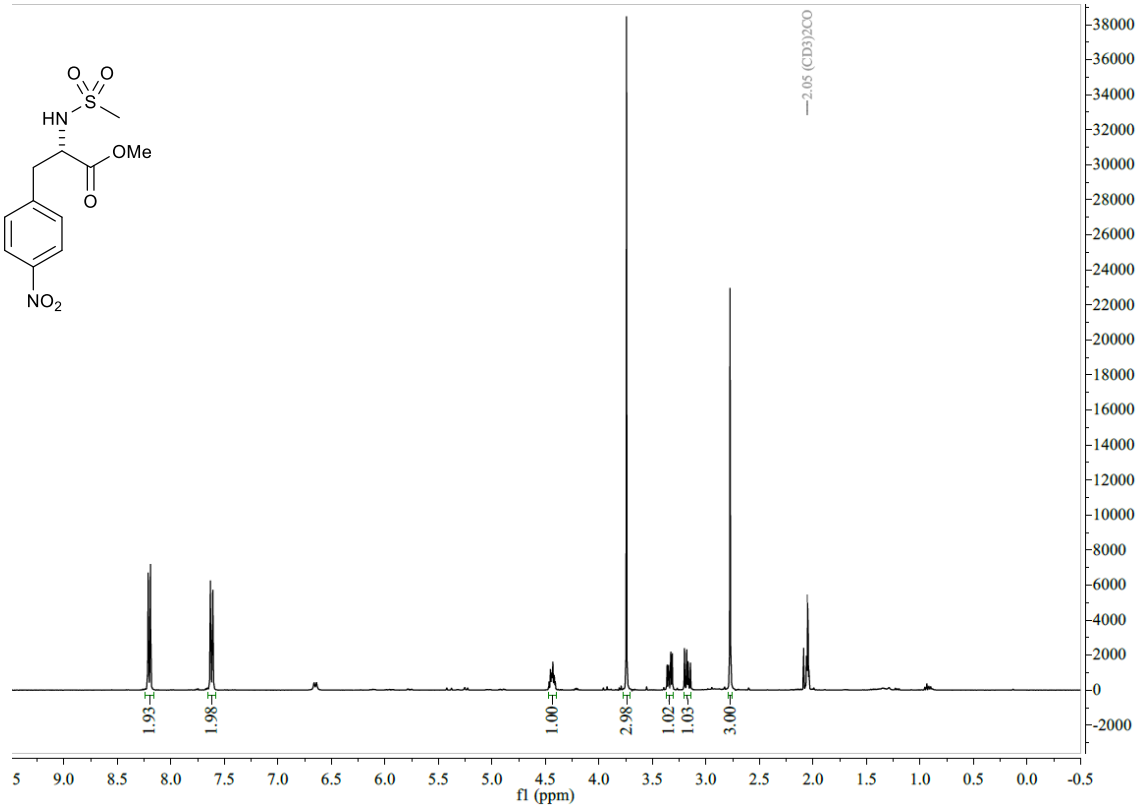

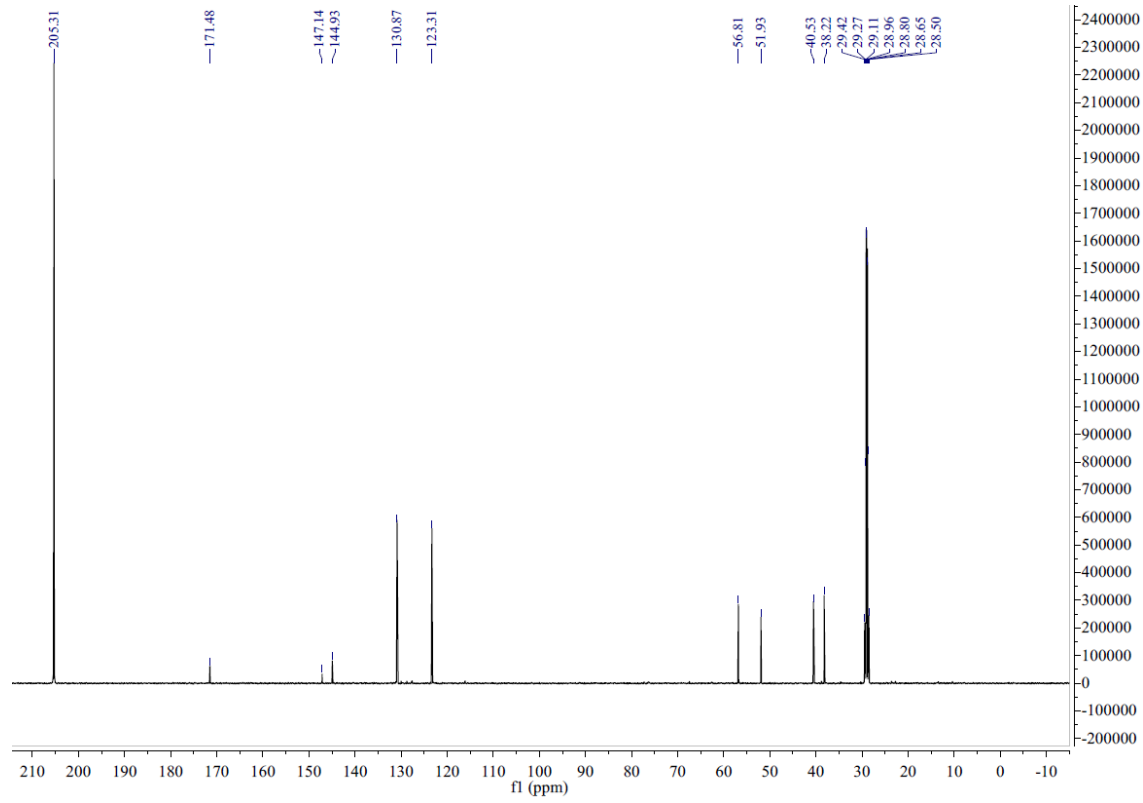

Methyl N-(4-chlorobenzyl)-N-(methylsulfonyl)-L-phenylalaninate (1.22.4a)

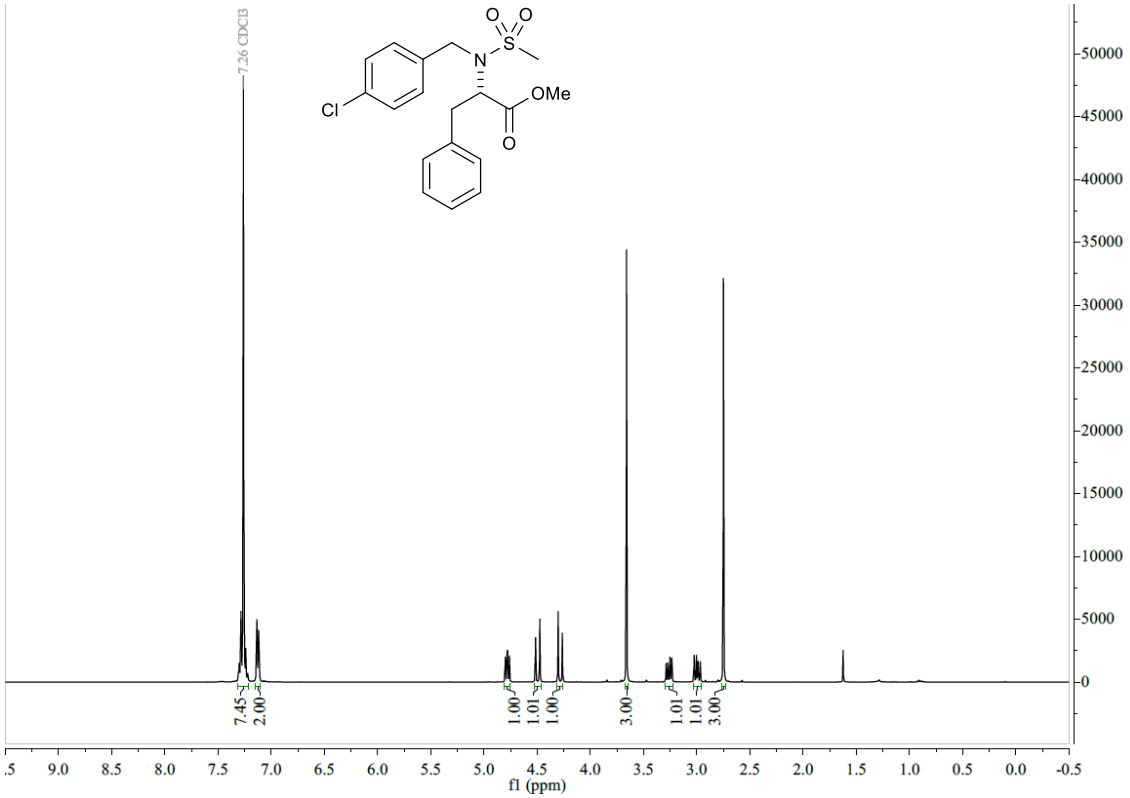

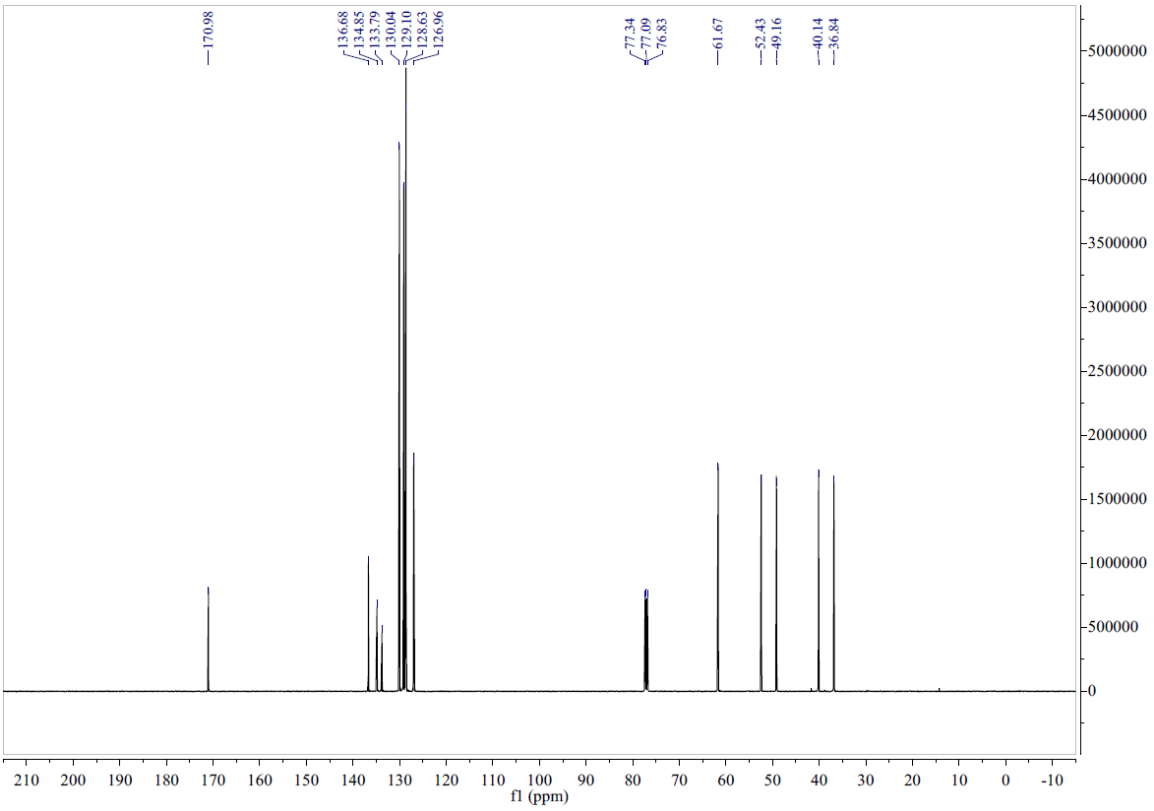

Methyl (S)-2-(N-(4-chlorobenzyl)methylsulfonamido)-3-(4-nitrophenyl)propanoate (1.22.4b)

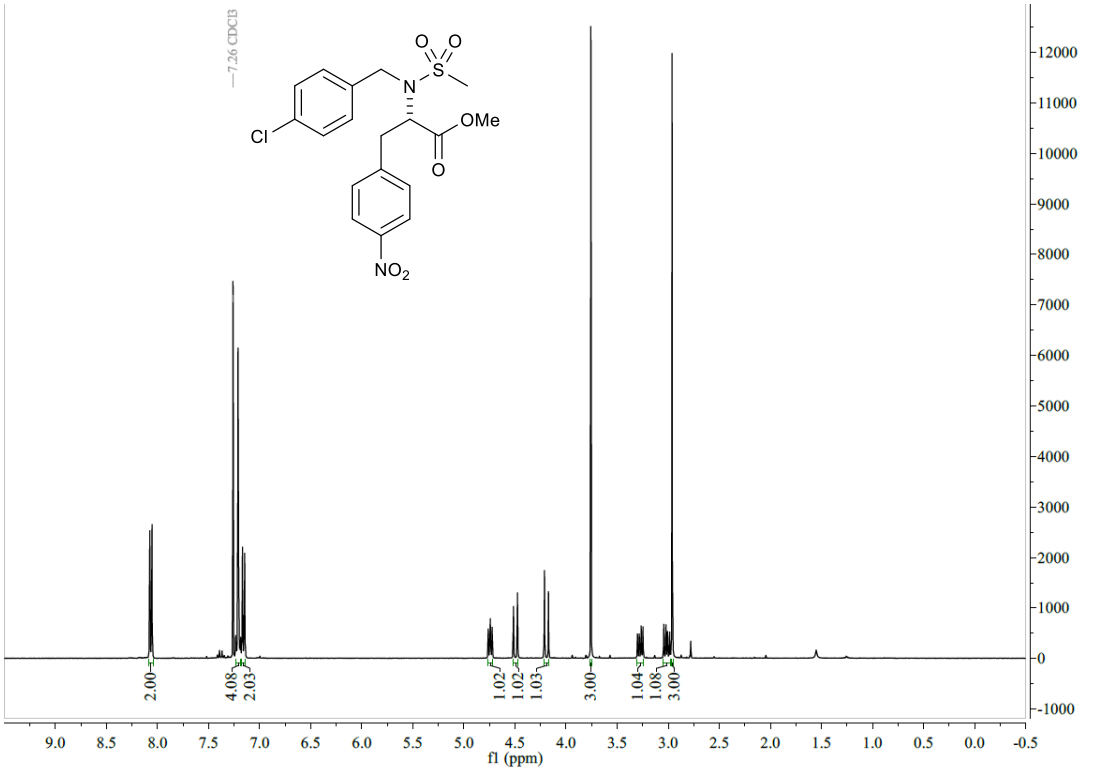

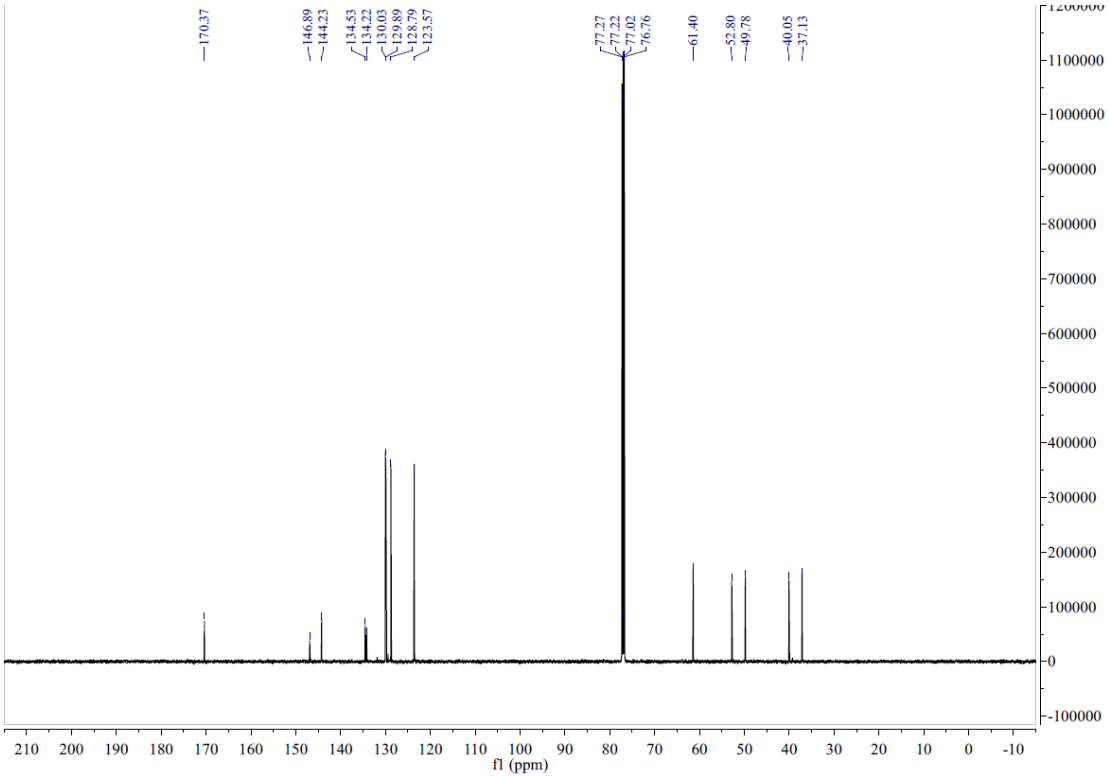

Methyl N-benzyl-N-methylsulfonyl-L-phenylalaninate (1.22.4c)

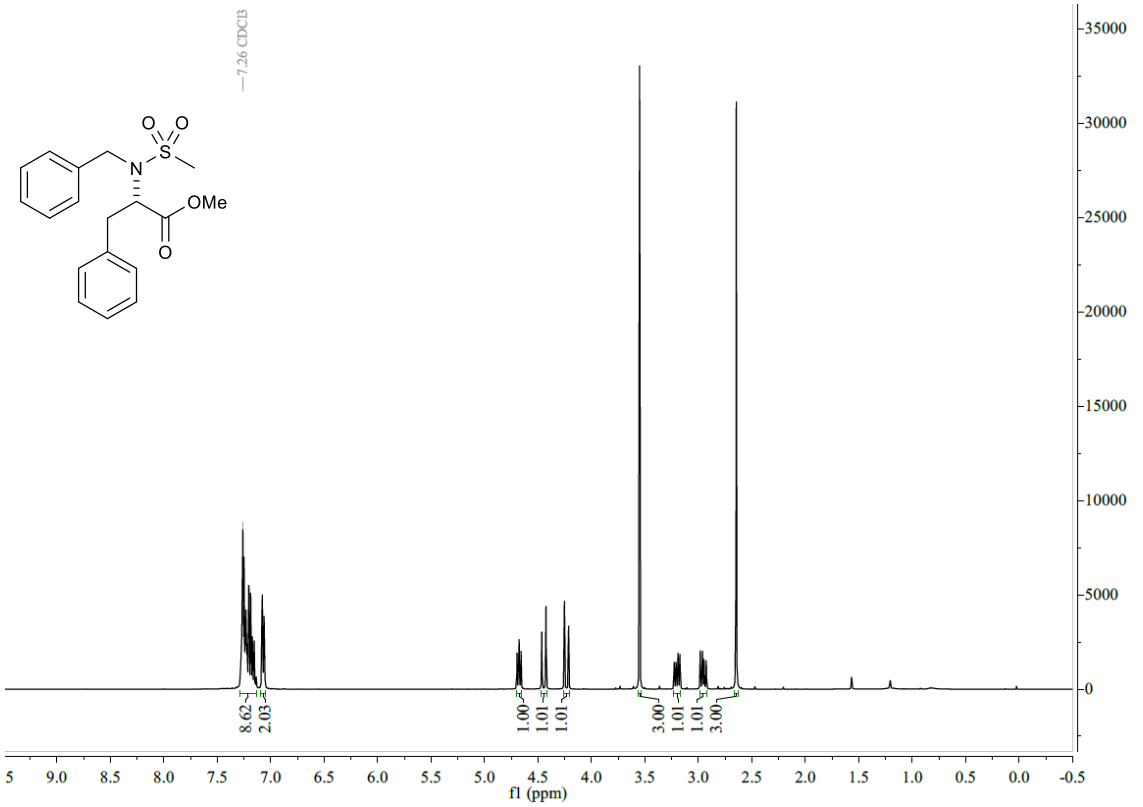

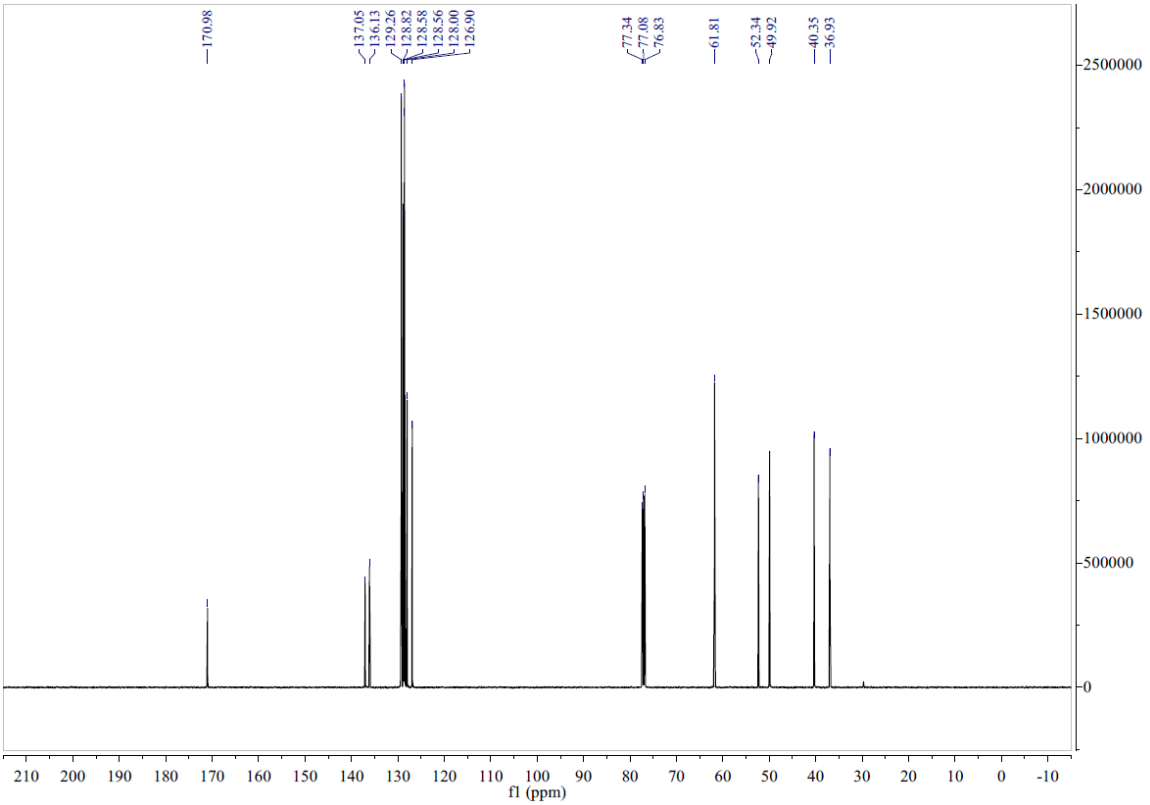

Methyl (S)-2-(N-benzylmethylsulfonamido)-3-(4-nitrophenyl)propanoate (1.22.4d)

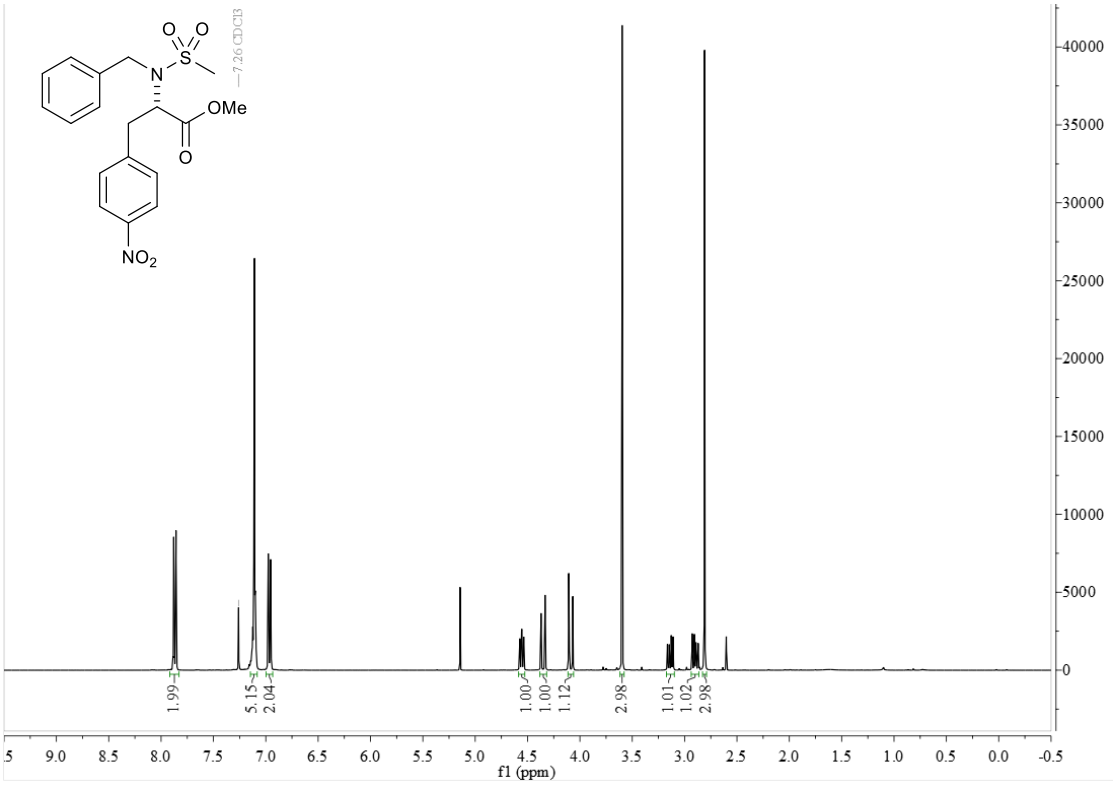

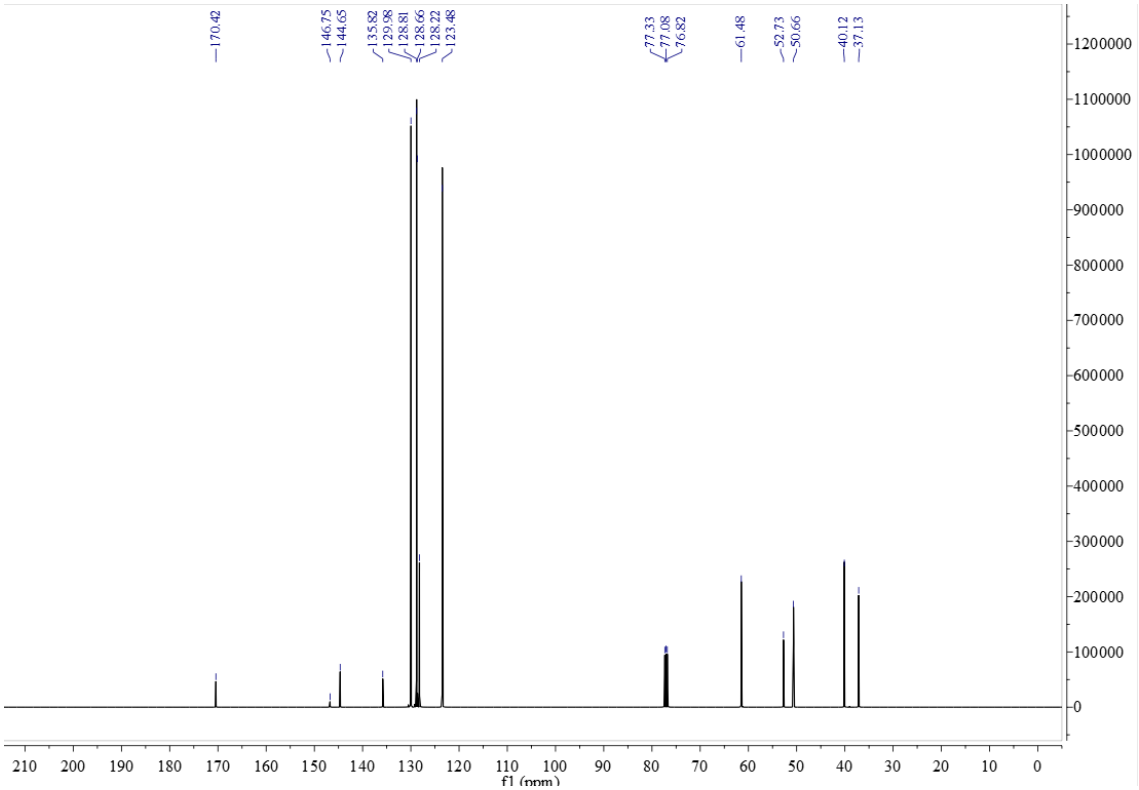

Methyl N-(4-fluorobenzyl)-N-(methylsulfonyl)-L-phenylalaninate (1.22.4e)

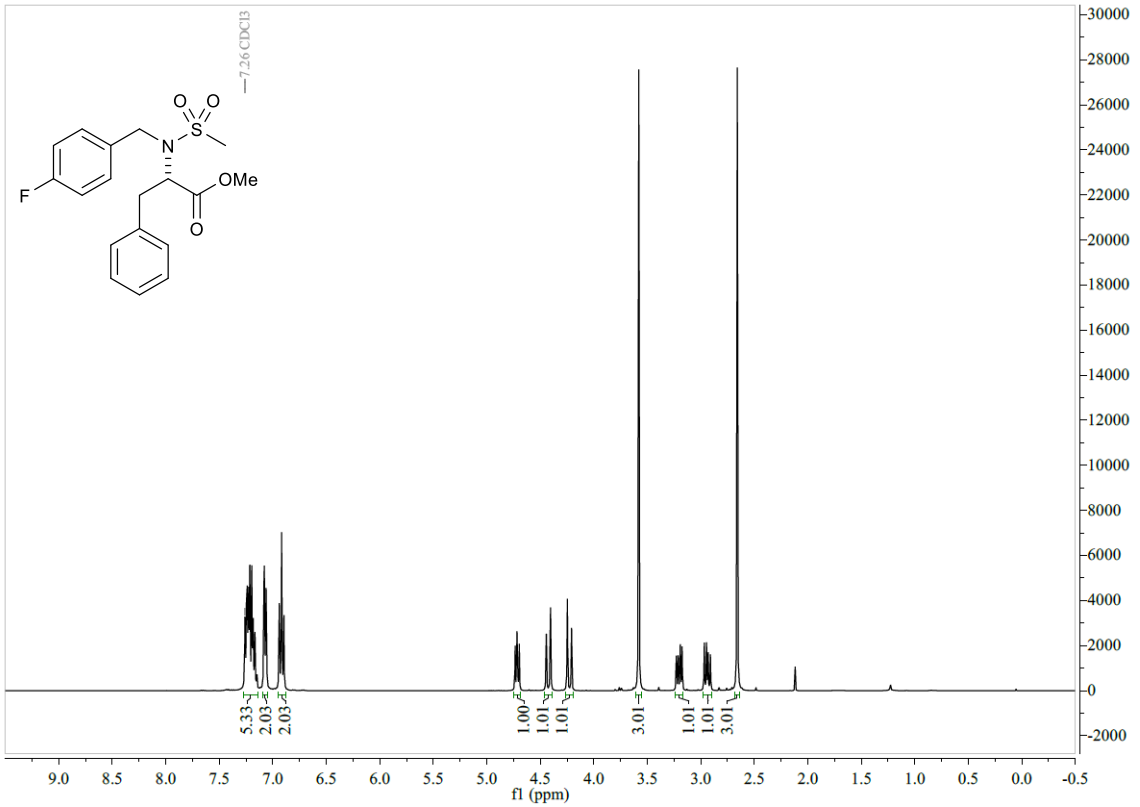

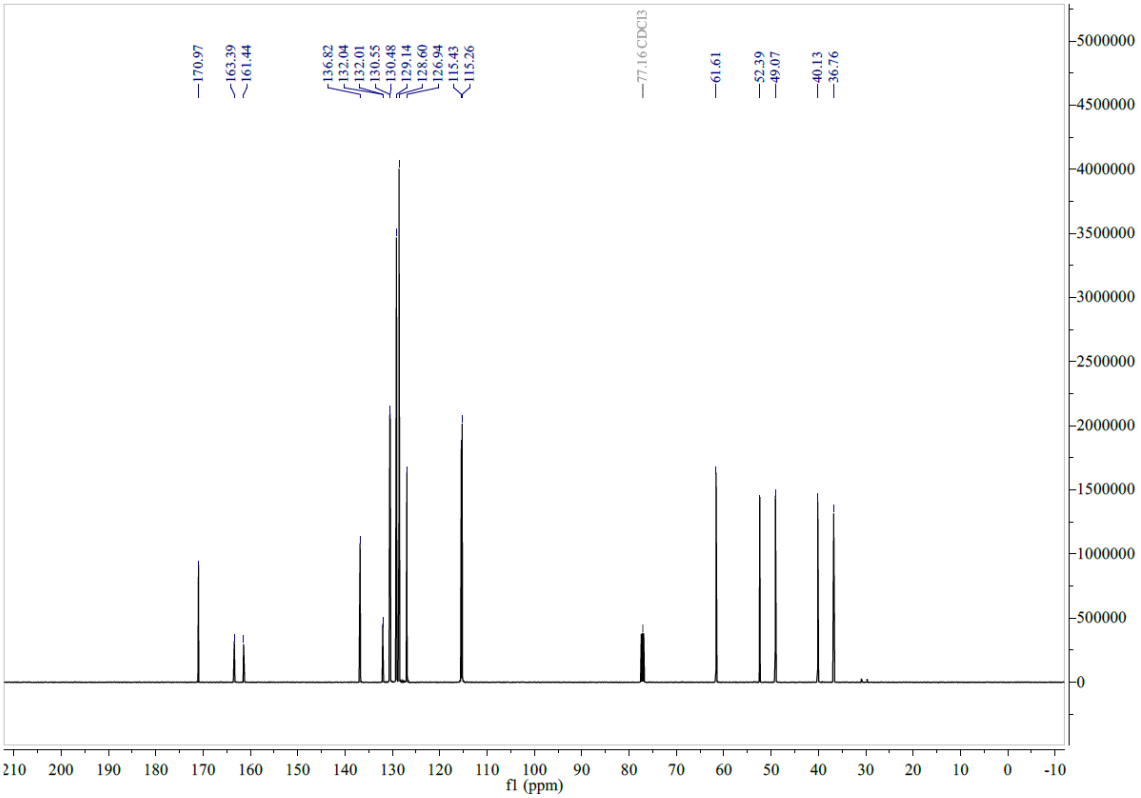

Methyl (S)-2-(N-(4-fluorobenzyl)methylsulfonamido)-3-(4-nitrophenyl)propanoate (1.22.4f)

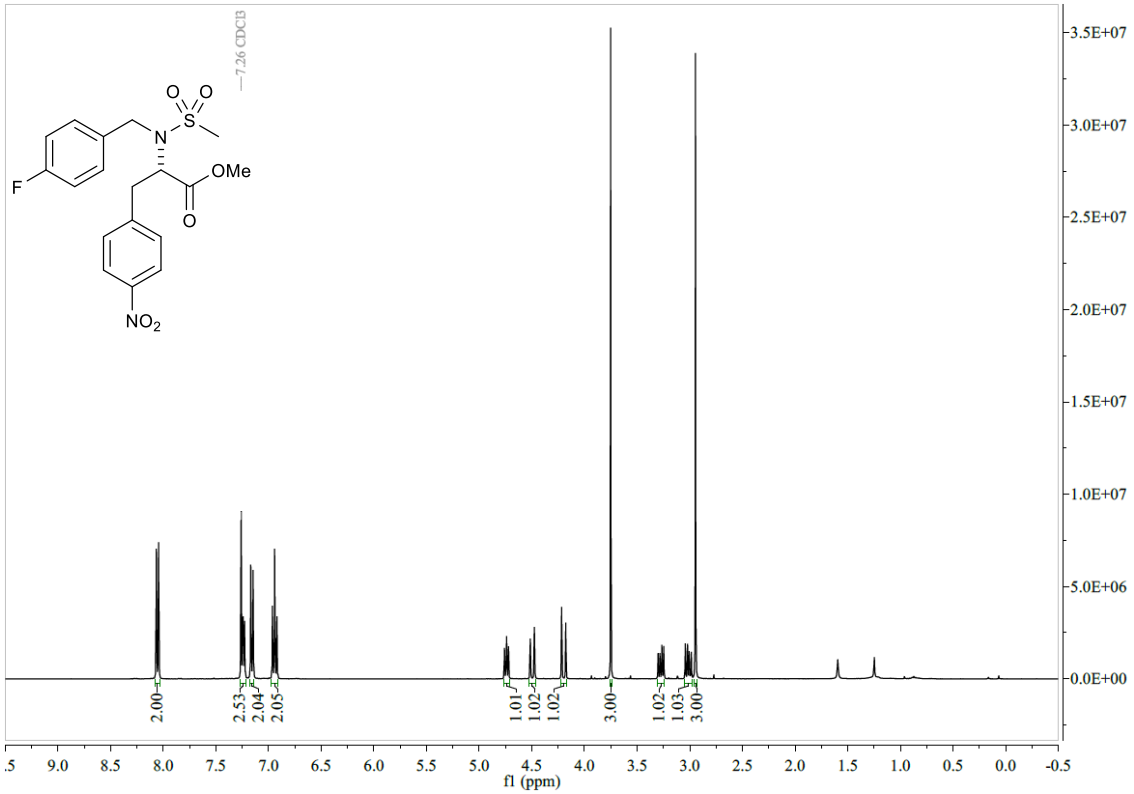

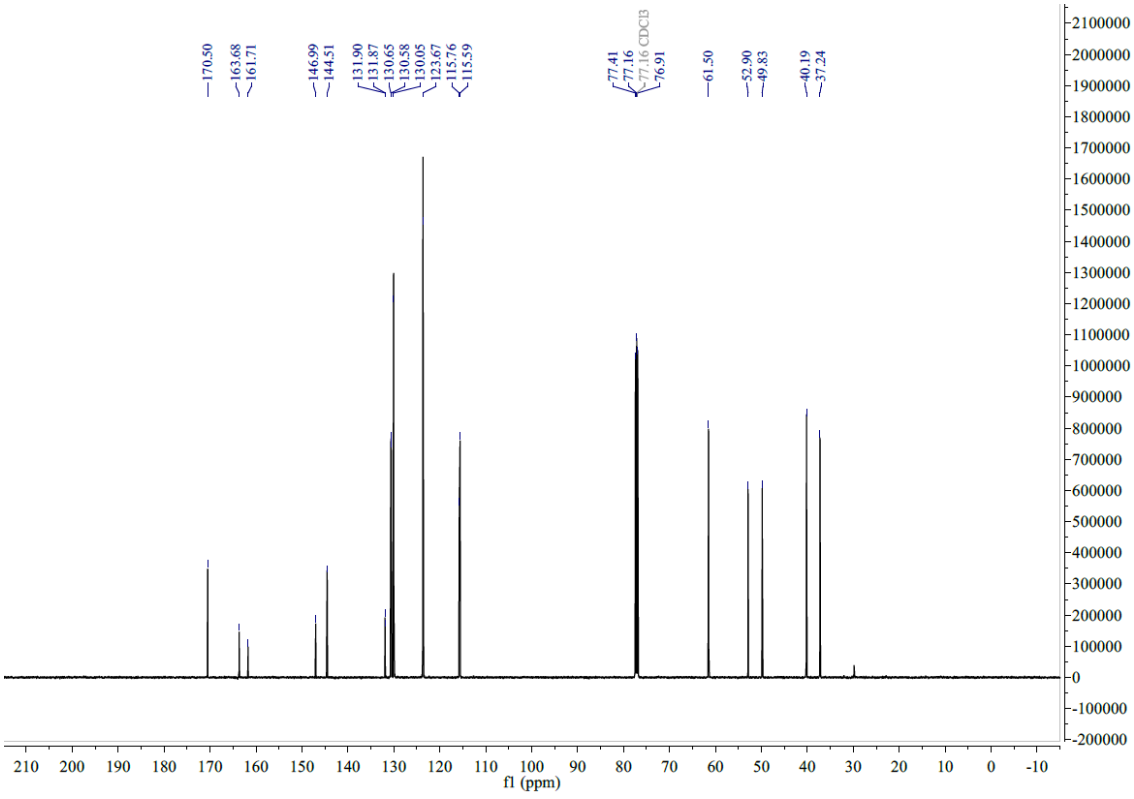

(S)-3-benzyl-2-(4-chlorobenzyl)isothiazolidin-4-one 1,1-dioxide (1.22.5a)

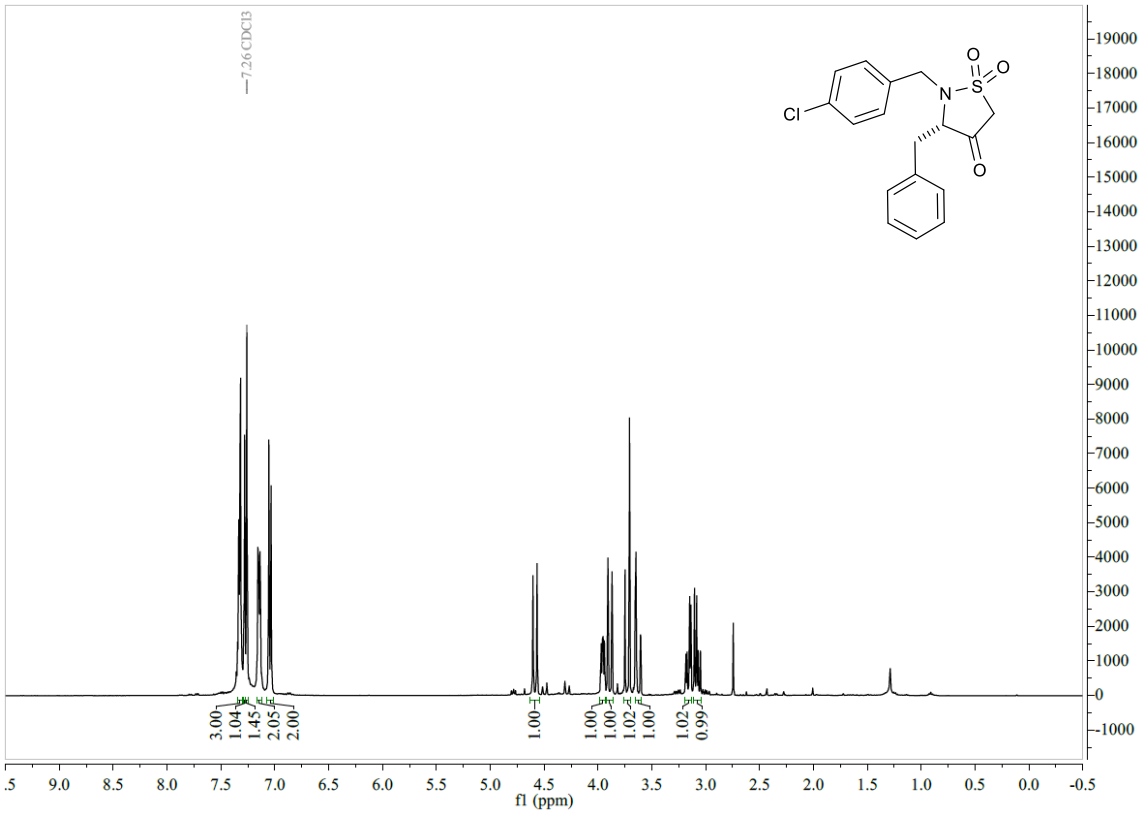

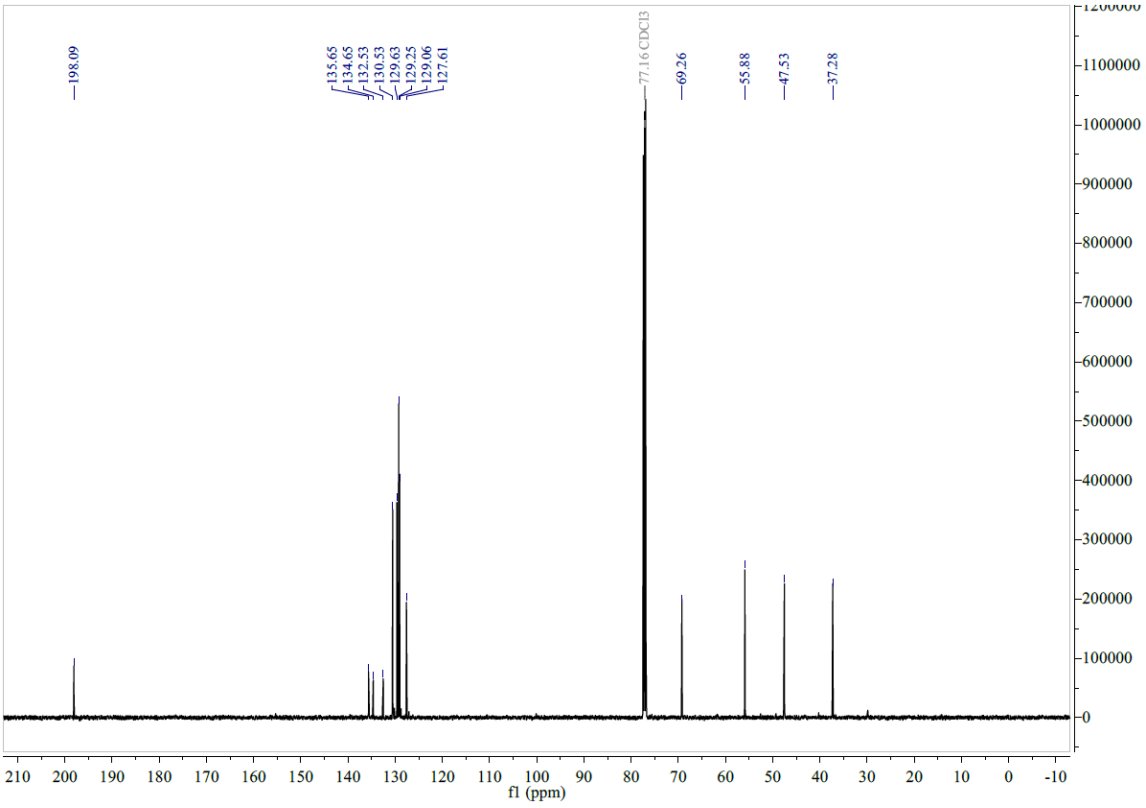

(S)-2-(4-chlorobenzyl)-3-(4-nitrobenzyl)isothiazolidin-4-one 1,1-dioxide (1.22.5b)

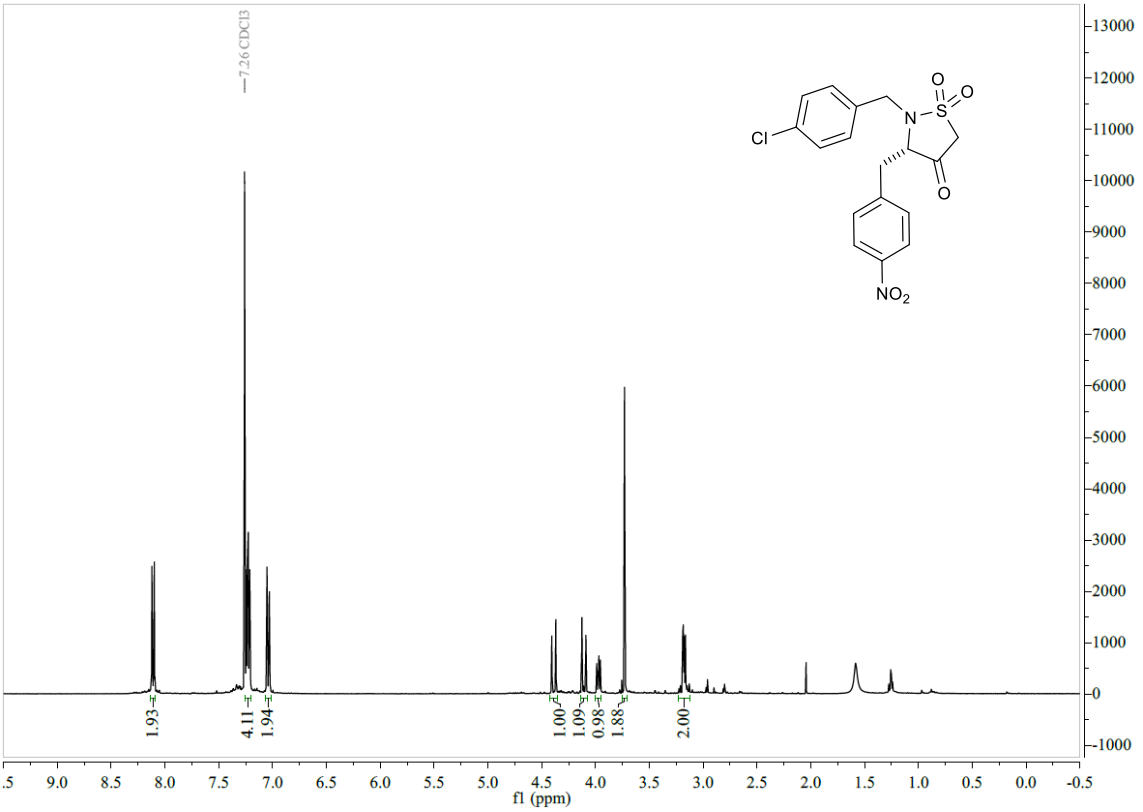

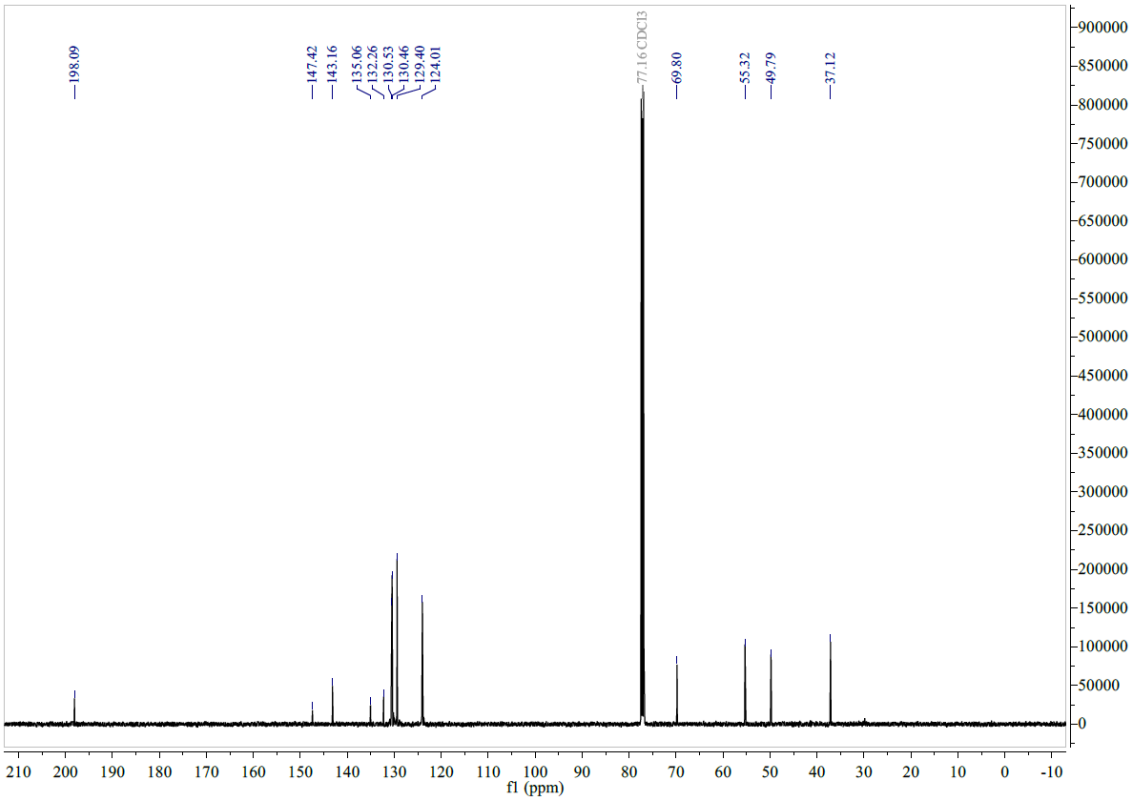

(S)-2,3-dibenzylisothiazolidin-4-one 1,1-dioxide (1.22.5c)

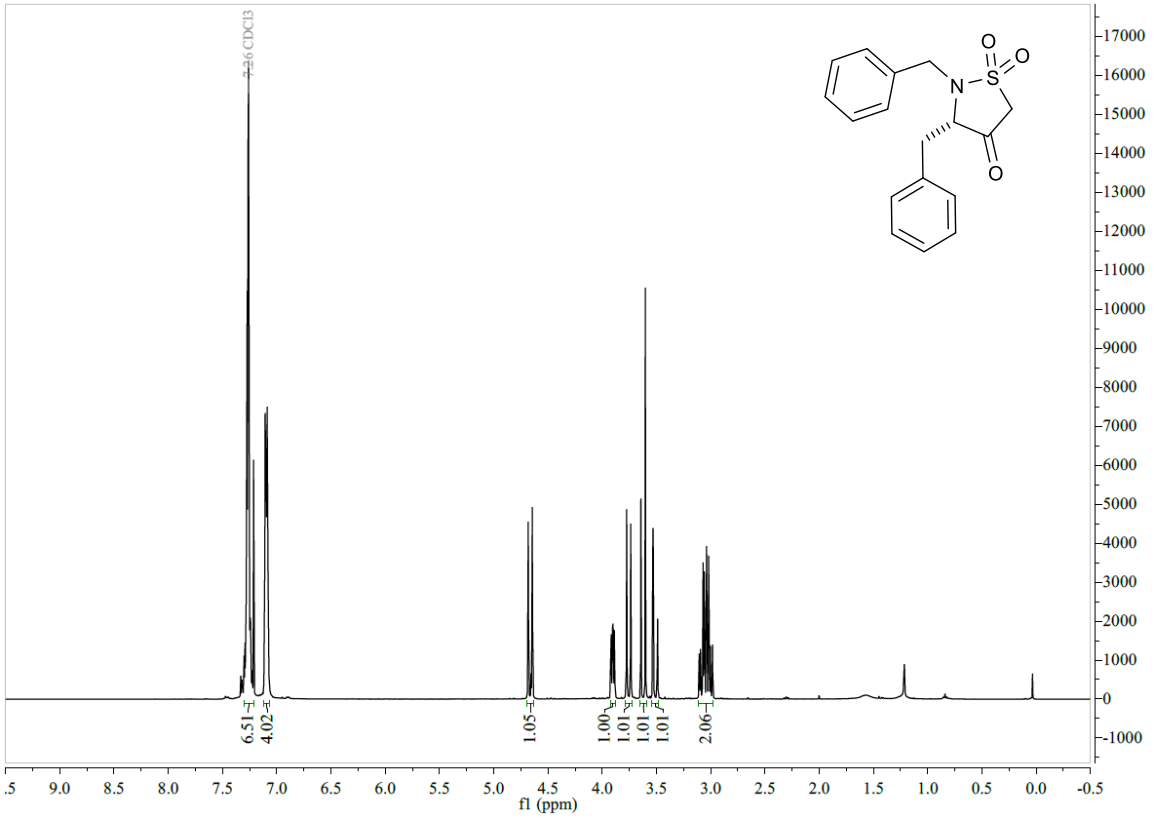

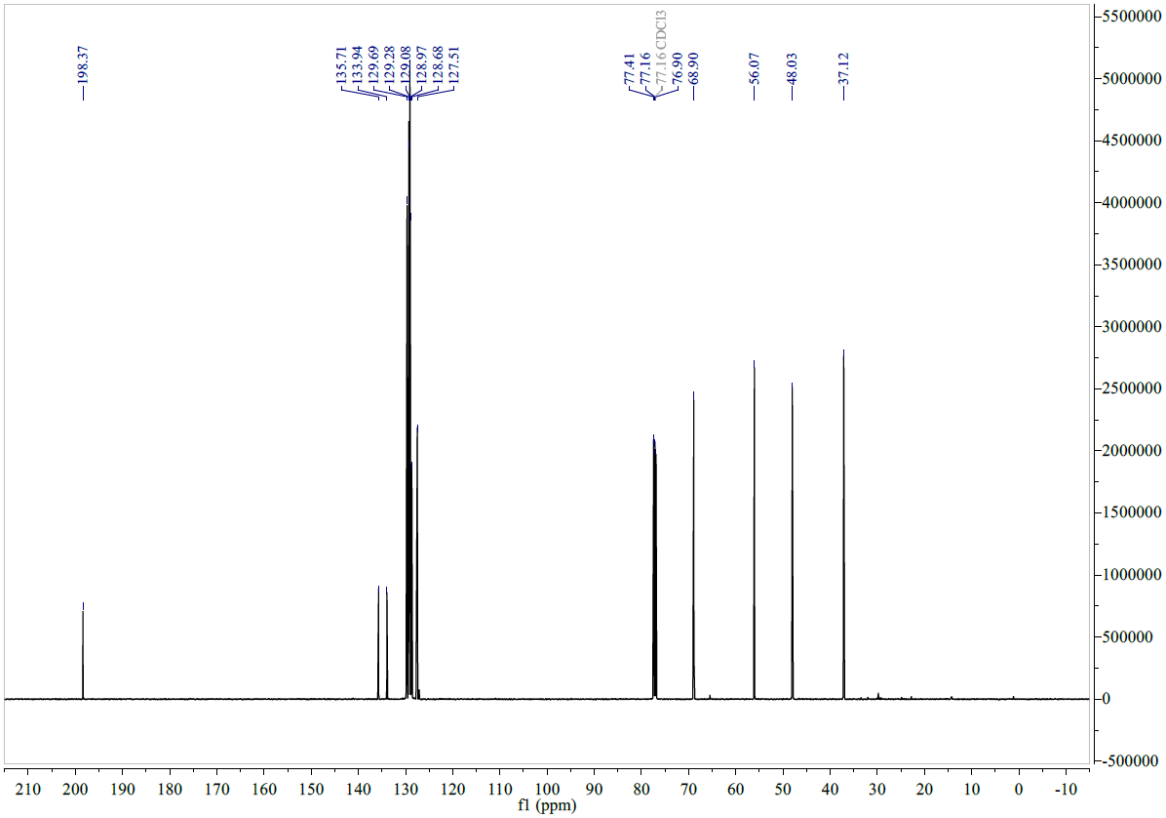

(S)-2-benzyl-3-(4-nitrobenzyl)isothiazolidin-4-one 1,1-dioxide (1.22.5d)

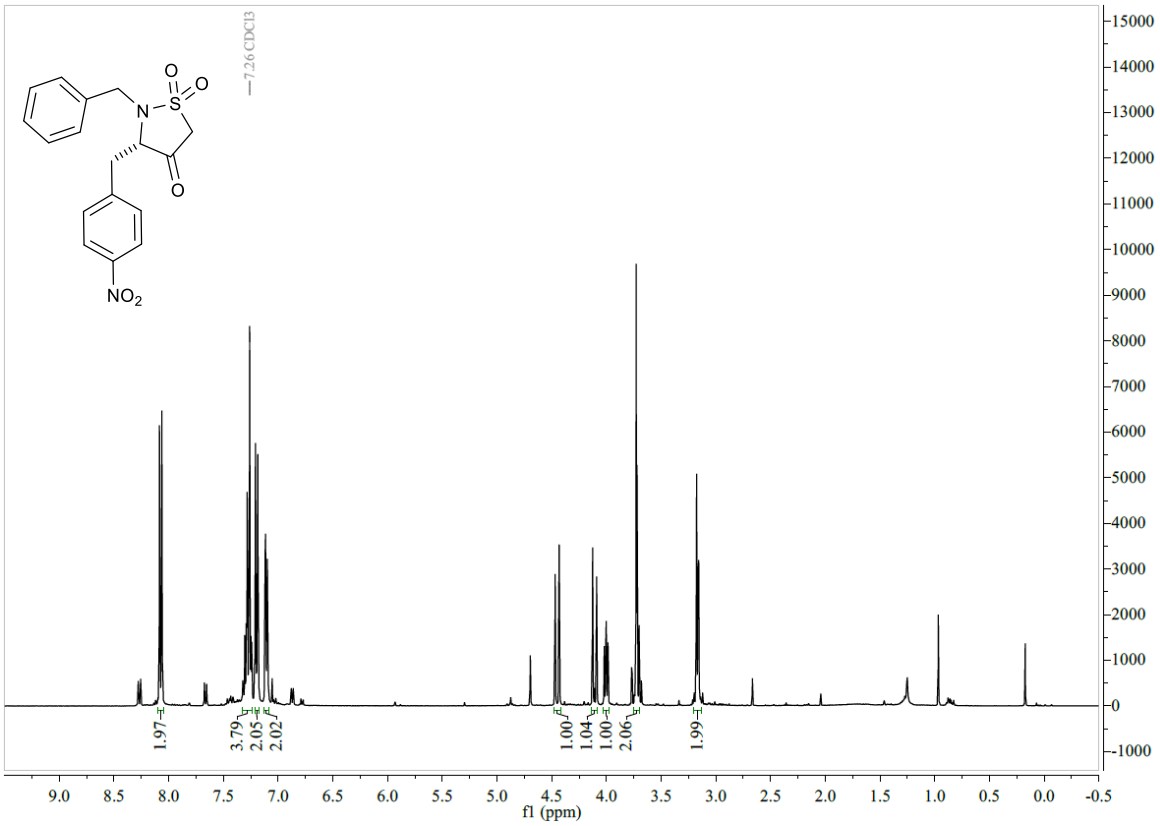

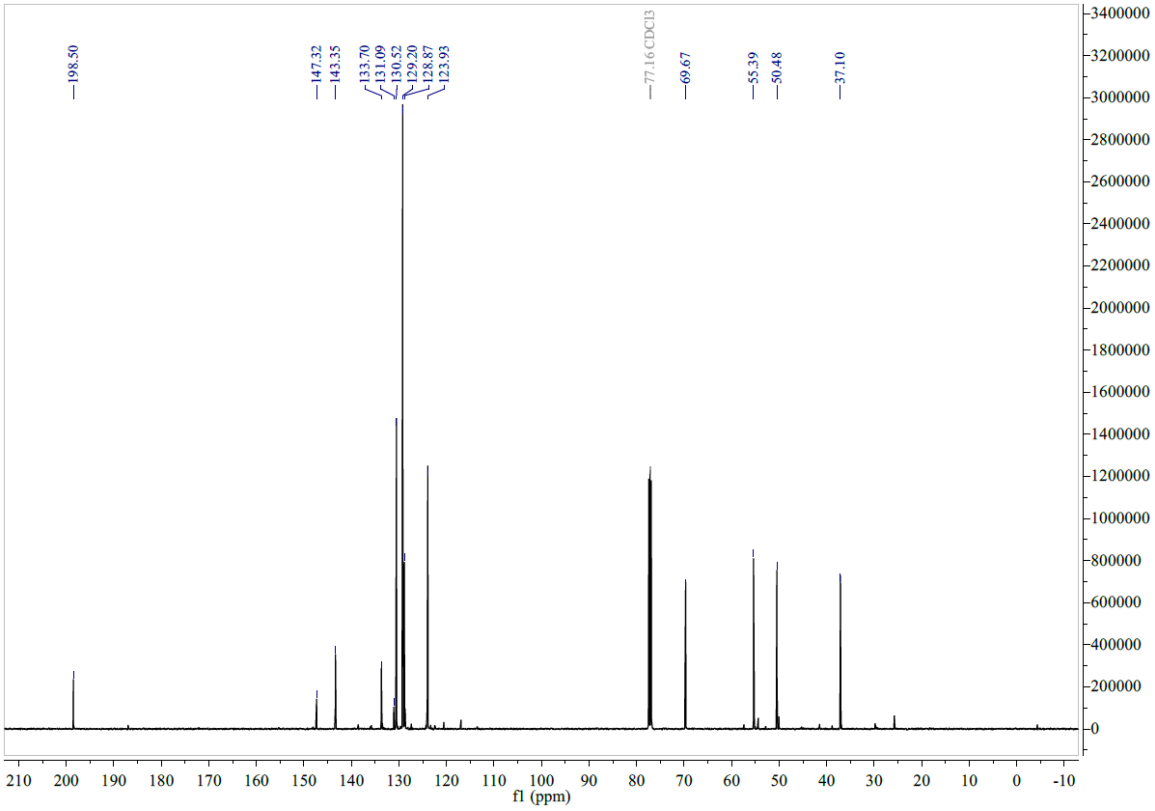

(S)-3-benzyl-2-(4-fluorobenzyl)isothiazolidin-4-one 1,1-dioxide (1.22.5e)

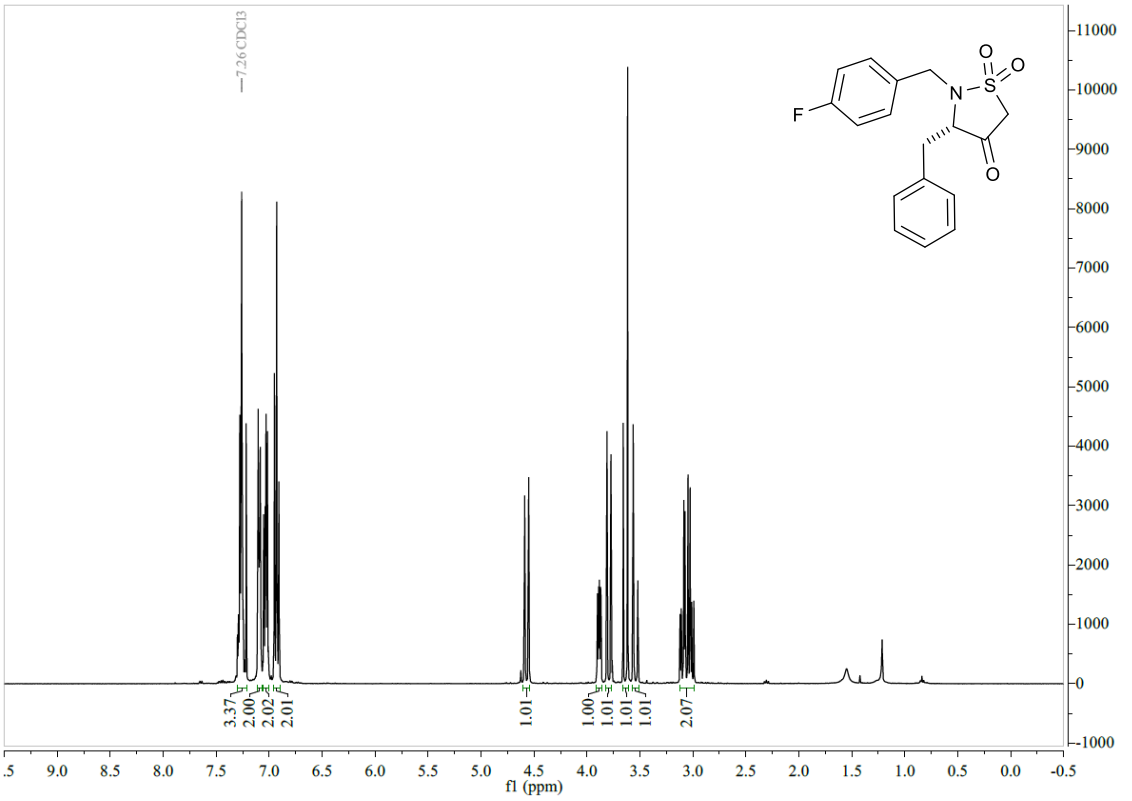

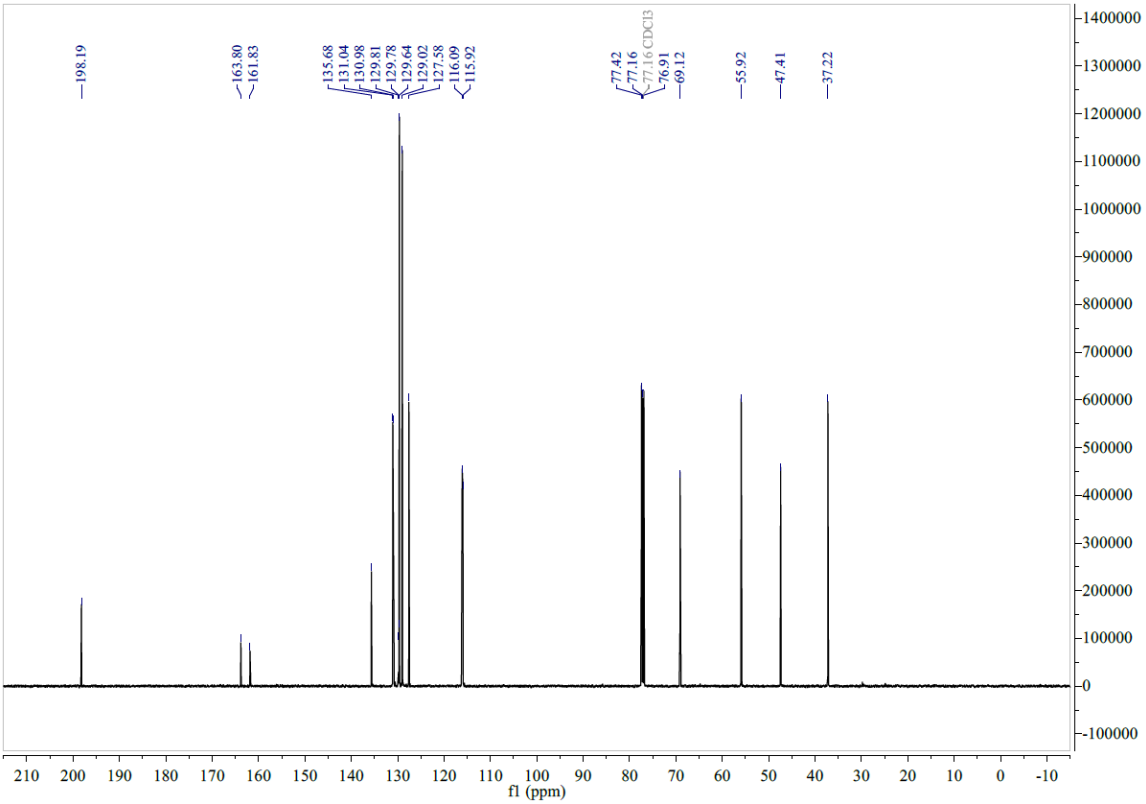

(S)-2-(4-fluorobenzyl)-3-(4-nitrobenzyl)isothiazolidin-4-one 1,1-dioxide (1.22.5f)

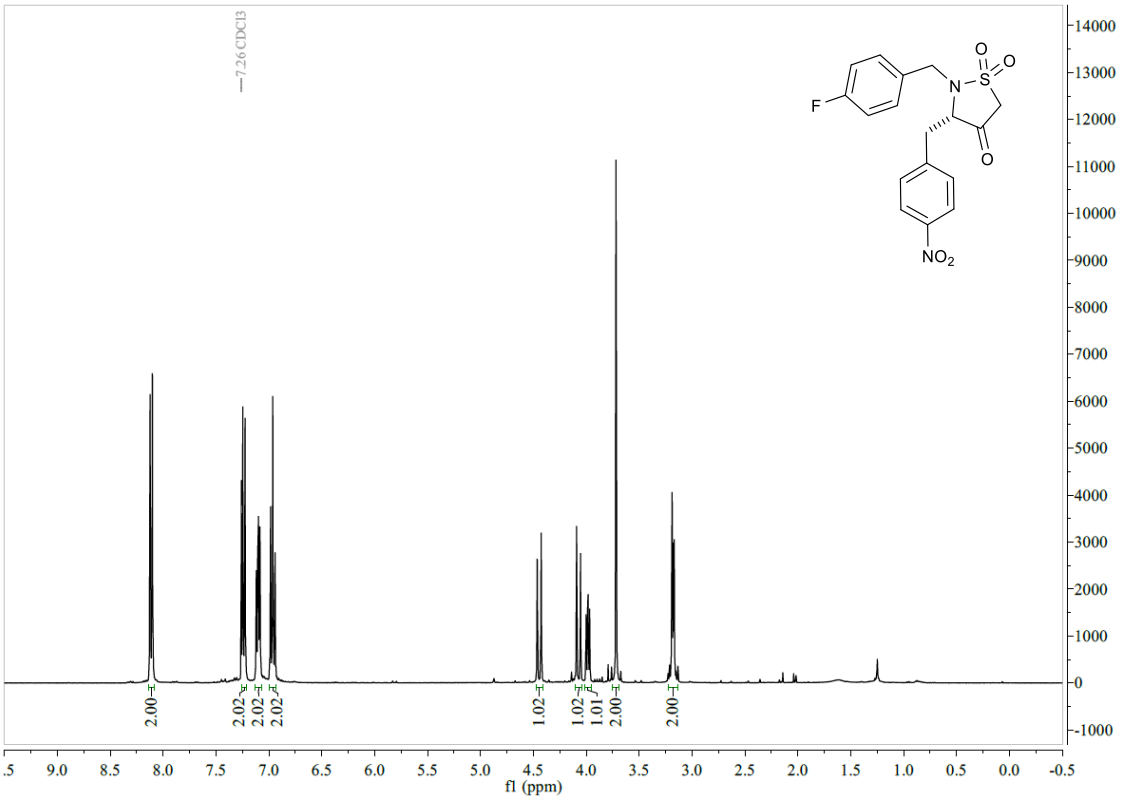

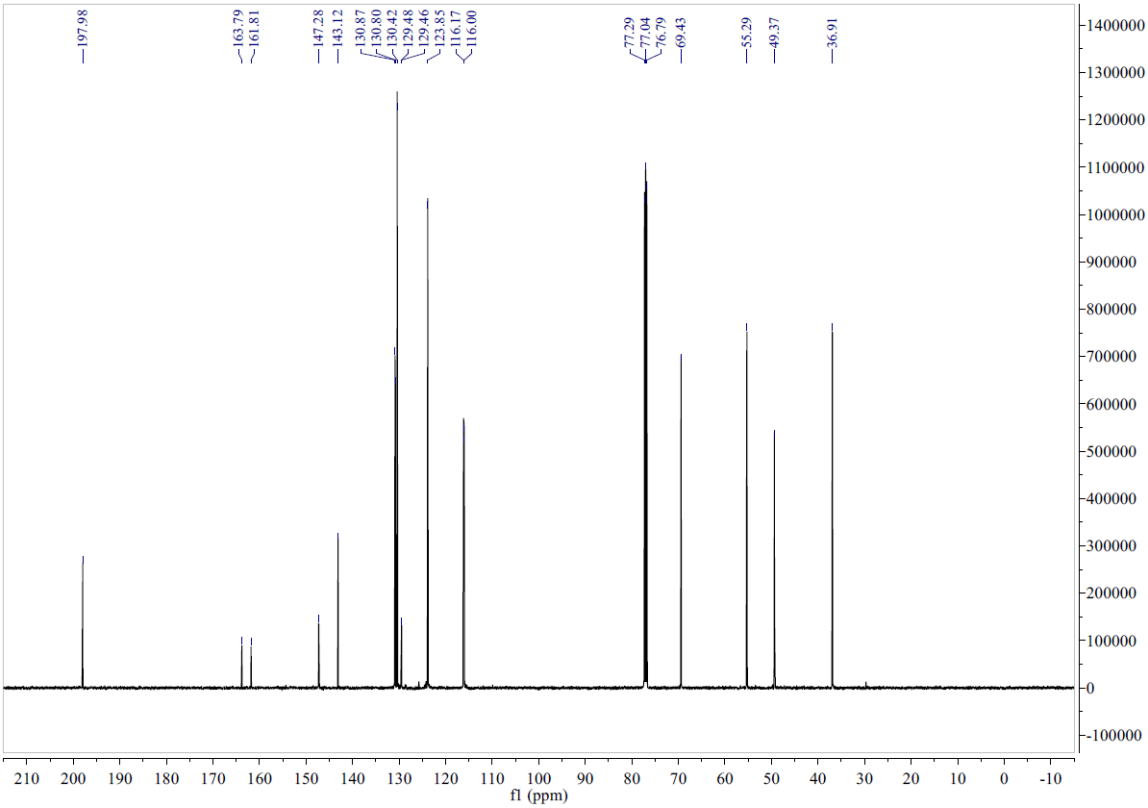

(S,E)-3-benzyl-2-(4-chlorobenzyl)-5-(4-methoxybenzylidene)isothiazolidin-4-one 1,1-dioxide (1.27.1a)

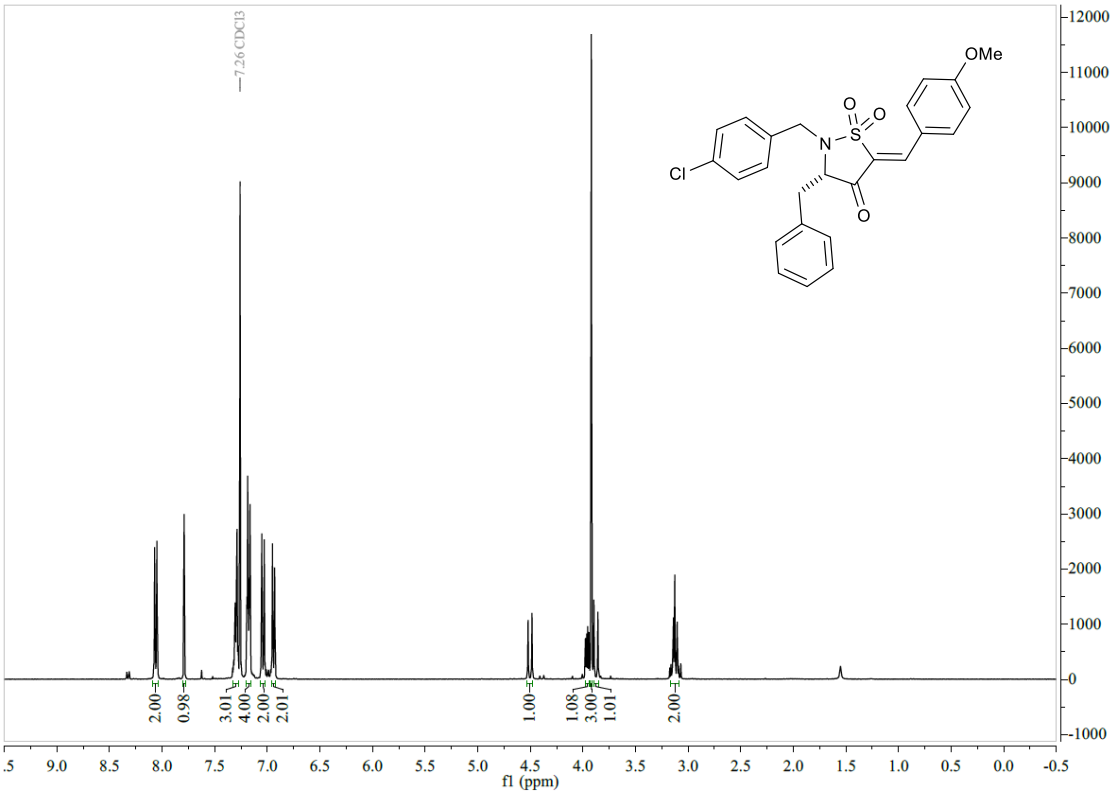

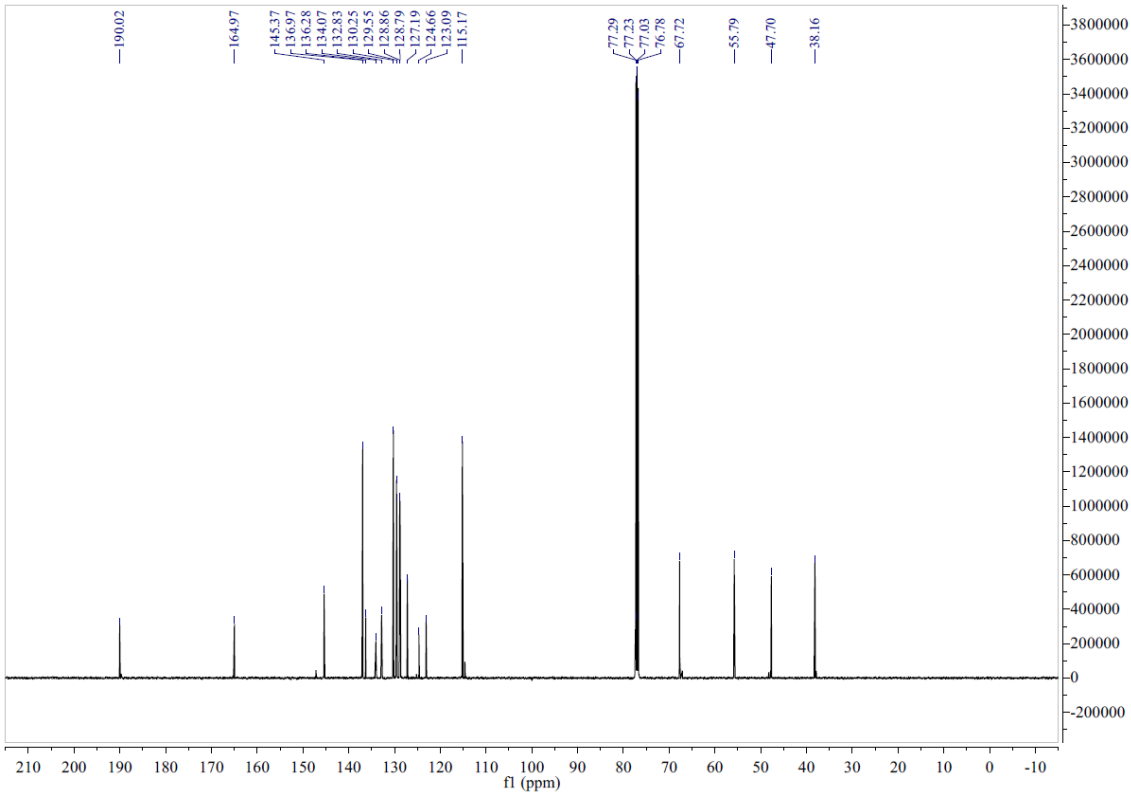

(S,E)-3-benzyl-2-(4-chlorobenzyl)-5-(4-fluorobenzylidene)isothiazolidin-4-one 1,1-dioxide (1.27.1b)

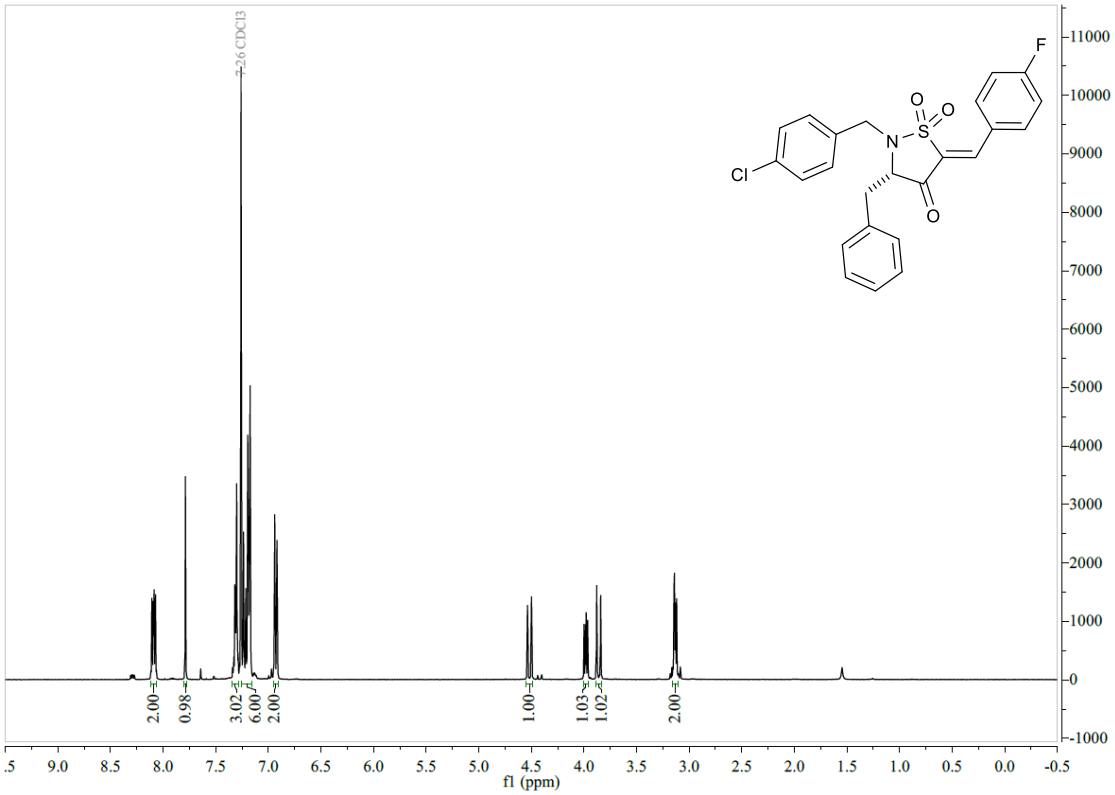

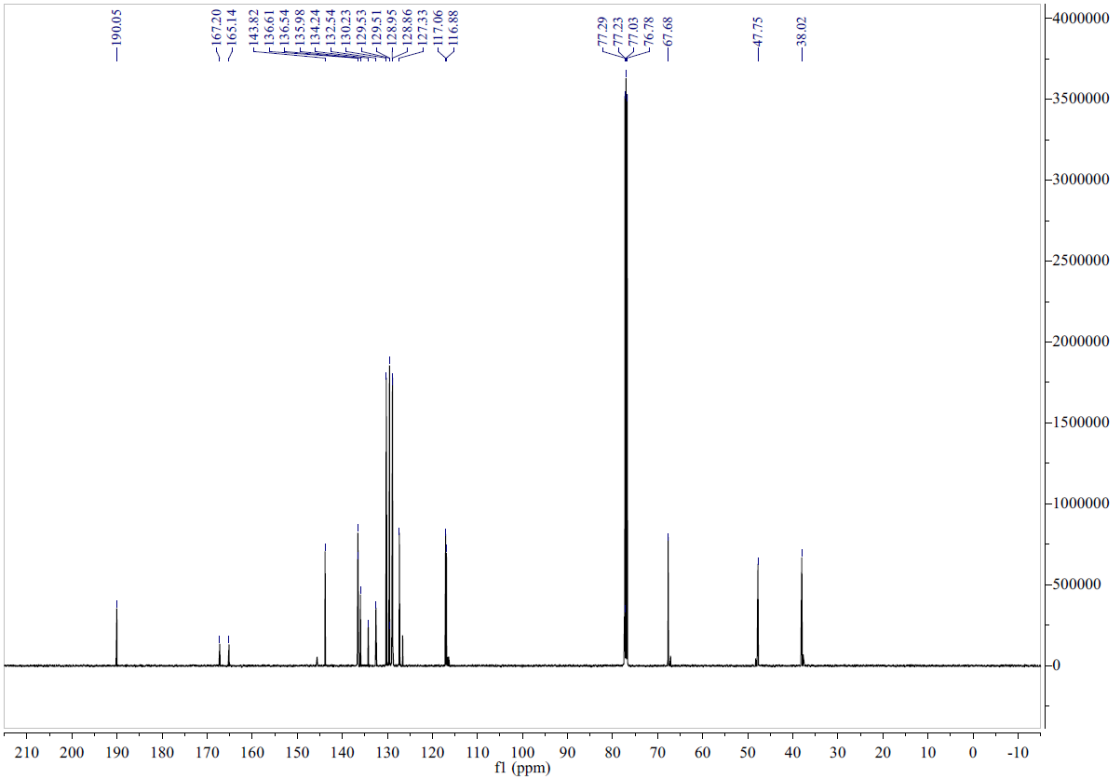

(S,E)-3-benzyl-5-benzylidene-2-(4-chlorobenzyl)isothiazolidin-4-one 1,1-dioxide (1.27.1c)

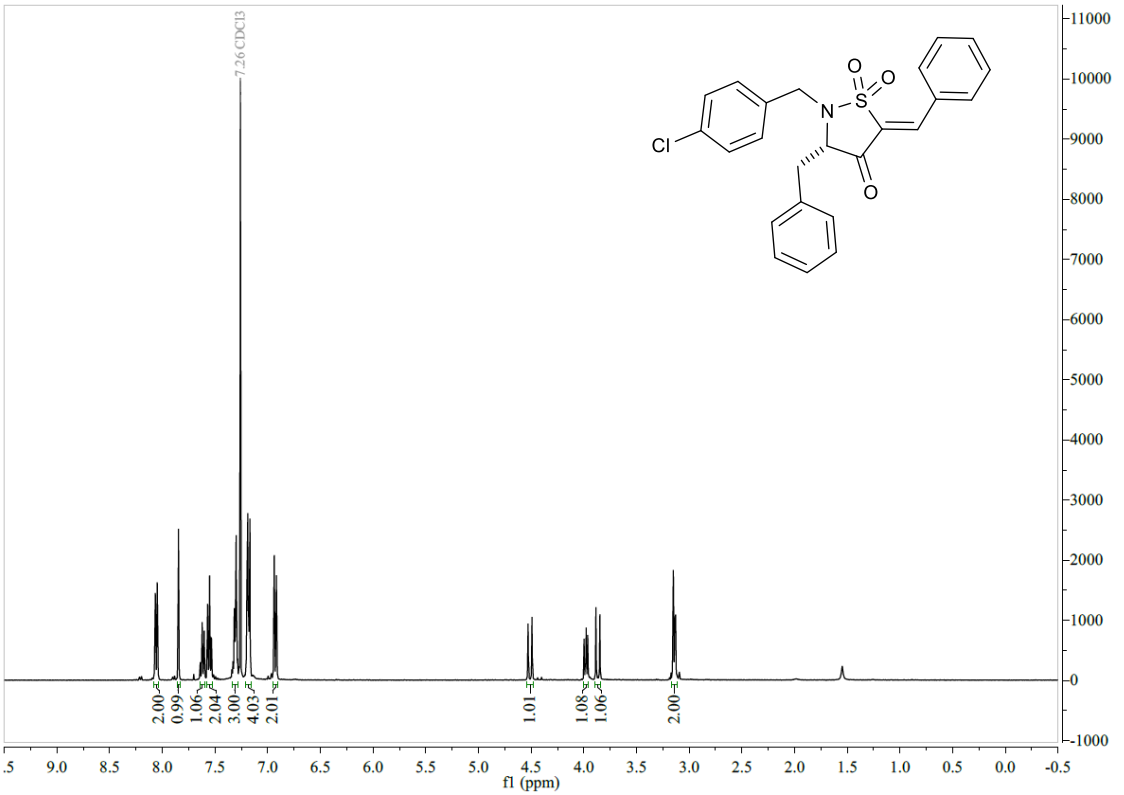

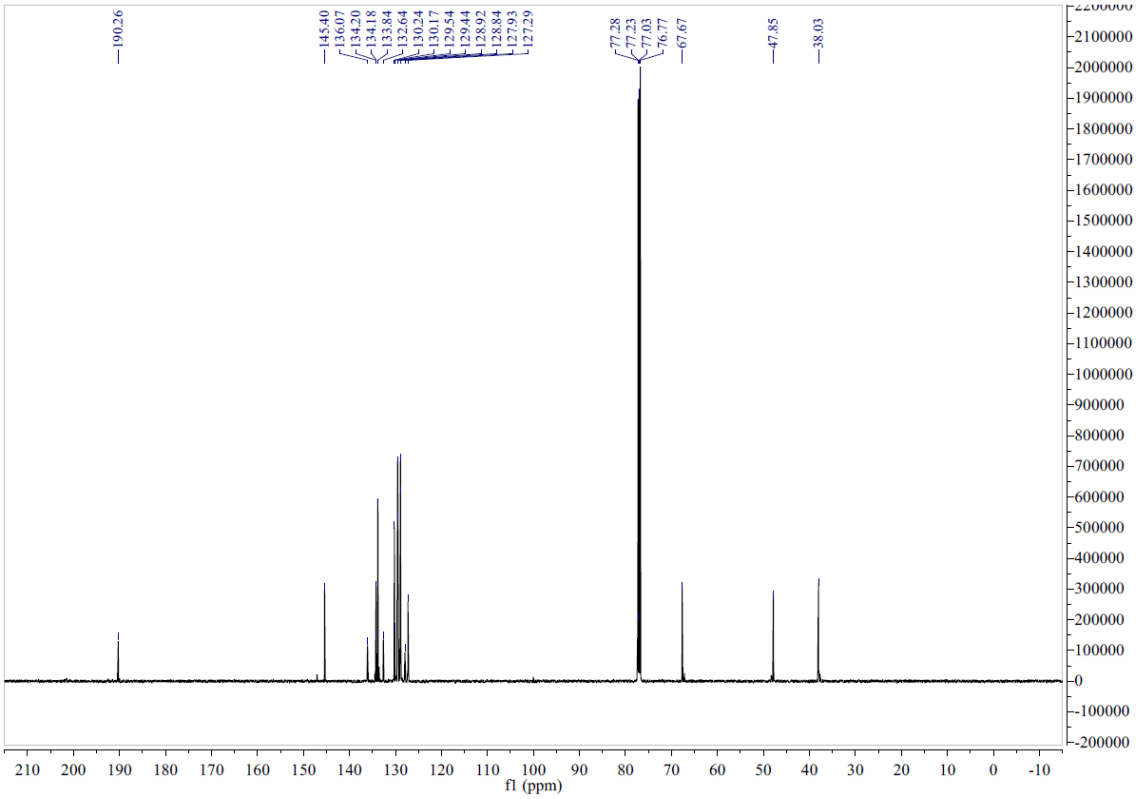

(S,E)-2-(4-chlorobenzyl)-5-(4-fluorobenzylidene)-3-(4-nitrobenzyl)isothiazolidin-4-one 1,1-dioxide (1.27.1d)

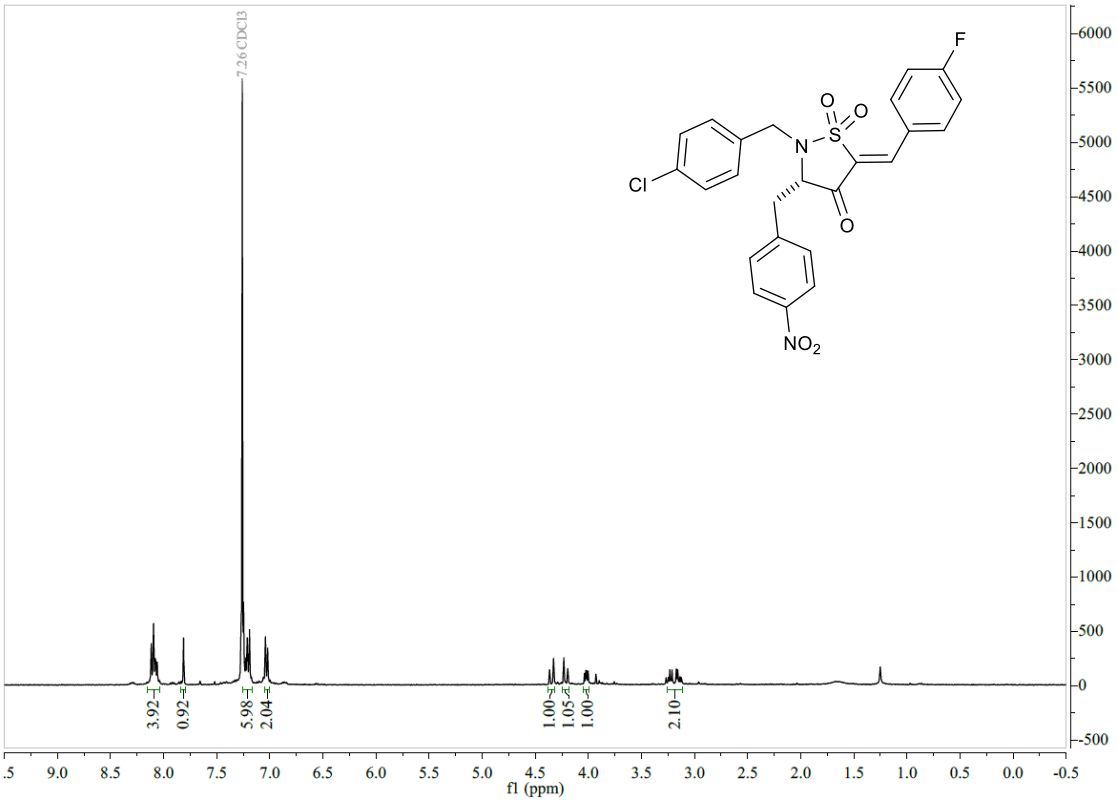

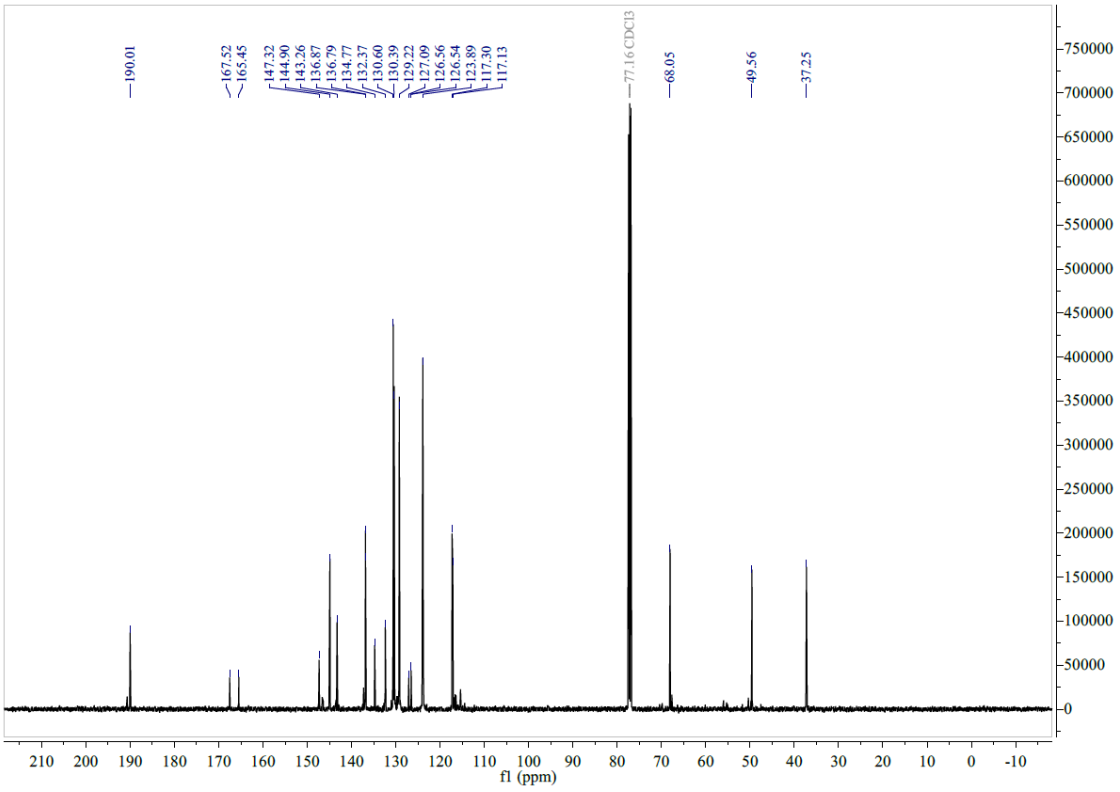

(S,E)-5-(benzo[d][1,3]dioxol-4-ylmethylene)-2-(4-chlorobenzyl)-3-(4-nitrobenzyl) isothiazolidin-4-one 1,1-dioxide (1.27.1e)

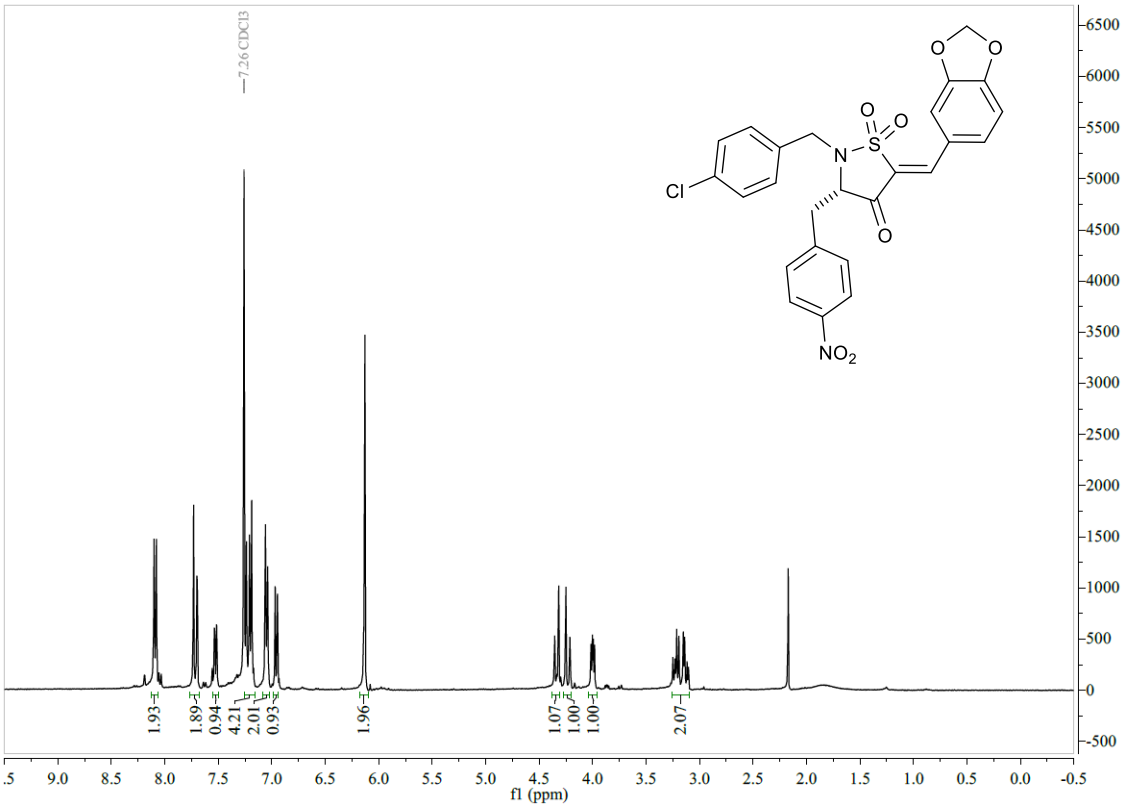

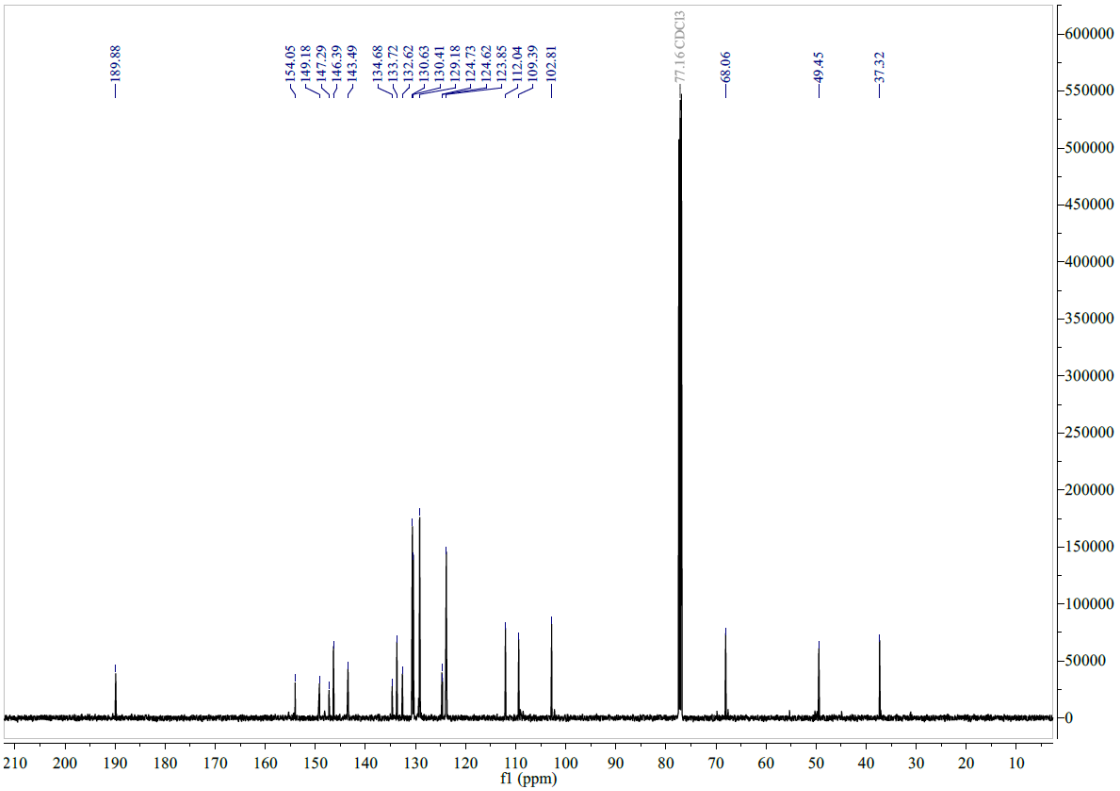

(S,E)-2,3-dibenzyl-5-(4-methoxybenzylidene)isothiazolidin-4-one 1,1-dioxide (1.27.1f)

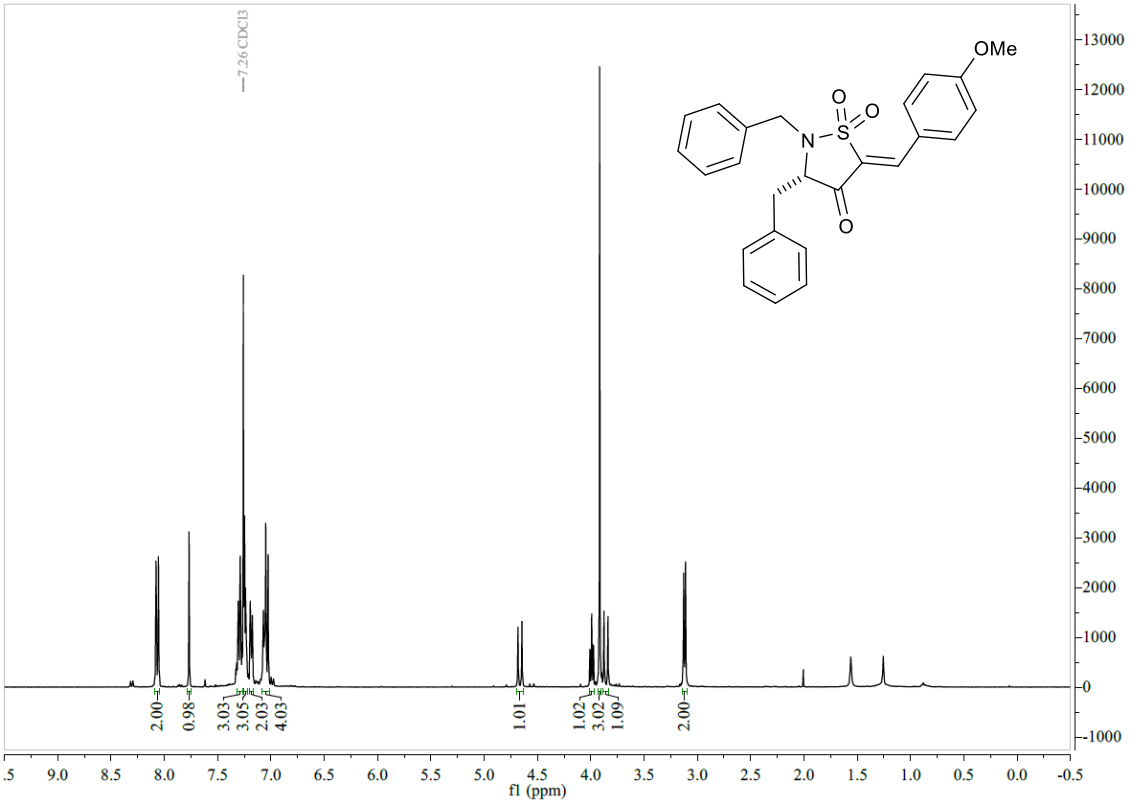

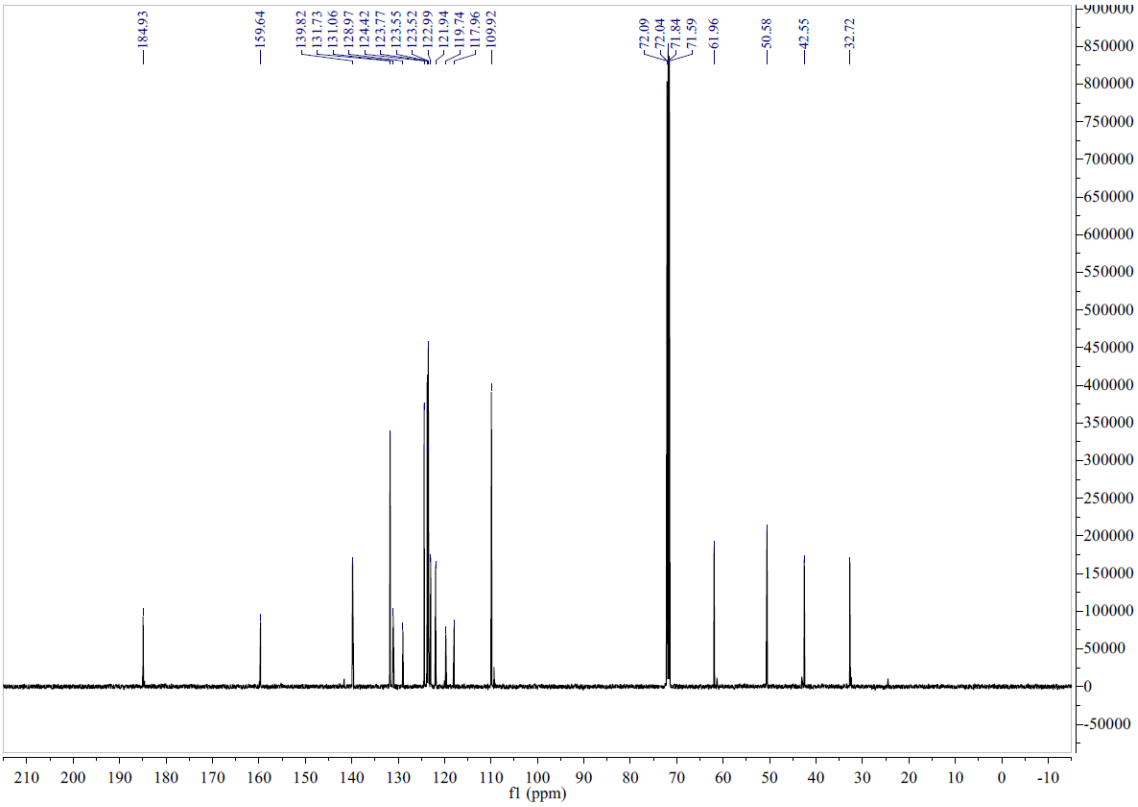

(S,E)-2,3-dibenzyl-5-(4-fluorobenzylidene)isothiazolidin-4-one 1,1-dioxide (1.27.1g)

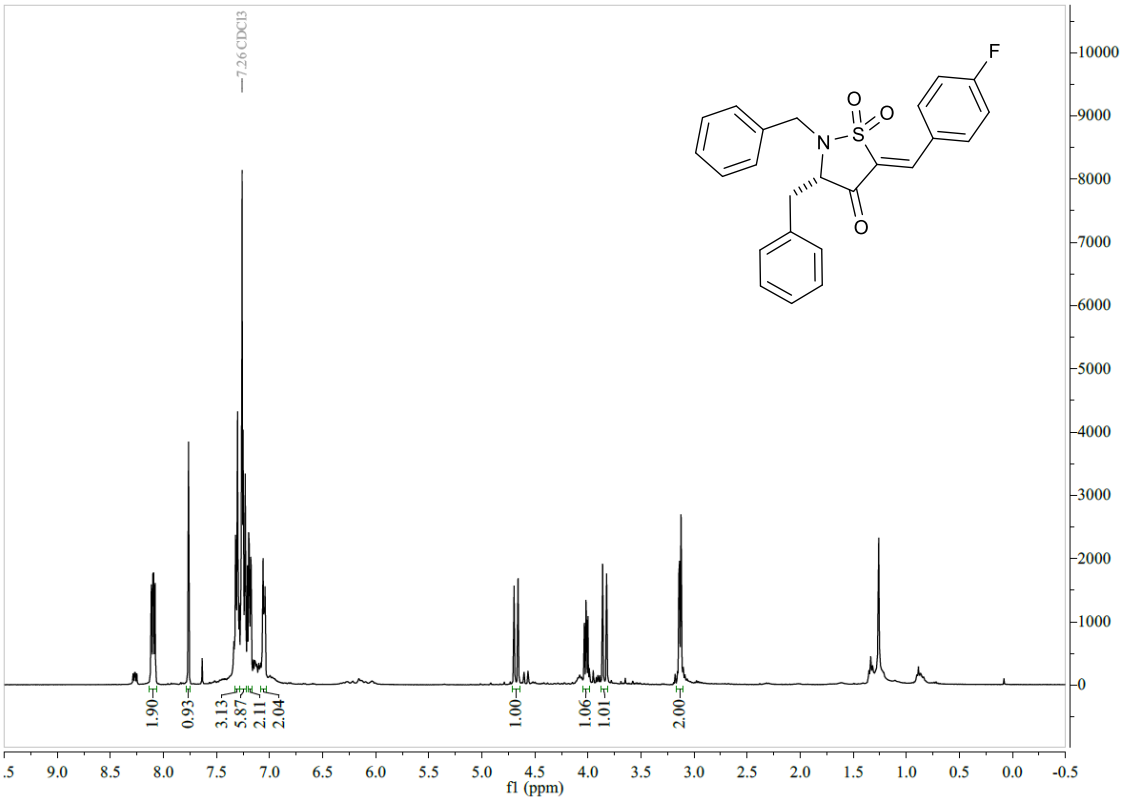

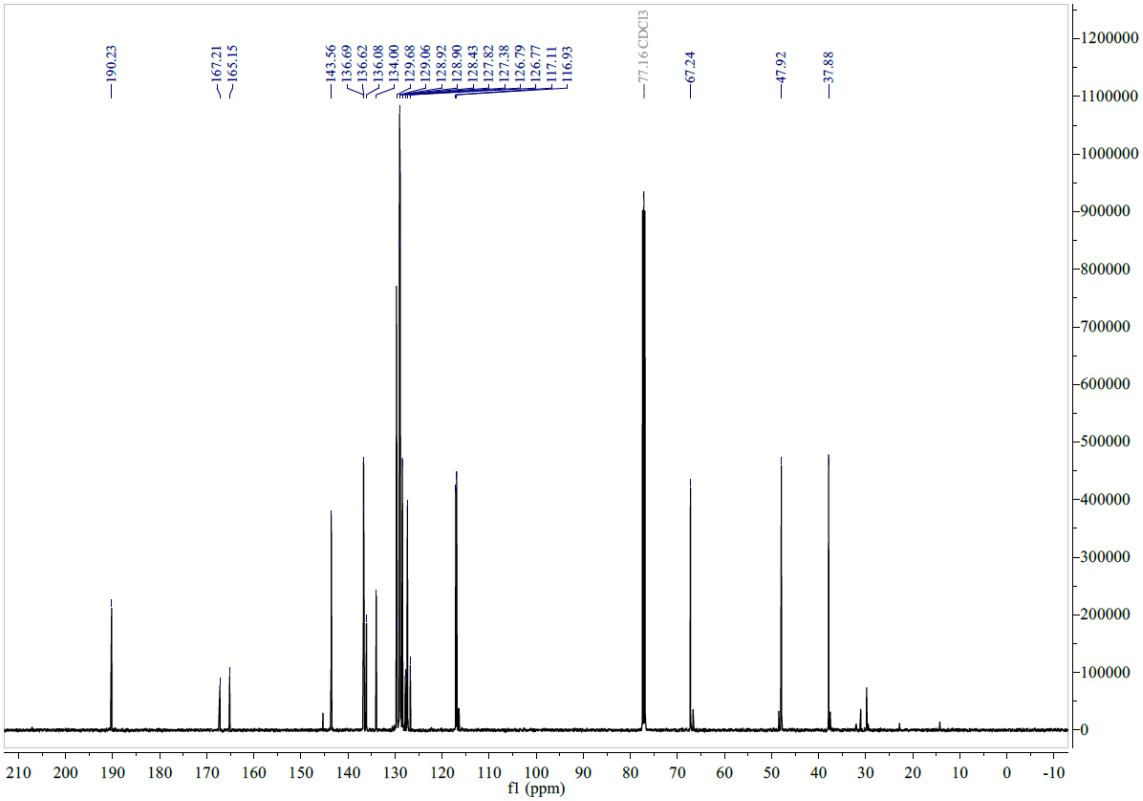

(S,E)-2-benzyl-5-(4-methoxybenzylidene)-3-(4-nitrobenzyl)isothiazolidin-4-one 1,1-dioxide (1.27.1h)

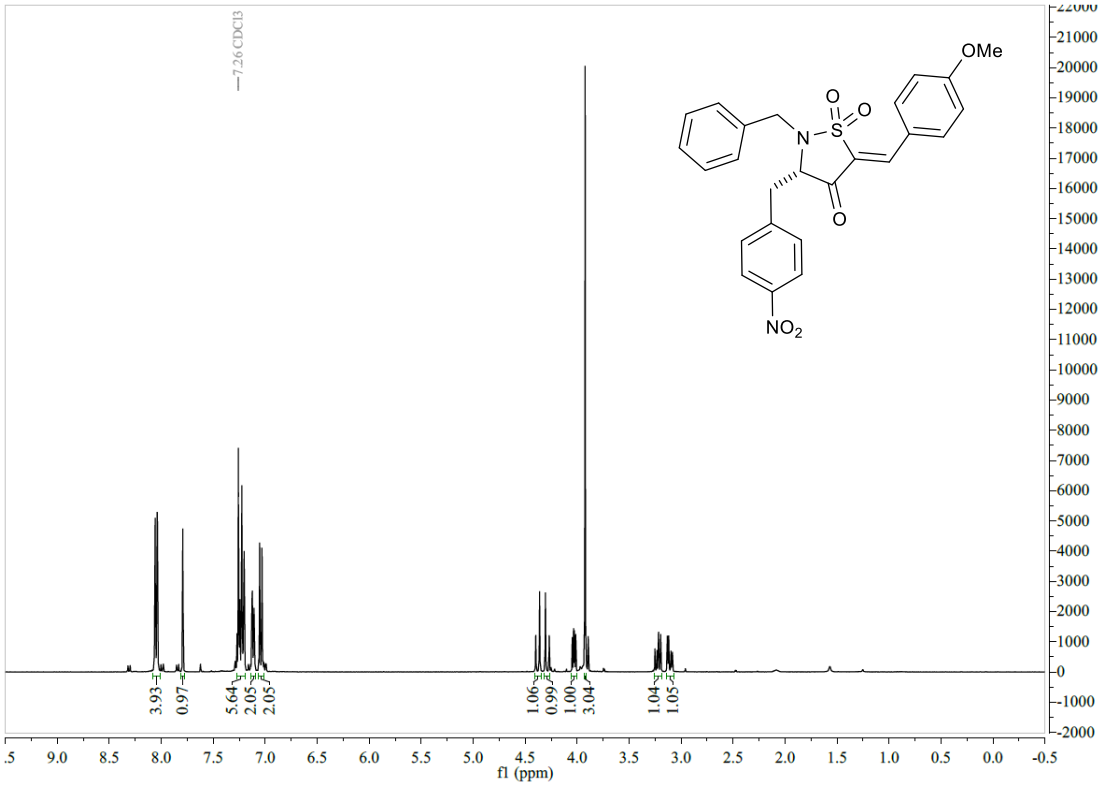

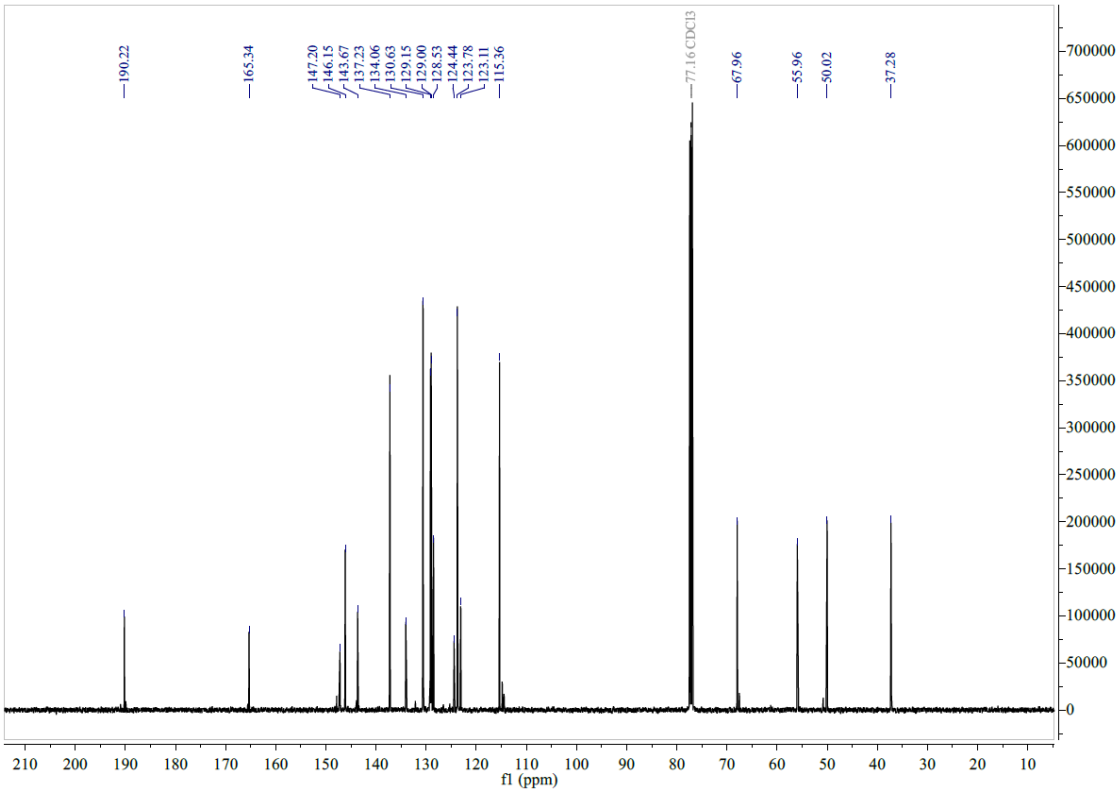

(S,E)-2-benzyl-5-(4-fluorobenzylidene)-3-(4-nitrobenzyl)isothiazolidin-4-one 1,1-dioxide (1.27.1i)

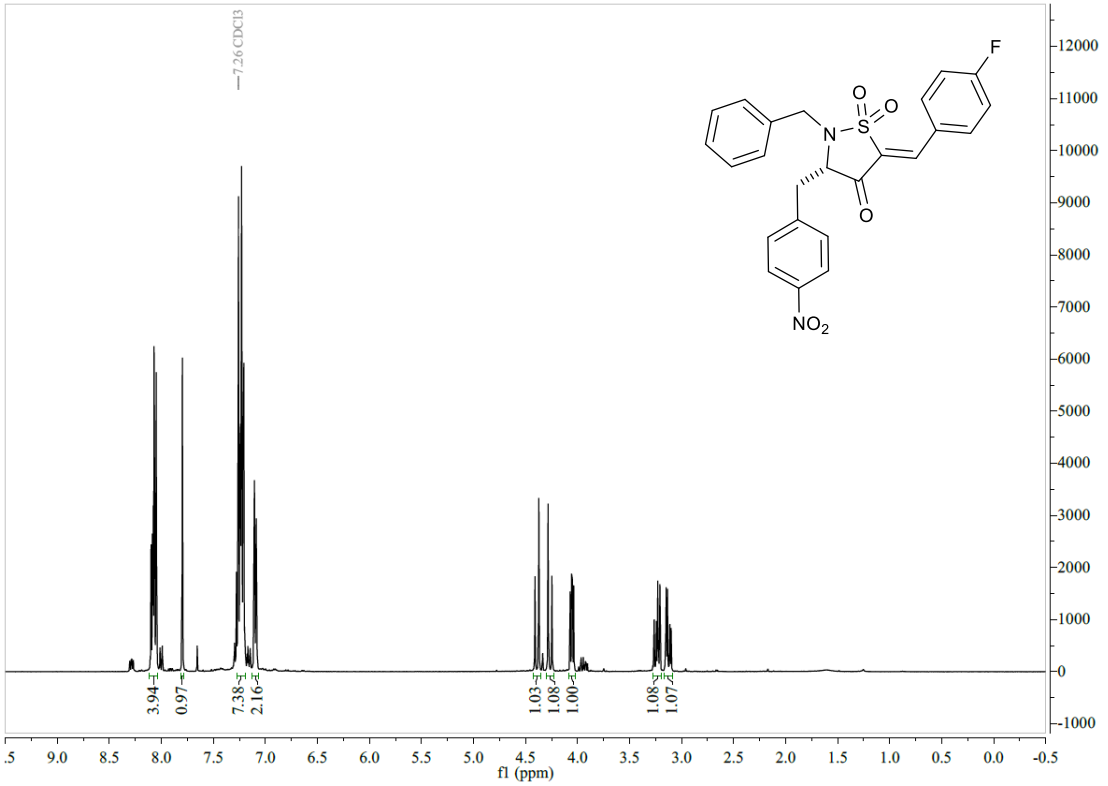

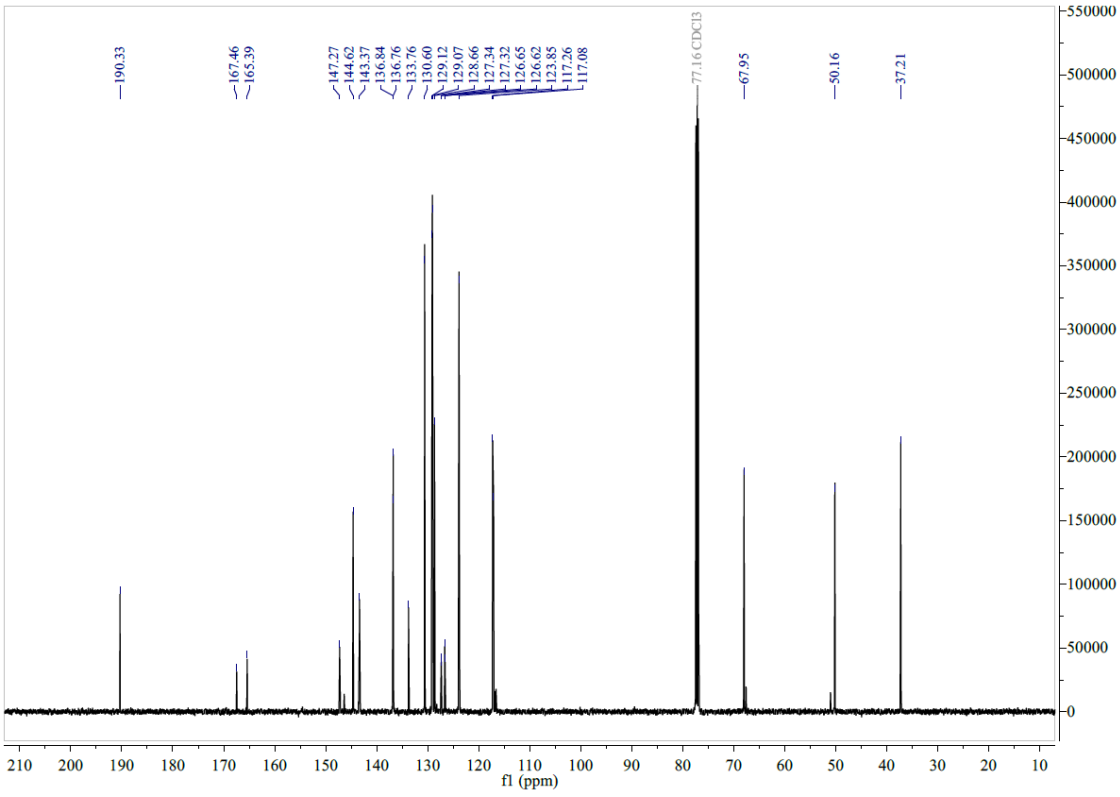

(S,E)-5-(benzo[d][1,3]dioxol-4-ylmethylene)-2-benzyl-3-(4-nitrobenzyl)isothiazolidin-4-one 1,1-dioxide (1.27.1j)

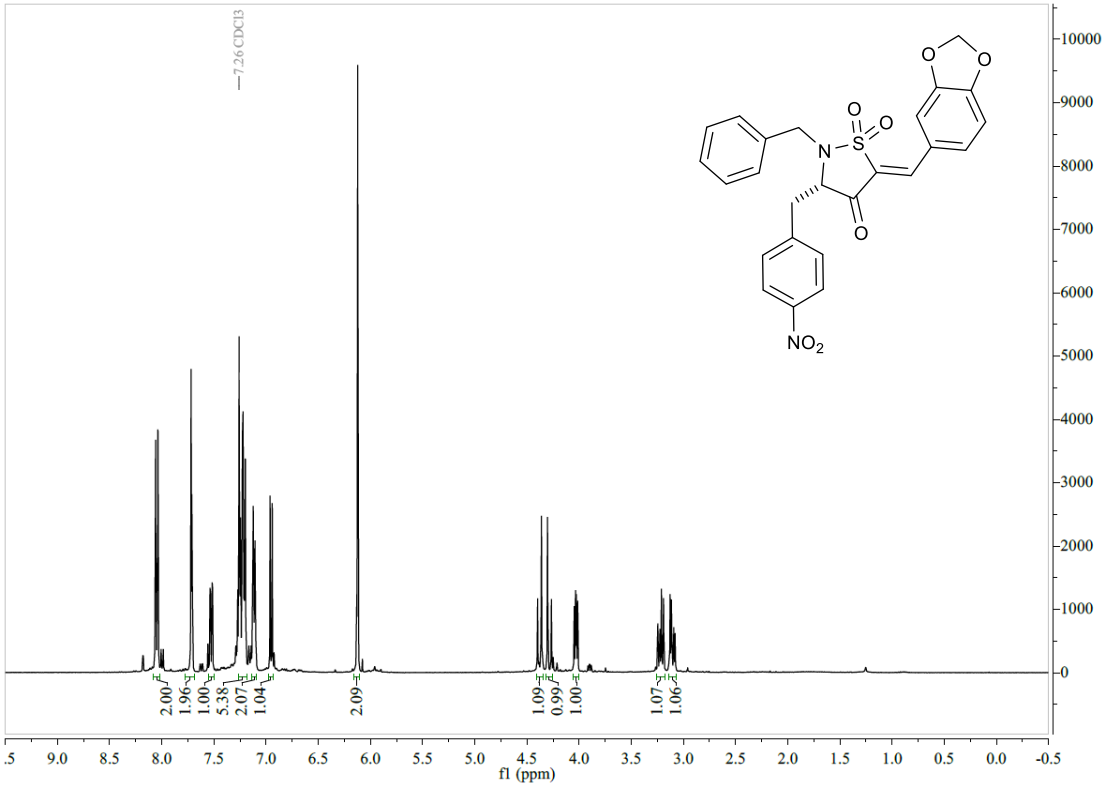

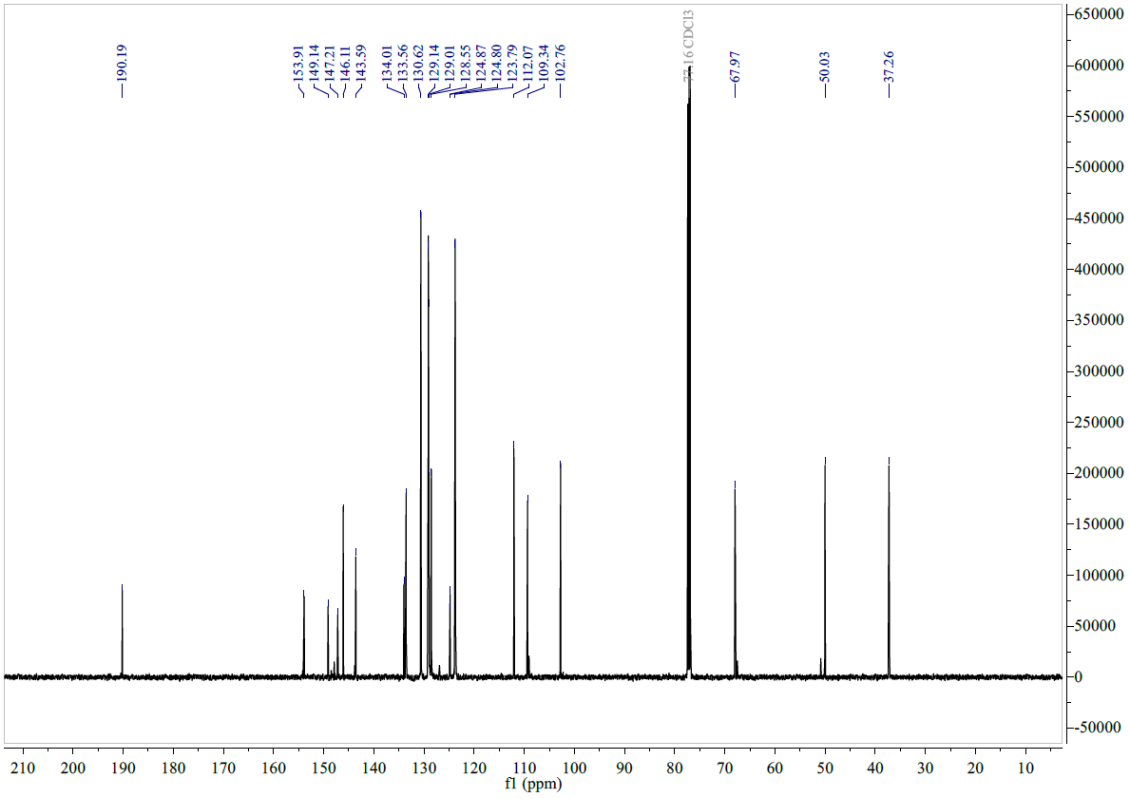

(S,E)-2-benzyl-5-((E)-3-(4-fluorophenyl)allylidene)-3-(4-nitrobenzyl)isothiazolidin-4-one 1,1-dioxide (1.27.1k)

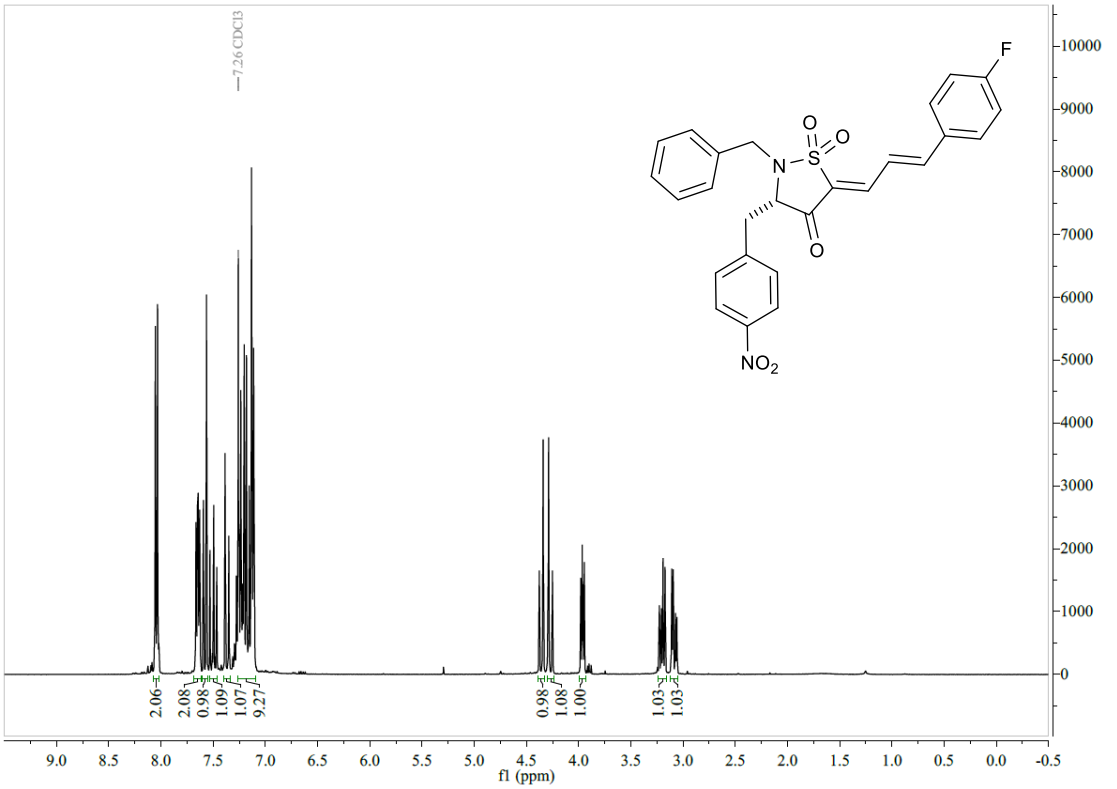

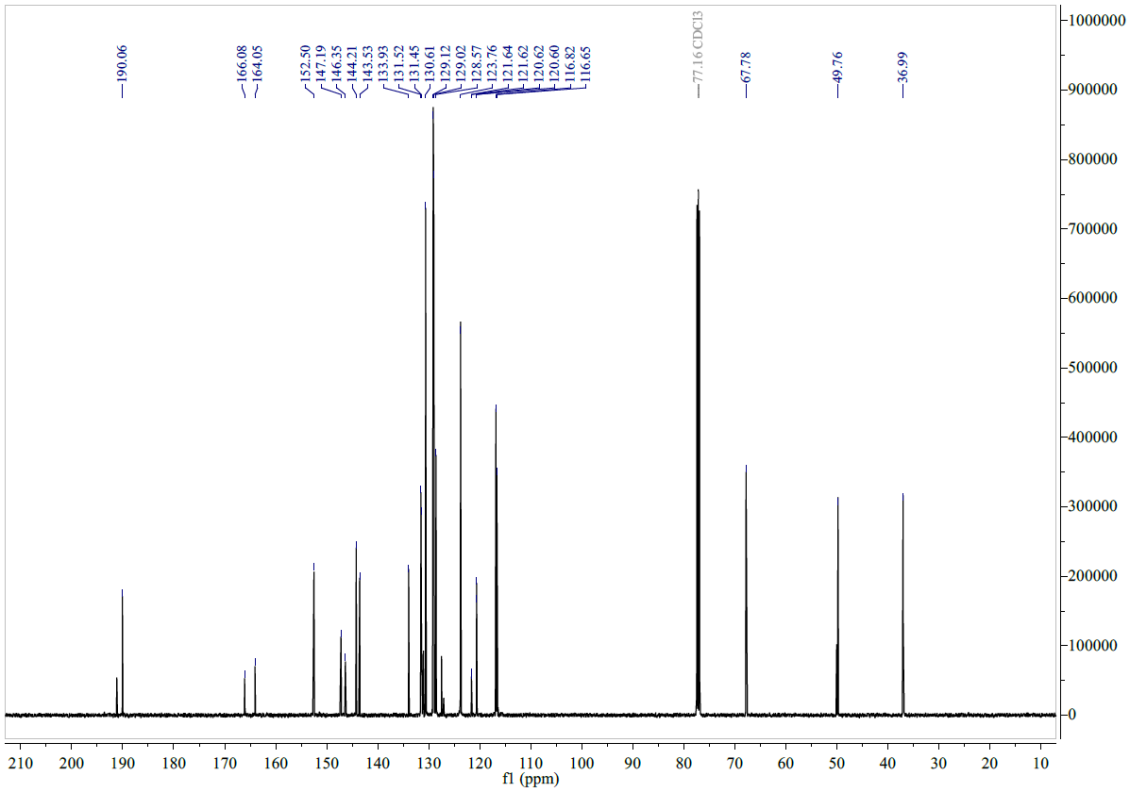

(S,E)-3-benzyl-2-(4-fluorobenzyl)-5-(4-methoxybenzylidene)isothiazolidin-4-one 1,1-dioxide (1.27.1l)

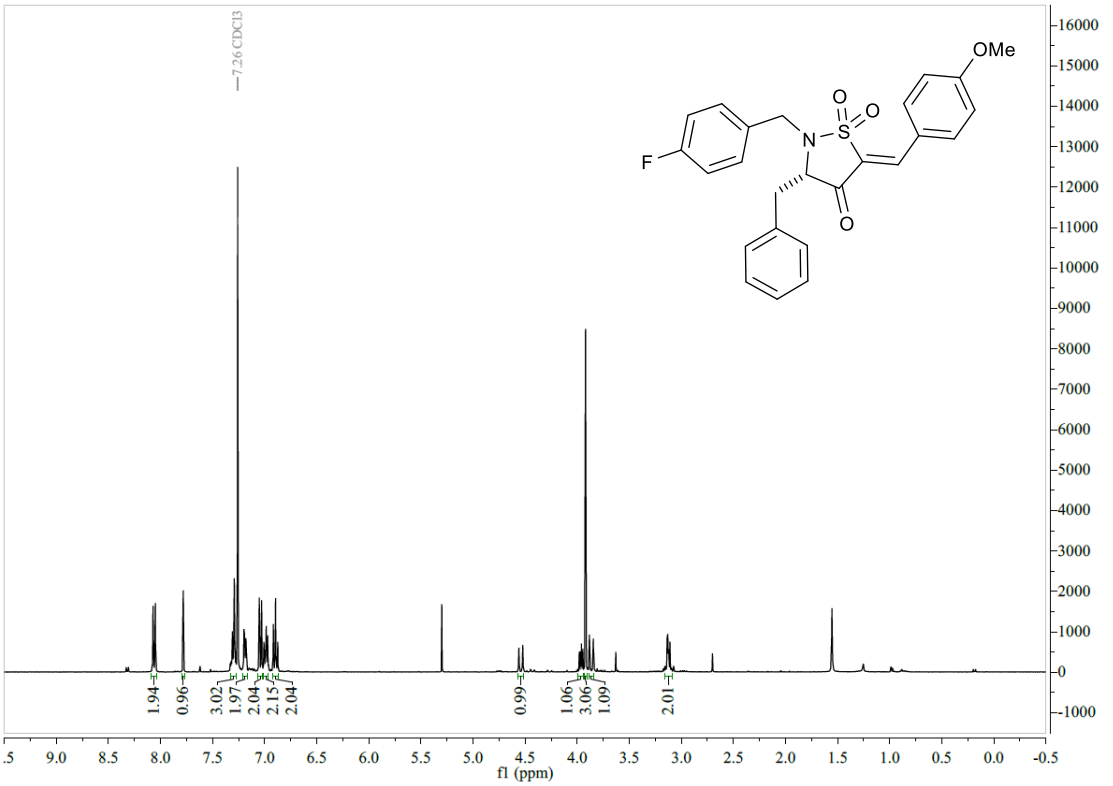

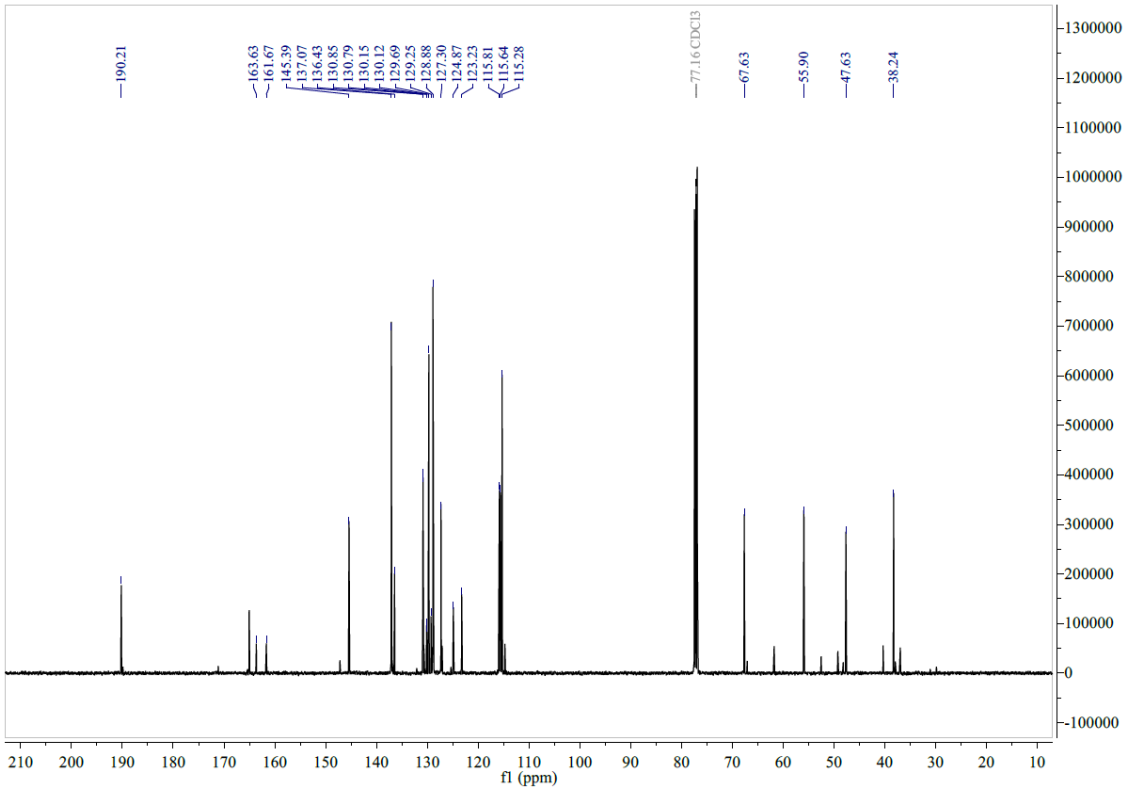

(S,E)-3-benzyl-2-(4-fluorobenzyl)-5-(4-fluorobenzylidene)isothiazolidin-4-one 1,1-dioxide (1.27.1m)

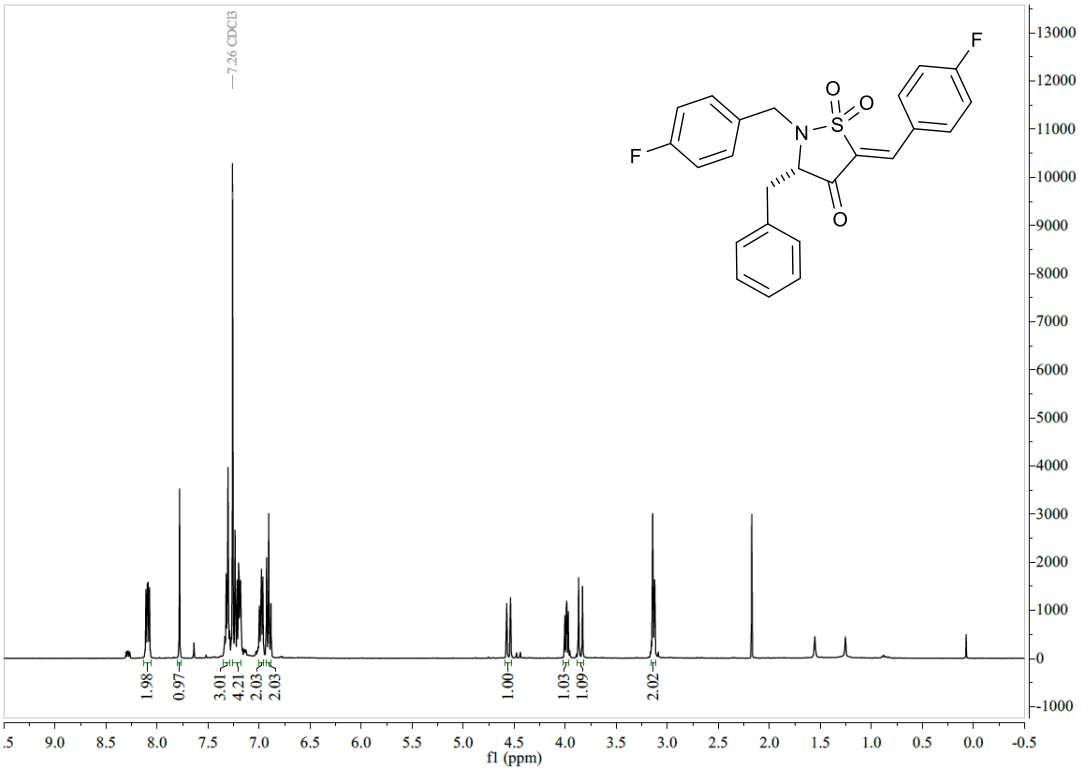

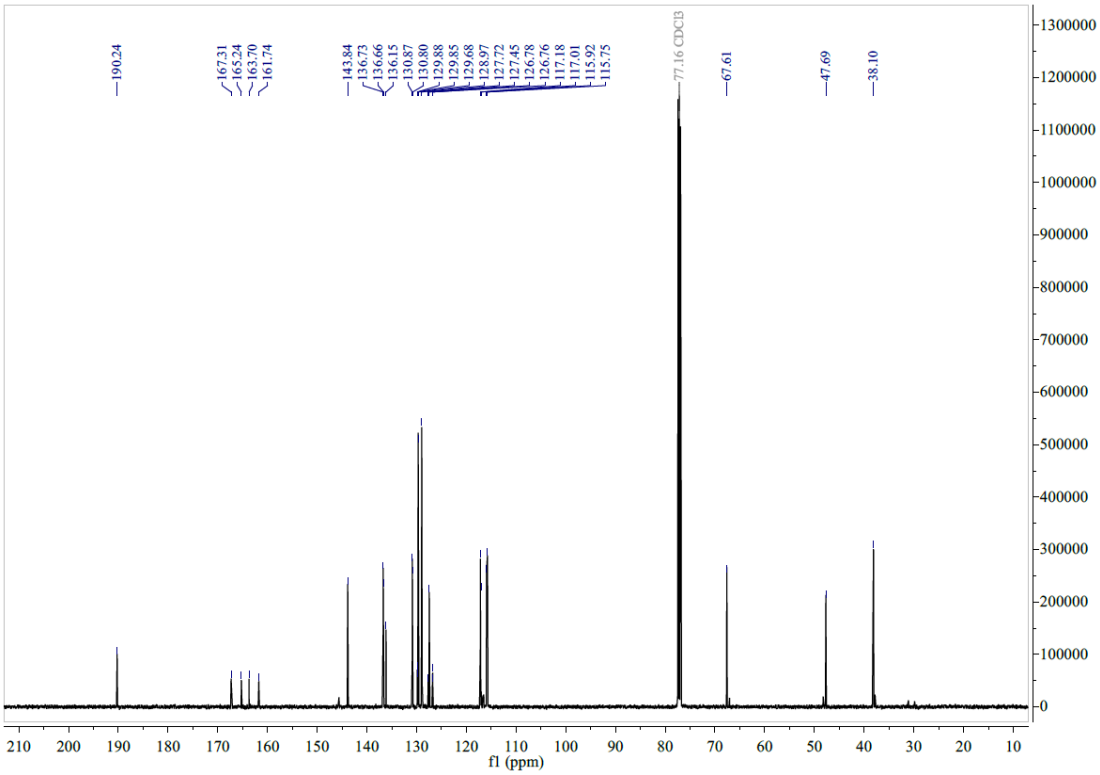

(S,E)-5-(benzo[d][1,3]dioxol-4-ylmethylene)-3-benzyl-2-(4-fluorobenzyl)isothiazolidin-4-one 1,1-dioxide (1.27.1n)

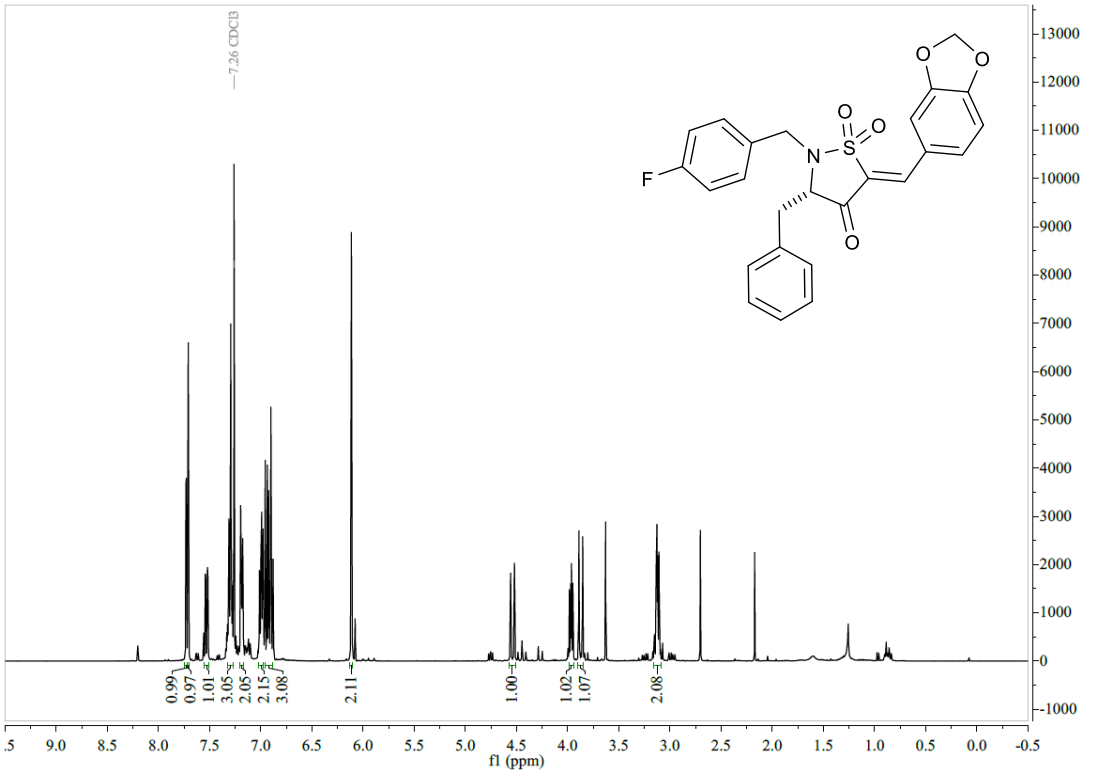

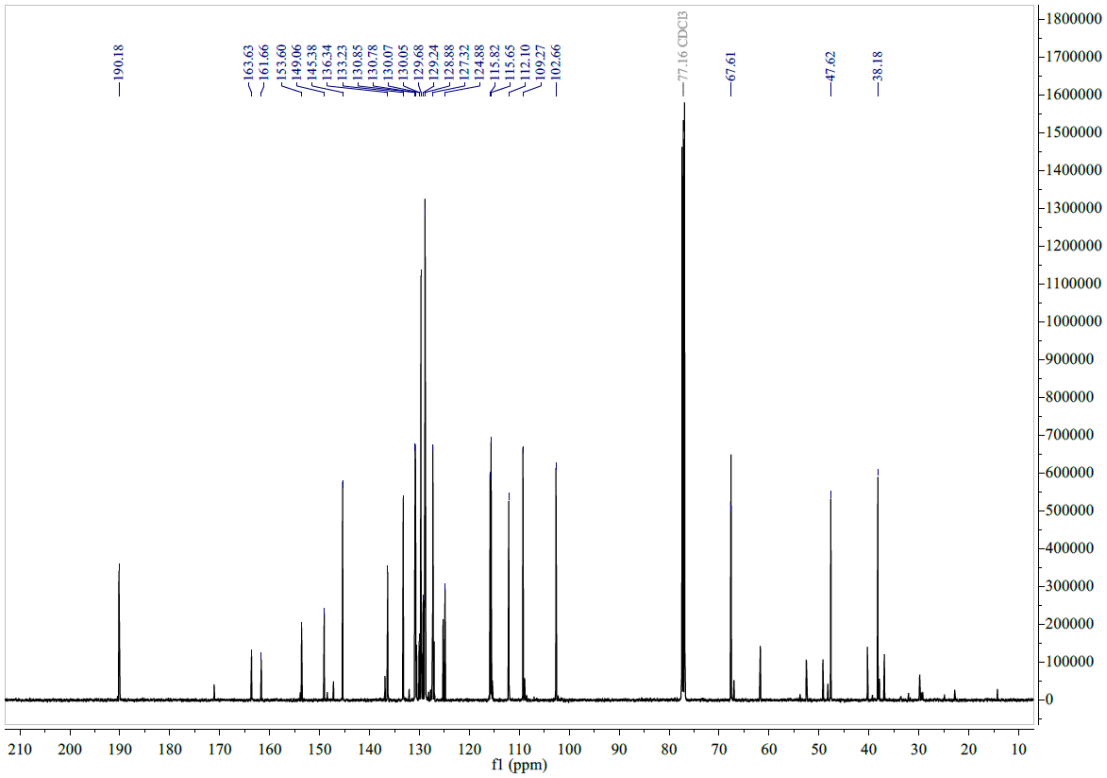

(S,E)-3-benzyl-2-(4-fluorobenzyl)-5-((E)-3-(4-fluorophenyl)allylidene)isothiazolidin-4-one 1,1-dioxide (1.27.1o)

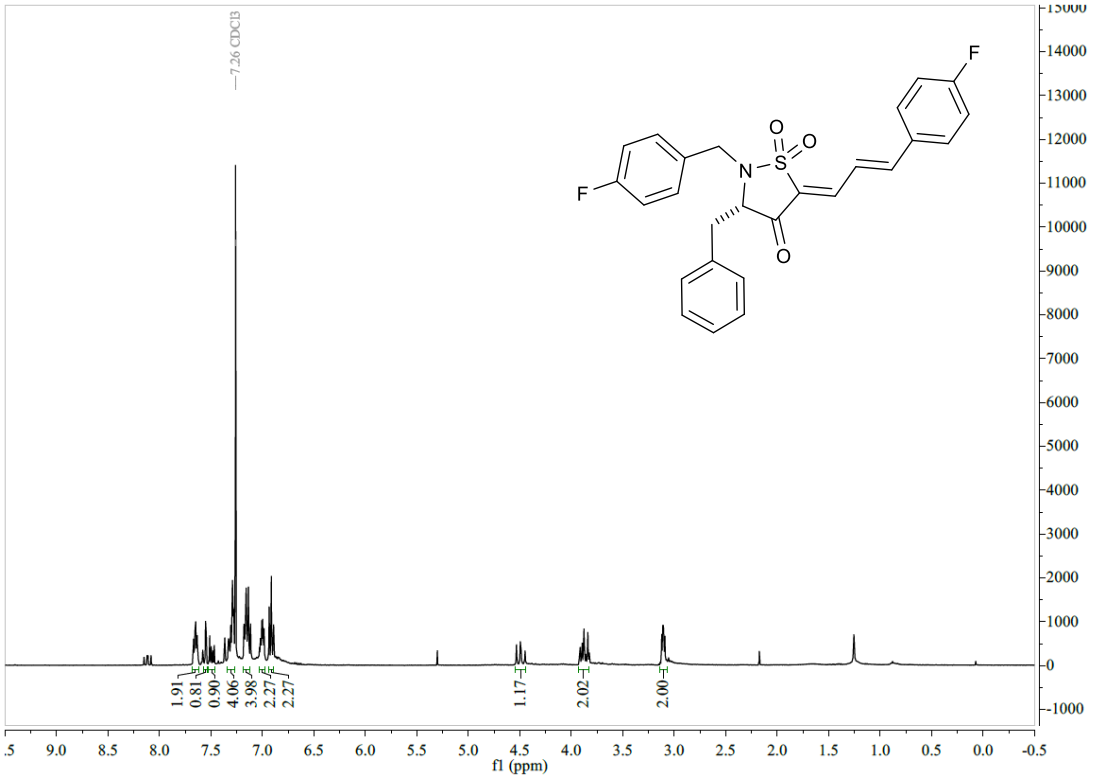

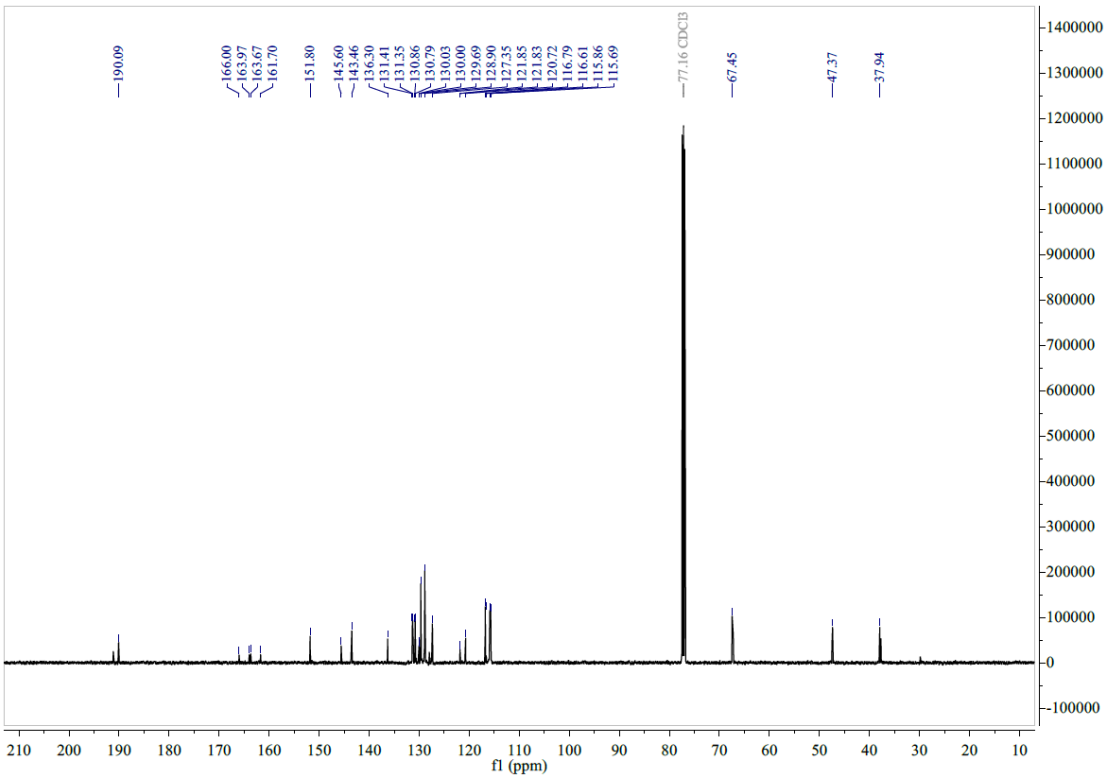

(S,E)-2-(4-fluorobenzyl)-5-(4-methoxybenzylidene)-3-(4-nitrobenzyl)isothiazolidin-4-one 1,1-dioxide (1.27.1p)

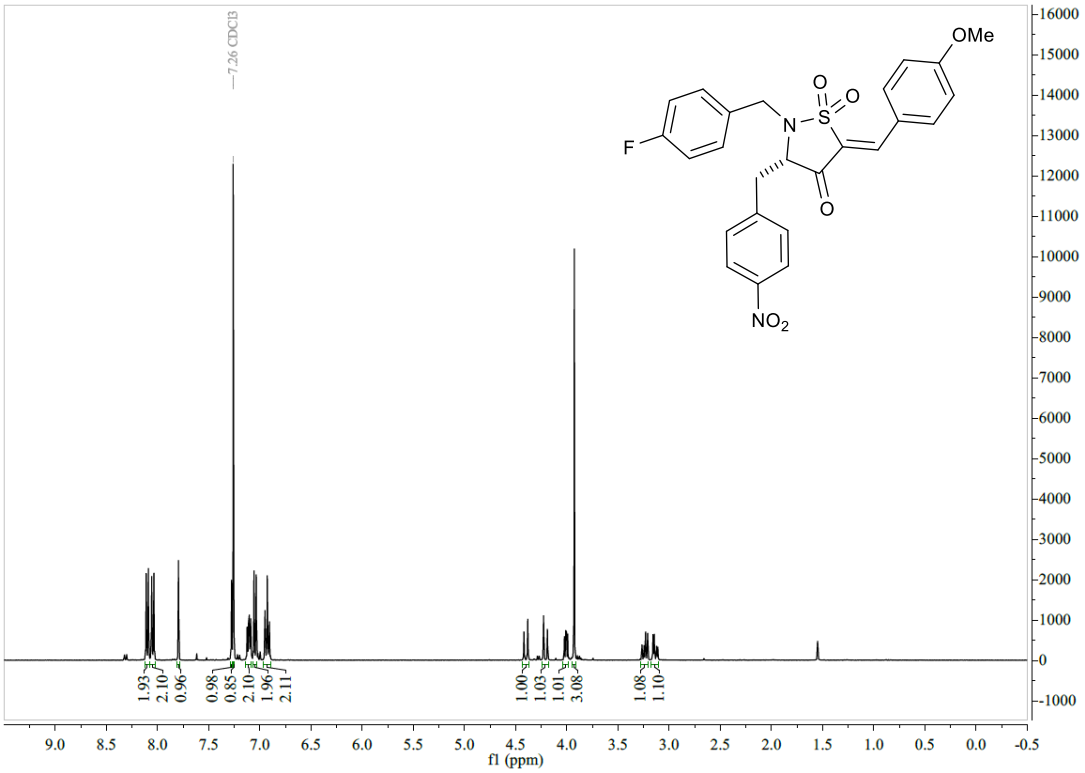

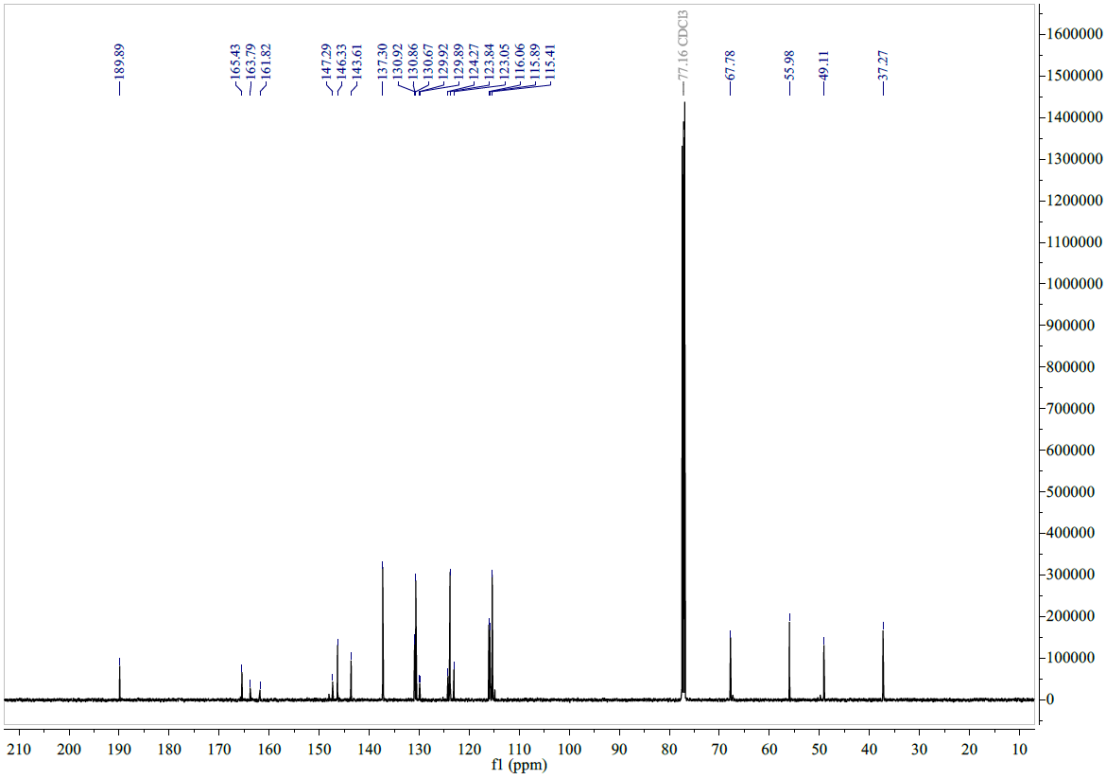

(S,E)-5-(benzo[d][1,3]dioxol-4-ylmethylene)-2-(4-fluorobenzyl)-3-(4-nitrobenzyl) isothiazolidin-4-one 1,1-dioxide (1.27.1q)

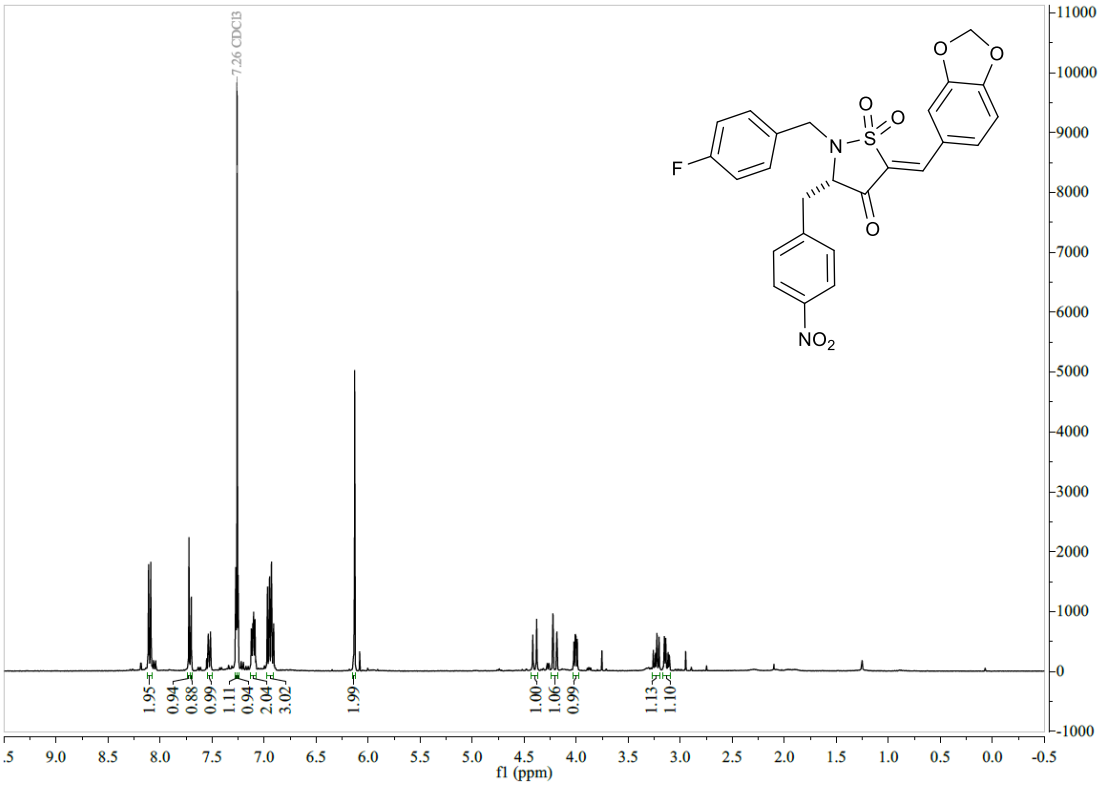

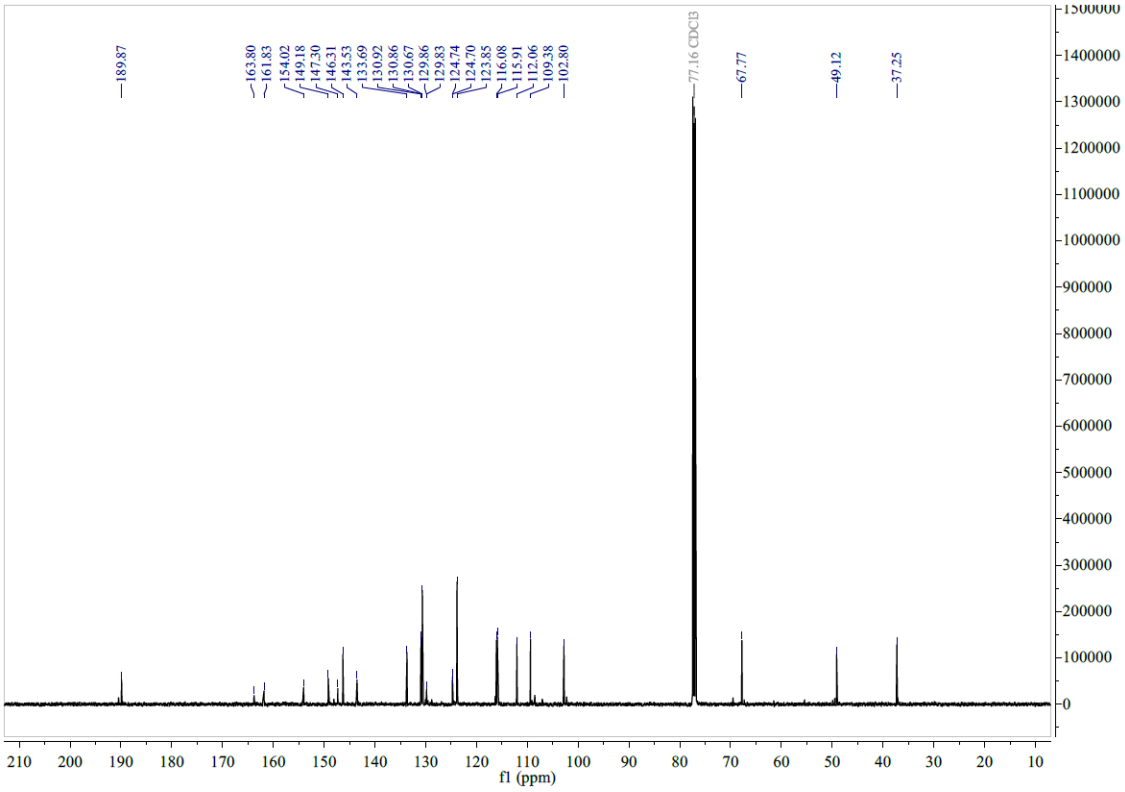

(S,E)-2-(4-fluorobenzyl)-5-((E)-3-(4-fluorophenyl)allylidene)-3-(4-nitrobenzyl) isothiazolidin-4-one 1,1-dioxide (1.27.1r)

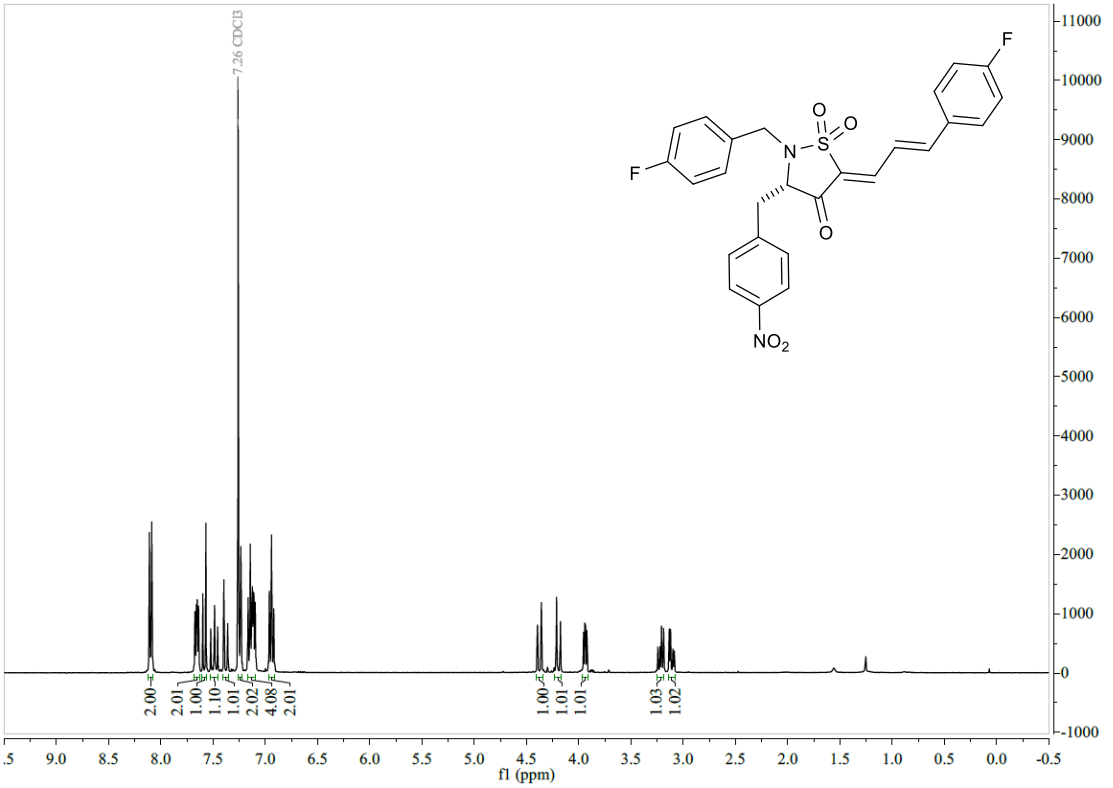

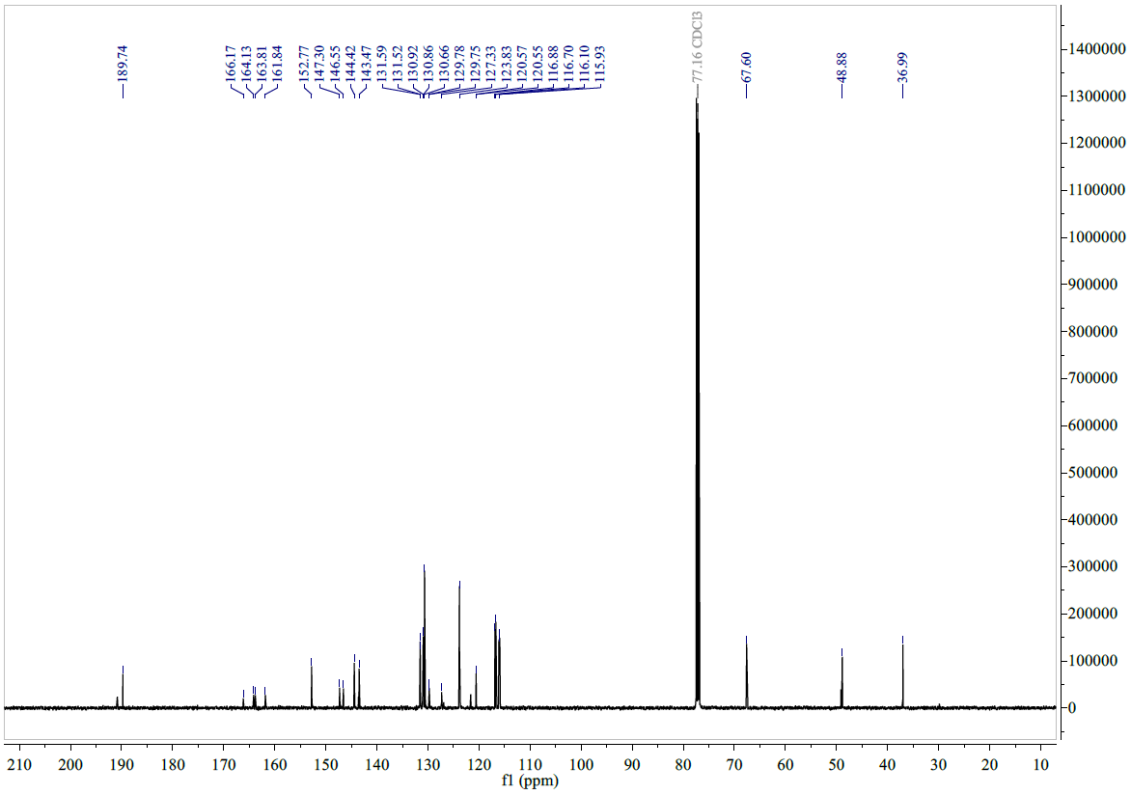

Methyl (S)-2-amino-3-(4-((tert-butyldimethylsilyl)oxy)phenyl)propanoate (2.7.3)

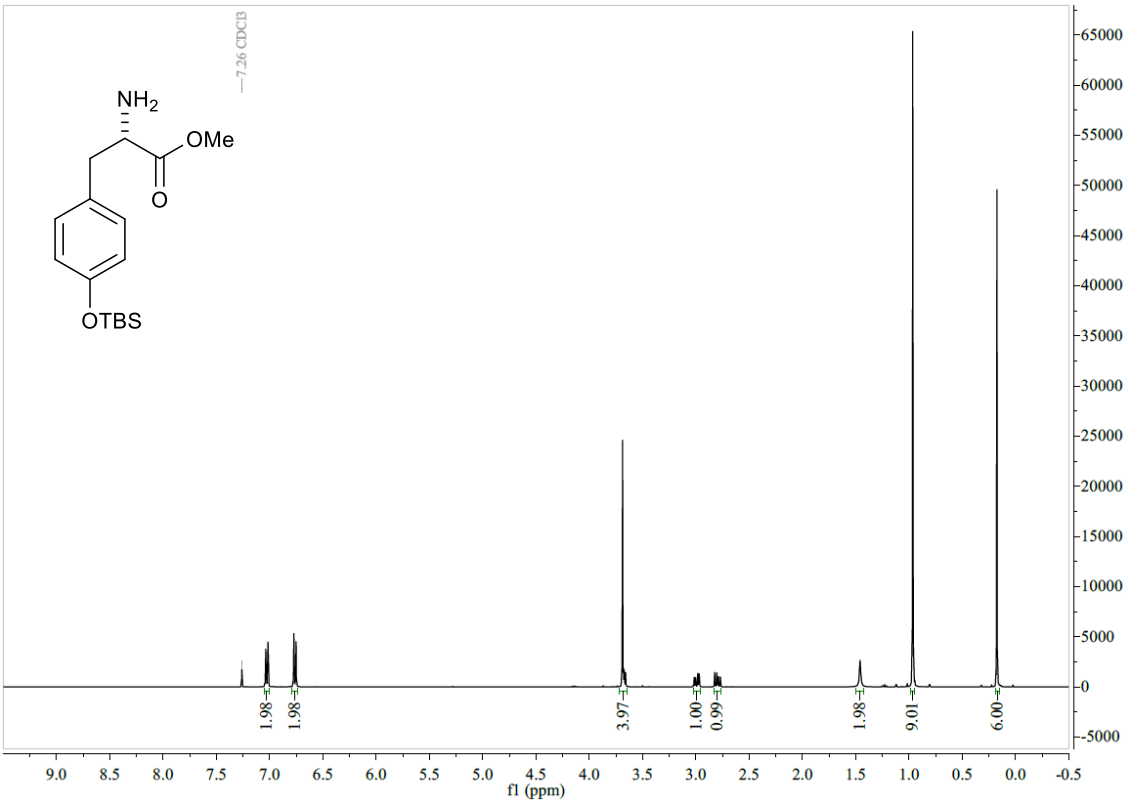

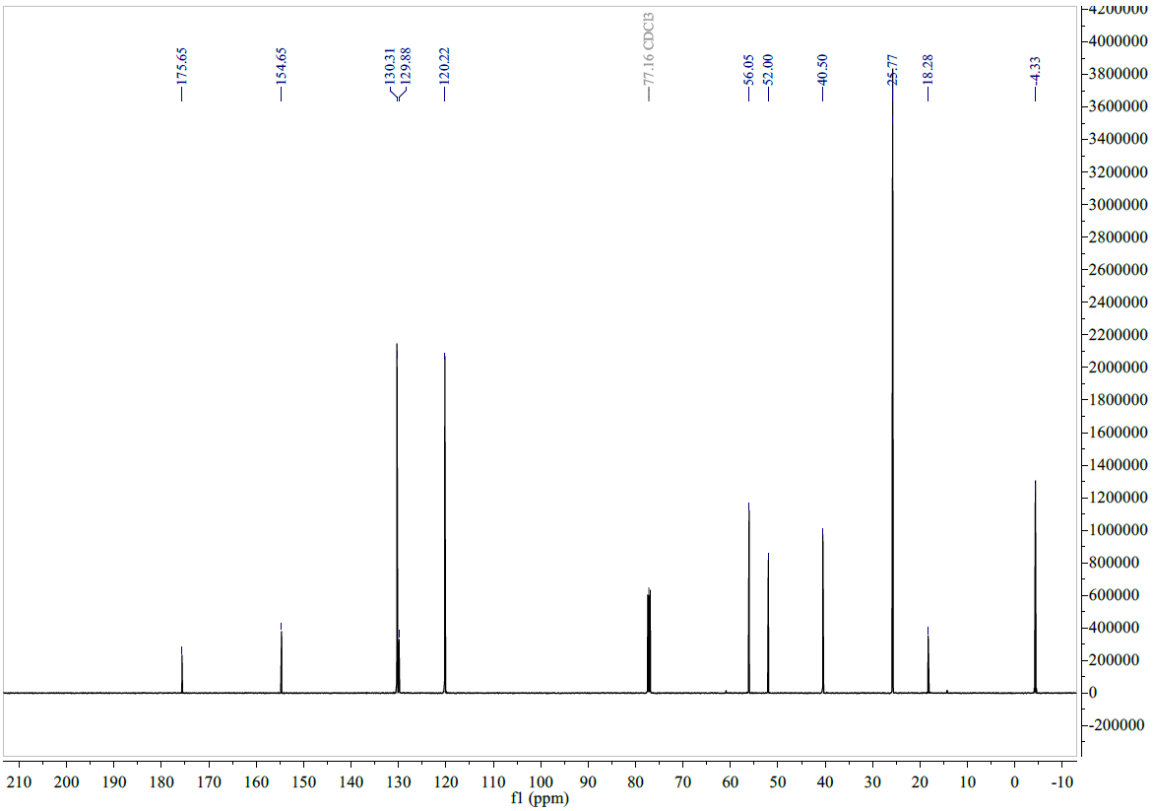

Methyl O-(tert-butyldimethylsilyl)-L-serinate (2.10.2)

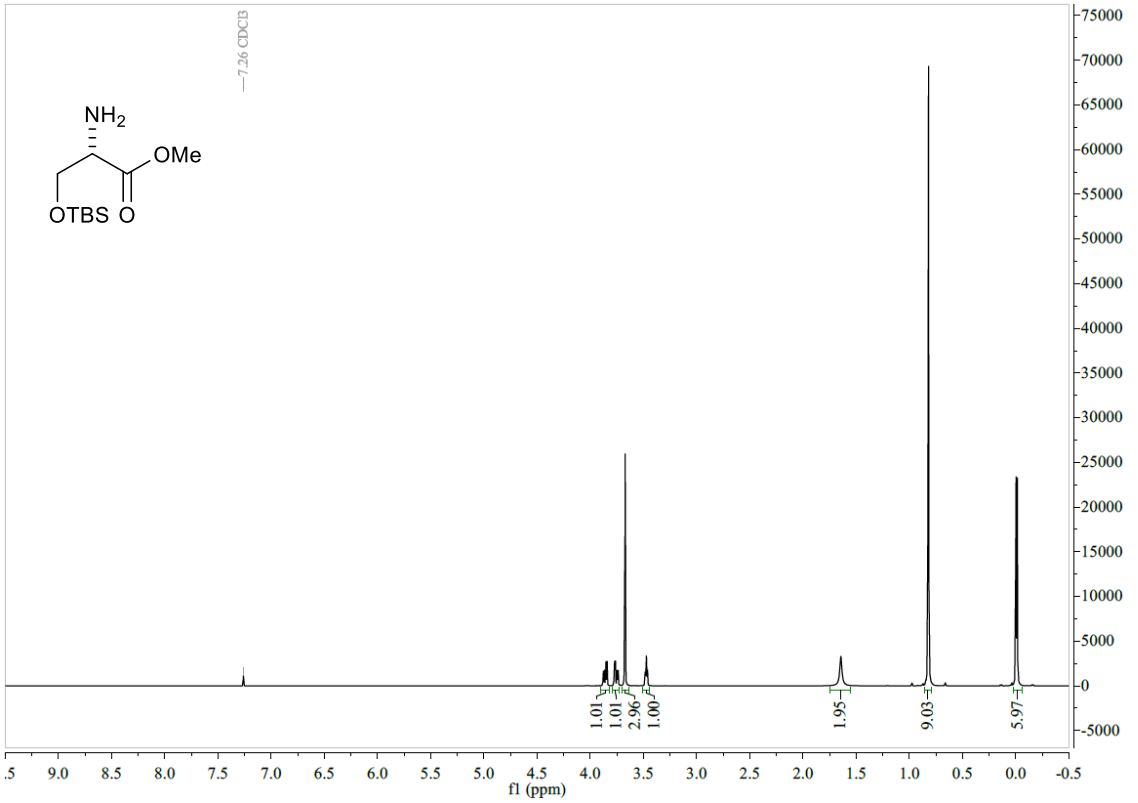

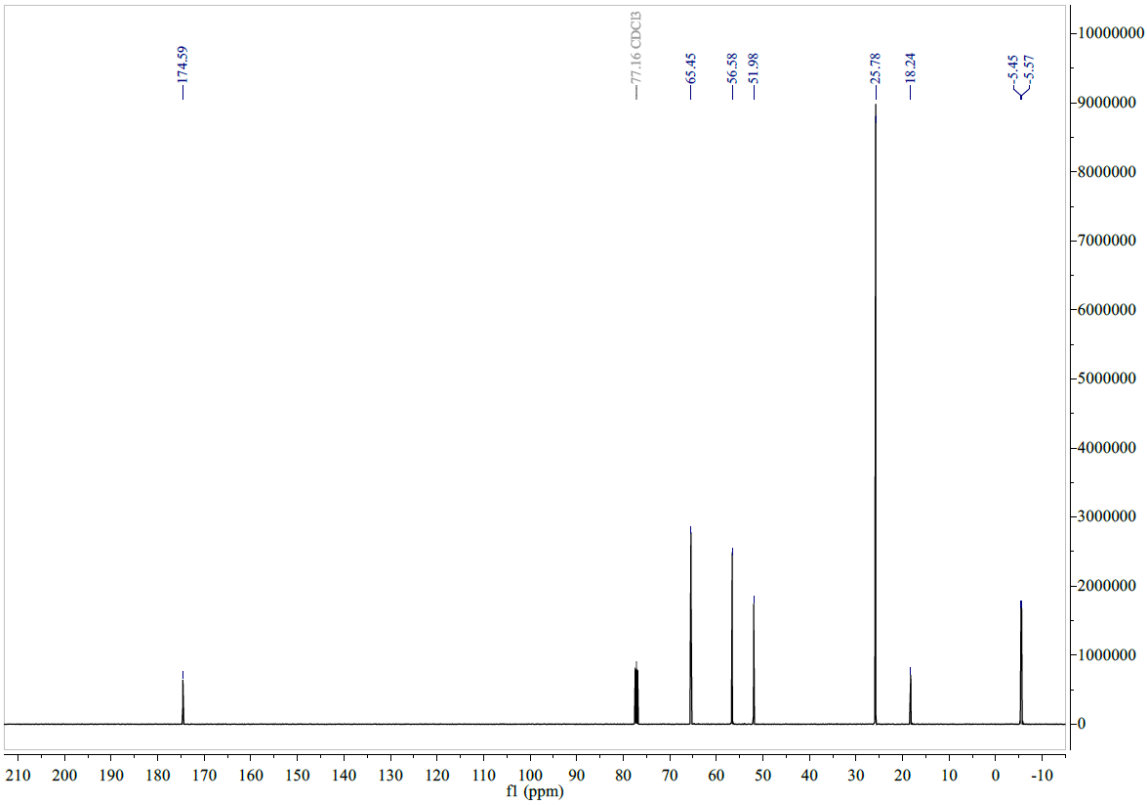

Methyl (S)-3-(4-((tert-butyldimethylsilyl)oxy)phenyl)-2-(methylsulfonamido)propanoate (2.7.4)

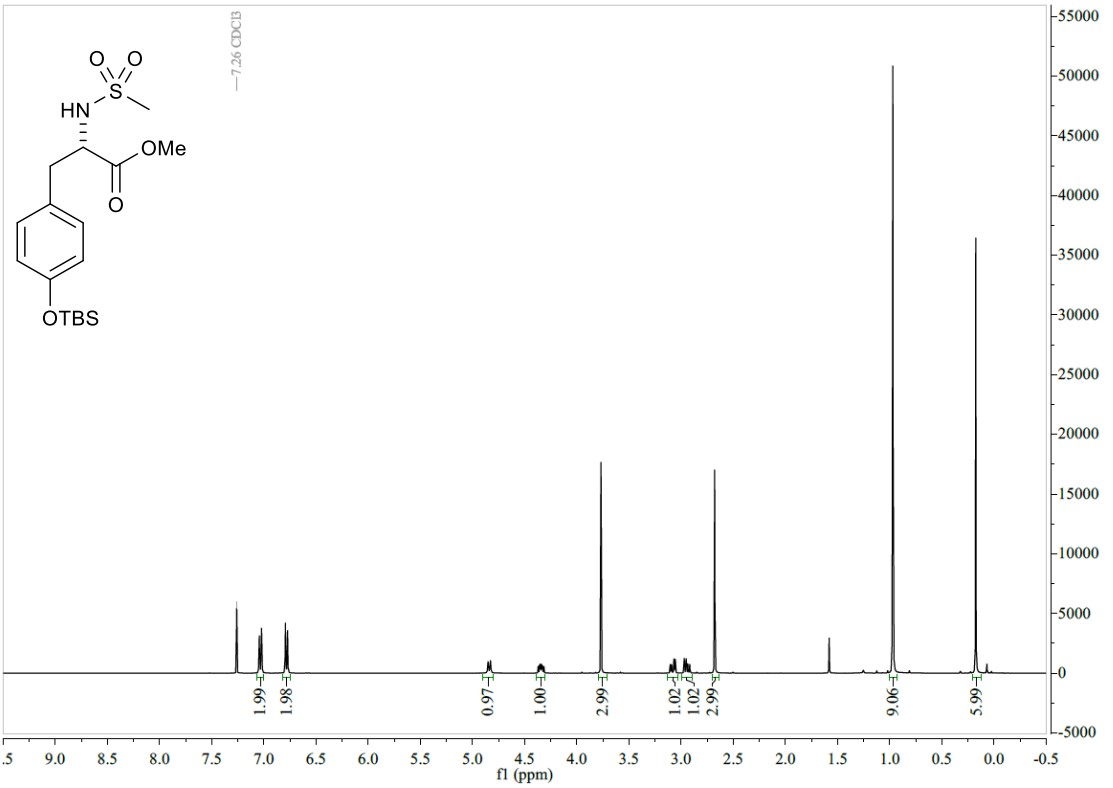

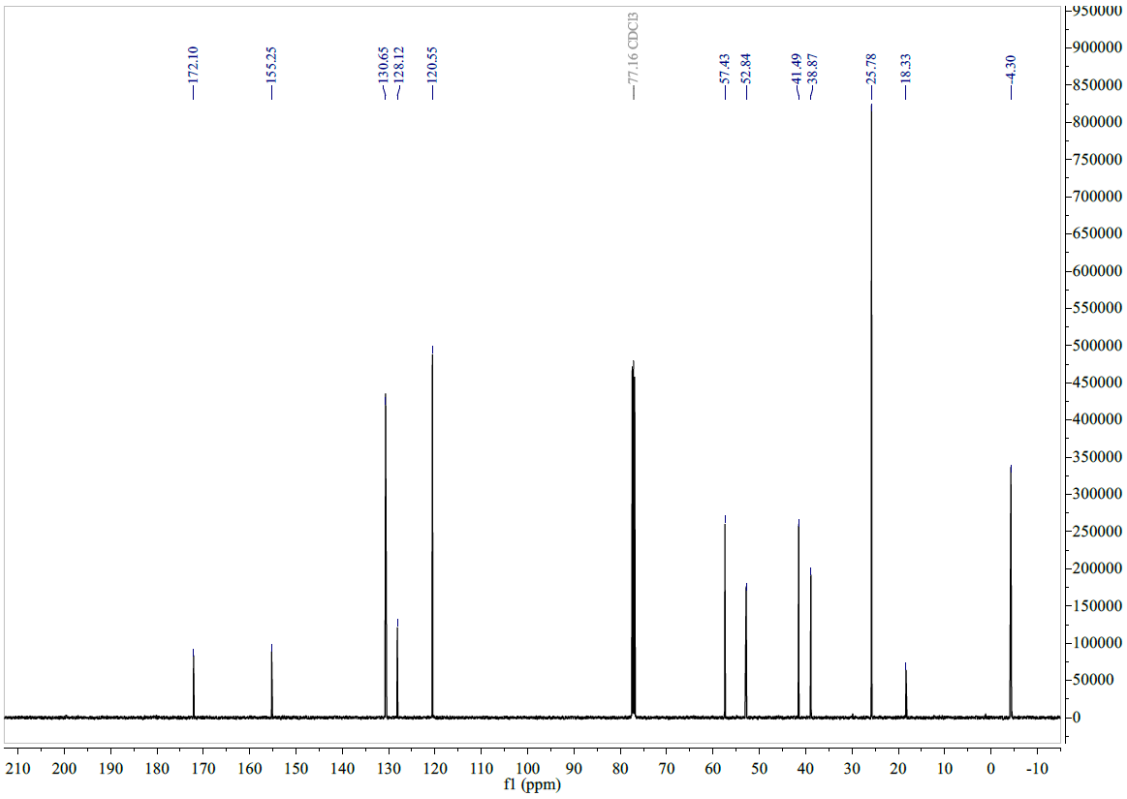

Methyl O-(tert-butyldimethylsilyl)-N-(methylsulfonyl)-L-serinate (2.10.3)

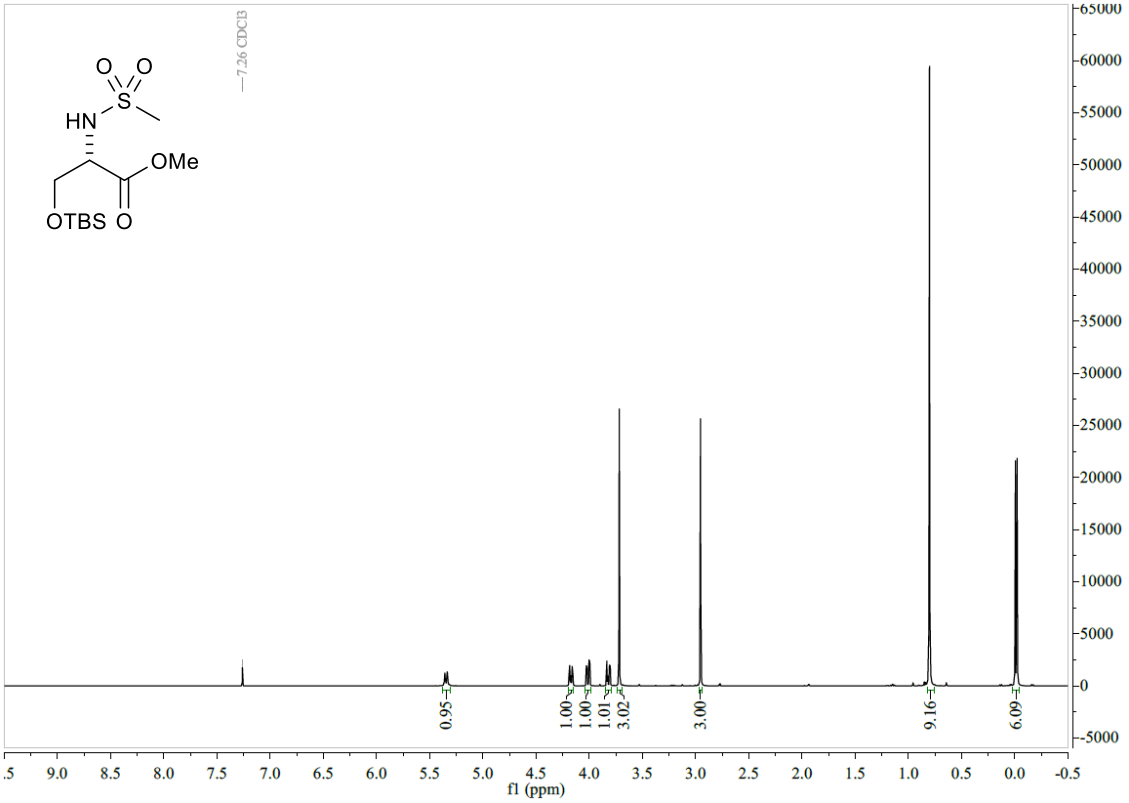

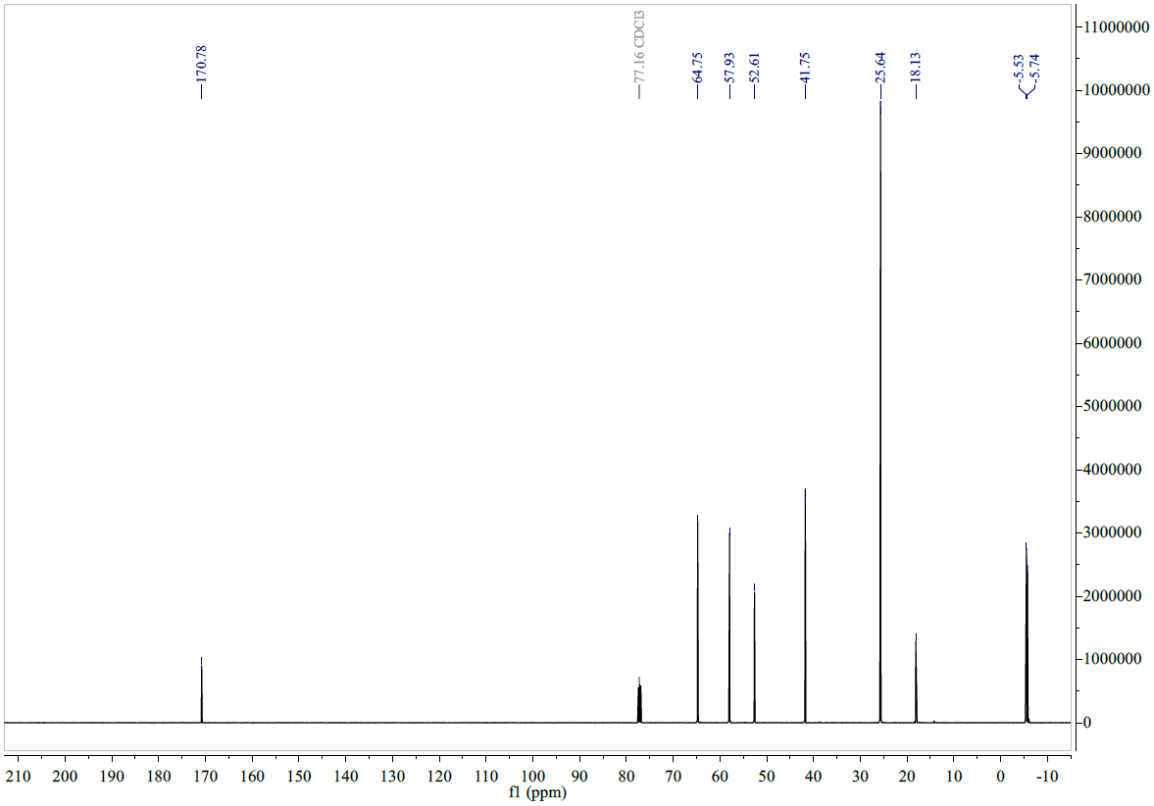

Methyl (S)-3-(4-((tert-butyldimethylsilyl)oxy)phenyl)-2-(N-(2-chlorobenzyl)methyl sulfonamido)propanoate (2.8.1a)

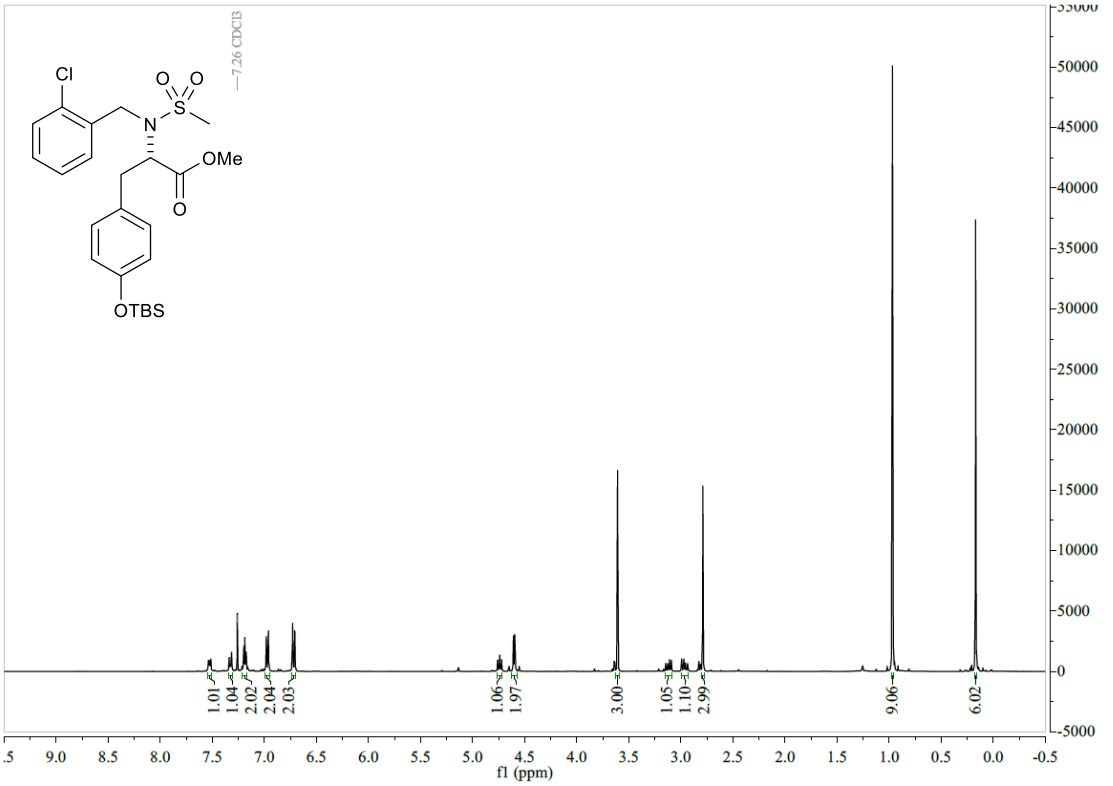

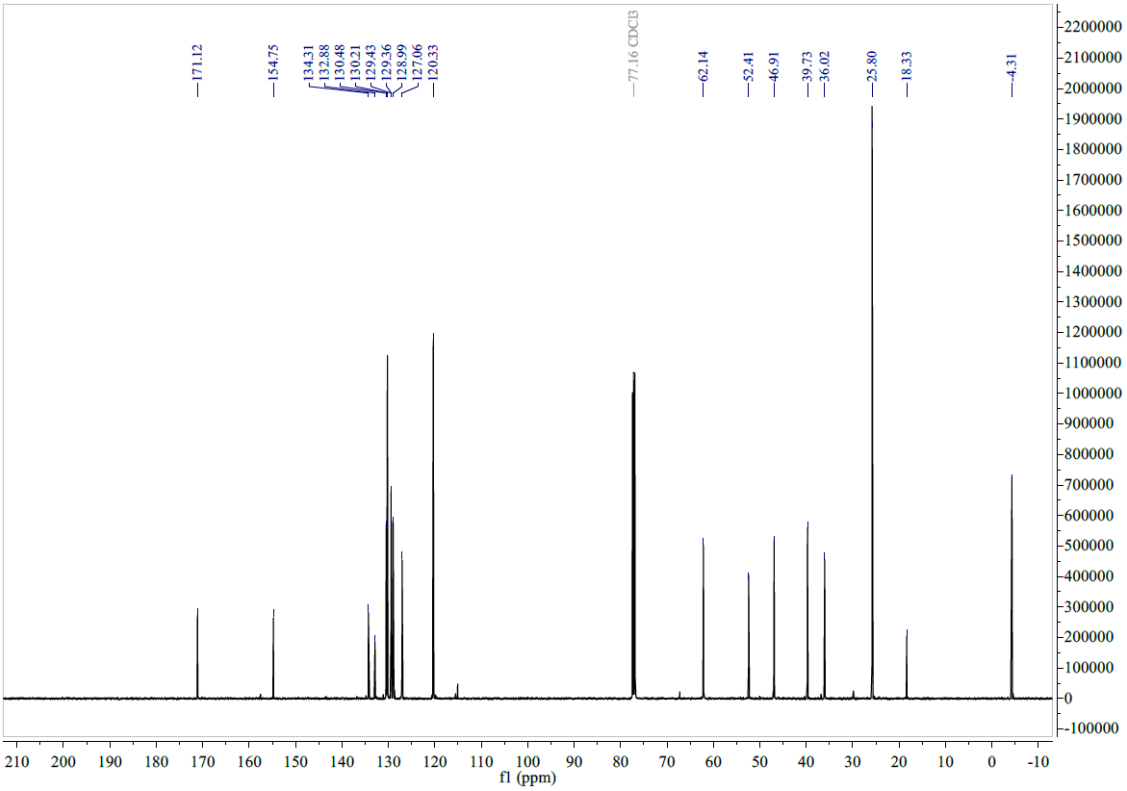

Methyl (S)-2-(N-benzylmethylsulfonamido)-3-(4-((tert-butyldimethylsilyl)oxy)phenyl) propanoate (2.8.1b)

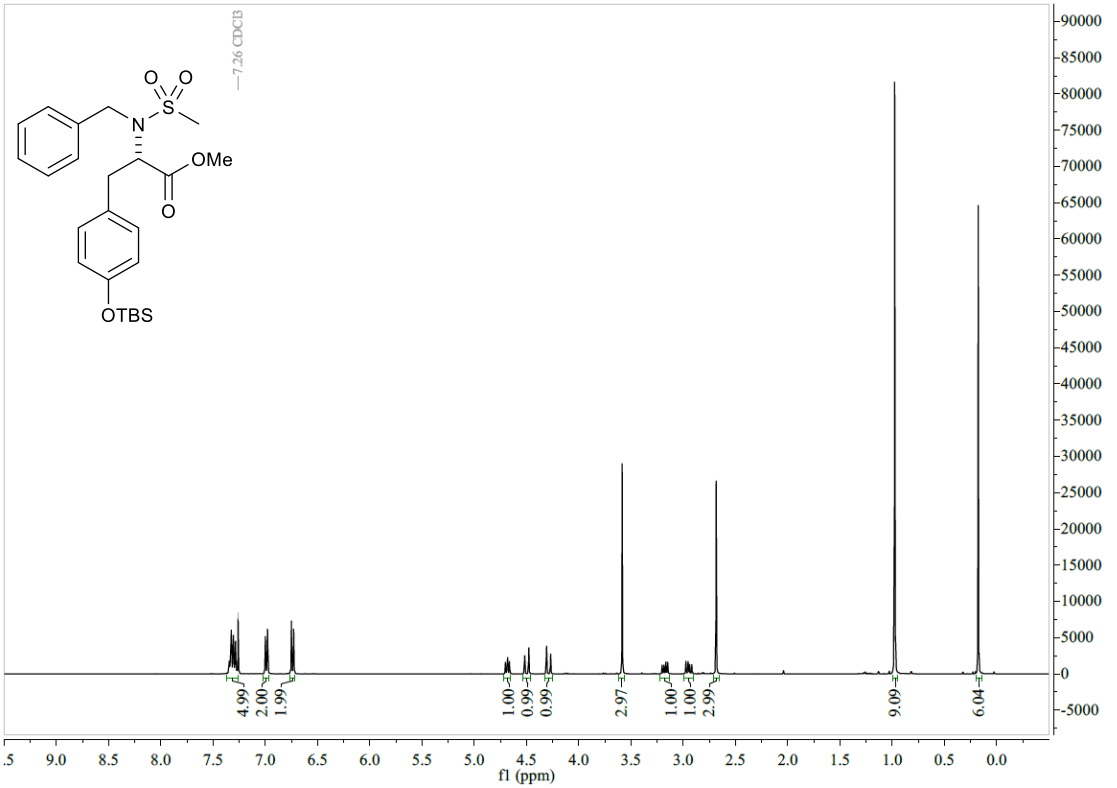

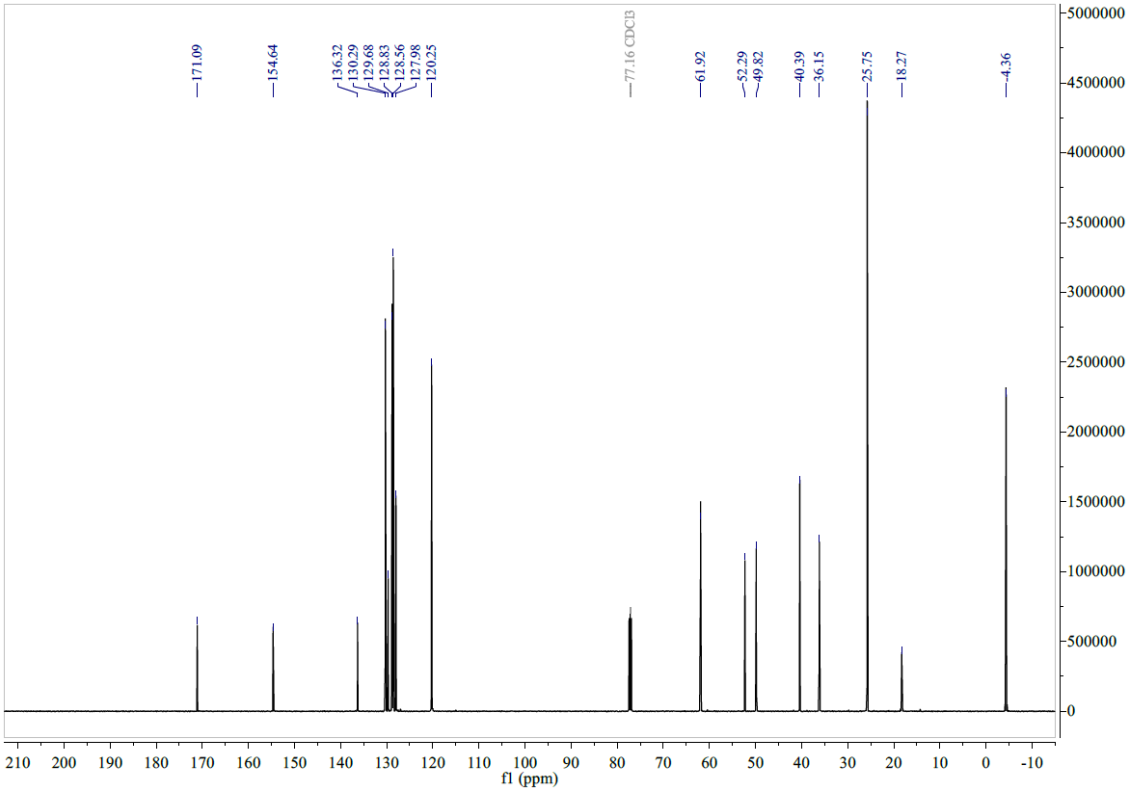

Methyl (S)-3-(4-((tert-butyldimethylsilyl)oxy)phenyl)-2-(N-(4-fluorobenzyl)methyl sulfonamido)propanoate (2.8.1c)

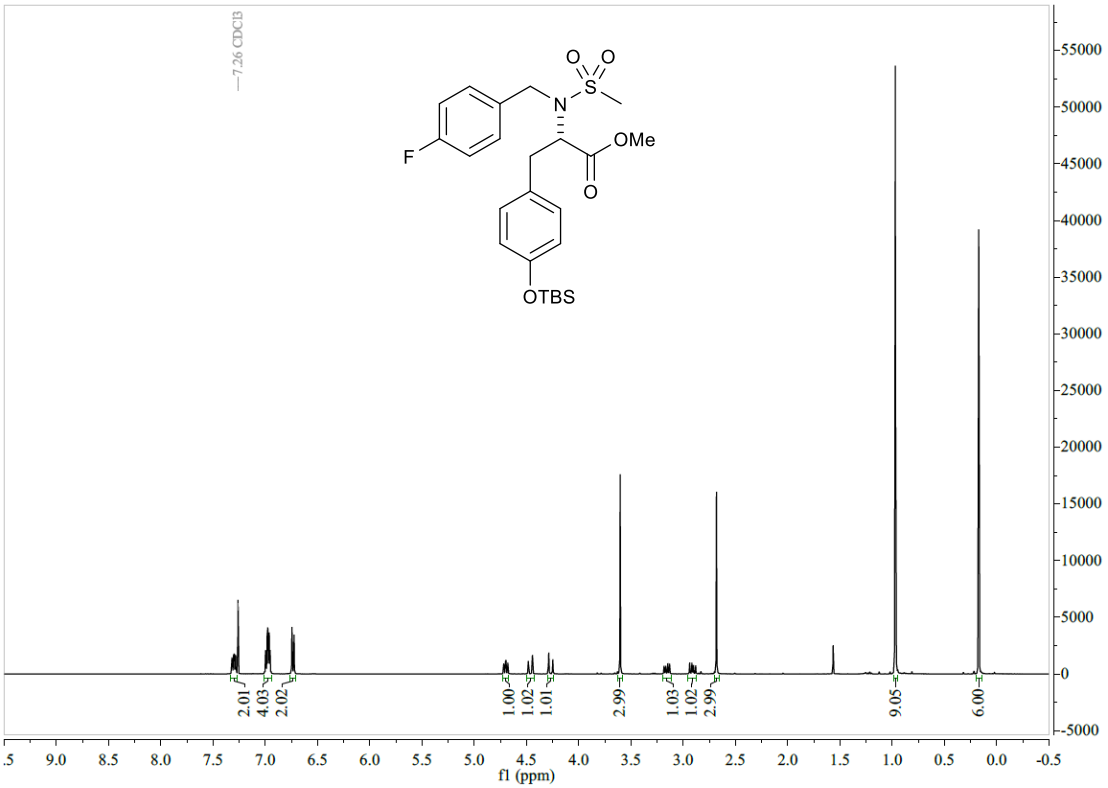

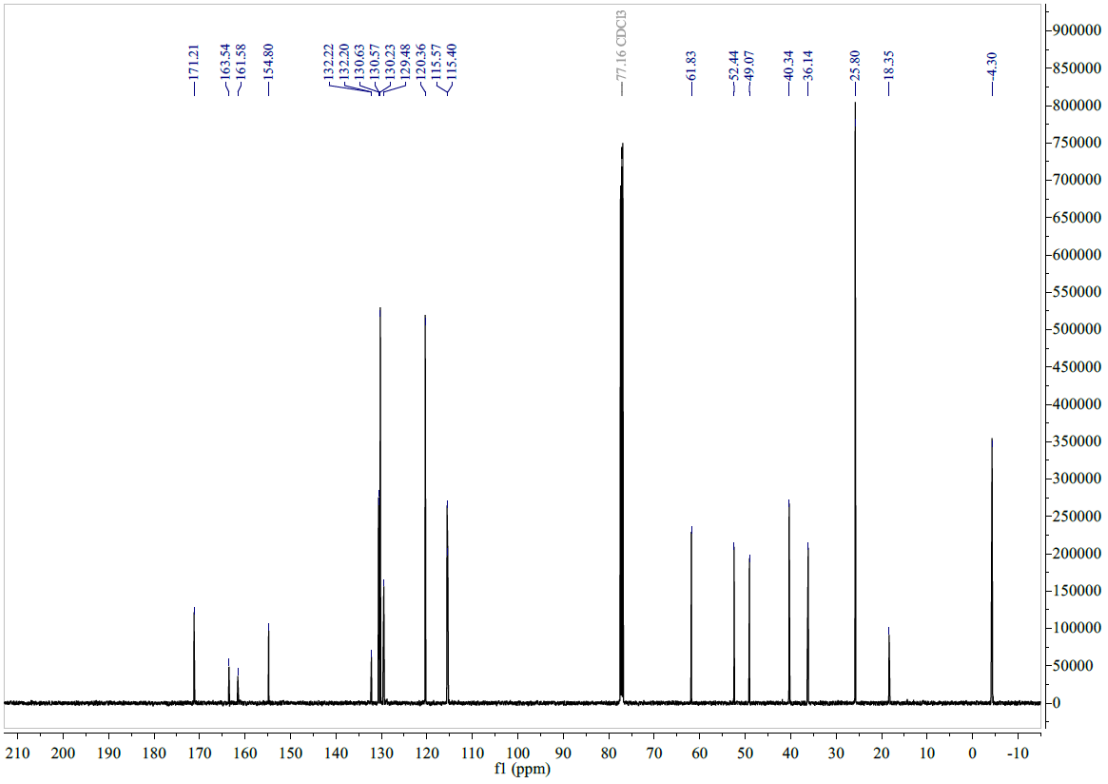

Methyl O-(tert-butyldimethylsilyl)-N-(2-chlorobenzyl)-N-(methylsulfonyl)-L-serinate (2.10.4a)

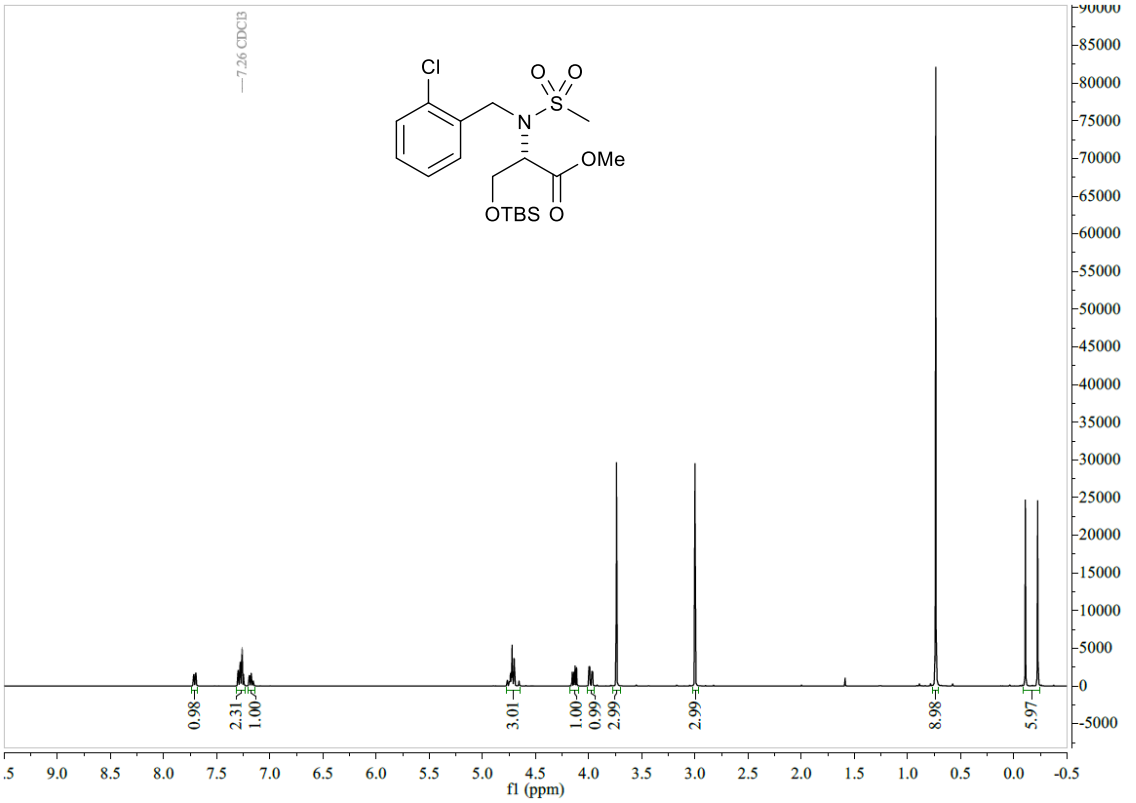

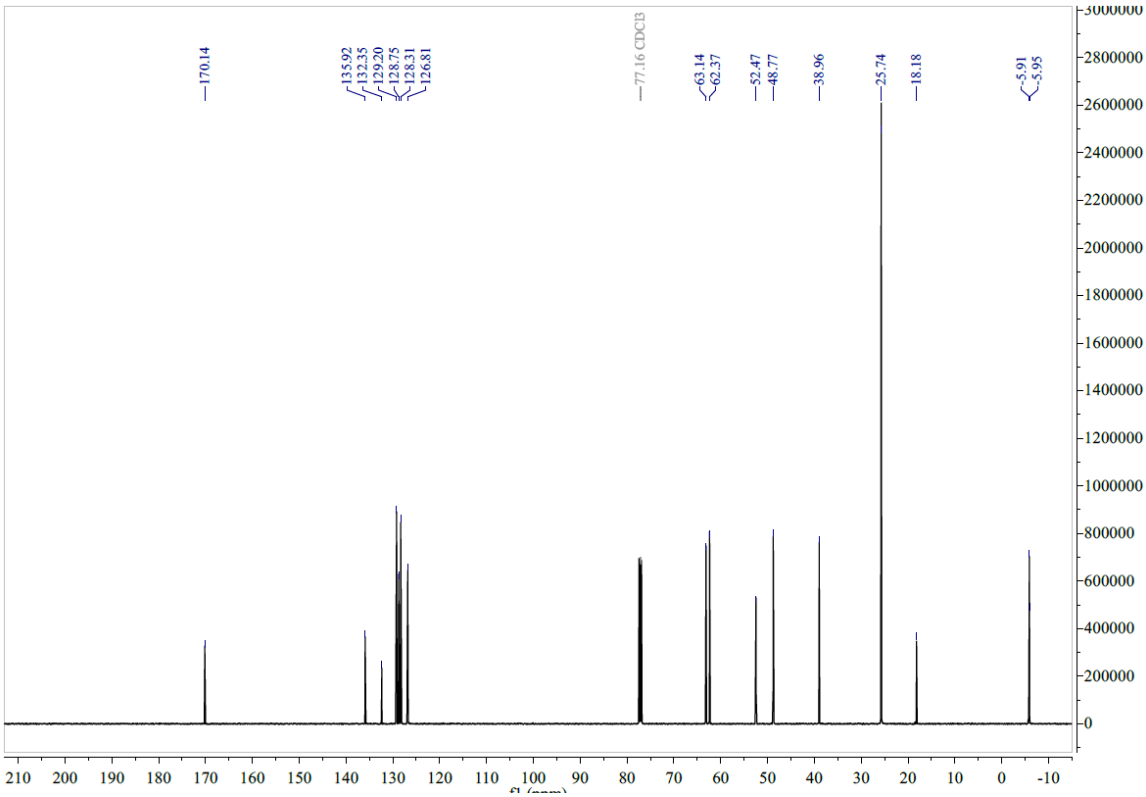

Methyl N-benzyl-O-(tert-butyldimethylsilyl)-N-(methylsulfonyl)-L-serinate (2.10.4b)

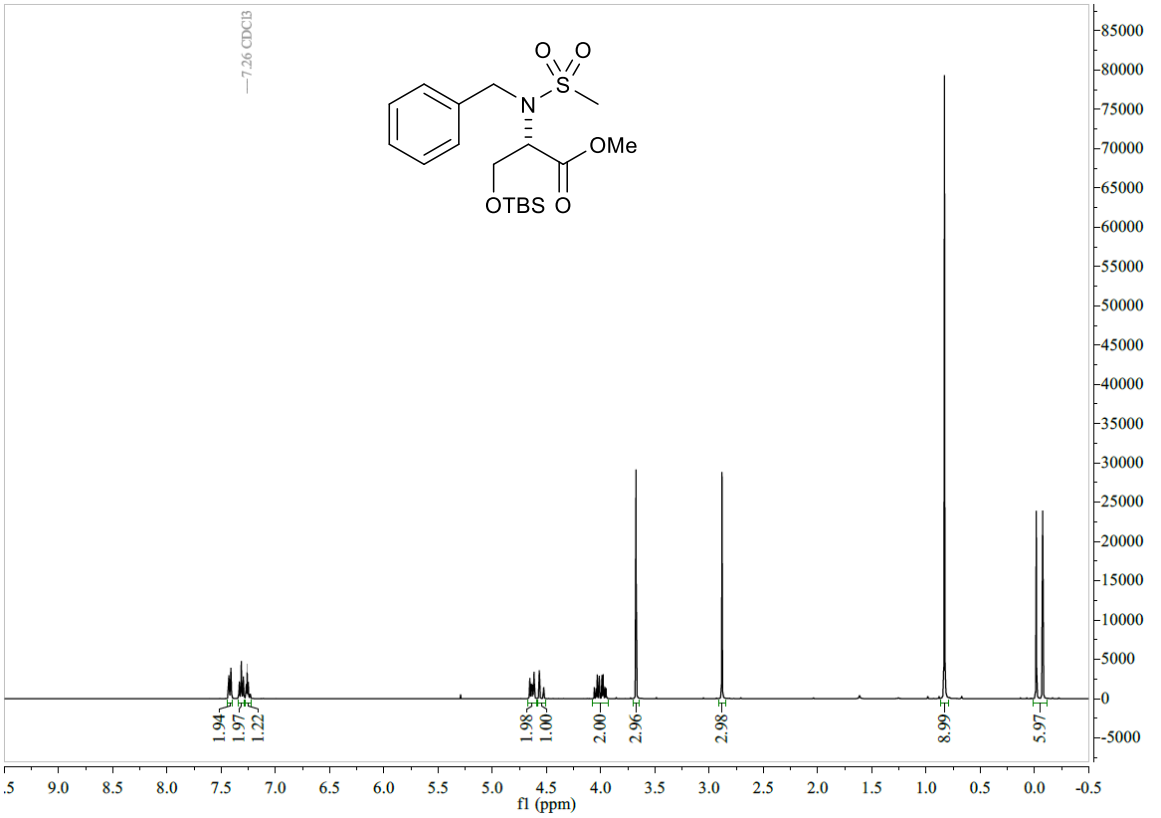

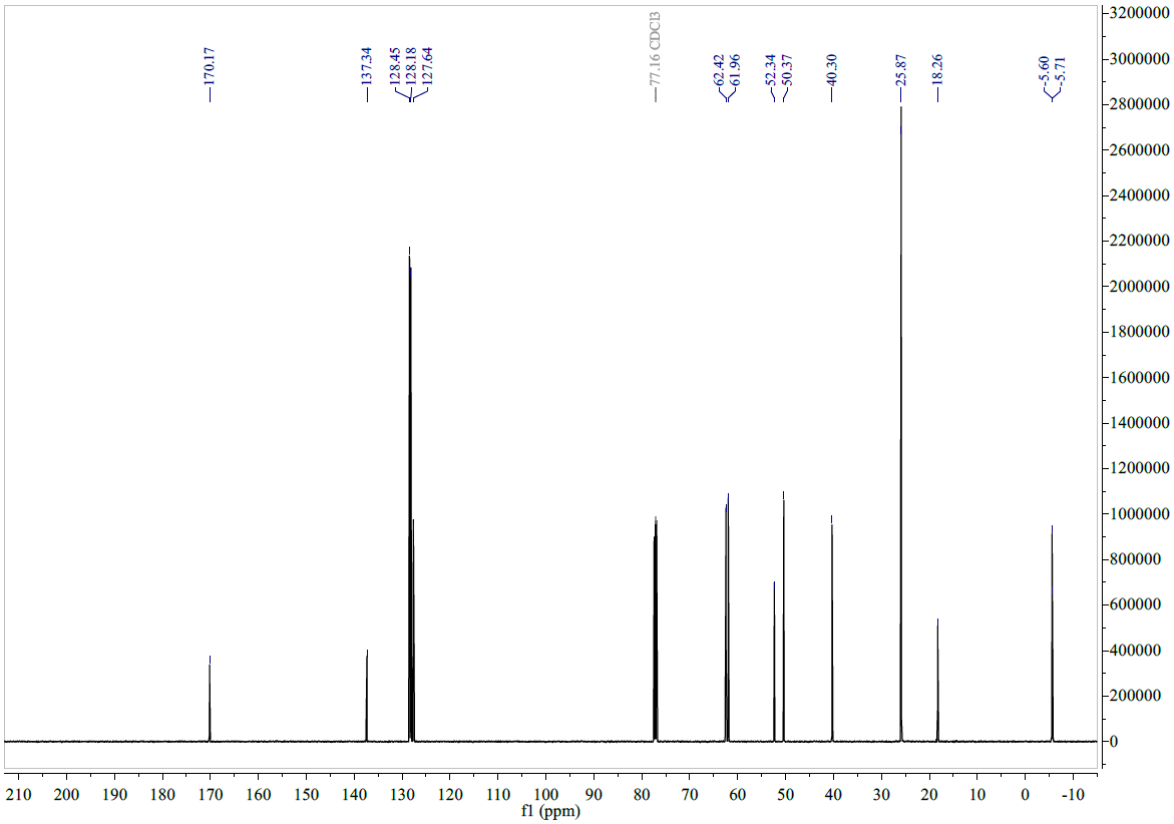

Methyl O-(tert-butyldimethylsilyl)-N-(4-fluorobenzyl)-N-(methylsulfonyl)-L-serinate (2.10.4c)

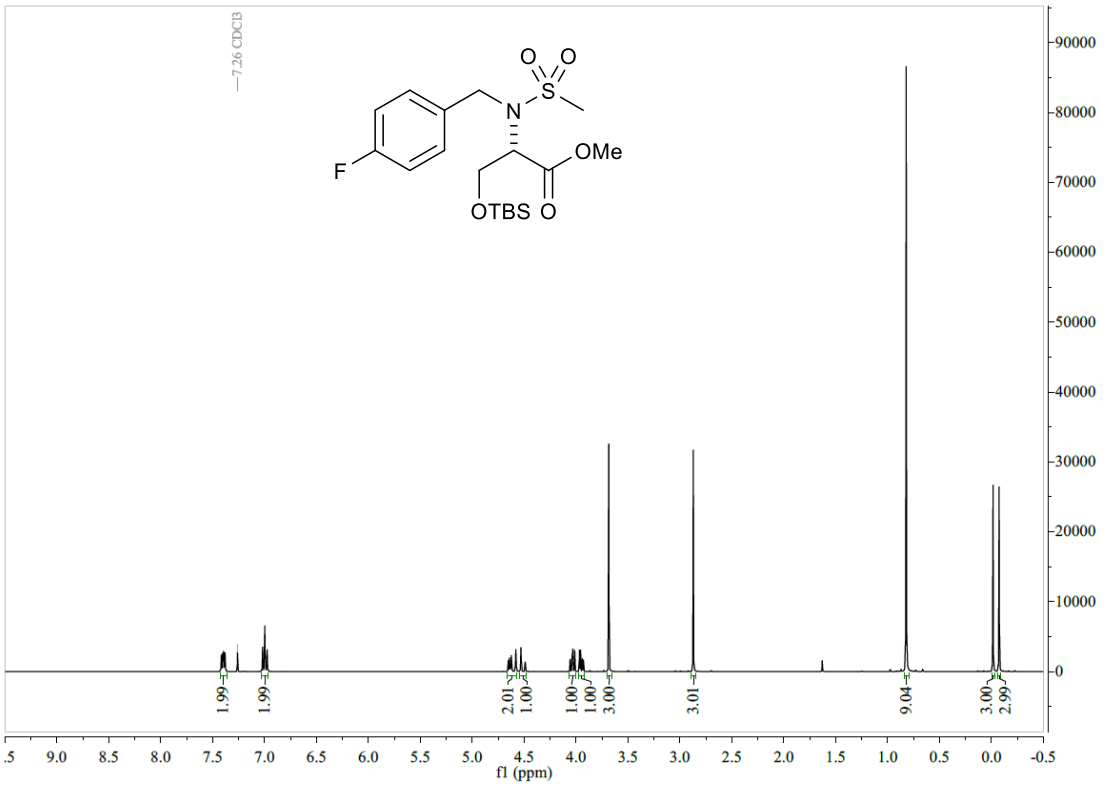

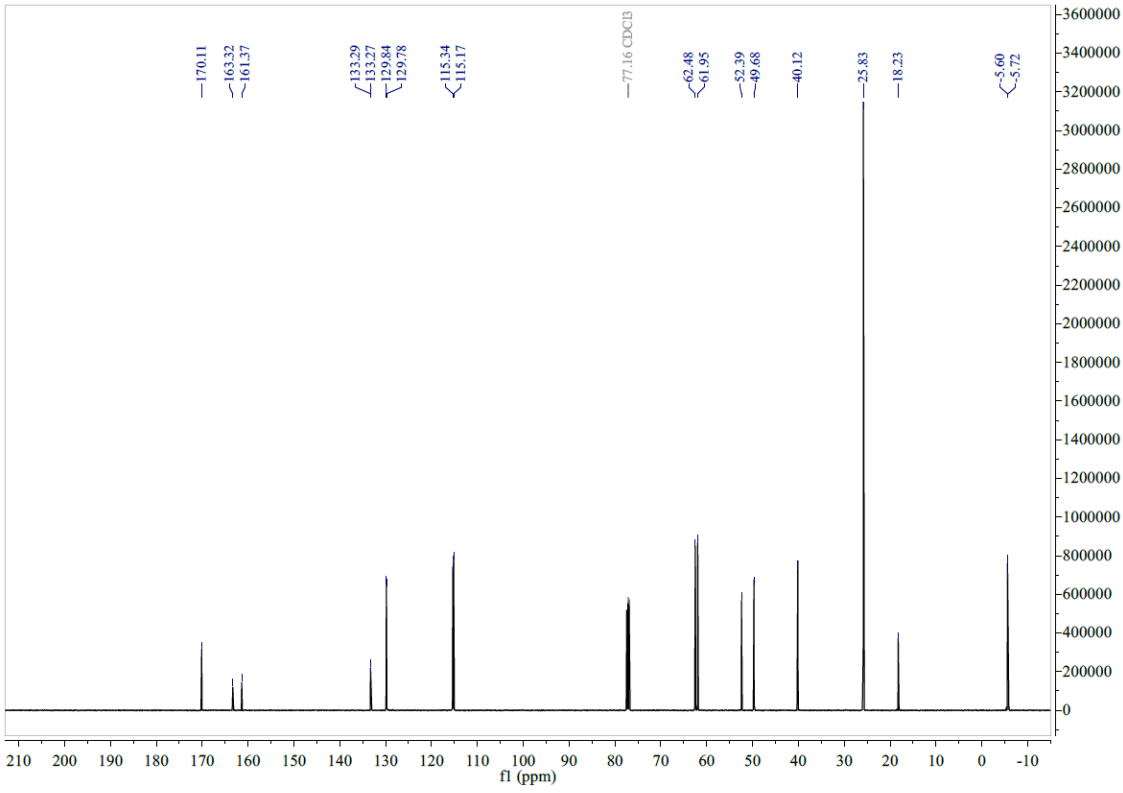

Methyl N-(2-chlorobenzyl)-N-(methylsulfonyl)-L-tyrosinate (2.9.1a)

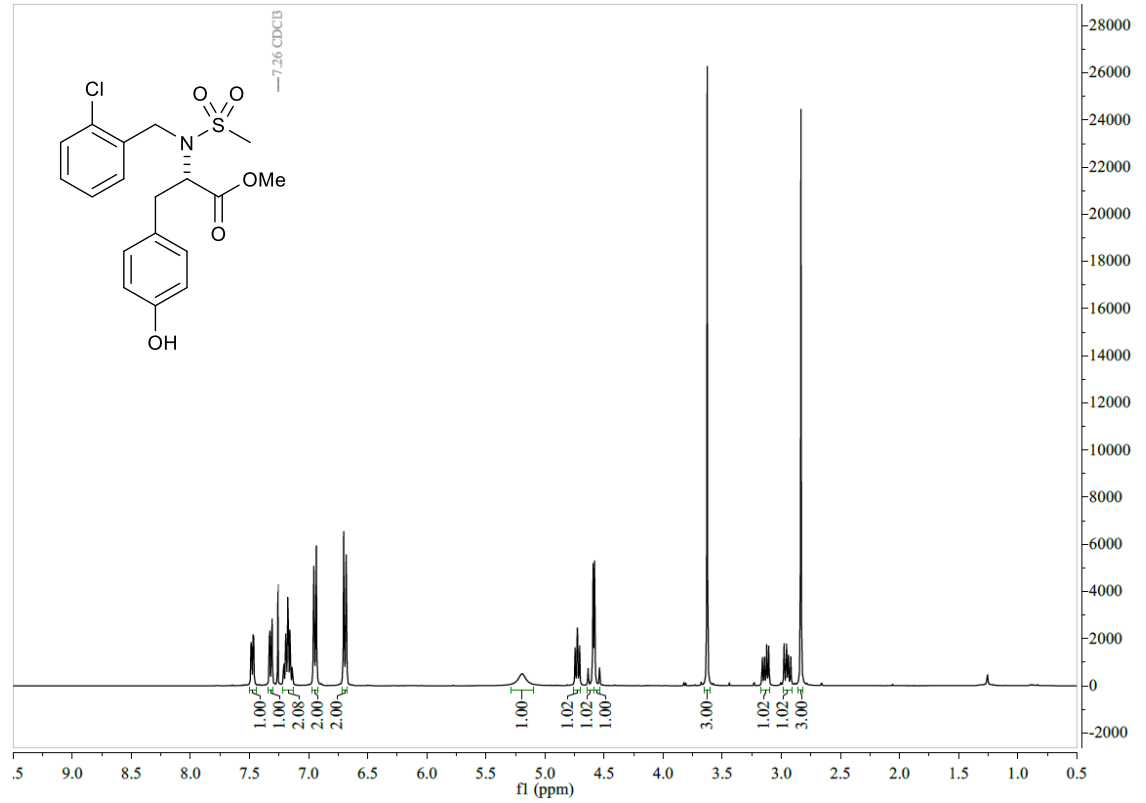

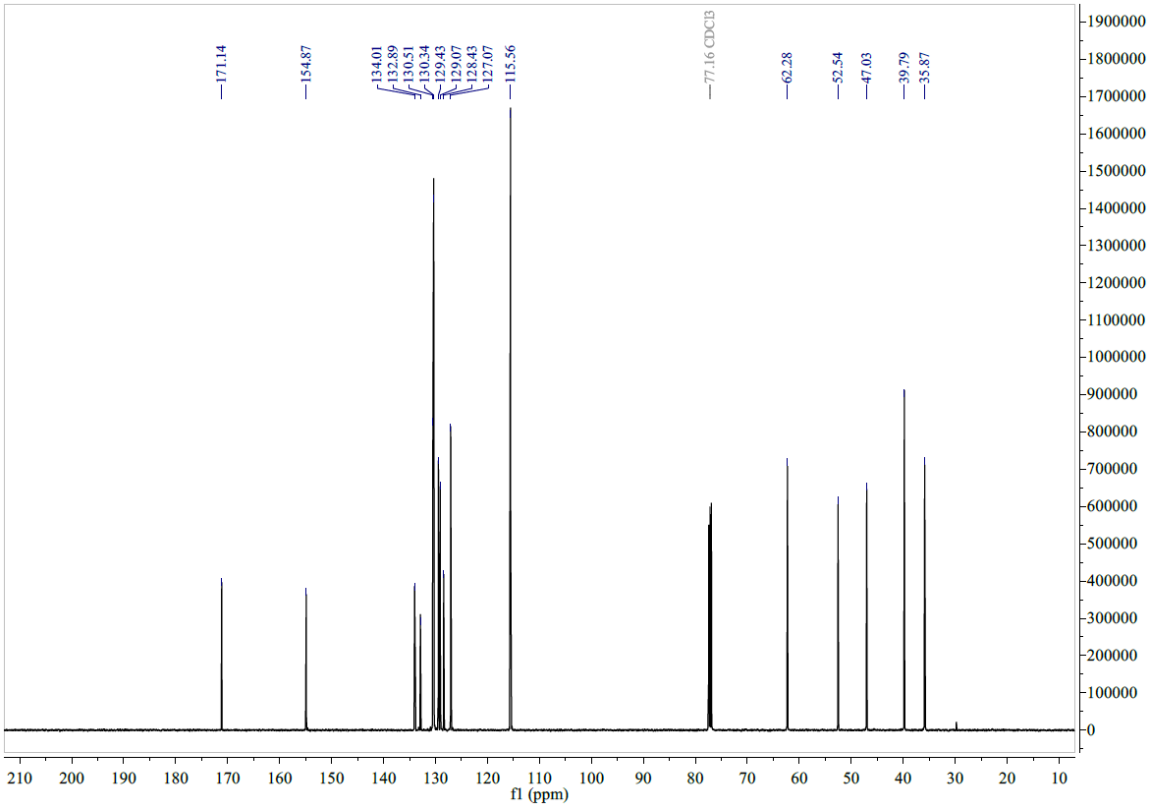

Methyl N-benzyl-N-(methylsulfonyl)-L-tyrosinate (2.9.1b)

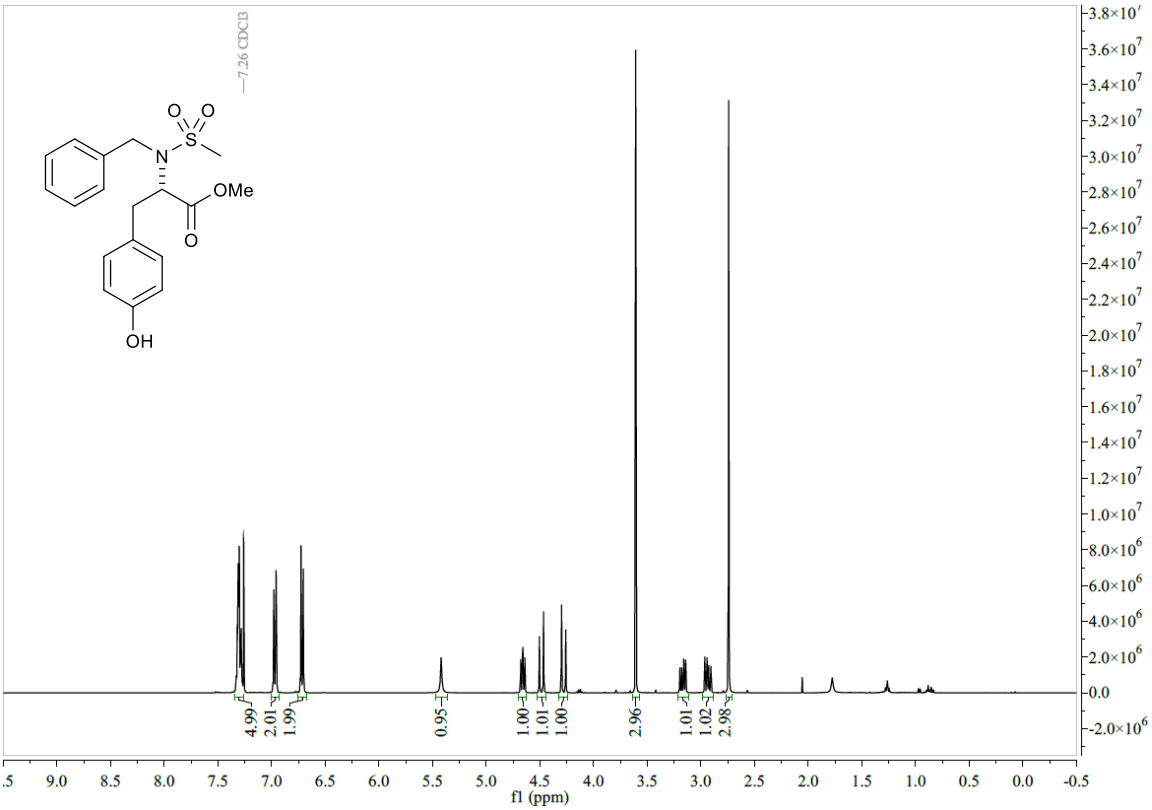

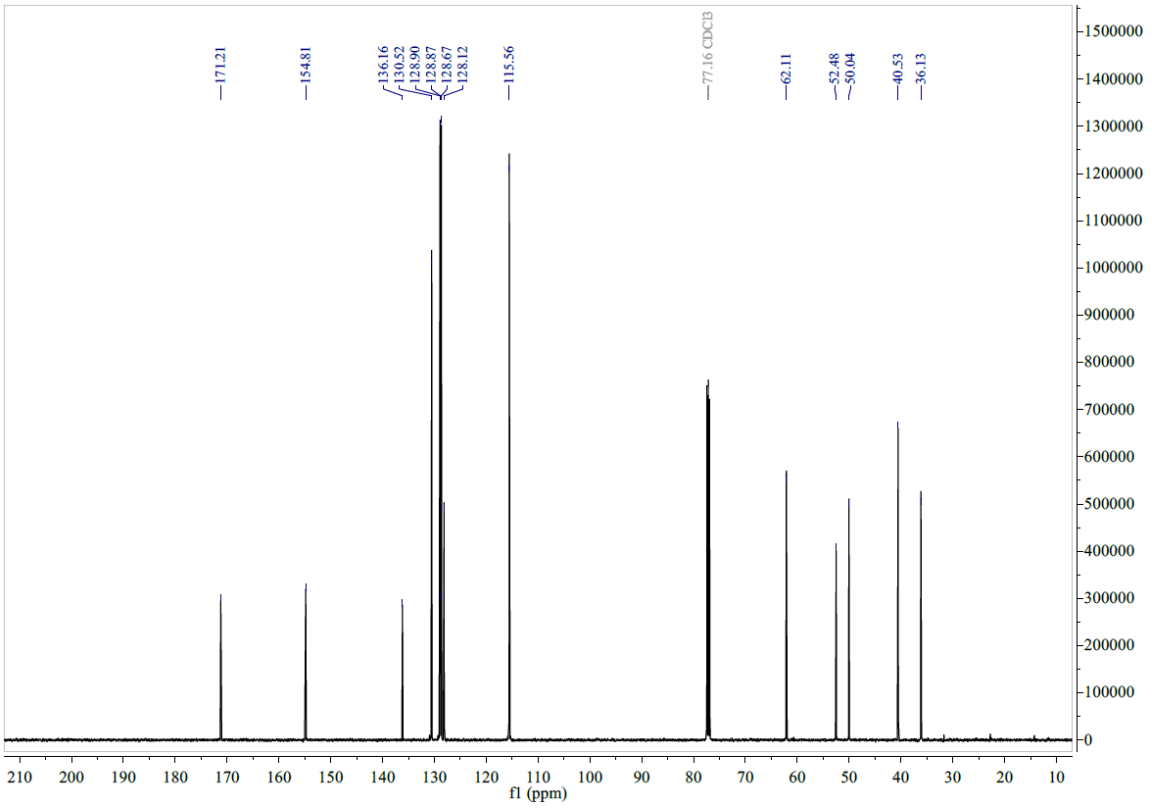

Methyl N-(4-fluorobenzyl)-N-(methylsulfonyl)-L-tyrosinate (2.9.1c)

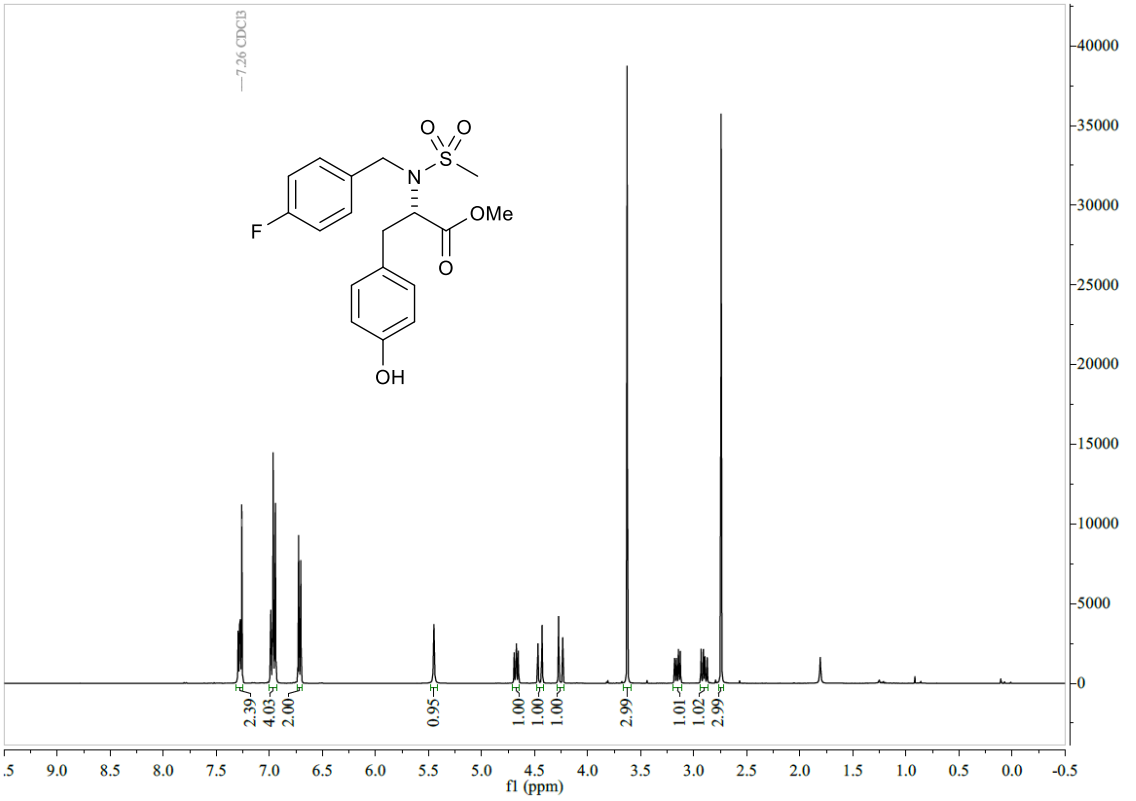

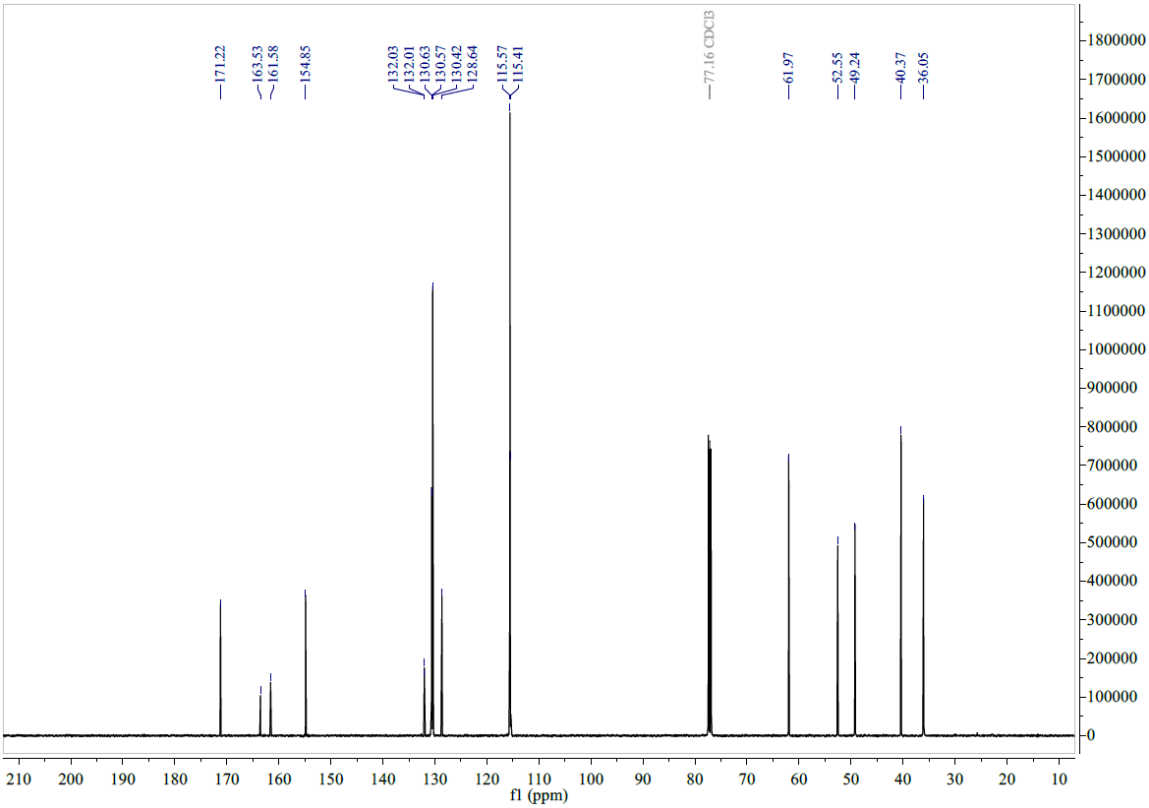

Methyl (S)-3-(4-(allyloxy)phenyl)-2-(N-(2-chlorobenzyl)methylsulfonamido)propanoate (2.9.2a)

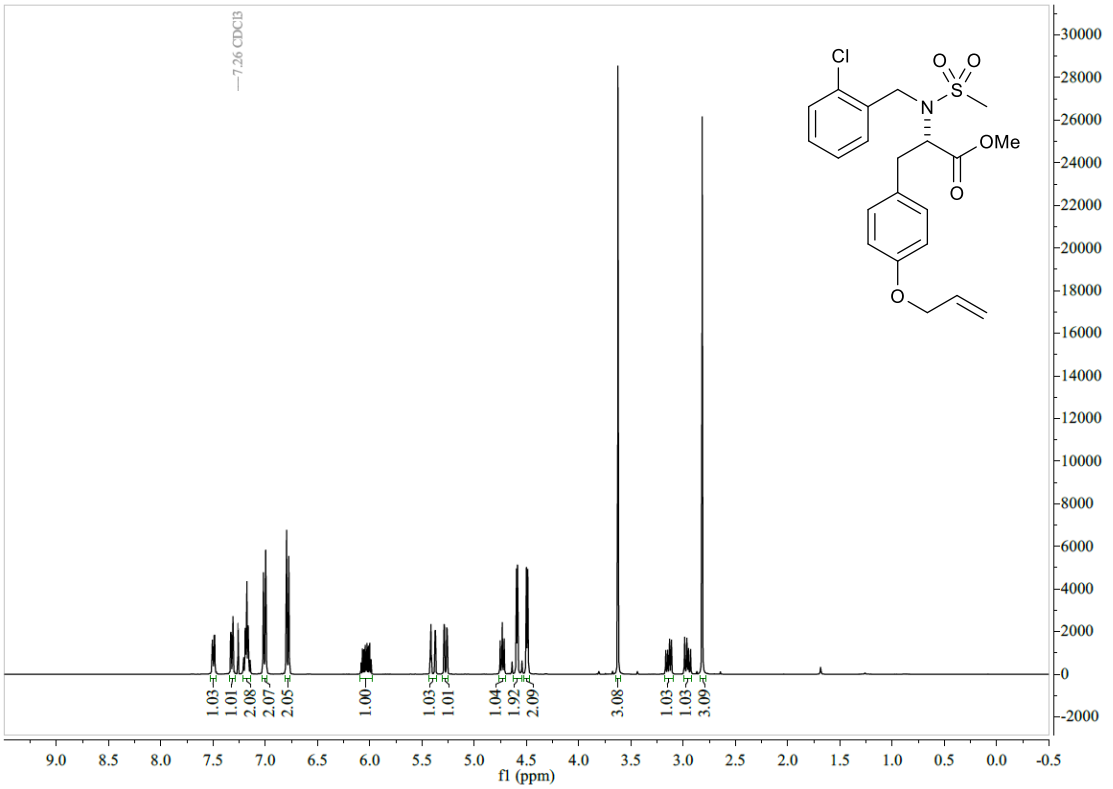

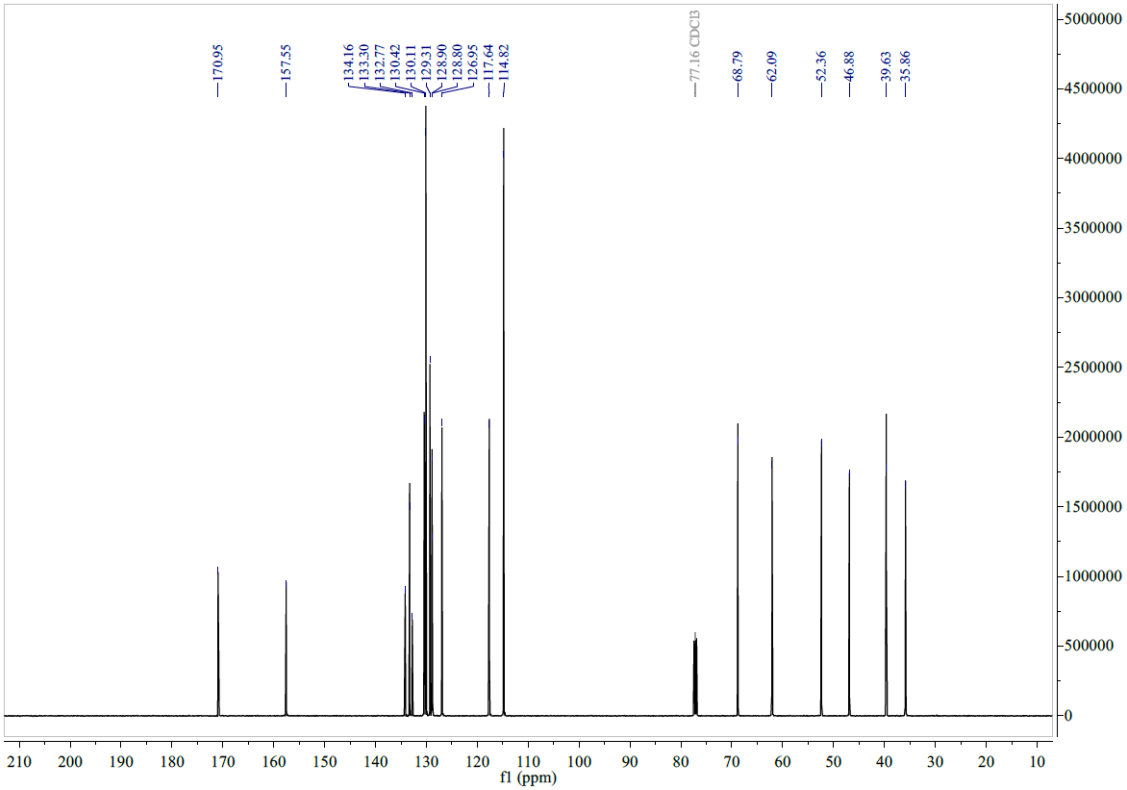

Methyl (S)-3-(4-(allyloxy)phenyl)-2-(N-benzylmethylsulfonamido)propanoate (2.9.2b)

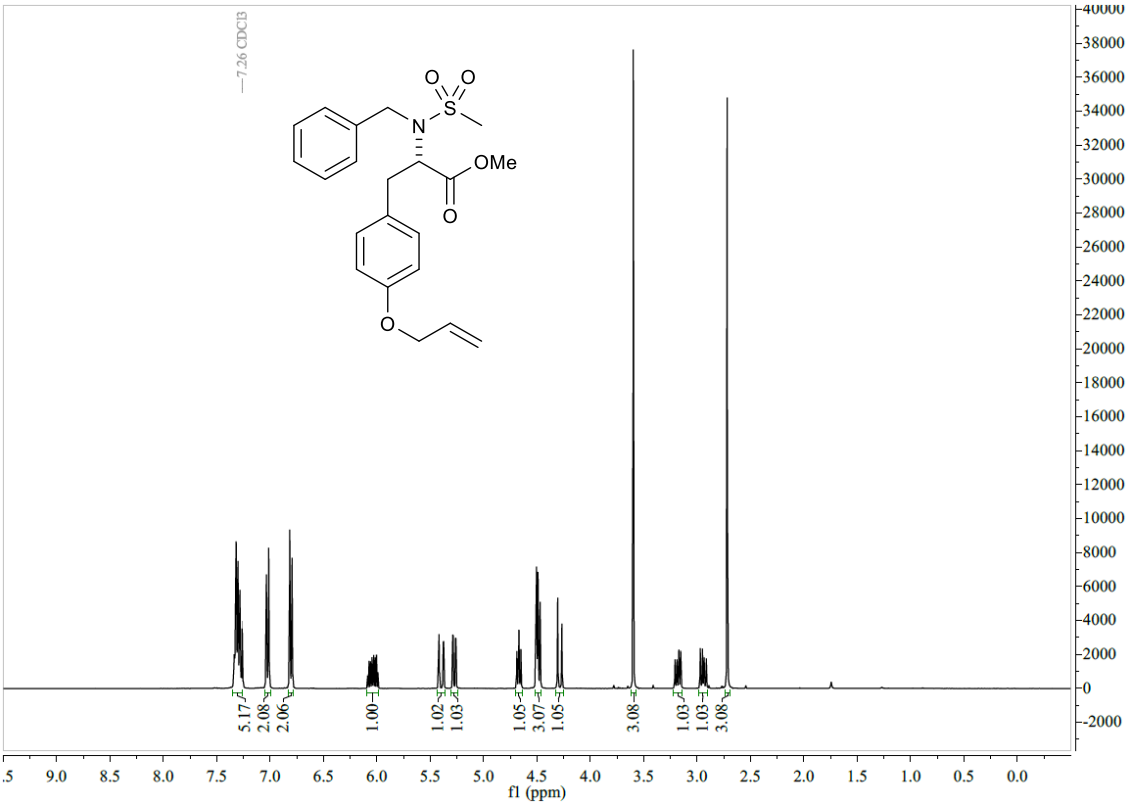

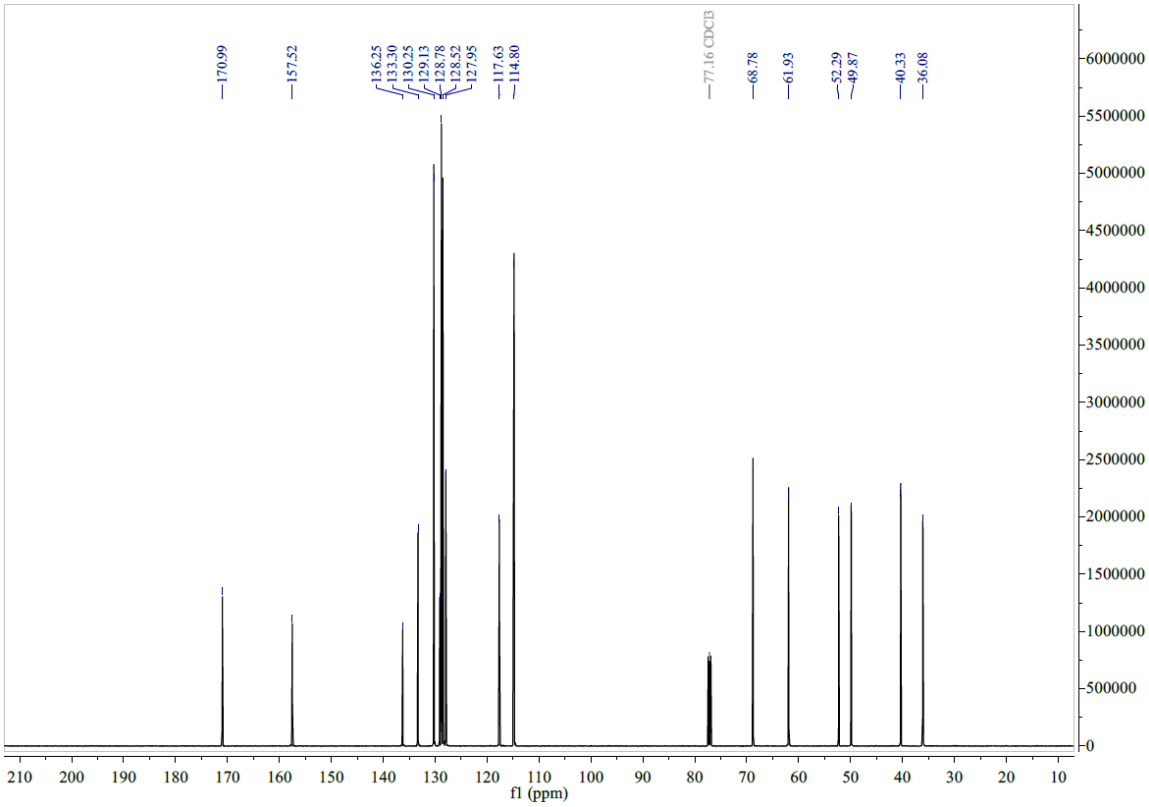

Methyl (S)-3-(4-(allyloxy)phenyl)-2-(N-(4-fluorobenzyl)methylsulfonamido)propanoate (2.9.2c)

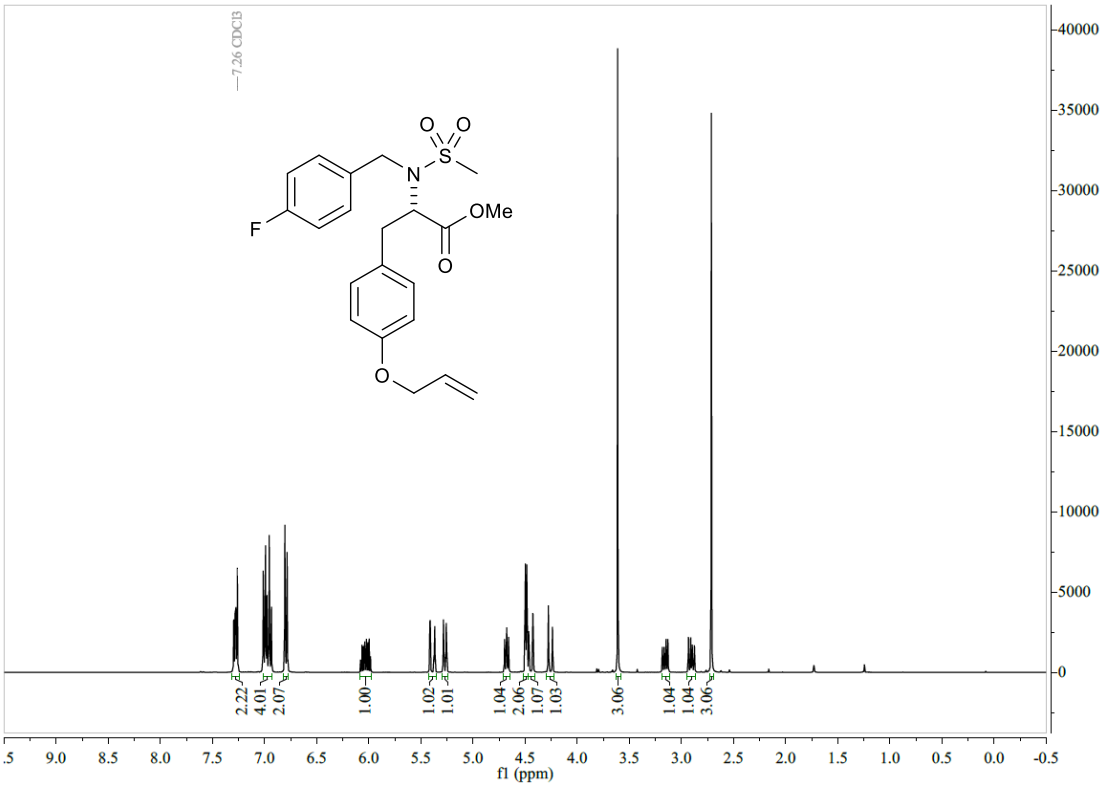

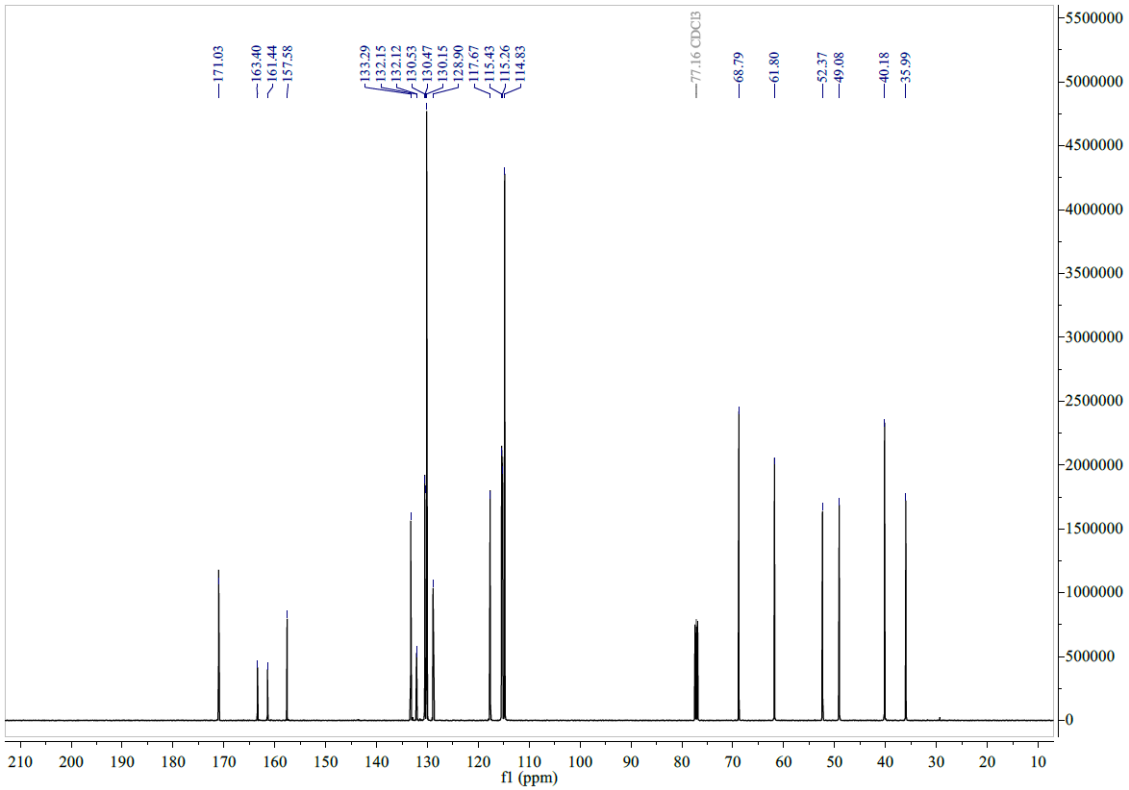

(S)-3-(4-(allyloxy)benzyl)-2-(2-chlorobenzyl)isothiazolidin-4-one 1,1-dioxide (2.9.3a)

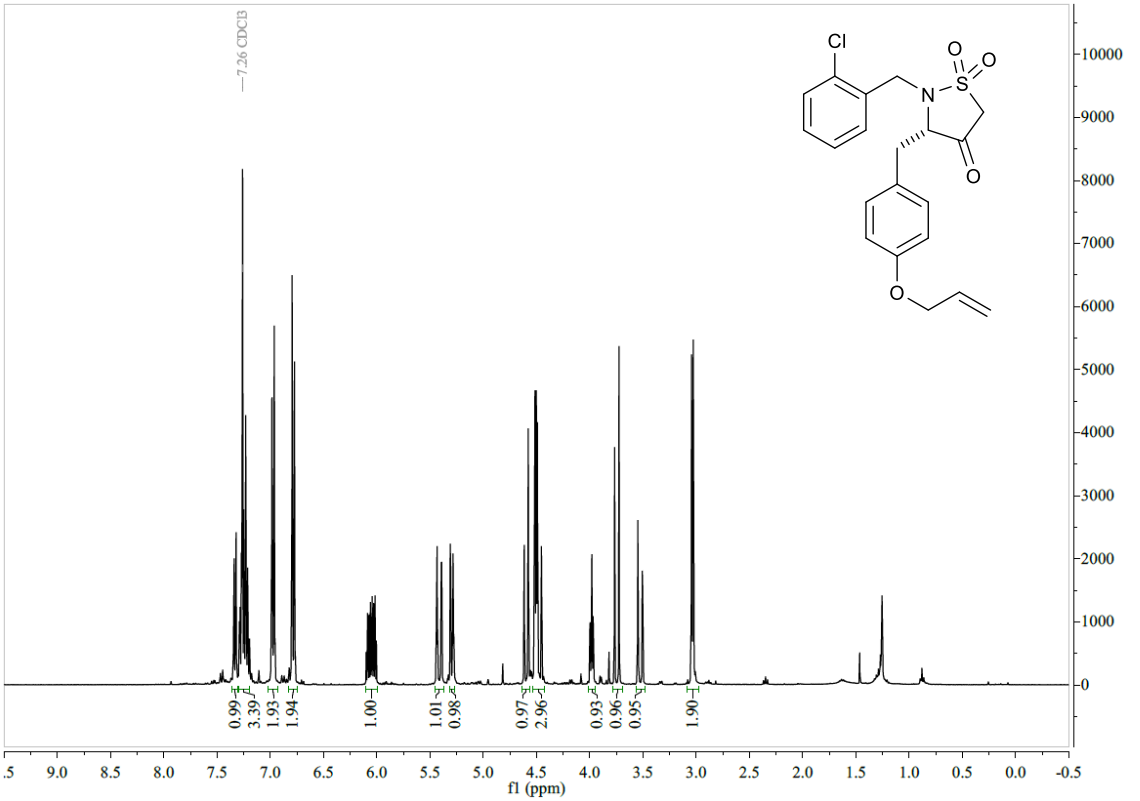

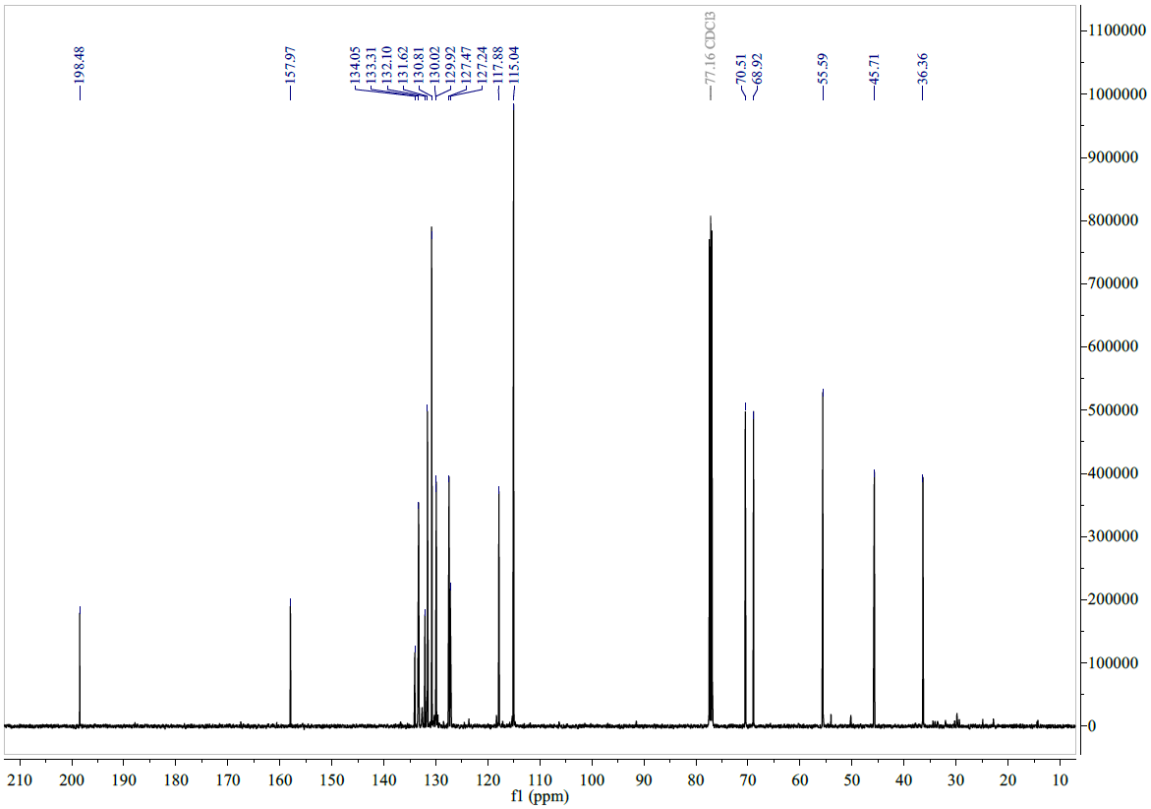

(S)-3-(4-(allyloxy)benzyl)-2-benzylisothiazolidin-4-one 1,1-dioxide (2.9.3b)

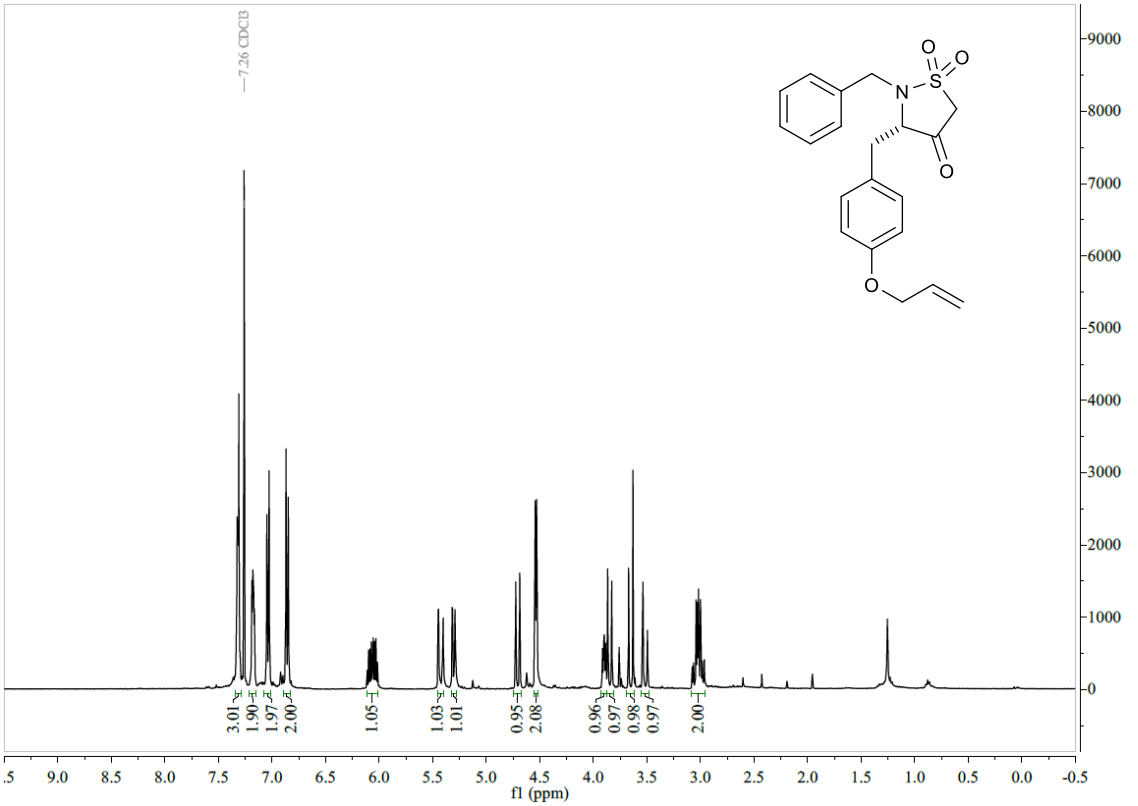

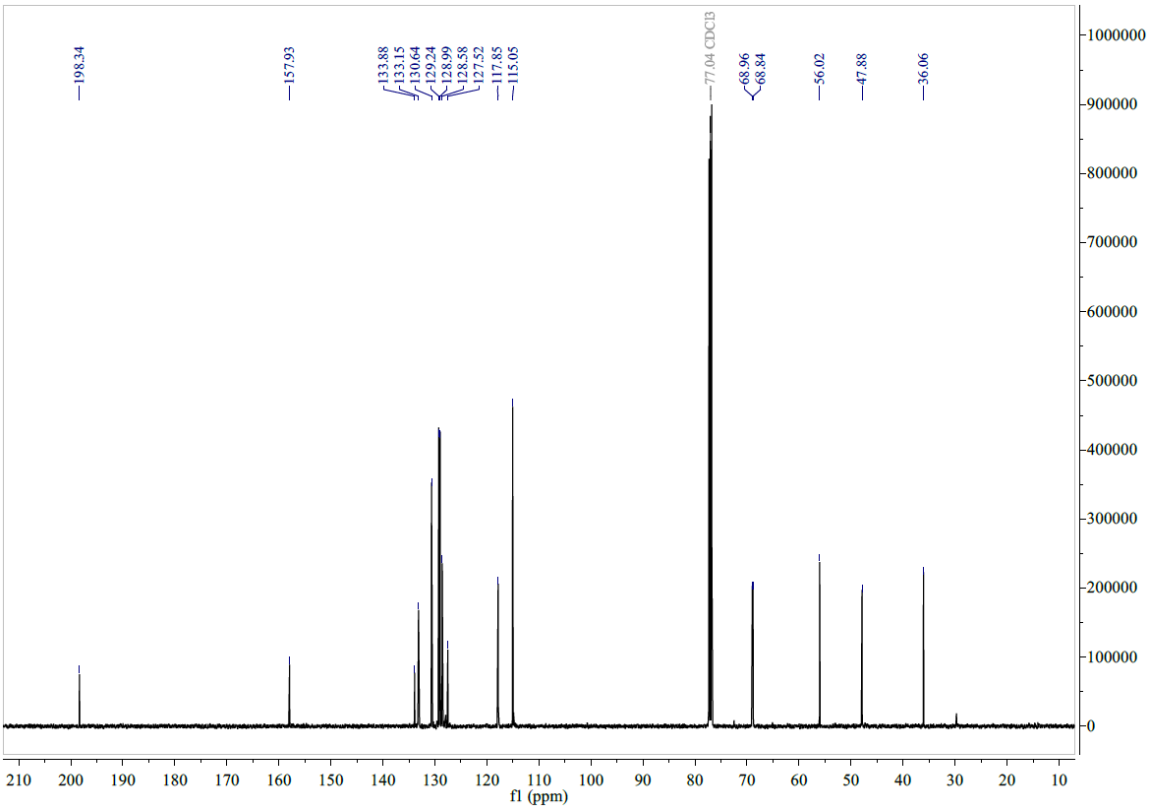

(S)-3-(4-(allyloxy)benzyl)-2-(4-fluorobenzyl)isothiazolidin-4-one 1,1-dioxide (2.9.3c)

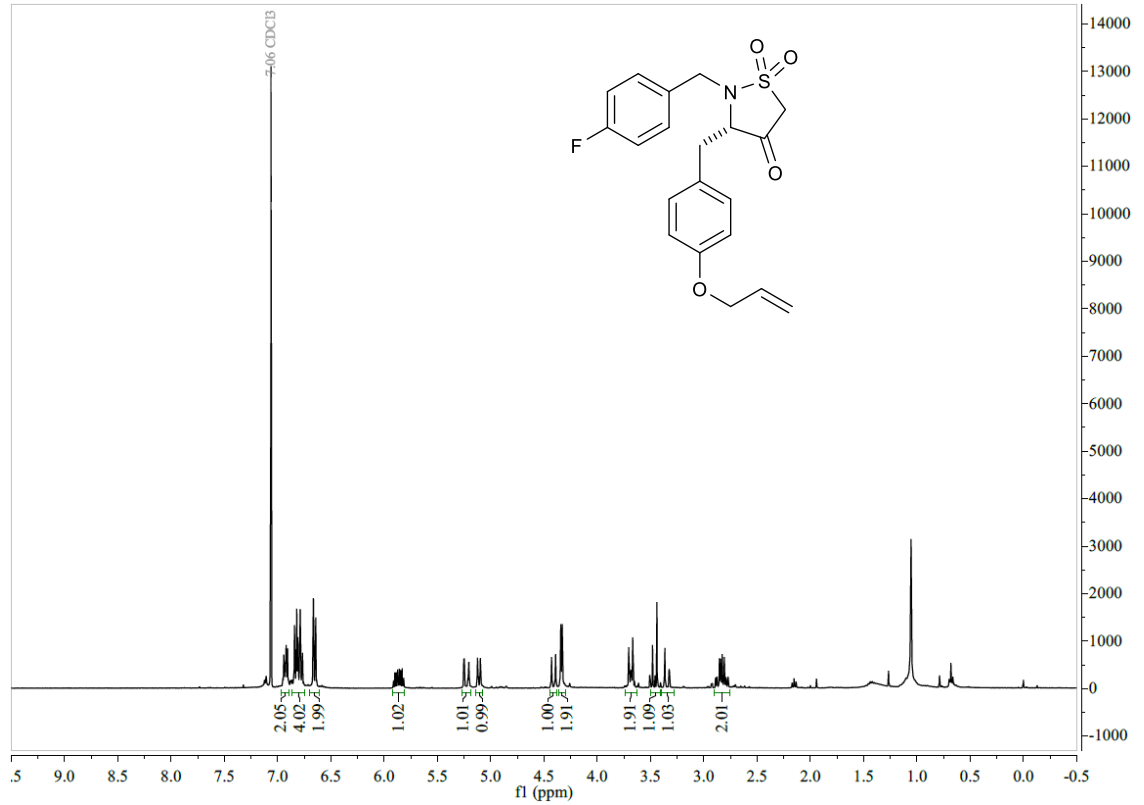

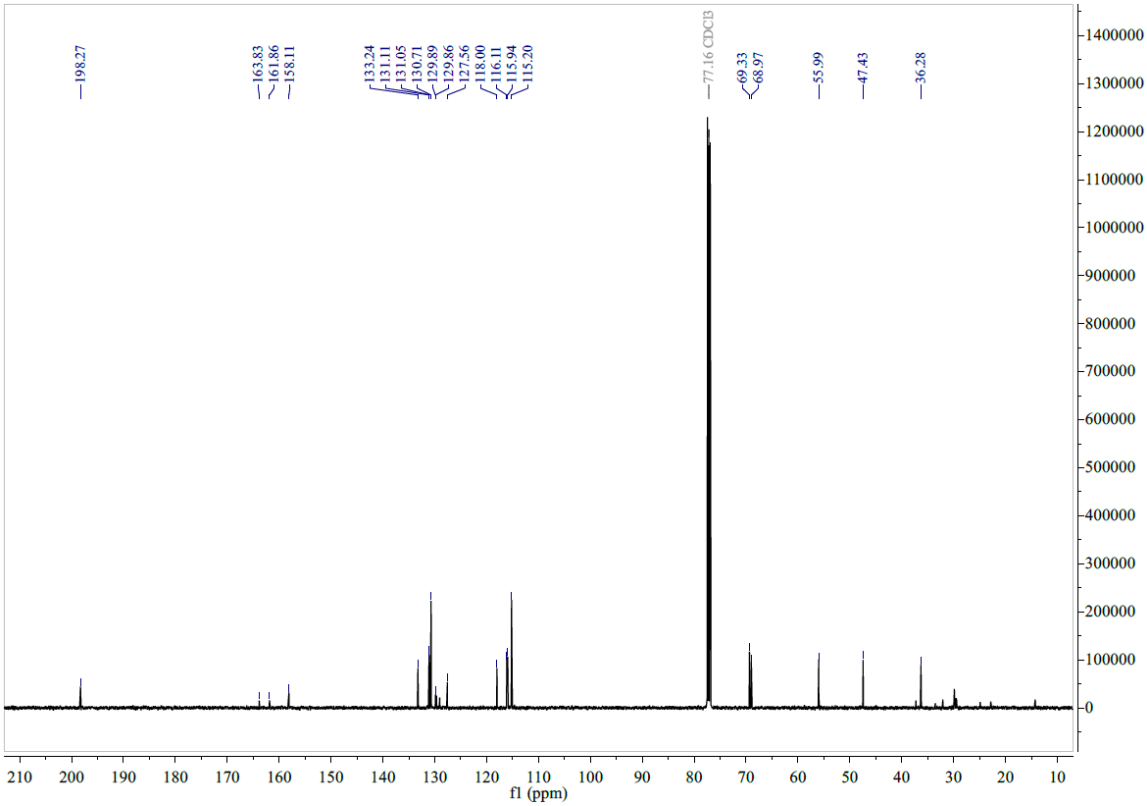

3-(but-3-en-1-yloxy)benzaldehyde (2.11.5)

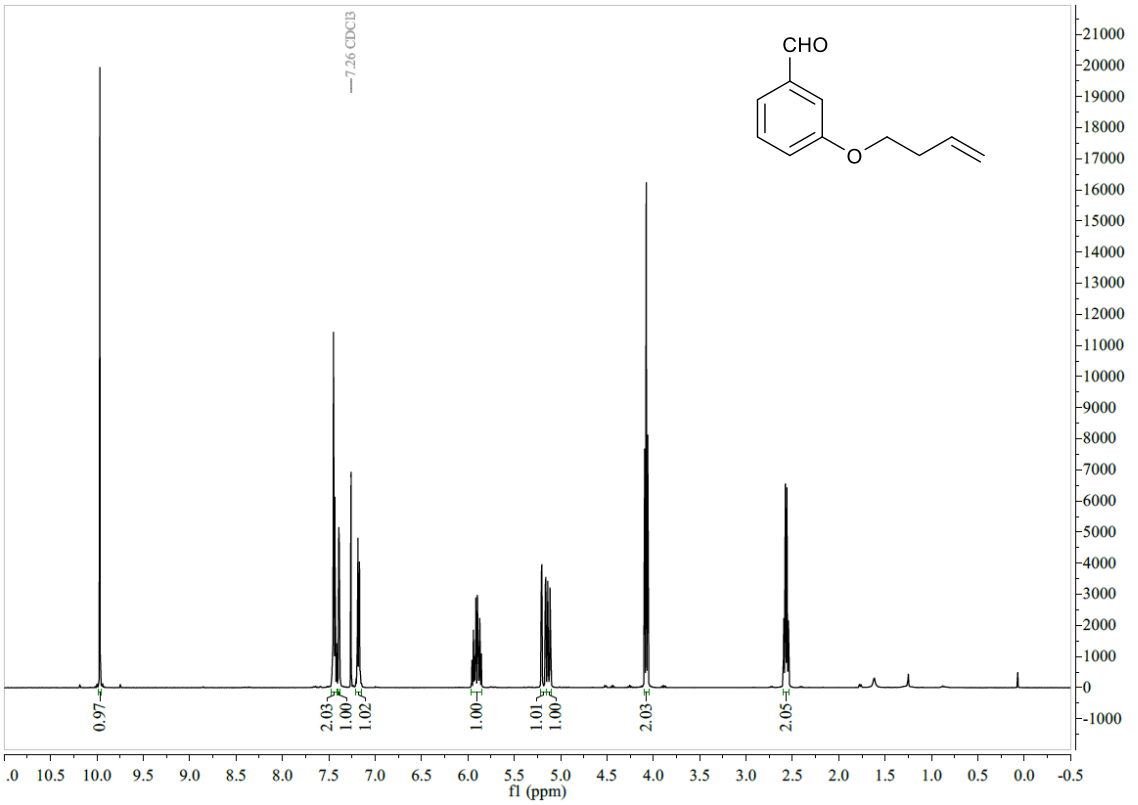

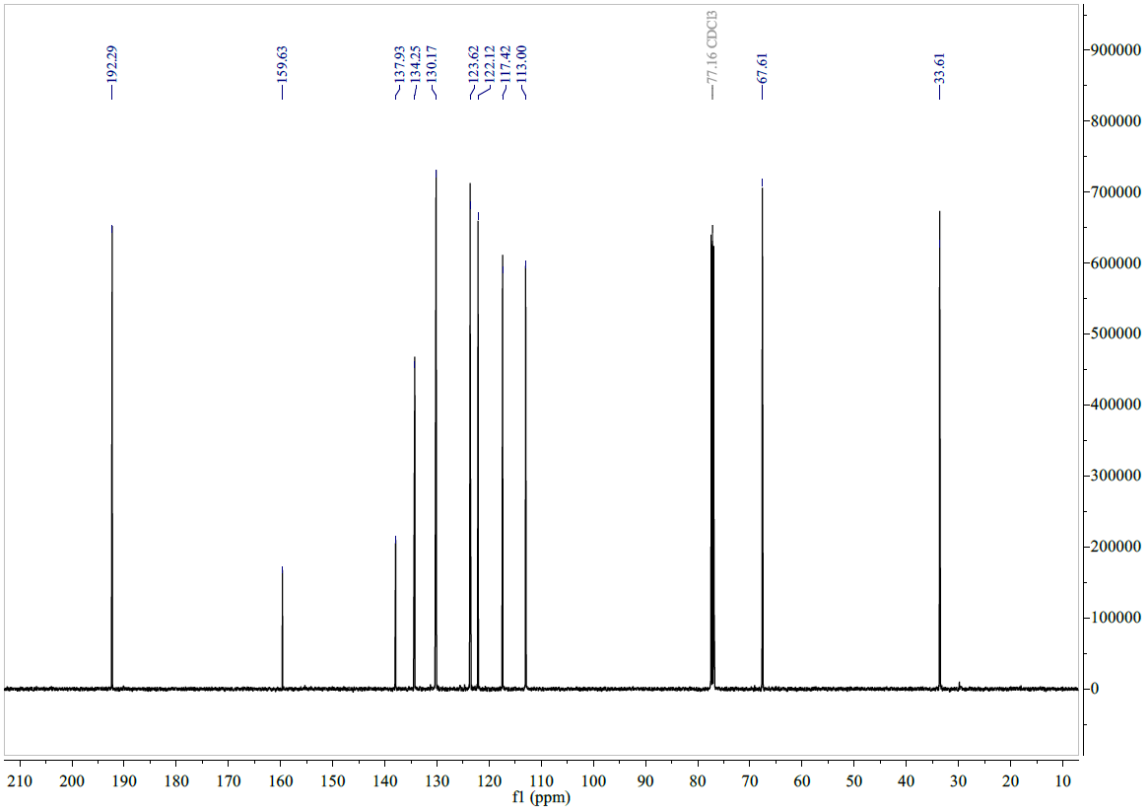

3-(pent-4-en-1-yloxy)benzaldehyde (2.11.4)

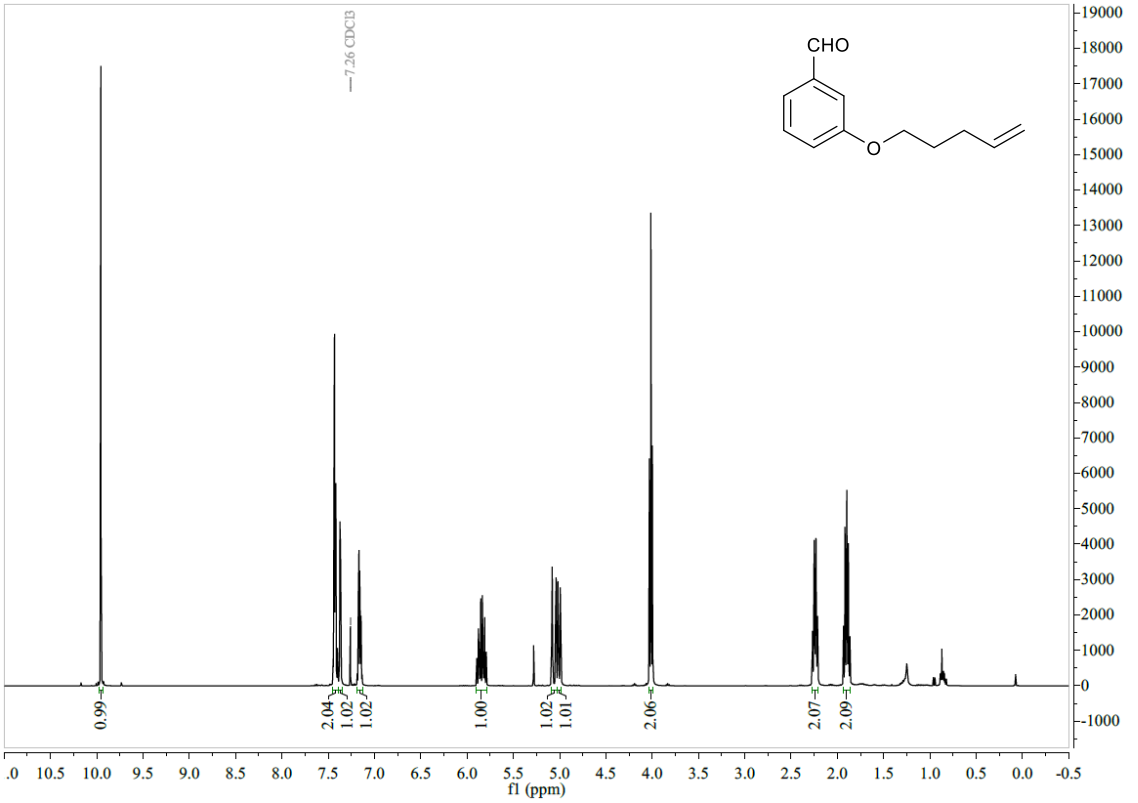

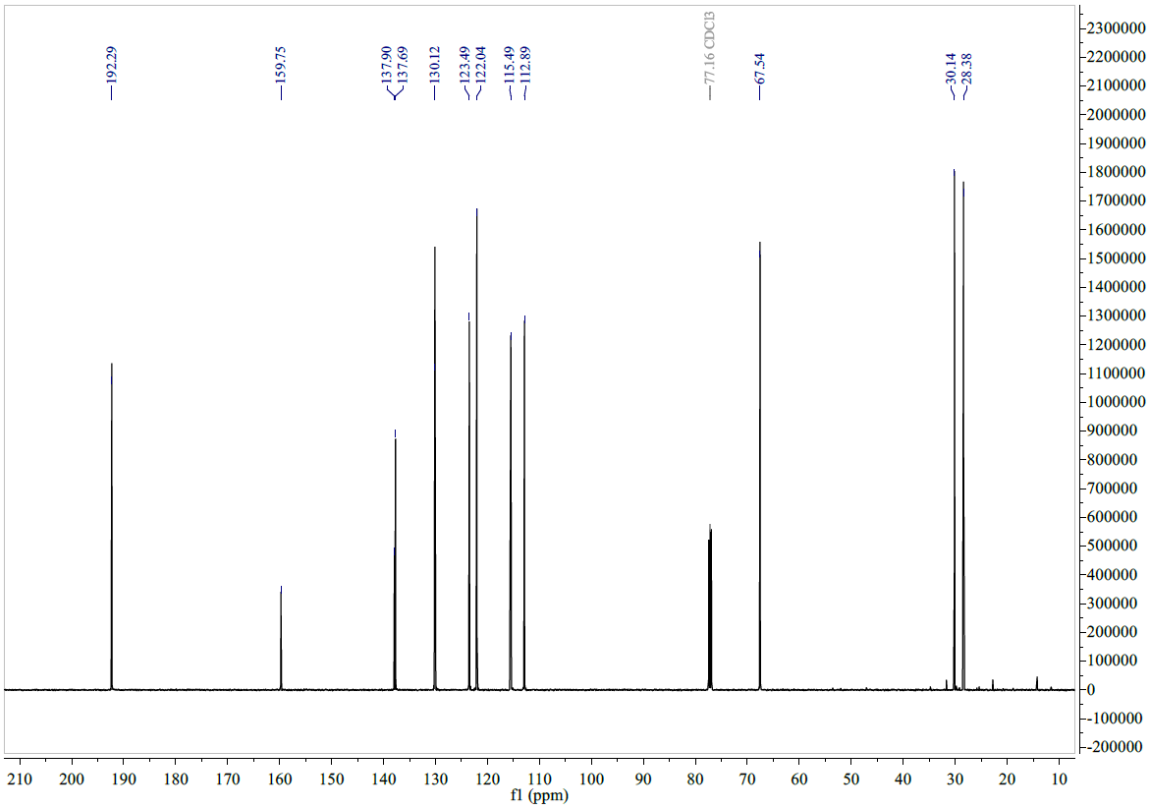

3-(hex-5-en-1-yloxy)benzaldehyde (2.11.6)

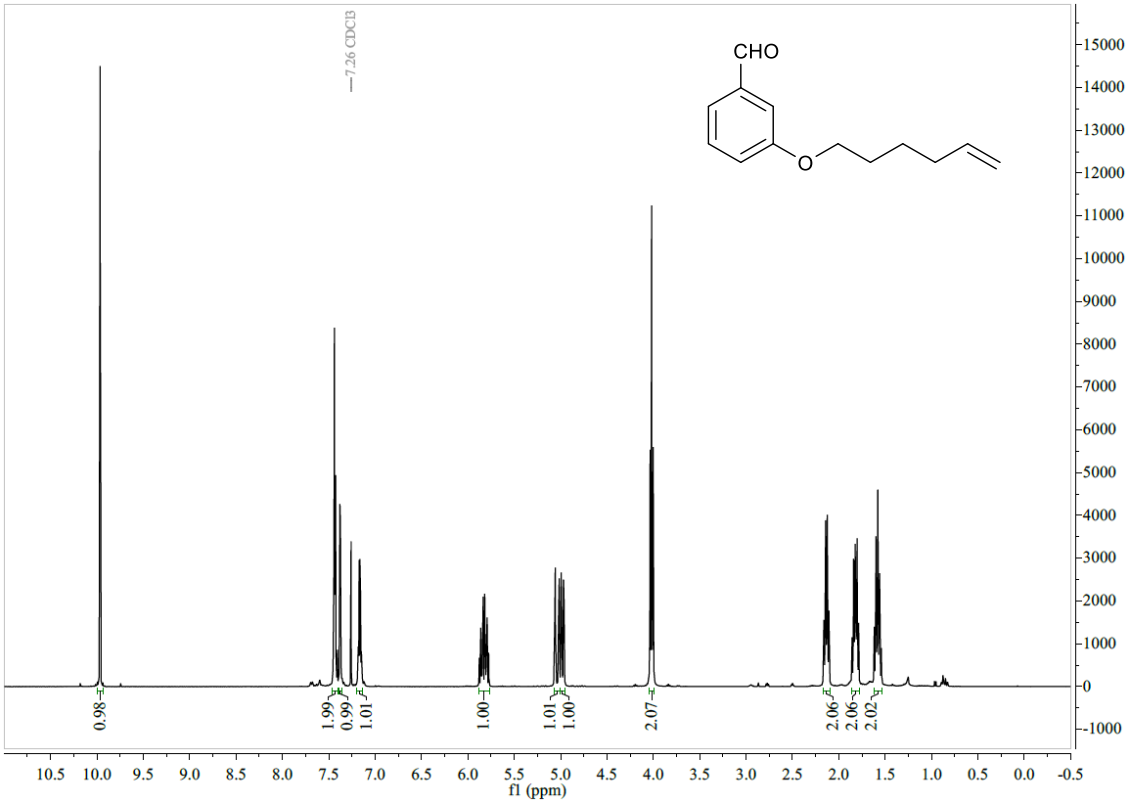

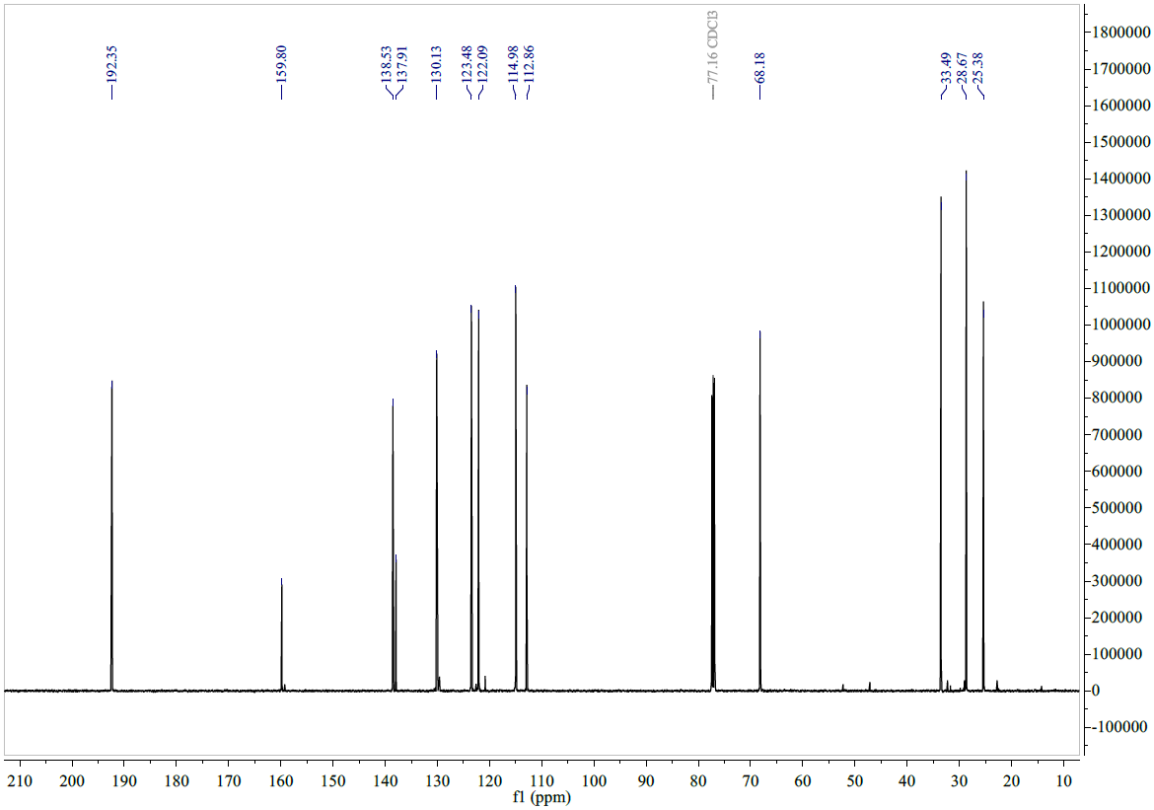

Crystal Structure for

$C_{25}H_{22}N_2O_6S$

Compound **1.27.1h**

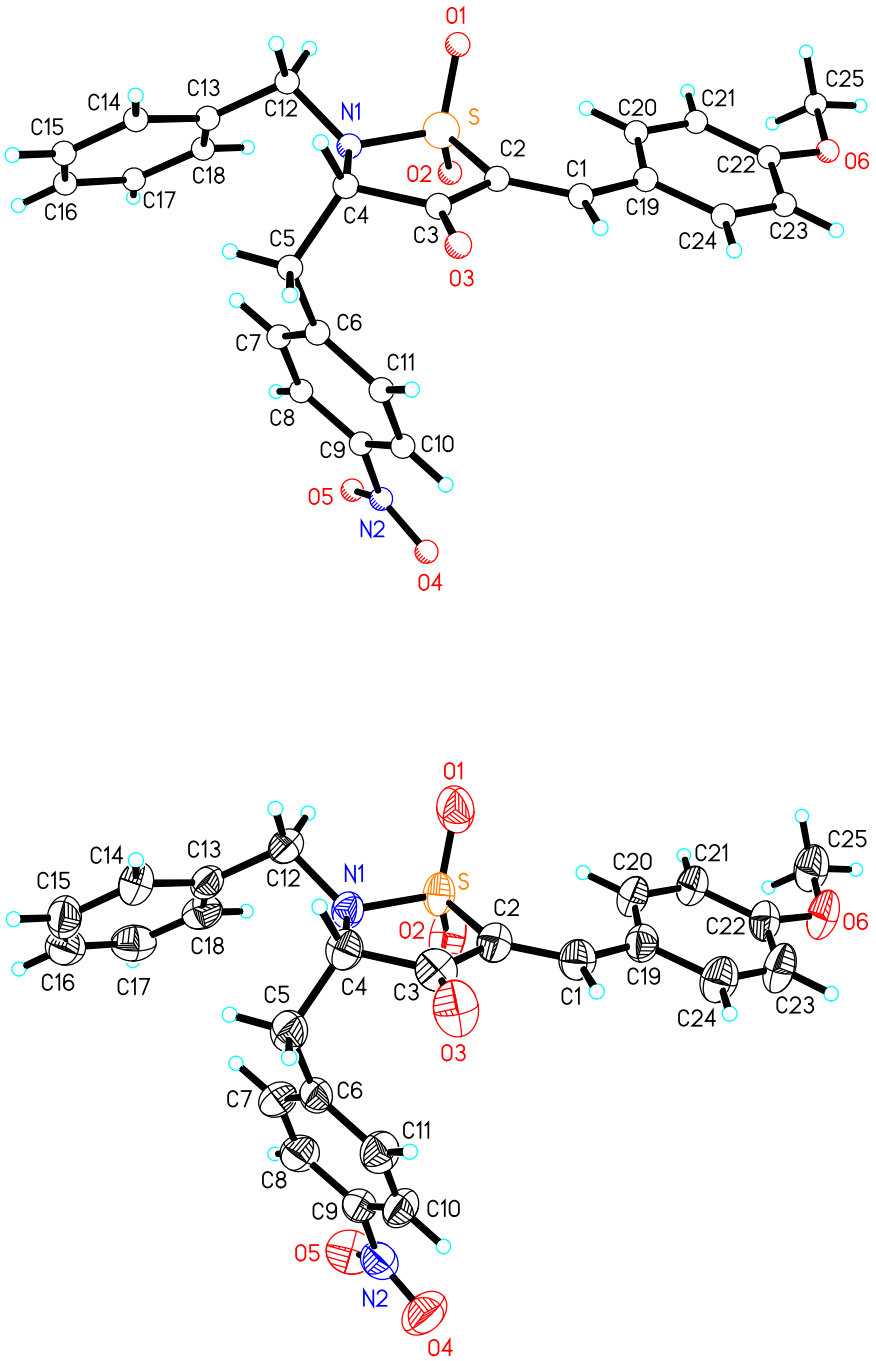

Crystal Structure for

$C_{25}H_{21}FN_2O_6S$

Compound **1.27.1p**